RICKY1 – a Novel Membrane Micro-Domain-Associated Player of Plant Immunity

Dissertation

zur Erlangung des Doktorgrades

an der Fakultät für Biologie der

Ludwig-Maximilians-Universität München

Institut für Genetik

vorgelegt von

CORINNA ANNA BUSCHLE

München, 2017

Die vorliegende Arbeit wurde im Bereich Genetik in der Arbeitsgruppe von Herrn Prof. Dr. Thomas Ott angefertigt.

Eidesstattliche Versicherung

Hiermit erkläre ich an Eides statt, dass ich die vorliegende Arbeit selbstständig, und ohne unerlaubte Hilfe von Dritten angefertigt habe.

München, den

_____
Corinna A. Buschle

Erklärung

Ich habe weder anderweitig versucht, eine Dissertation einzureichen oder mich einer Doktorprüfung zu unterziehen, noch habe ich diese Dissertation oder Teile derselben einer anderen Prüfungskommission vorgelegt.

München, den

_____
Corinna A. Buschle

Table of Contents

List of Figures

1. Summary

1.1. Summary

Plants as sessile organisms are exposed to a variety of abiotic and biotic stresses in their surrounding. Their fitness heavily relies on a fast perception of external stimuli and an efficient cellular modulation to adapt to the rapidly changing environmental conditions. The ultimate need is to immediately respond to microbial infections in order to ensure tissue and/or host survival.

Increasing evidence indicates the significance of pre-assembled protein complexes in distinct domains of the plasma membrane (PM). The compartmentalization facilitates an efficient signal transduction in a spatially confined three-dimensional space. Remorins are accepted micro-domain marker proteins and are thought to mediate the assembly of active signaling platforms at the PM. Therefore, the hypothesized scaffold protein REM1.2 was used as a bait to identify new signaling components.

In this study, I characterized a so far undescribed leucine-rich repeat receptor-like kinase RICKY1 (REMORIN INTERACTING KINASE IN YEAST 1) with respect to its interaction with remorins, its subcellular organization and its role in plant defense.

Data obtained from the heterologous yeast system, indicate a specific interaction between RICKY1 and REM1.2 in a phosphorylation-dependent manner.

In planta, RICKY1 localizes to the PM and is organized in small and dynamic micro-domains. Co-localization analyses revealed a positive correlation between RICKY1-labeled micro-domains and REM1.2 and REM1.3. Image-based interaction studies verified a direct interaction between RICKY1 and REM1.2, even though all three proteins might be part of the same protein complex. Interestingly, REM1.2 has an impact on the lateral mobility of RICKY1, emphasizing its role as scaffold protein.

Pathogen infection assays showed an increased susceptibility of *ricky1* mutants to various phytopathogens. In line with these data, RICKY1 accumulates around oomycete haustoria.

A detailed characterization of several flg22-induced defense responses demonstrated the involvement of RICKY1 in the late production of callose. In contrast, early and intermediate defense mechanisms were not affected in *ricky1* plants. These results suggest that RICKY1 is indeed a new, micro-domain associated player in plant immunity.

1.2. Zusammenfassung

Auf Grund ihrer sesshaften Lebensweise sind Pflanzen direkt und unausweichlich einer Vielzahl von biotischen und abiotischen Stressfaktoren ausgesetzt. Um sich solch stetig wechselnden Umweltbedingungen anzupassen, entwickelten sie eine einmalige Vielzahl effizienter Perzeptionssysteme auf ihren Zelloberflächen und hochkomplexe Mechanismen zur zellulären Regulierung. Diese sind auch und in besonderem Maße essentiell für die Interaktion mit verschiedenen Phytopathogenen. Einer dieser Mechanismen ist die Stimulus-unabhängige und meist konstitutive Prä-Assemblierung funktioneller Multiproteinkomplexe. Eine solche Kompartimentierung ermöglicht eine schnelle und physikalische Assoziation einzelner Komponenten und somit eine wirkungsvolle Signaltransduktion in einem räumlich abgegrenzten Bereich. Remorine sind anerkannte Markerproteine für Mikrodomänen und vielversprechende Kandidaten für die Bildung von Signalweiterleitungszentren an der Plasmamembran. Aus diesem Grund wurde REM1.2 ausgewählt, um neue Mikrodomänen-assoziierte Signalproteine zu identifizieren und zu charakterisieren.

In dieser Studie wurde die im Rahmen eines Hefescreen identifizierte und bisher unbekannte Rezeptor-ähnliche Kinase RICKY1 (REMORIN INTERACTING KINASE IN YEAST 1) mit Blick auf ihre Interaktion mit Remorinen, ihre subzellulare Organisation und ihre Rolle während der pflanzlichen Immunabwehr untersucht.

In Pflanzen ist RICKY1 in kleinen, mobilen Mikrodomänen an der Plasmamembrane lokalisiert. Co-Lokalisationsstudien zeigten eine positive Korrelation zwischen RICKY1-markierten Mikrodomänen und REM1.2 und REM1.3. Die im Rahmen dieser Doktorarbeit durchgeführten Interaktionsstudien wiesen dabei allerdings vorwiegend auf eine direkte und möglicherweise phosphorylierungsabhängige Interaktion zwischen RICKY1 und REM1.2 hin. Obwohl das zu REM1.2 nahe verwandte Remorin REM1.3 Teil des hetero-oligomeren Komplexes ist, interagiert RICKY1 kaum mit diesem Protein. Die erhöhte lateral Mobilität des Rezeptors in REM1.2-defizienten Mutanten unterstützt die vermutete Funktion von Remorinen als molekulare Gerüstproteine.

Die Untersuchung von *ricky1* Mutanten demonstrierte eine erhöhte Anfälligkeit gegenüber verschiedenen Pathogenen. Zusätzlich lokalisiert RICKY1 um die Haustorien eines Oomyzets. Eine detaillierte Analyse zeigte, dass RICKY1 bei der flg22-induzierten Callose-Produktion involviert ist. Im Gegensatz dazu sind frühere Verteidigungsmechanismen in *ricky1* nicht beeinträchtigt. Diese Ergebnisse zeigen deutlich, dass es sich bei RICKY1 tatsächlich um eine neue, Mikrodomänen-assoziierte Komponente der pflanzlichen Immunabwehr handelt.

2. Introduction

2.1. Plant Immunity

2.1.1.   Receptor-Like Kinases in Plant Defense

Plants are exposed to a multitude of co-existing abiotic and biotic stresses in their environment. Because of their sessile lifestyle, they are particularly dependent on a fast and efficient monitoring system to adapt to changing conditions. A fine-tuned balance between growth and induced stress responses is crucial for a maintained fitness and consequently for their survival. This especially applies for the interaction between plants and various phytopathogens in their surrounding (Huot *et al.*, 2014).

In contrast to vertebrates, plants lack an adaptive immune system and exclusively rely on innate immune responses (Spoel & Dong, 2012). Nevertheless many plants are resistant to a broad range of phytopathogens. This phenomenon is called non-host resistance and is based on multiple tiers of plant defense (Thordal-Christensen, 2003; Gill *et al.*, 2015). For a successful infection, potential pathogens have to overcome constitutive, physical barriers such as the waxy cuticle and the rigid cell wall (CW) and bear several antimicrobial compounds (Malinovsky *et al.*, 2014; Miedes *et al.*, 2014; Serrano *et al.*, 2014; Piasecka *et al.*, 2015). Furthermore, the recognition of conserved pathogen- or microbe-associated molecular pattern (PAMPs, MAMPs) by pattern-recognition receptors (PRRs) triggers induced defense responses leading to the PAMP-triggered immunity (PTI) (Jones & Dangl, 2006). MAMPs are generally characterized by their highly conserved structure, their significance for the fitness of the pathogen and their absence in the host. The latter is crucial to enable the differentiation between self and non-self (Medzhitov & Janeway, 2002).

The perception of pathogenic components by PRRs is a common feature of plants and vertebrates. However, besides several similarities also obvious differences exist between them (Nürnberger *et al.*, 2004; Jones & Dangl, 2006; Ronald & Beutler, 2010).

Well-characterized animal PRRs are the membrane-localized Toll-like receptors (TLR), comprising 10 and 12 members in humans and mice, respectively. They consist of extracellular leucine-rich repeats (LRRs), a transmembrane (TM) domain and an intracellular Toll-interleukin 1 (IL-1) receptor (TIR) domain. The latter forms a docking platform for TIR-containing adapters. Because TLRs lack a kinase domain, the additional recruitment of IL-1

receptor-associated (IRAK) and Pelle kinases is essential to propagate the signal to downstream components (Aderem & Ulevitch, 2000; O'Neill & Bowie, 2007; Kawai & Akira, 2010). Animals are able to detect MAMPs outside as well as inside of the cell (Hansen *et al.*, 2011), whereas all known plant PRRs, receptor-like kinases (RLKs) and receptor-like proteins (RLPs), are exclusively located at the plasma membrane (PM) (Macho & Zipfel, 2014).

RLKs are composed of a variable extracellular region, a single TM domain and a cytoplasmic kinase domain. RLPs display a similar overall structure, but lack the intracellular kinase domain (Shiu & Bleecker, 2001a). RLPs are therefore thought to collaborate with interacting RLKs to propagate the signal (Zipfel, 2014). The monophyletic family of RLKs comprises over 600 members in *Arabidopsis thaliana* (hereafter *Arabidopsis*) and thus 2.5 % of all protein coding genes (Shiu & Bleecker, 2001b). However, several annotated RLKs do not contain a TM-spanning domain and are hence called receptor-like cytoplasmic kinases (RLCK). Intriguingly, kinase domains of RLKs and RLCKs are phylogenetically related to *Drosophila* Pelle and human IRAK kinases (Shiu & Bleecker, 2001b).

RLKs can be divided into 46 subgroups based on the sequence of their kinase domains and the appearance of their variable extracellular domains (ECDs). The latter enable PRRs to perceive diverse biotic signals in the apoplast. Among them, LRRs constitute the most frequent motif in the ECDs of plant RLKs (Shiu & Bleecker, 2001a; Shiu & Bleecker, 2003).

Interestingly, animal and plant PRRs often recognize different epitopes of the same pathogenic components (Felix *et al.*, 1999; Smith *et al.*, 2003; Zipfel & Felix, 2005; Neyen & Lemaitre, 2016). The animal receptor TLR5, for example, binds a conserved part of the bacterial flagellin that is buried in the flagellar filament (Hayashi *et al.*, 2001; Mizel *et al.*, 2003; Smith *et al.*, 2003). In contrast, the LRR-receptor kinase (RK) FLS2 (FLAGELLIN SENSING 2) senses an N-terminal 22 amino acid peptide, referred to as flg22 (Felix *et al.*, 1999; Gomez-Gomez & Boller, 2000). TLR5 and FLS2 do not share a high sequence similarity, except for the presence of LRRs in their extracellular part, indicating an independent, convergent evolution (Smith *et al.*, 2003).

The ectodomain of FLS2 consists of 28 LRRs of which 14 (LRR3-16) are directly involved in flg22 binding (Chinchilla *et al.*, 2006; Sun *et al.*, 2013). Upon flg22 perception FLS2 interacts with its co-receptor BAK1/SERK3 (BRASSINOSTEROID INSENSITIVE 1 (BRI1)-ASSOCIATED RECEPTOR KINASE 1/ SOMATIC EMBRYOGENESIS RECEPTOR KINASE 3) that is required for the complete activation of downstream defense responses (Chinchilla *et al.*, 2007). Surprisingly, the C-terminal region of FLS2-bound flg22 is additionally recognized by BAK1 and acts as molecular glue to stabilize the interaction (Sun *et al.*, 2013).

The majority of higher plants is able to respond to flg22 treatments (Boller & Felix, 2009). Accordingly, FLS2 orthologs have been identified in tobacco (*Nicotiana benthamiana*), tomato (*Solanum lycopersicum*), rice (*oryza sativa*) and grapevine (*Vitis vinifera*) (Hann & Rathjen, 2007; Robatzek *et al.*, 2007; Takai *et al.*, 2008; Trda *et al.*, 2014). Additionally, another flagellin epitope, called flgII-28, was shown to induce defense responses exclusively in distinct Solanaceae species (Cai *et al.*, 2011; Veluchamy *et al.*, 2014). However, flgII-28 is not recognized by the receptor FLS2 (Clarke *et al.*, 2013), but by the LRR-RK FLS3 (Hind *et al.*, 2016).

Another well-studied PRR is the LRR-RLK EFR (EF-TU RECEPTOR) that perceives conserved N-acetylated epitopes of the bacterial elongation factor EF-TU (elf18 and elf26) (Kunze *et al.*, 2004; Zipfel *et al.*, 2006). In contrast to flg22, the sensing of elf18 is restricted to Brassicaceae (Boller & Felix, 2009). Fascinatingly, the heterologous expression of AtEFR in tobacco and tomato plants results in the responsiveness to EF-TU. These results suggest that the transfer of PRRs can be used to engineer disease resistance in different plant species (Lacombe *et al.*, 2010). Likewise, the Brassicaceae-specific, B-type lectin S-domain (SD)-1 RLK LORE (LIPOOLIGOSACCHARIDE-SPECIFIC REDUCED ELICITATION) can confer the sensitivity to lipopolysaccharides (LPS) to *N. benthamiana* and *N. tabacum* (Ranf *et al.*, 2015).

In addition to bacterial compounds, also fungal-derived pattern can be recognized by plant PRRs. In rice, homodimers of the lysin motif (LysM)-containing RLP CEBiP (CHITIN ELICITOR-BINDING PROTEIN) were shown to bind the fungal CW component chitin. The subsequent heterodimerization with OsCERK1 (CHITIN ELICITOR RECEPTOR KINASE 1) results in a sandwich-type receptor complex (Shimizu *et al.*, 2010; Hayafune *et al.*, 2014). In *Arabidopsis*, CERK1 was previously thought to constitute the unique chitin receptor (Miya *et al.*, 2007; Petutschnig *et al.*, 2010; Liu *et al.*, 2012). However, only recently LYK5 (LYSIN MOTIF RECEPTOR LIKE KINASE 5) was shown to bind chitin with a higher affinity than AtCERK1 (Cao *et al.*, 2014). Accordingly, the inactive kinase LYK5 is crucial for chitin-induced responses and acts in concert with CERK1 (Cao *et al.*, 2014). In line with these data, CERK1 was additionally shown to function as co-receptor during the perception of bacterial peptidoglycans (PGN) by the RLPs LYM1 (LysM DOMAIN-CONTAINING GLYCOSYLPHOSPHATIDYLINOSITOL-ANCHORED PROTEIN 1) and LYM3 (Gimenez-Ibanez *et al.*, 2009a; Gimenez-Ibanez *et al.*, 2009b; Willmann *et al.*, 2011).

In addition to MAMPs, also endogenous plant-derived signal, so-called DAMPs (damage-associated molecular pattern), can induce different defense responses. For instance, plants actively release adenosine 5´-triphosphate (ATP) to the apoplast in response to abiotic,

biotic and mechanical stresses (Tanaka *et al.*, 2010; Dark *et al.*, 2011; Choi, J *et al.*, 2014). Only recently, the lectin receptor kinase DORN1 (DOES NOT RESPOND TO NUCLEOTIDES 1) was identified as receptor for extracellular ATP (Choi, J *et al.*, 2014). Furthermore, the LRR-RLKs PEPR1 (PEP1 RECEPTOR 1) and PEPR2 are known to bind endogenous AtPep1 peptides and might play a role for spreading the signal from damaged to not yet infected cells (Huffaker *et al.*, 2006; Yamaguchi *et al.*, 2006; Krol *et al.*, 2010; Yamaguchi *et al.*, 2010; Ross *et al.*, 2014). Interestingly, even PEPR1 and PEPR2 interact with the co-receptor BAK1 in a ligand-dependent manner (Postel *et al.*, 2010; Schulze *et al.*, 2010).
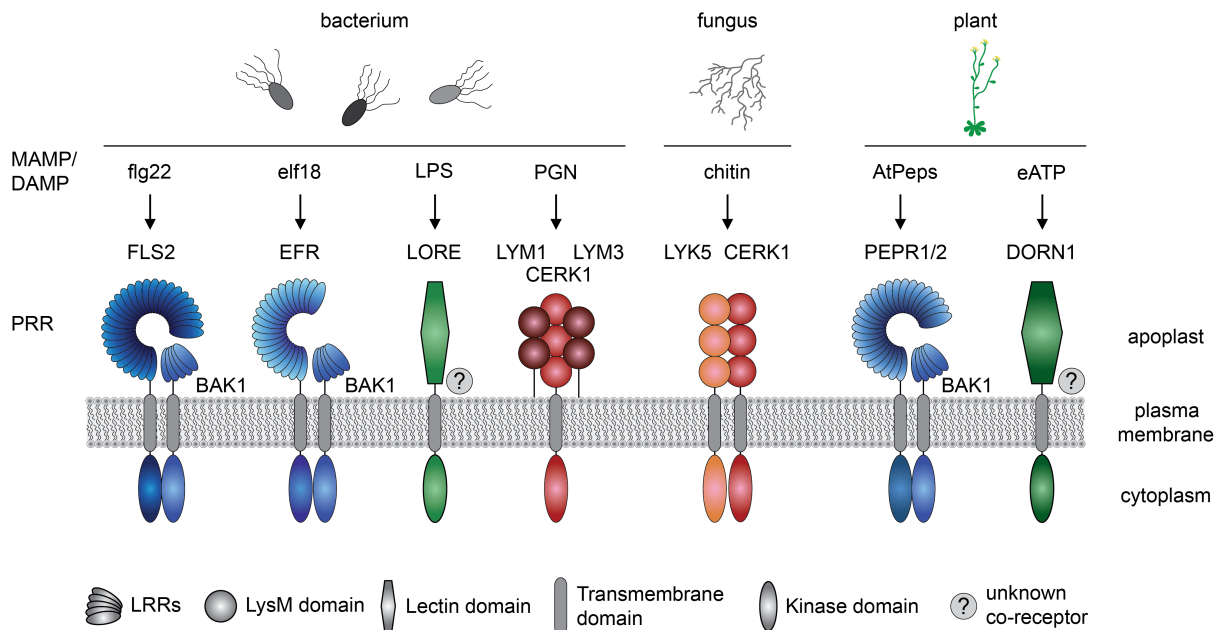
Fig. 2.1 PM-localized PRRs recognize MAMPs and DAMPs with their variable extracellular domains

Microbe- and damage-associated molecular pattern (MAMPs and DAMPs) are bacteria-, fungus or plant-derived components that are perceived by pattern-recognition receptors (PRRs). Leucine-rich repeat (LRR) receptor-like kinases are able to sense proteins or peptides. Accordingly, the LRR-RLKs FLS2, EFR and PEPR1/2 bind flg22, elf18 and AtPeps, respectively. Lysin motif (LysM)-RLKs such as LYM1/3 and LYK5 recognize the carbohydrate-based ligands peptidoglycan (PGN) and chitin, respectively. The lectin domain-containing RLKs LORE and DORN1 perceive lipopolysaccharides (LPS) and extracellular ATP (eATP), respectively. The LRR-RLK BAK1 functions as co-receptor for LRR-RKs, whereas the LysM-RLK CERK1 interacts with other LysM-RKs. If also LORE and DORN1 act together with co-receptors is not known so far.

Additionally, BAK1 itself or closely related, partially redundant members of the SERK family interact with diverse LRR-RKs involved in various signaling pathways including brassinosteroid (BR) signaling (BRI1; BRASSINOSTEROID INSENSITIVE 1) cell expansion (PSKR1; PHYTOSULFOKINE (PSK) RECEPTOR 1) and floral organ abscission

(HAE/HSL2; HAESA/HAE-LIKE 2) (Li *et al.*, 2002; Nam & Li, 2002; Gou *et al.*, 2012; Wang *et al.*, 2015a; Ma *et al.*, 2016; Meng *et al.*, 2016). In contrast, CERK1 specifically binds to PRRs with extracellular LysM domains (Willmann *et al.*, 2011; Cao *et al.*, 2014; Hayafune *et al.*, 2014). In line with this, CERK1 is not involved in flg22 sensing and chitin perception is independent of BAK1 (Shan *et al.*, 2008; Wan *et al.*, 2008).

How co-receptors coordinate with the variety of interacting RLKs in a spatiotemporal-defined manner and how signaling specificity is achieved needs to be further investigated (Ma *et al.*, 2016). So far, the characterization of the hypoactive BAK1-5 allele highlights the importance of discriminative phosphorylation events. While defense-related responses are reduced in *bak1-5* mutants, other BAK1-related pathways such as BR-signaling and cell death are not affected (Schwessinger *et al.*, 2011). Intriguingly, first transphosphorylation events between BAK1 and FLS2/BRI1 occur within seconds after ligand perception, indicating pre-assembled protein complexes (Schulze *et al.*, 2010). However, the analysis of BAK1 and FLS2 real-time dynamics suggests hetero- as well as homodimerization only upon flg22 treatment (Somssich *et al.*, 2015). Only recently, the malectin-like RLK FER (FERONIA) was proposed to act as a RALF23 (RAPID ALKALINIZATION FACTOR 23)-regulated scaffold for the formation of immunity-related complexes (Stegmann *et al.*, 2017). In *Arabidopsis,* 34 endogenous RALF peptides are produced upon changing environmental conditions and contribute to different signaling pathways (Wu *et al.*, 2007; Matos *et al.*, 2008; Haruta *et al.*, 2014; Stegmann *et al.*, 2017). Because FER is able to bind several RALFs, the authors hypothesized that various FER-RALF modules influence distinct signaling pathways by regulating the complex assembly of diverse receptors (Stegmann *et al.*, 2017).

Within few minutes upon ligand binding multimeric protein complexes are assembled including several cytoplasmic proteins such as RLCKs (Lin *et al.*, 2013b). One of the best-studied RLCKs in plant immunity is BIK1 (BOTRYTIS-INDUCED KINASE 1) (Veronese *et al.,* 2006). BIK1 as well as closely related PBL (AVRPPHB SUSCEPTIBLE 1 (PBS1)-like) proteins interact with FLS2 and BAK1 in non-stimulated cells. Upon flg22 treatment BIK1 gets phosphorylated by BAK1 and in turn transphosphorylates BAK1 and FLS2 (Lu *et al.*, 2010; Zhang *et al.*, 2010). Subsequently BIK1 dissociates from the complex and activates downstream signaling components (Lu *et al.*, 2010; Kadota *et al.*, 2014; Li *et al.*, 2014). In addition to FLS2, BIK1 associates with EFR, CERK1, PEPR1 and BRI1 prior to ligand perception (Zhang *et al.*, 2010; Lin *et al.*, 2013a; Liu *et al.*, 2013). However, in contrast to its

function as positive regulator of immune-related responses, BIK1 plays a negative role in BR-signaling (Lin *et al.*, 2013a).

2.1.2.   Plant Defense Responses

One of the first detectable cellular changes is the increased influx of extracellular Ca^{2+} ions to the cytosol occurring seconds to minutes upon MAMP/DAMP perception (Boller, 1995; Blume *et al.*, 2000; Lecourieux *et al.*, 2002). The subsequent activation of additional PM-localized transporters (influx: H^+; efflux: K^+, Cl^-; NO_3^-) results in an immediate extracellular alkalinization and a depolarization of the PM (Jeworutzki *et al.*, 2010). Intriguingly, the Ca^{2+} ATPase ACA8 (ARABIDOPSIS-AUTOINHIBITED CA2+ ATPASE 8) associates with FLS2, indicating the proximity of defense response-related components and the receptor complex. Accordingly, ACA8 and the closely related ACA10 were shown to participate in the fine regulation of Ca^{2+} levels (Frei dit Frey *et al.*, 2012). These are important for the activation of downstream CALCIUM-DEPENDENT PROTEIN KINASES (CPK or CDPK) (Schulz *et al.*, 2013). CPK4, 5, 6, 11, for example, are involved in plant immunity and positively regulate the production of reactive oxygen species (ROS) (Boudsocq & Sheen, 2013; Dubiella *et al.*, 2013).

In *Arabidopsis,* the NADPH oxidase RBOHD (RESPIRATORY BURST OXIDASE HOMOLOG D) is responsible for the MAMP-induced ROS burst (Nühse *et al.*, 2007; Zhang *et al.*, 2007). In line with this, RBOHD is differentially phosphorylated by CPK5 as well as BIK1 and close homologs upon MAMP treatment (Benschop *et al.*, 2007; Nühse *et al.*, 2007; Dubiella *et al.*, 2013; Kadota *et al.*, 2014; Li *et al.*, 2014). Together, the two-step regulation of RBOHD activity is thought to maintain its signaling specificity (Kadota *et al.*, 2015). Interestingly, ROS can in turn induce an increase in cytoplasmic Ca^{2+} levels and thereby enhance the CPK5-mediated phosphorylation of RBOHD (Pei *et al.*, 2000; Rentel & Knight, 2004; Dubiella *et al.*, 2013). Moreover, also BIK1 is a positive regulator of the Ca^{2+} burst (Li *et al.*, 2014; Ranf *et al.*, 2014), indicating a complex interplay between Ca^{2+}- and ROS-mediated responses.

ROS itself is thought to be toxic for phytopathogens and might impede their invasion (Bradley *et al.*, 1992; Luna *et al.*, 2011; Macho *et al.*, 2012). Furthermore, ROS acts as a second messenger in cell-to-cell communication to activate ROS in neighboring cells and to induce defense responses in distal leaves (Miller *et al.*, 2009; Dubiella *et al.*, 2013; Choi, WG *et al.,* 2014; Gilroy *et al.*, 2014). ROS and Ca^{2+}-regulated proteins such as CPKs are

involved in signal transduction by interacting with downstream components (Boudsocq *et al.*, 2010; Dubiella *et al.*, 2013; Gao *et al.*, 2013).

In addition, mitogen-activated protein kinases (MAPKs) play a crucial role for the connection of PM-localized receptor complexes and downstream components including various transcription factors. The phosphorylation-dependent signaling cascade is mediated by three types of kinases: Upstream MAPK kinase kinases (MAPKKKs) phosphorylate MAPK kinases (MAPKKs) that, in turn, finally activate MAPKs (Meng & Zhang, 2013). In *Arabidopsis*, 60 MAPKKKs, 10 MAPKKs and 20 MAPKs have been identified (Ichimura *et al.*, 2002), highlighting the complexity of this pathway. Only recently, the RLCK PBL27 was shown to directly connect the chitin-induced LYK5/CERK1 complex with the MAPK signaling cascade by interacting with both, CERK1 and MAPKKK5 (Yamada *et al.*, 2016). In contrast, the intermediary kinase was not yet identified for the flg22-induced MAPK cascade. However, four MAPKs, namely MPK (MITOGEN-ACTIVATED PROTEIN KINASE) 3, 4, 6 and 11, are activated upon flg22 treatment (Nühse *et al.*, 2000; Asai *et al.*, 2002; Bethke *et al.*, 2012). Accordingly, two distinct pathways have been suggested: On the one hand the MEKK1 (MAPK/ERK KINASE KINASE 1) - MKK1/2 (MITOGEN-ACTIVATED PROTEIN KINASE KINASE 1,2) - MPK4 cascade (Ichimura *et al.*, 2006; Nakagami *et al.*, 2006; Suarez-Rodriguez *et al.*, 2007; Qiu *et al.*, 2008). On the other hand the MKK4/5 – MPK3/6 cascade that is initiated by so far unknown MAPKKK(s) (Asai *et al.*, 2002; Ren *et al.*, 2002; Ichimura *et al.*, 2006). Targets of MAPKs are mainly defense-related transcription factors that modulate plant gene expression. Therefore, MAPK signaling cascades play an important role for several defense responses including the biosynthesis of hormones and antimicrobial compounds as well as stomatal closure (Petersen *et al.*, 2000; Kim & Zhang, 2004; Gudesblat *et al.*, 2007; Takahashi *et al.*, 2007; Ren *et al.*, 2008; Xu *et al.*, 2008; Jammes *et al.*, 2009; Pitzschke & Hirt, 2009; Han *et al.*, 2010; Ishihama *et al.*, 2011; Mao *et al.*, 2011; Li, GJ *et al.*, 2012).

One of the later defense responses (occurring hours after MAMP perception) is the enhanced production of the CW component callose (Gomez-Gomez *et al.*, 1999; Luna *et al.*, 2011). The polysaccharide, composed of β-1,3-linked glucose residues, is synthesized by a family of PM-localized GSL (GLUCAN SYNTHASE-LIKE) proteins composed of 12 members in *Arabidopsis* (Richmond & Somerville, 2000). So far, different GSLs have been shown to play a role in fertility, cell division and structural reinforcements upon wounding or pathogen infection (Hong *et al.*, 2001; Jacobs *et al.*, 2003; Nishimura *et al.*, 2003; Enns *et al.*, 2005; Ellinger & Voigt, 2014; Cui & Lee, 2016). Among them, GSL5/PMR4 (POWDERY MILDEW

RESISTANT 4) is the main contributor to immunity-related callose depositions (Jacobs *et al.*, 2003; Nishimura *et al.*, 2003). Accordingly, the flg22-triggered increase in callose production is exclusively dependent on GSL5. In contrast, further GSL(s) seem to be marginally involved in the chitosan-induced biosynthesis of callose (Luna *et al.*, 2011).

The role of callose in plant defense is still under debate (Jacobs *et al.*, 2003; Nishimura *et al.*, 2003; Ellinger *et al.*, 2013; Eggert *et al.*, 2014), but recent results indicate the significance of a spatiotemporal regulation of callose synthesis to diminish pathogen penetration success (Eggert *et al.*, 2014; Ellinger & Voigt, 2014).
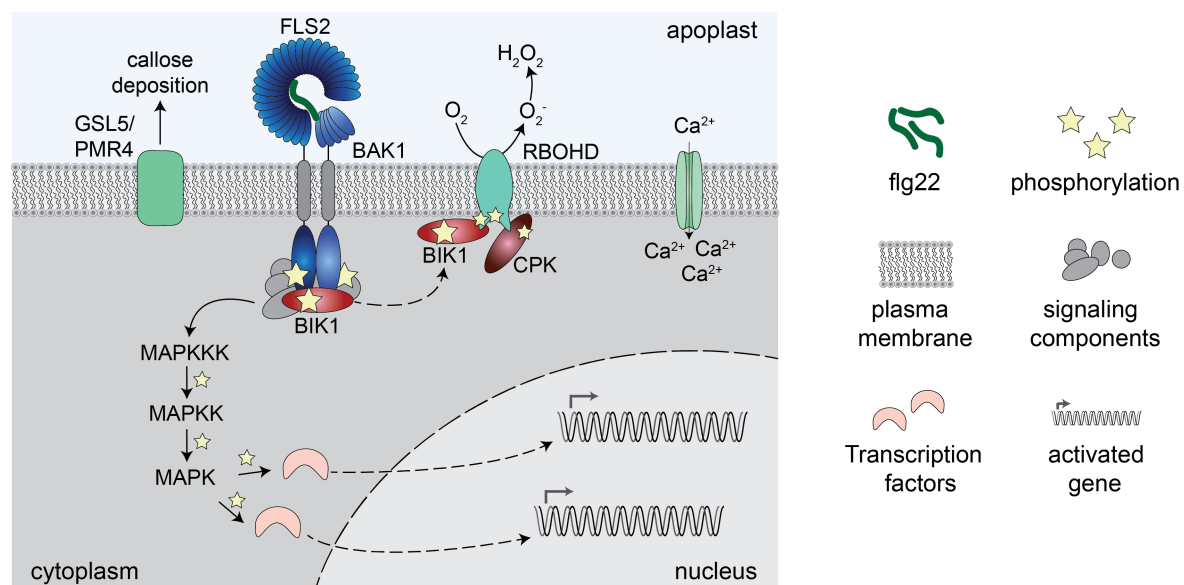
Fig. 2.2 Flg22-induced signaling pathway and defense responses

The binding of flg22 to the receptor-kinase FLS2 results in an immediate complex formation with the co-receptor BAK1 followed by auto- and transphosphorylation events. Subsequently, larger receptor complexes are assembled including several cytoplasmic proteins such as BIK1. Upon phosphorylation, BIK1 dissociates from the complex (dashed line). Within few minutes, first cellular changes occur such as the increased Ca^{2+} influx and the production of reactive oxygen species by RBOHD. The phosphorylation of RBOHD by BIK1 and several CPKs is crucial for its activation. The MAPK signaling cascade transfers the PM-derived signal to downstream components including various transcription factors. These finally ensure the modulation of gene expression. GSL5/PMR4 increasingly produces callose hours after flg22 perception. Components are not to scale.

2.1.3.   Effector-Triggered Immunity

Successful phytopathogens overcome PTI-responses by manipulating plant immunity-related components. Therefore, pathogens secrete a diverse range of effector proteins inside the host cell (Petre & Kamoun, 2014; Green & Mecsas, 2016). The bacterial model strain *Pseudomonas syringae* pv. *tomato* (*Pto*) DC3000, for example, produces 28 well-

expressed effectors and their complete deletion results in a highly diminished infection process (Cunnac *et al.*, 2011; Lindeberg *et al.*, 2012). Effectors target plant proteins involved in all aspects of plant immunity ranging from the MAMP detecting receptors at the PM to MAPKs cascade and transcriptional reprogramming in the nucleus (Büttner, 2016). These manipulations result in an increased pathogen infection success, referred to as effector-triggered susceptibility (ETS) (Jones & Dangl, 2006). However, effectors can be recognized by distinct plant species leading to an effector-triggered immunity (ETI). ETI and PTI share several defense responses, but ETI is extended, more effective and often associated with locally restricted cell death, called hypersensitive response (HR). This evolutionary arm race between plants and phytopathogens is illustrated by the zigzag model proposed by Jones and Dangl (Jones & Dangl, 2006). Responsible for the detection of pathogenic effectors are proteins encoded by plant resistance (R) genes (Flor, 1971). The largest group constitutes a polymorphic family of intracellular nucleotide-binding-LRR (NB-LRR) receptors (Van der Biezen & Jones, 1998). These can either directly interact with effectors or monitor changes in effector target proteins. Regarding the latter, two distinct models can be distinguished. In the "guard" model, the guardees are virulence targets and contribute to the pathogen infection success in plants lacking the corresponding NB-LRR. In contrast, so-called decoys have no function in virulence, but mimic actual effector targets (Cesari *et al.*, 2014; Khan *et al.*, 2016).

One of the best-characterized effector targets is the small, PM-localized protein RIN4 (RPM1 INTERACTING PROTEIN 4). RIN4 is a negative regulator of plant immunity (Kim *et al.*, 2005; Liu *et al.*, 2009; Lee *et al.*, 2015) and is differentially modulated by several effectors including AvrRpm1, AvrB and AvrRpt2 (Mackey *et al.*, 2002; Axtell & Staskawicz, 2003; Mackey *et al.*, 2003). AvrRpm1 and AvrB trigger the phosphorylation of RIN4 that is sensed by the NB-LRR RPM1 (RESISTANCE TO PSEUDOMONAS SYRINGAE PV. MACULICOLA) (Mackey *et al.*, 2002). Both effectors have no obvious kinase activity and therefore rely on plant kinases. Accordingly, AvrB mediates RIN4 phosphorylation by the cytoplasmic kinase RIPK (RPM1-INDUCED PROTEIN KINASE) (Liu *et al.*, 2011). Interestingly, another effector, namely AvrPphB, was shown to cleave RIPK to prevent the activation of RPM1 (Russell *et al.*, 2015). Even AvrRpt2 blocks RPM1-induced ETI by a direct cleavage of RIN4 (Axtell *et al.*, 2003; Chisholm *et al.*, 2005; Kim *et al.*, 2005). Nevertheless, the absence of RIN4 is perceived by the NB-LRR RPS2 (RESISTANCE TO PSEUDOMONAS SYRINGAE 2) and gives rise to ETI (Bent *et al.*, 1994; Mindrinos *et al.*, 1994; Axtell & Staskawicz, 2003; Mackey *et al.*, 2003).

Another important aspect of effector-mediated host manipulations affects various phytohormone-signaling pathways (Kazan & Lyons, 2014). In this regard, salicylic acid (SA), jasmonic acid (JA) and ethylene (ET) are the main defense-associated hormones (Campos *et al.*, 2014; Kumar, 2014; Broekgaarden *et al.*, 2015). While SA simultaneously mediates resistance against biotrophic and susceptibility against necrotrophic pathogens, JA and ET have opposing functions. JA and ET act synergistically to enhance the immunity against necrotrophs and to diminish defense against biotrophs (Thomma *et al.*, 1998; Glazebrook, 2005). Additionally, other hormones including auxin, cytokinin, abscisic acid or gibberellins play a role during plant-pathogen interactions (Shigenaga & Argueso, 2016). The complex interdependencies between different hormones make them worthwhile targets for manipulations by phytopathogens (Kazan & Lyons, 2014). Besides indirect influences of hormone pathways, pathogens can also directly regulate distinct signaling processes. In line with the latter, several *P. syringae* pathovars are able to produce the phytotoxin coronatine (COR), which mimics a bioactive JA conjugate (Mitchell, 1982; Ullrich *et al.*, 1993; Weiler *et al.*, 1994; Bender *et al.*, 1999; Fonseca *et al.*, 2009). Accordingly, COR can activate JA-mediated and suppress SA-related signaling pathways (Geng *et al.*, 2014). As a consequence, COR counteracts MAMP-triggered stomatal closure and is able to reopen stomata to facilitate the bacterial infection process (Melotto *et al.*, 2006; Zheng *et al.*, 2012).

2.2. Compartmentalization of the Plasma Membrane

PMs separate the interior of the cell from abiotic and biotic stresses in the outside environment. Since they harbor PRRs and associated protein complexes, PMs constitute an important factor in plant immunity (Monaghan & Zipfel, 2012). Fascinatingly, the functional compartmentalization of the PM is thought to play an essential role for the efficiency of signaling processes (Urbanus & Ott, 2012).

2.2.1.   The Fluid Mosaic Model

The first generally accepted model of the PM was proposed by Singer and Nicolson back in 1972 (Singer & Nicolson, 1972). In their "fluid mosaic model" the authors described functional membranes as two-dimensional liquids composed of lipids and proteins. Bilayers of homogenously distributed phospholipids served thereby as solvent for freely diffusing

integral and peripheral proteins. Because of the loose PM-attachment of the latter, they were considered as not important for the membrane structure. In contrast, integral proteins were thought to be the crucial determinants for the structural integrity of membranes (Singer & Nicolson, 1972). The idea of a continuous and unconfined lateral diffusion of proteins and lipids along the entire membrane was supported by experimental data obtained by Frye and Edidin (Frye & Edidin, 1970). They demonstrated that a virus-induced fusion of different cell types leads to the total intermixing (mosaicims) of surface antigens of both cells at the PM of the heterokaryonts (Frye & Edidin, 1970).

Nevertheless, even Singer and Nicolson did not exclude the possibility of rare nonrandom distributions in some membranes (Singer & Nicolson, 1972).

However, since then many reports pointed out that the architecture of cell membranes is much more complex than explained and implied by the fluid mosaic model.

2.2.2.   The Picket Fence Model

Several experiments revealed that PM components are not freely diffusing along the entire membrane, but are restricted by the membrane-associated cytoskeleton (MSK) (Kusumi *et al.*, 2005).

In 1980, Sheetz and colleagues showed an increased diffusion coefficient for the TM protein band 3 in erythrocyte mutants lacking the spectrin MSK network (Sheetz *et al.*, 1980). In line with this, a drug-induced enhancement of the network decreases the lateral diffusion of band 3 significantly (Tsuji & Ohnishi, 1986; Tsuji *et al.*, 1988). Even the diffusion rate of the phospholipid DOPE (1,2-dioleoyl-sn-glycero-3-phosphoethanolamine) is dependent on and influenced by the actin MSK. Besides the free diffusion of DOPE within a cytoskeleton-restricted compartment, the lipid is occasionally able to hop to neighboring compartments (Fujiwara *et al.*, 2002). This so-called "hop diffusion" is also reported for TM domain-containing proteins such as the transferrin receptor TfR or the α_2-macroglobuline receptor α2M-R (Sako & Kusumi, 1994; Fujiwara *et al.*, 2002).

These new insights were then summarized in the "picket fence model" of the PM. Therein, the authors postulated the combined influence of the actin-based membrane cytoskeleton (fence) and MSK-associated PM proteins (pickets) on the diffusion rates of PM components (Fujiwara *et al.*, 2002; Kusumi *et al.*, 2005). Only recently, single-particle tracking confirmed comparable compartments sizes for the transferrin receptor TfR and the phospholipid DOPE

that match the mesh size of the actin MSK located within 8.8 nm from the PM (Fujiwara *et al.*, 2016).

2.2.3.   The Lipid Raft Model

Additionally, increasing evidence suggested lateral inhomogeneity of membrane components.

In this regard, a spectroscopic technique revealed the heterogeneous distribution of phospholipids in the microsomal membrane of liver. Thereby, patches of phospholipids differed in their fluidity compared to the surrounding bulk phase (Stier & Sackmann, 1973). Also the lipid asymmetry of the PM contradicts the fluid mosaic model. While sphingomyelins and glycosphingolipids are enriched in the exoplasmic leaflet, phosphatidylserines and phosphatidyethanolamines are more abundant in the cytoplasmic surface of the bilayer (Van Meer, 1989; Devaux & Morris, 2004).

The propensity of sphingolipids and cholesterol to associate and form mobile clusters in the membrane bilayer finally led to the "lipid raft model" postulated by Simons and Ikonen (Simons & Ikonen, 1997). The concept of lipid raft formation is based on the lateral association of sphingolipids via weak interactions between their carbohydrate heads. The gaps caused by their mainly saturated lipid hydrocarbon chains are filled with stabilizing cholesterol molecules. The resulting highly packed, ordered rafts are surrounded by loosely packed, disordered liquids (Simons & Ikonen, 1997). These lipid rafts were thought to mediate platforms for the attachment of GPI-anchored, TM domain-containing or acylated proteins (Skibbens *et al.*, 1989; Brown & Rose, 1992; Casey, 1995; Simons & Ikonen, 1997). Because of their specific protein composition, these clusters were thought to function in membrane trafficking and signaling (Simons & Ikonen, 1997; Lingwood & Simons, 2010).

Since lipid rafts could not be visualized by light microscopy, their existence was mainly supported by the insolubility of membrane components in nonionic detergents (Triton X-100, at 4°C) (Brown & Rose, 1992). The localization of proteins or lipids in detergent-insoluble (DIM) or detergent-resistant membrane (DRM) fractions was considered as evidence for their association with functional rafts (Brown & Rose, 1992; Brown & London, 1998; Schroeder *et al.,* 1998; Mongrand *et al.*, 2004). Doubts have been raised about the validity of this method. Increasing evidence indicated that DRMs do not correspond to functional lipid rafts in living cells (Zurzolo *et al.,* 2003). The differential solubility of distinct components as

well the formation of aggregates and artifacts during the extraction process can influence the localization to DRMs. Additionally, the complex spatiotemporal organization of the PM is not illustrated by DRMs (Heerklotz, 2002; Munro, 2003; Zurzolo *et al.*, 2003; Brown, 2006; Kierszniowska *et al.*, 2009; Tanner *et al.*, 2011). In line with the latter, yeast DRM fractions have been shown to simultaneously contain proteins that are known to localize to distinct, non-overlapping compartments or to be homogeneously distributed at the PM (Malínská *et al.*, 2003; Lauwers *et al.*, 2007; Berchtold & Walther, 2009).

However, a stimulus-induced change in protein solubility could still be of value. It might represent an altered membrane environment of a protein and could possibly indicate its subcellular re-localization (Tanner *et al.*, 2011). Accordingly, the receptor kinase FLS2 and other defense-related proteins were demonstrated to be more abundant in DRMs after flg22 elicitation compared to untreated controls. These results suggest a massive reorganization of the PM during plant immunity (Keinath *et al.*, 2010).

In 2006, biophysicists, biochemists and cell biologists decided collectively to replace the term "lipid raft" with "membrane raft" (Pike, 2006). This term should highlight the contributions of both lipids and proteins to the formation of these raft clusters. They likewise agreed on the definition that membrane rafts are small, heterogeneous and dynamic domains enriched in sterols and sphingolipids. Additionally, larger platforms could be formed through protein-protein and protein-lipid interactions (Pike, 2006).

2.2.4.   The   Hierarchical   Three-Tired   Meso-Scale   Domain Architecture of the Plasma membrane

Even though different models were suggested to explain the specific features of the PM (Simons & Ikonen, 1997; Kusumi *et al.*, 2005), so far no evidence indicates that they might exclude each other (Kusumi *et al.*, 2012). Therefore, Kusumi and colleagues postulated the "three-tiered meso-scale domain architecture" of the PM, combining ideas of the "picket fence" and the "membrane raft" hypotheses (Kusumi *et al.*, 2012).

In the first tier, the membrane cytoskeleton "fence" and associated protein "pickets" subdivide the PM into 40-300 nm compartments. PM components can overcome these barriers by non-Brownian hop diffusion occurring every 1 - 50 ms. But within these compartments, lipids and proteins undergo simple Brownian diffusion and show diffusion

coefficients that are comparable to those measured in artificial membranes (Lindblom *et al.*, 1981; Lee *et al.*, 1993; Ladha *et al.*, 1996; Murase *et al.*, 2004; Samiee *et al.*, 2006; Kusumi *et al.*, 2012). These results suggest that the fluid mosaic model is still suitable for molecular events occurring within small areas of the PM (Kusumi *et al.*, 2012).

In the second tier, "raft domains", enriched in cholesterol, glycosphingolipids and GPI-anchored proteins, enable an additional compartmentalization of the PM into 2 – 20 nm-sized areas. Of special importance is the differentiation between raft domains before and after stimulation. While non-stimulated rafts are highly dynamic and often short in lifetime, stimulated rafts are considered to be larger and laterally stable. This is achieved by activated raft-associated receptors forming oligomers and assembling additional cholesterol and saturated lipids to the receptor-cluster rafts (Janes *et al.*, 1999; Suzuki *et al.*, 2007; Kusumi *et al.*, 2012).

In the third tier, dynamic protein complex domains enable an additional differentiation in 3 - 10 nm compartments. They are exclusively formed by protein-protein interactions and can be divided into three distinct types: complexes based on oligomers of membrane-anchored proteins, induced by scaffold proteins or mediated by coat proteins (Kusumi *et al.*, 2012). Interestingly, the latter domain can enlarge up to 100 nm (Parton & Simons, 2007). These higher order protein complexes are considered to be important for many cellular processes as signaling or membrane trafficking.

2.2.5.   The Cell Wall-Plasma Membrane-Cytoskeleton Continuum

The different models of the PM described above are mainly based on results obtained in animal cells or artificial membranes. However, besides many similarities, also several differences were found between micro-domains in plant and animal PMs. While the latter are reported to be small and highly dynamic rafts, the majority of plant micro-domains are thought to be larger and laterally stable over time (Tanner *et al.*, 2011; Malinsky *et al.*, 2013). In contrast to animal, plant PMs are not only influenced by the attached cytoskeleton, but also by the surrounding CW. All three components constitute the cell surface continuum of plants and form the interface between the cellular inside and the outside environment (Baluška *et al.*, 2003; McKenna *et al.*, 2014; Liu *et al.*, 2015a; Liu *et al.*, 2015b). The close contact between the PM and the CW is mainly caused by the tremendous turgor pressure within the cell (Coster *et al.*, 1977; Beauzamy *et al.*, 2014). The mechanically strong CW

constrains the turgor pressure and protects the cell against rupture. It additionally allows a high extensibility during cell expansion and growth. Both opposing features are feasible due to their heterogeneous composition and a dynamic remodeling in a spatiotemporal-defined manner (Burton *et al.*, 2010; Peaucelle *et al.*, 2012; Cosgrove, 2016). Many of these processes are regulated by interdependencies between the CW, the PM and the cytoskeleton.

Cellulose fibrils, the main component of the CW, are synthesized at the PM by the cellulose synthase complex (CSC). The CSC is composed of hexagonally arranged cellulose synthases (CesAs) and additionally associated proteins (Mueller *et al.*, 1976; Mueller & Brown, 1980; McFarlane *et al.*, 2014). During cellulose synthesis the complex moves along cortical microtubules (Paredez *et al.*, 2006; Paredez *et al.*, 2008), while its localization to and maintenance at the PM is influenced by actin (Sampathkumar *et al.*, 2013). In this regard, the protein POM2/CSI1 (CELLULOSE SYNTHASE-INTERACTIVE PROTEIN 1) was demonstrated to play a role in mediating the link between the CSC and the microtubules by binding to both components (Gu *et al.*, 2010; Bringmann *et al.*, 2012; Lu *et al.*, 2012a). In addition, only recently two PM-localized units of the CSC, CC1 and 2 (COMPANION OF CELLULOSE SYNTHASE 1 and 2), were reported to interact with CSC and microtubules. Interestingly, the proteins were shown to promote the re-assembly of microtubules after their salt stress-induced depolymerization (Endler *et al.*, 2015). Together these data clearly highlight the impact of the PM and the cytoskeleton on the plant CW by influencing the cellulose synthesis under normal and under stress conditions.

Conversely, the CW affects the localization and dynamic of PM-localized proteins (Feraru *et al.*, 2011; Martinière *et al.*, 2012). In this regard, the basal localization of the polar auxin transporter PIN1 (PIN-FORMED 1) was reported to be highly reduced in various *cesa* mutants (Feraru *et al.*, 2011). Additionally, the maintenance of apical and basal polarity of PIN2 and PIN1 was abolished in protoplasts, respectively. Even the lateral mobility of PIN2 was highly increased upon plasmolysis or treatment with the cellulose synthesis inhibitor isoxaben. These results might be explained by a direct connection between polar PM domains and the CW (Feraru *et al.*, 2011).
Accordingly, several proteins have been shown to physically link the PM and the CW by various mechanisms (Martinière *et al.*, 2011; Liu *et al.*, 2015a; Kohorn, 2016).
The RGD (Arg-Gly-Asp)-motif is mainly known to play a role in cell adhesion mediated by different integrin receptors in animals (Ruoslahti, 1996). However, different studies indicate

that even plants have RGD-recognizing proteins that could be involved in anchoring the CW to the PM (Schindler *et al.,* 1989; Katembe *et al.,* 1997; Canut *et al.,* 1998; Senchou *et al.,* 2004; Gouget *et al.,* 2006). The legume-like lectin receptor kinase LecRK-I.9, for example, was shown to play a role in the CW-PM continuum, probably via binding to endogenous RGD-containing peptides (Bouwmeester *et al.,* 2011). In addition, LecRK-I.9 was demonstrated to interact with the *Phytophthora infestans* RXLR-dEER effector IPI-O via the RGD motif of IPI-O (Gouget *et al.,* 2006). During pathogen infection, the competition between IPI-O and plant peptides leads to a reduced PM-CW adhesion that results in an increased susceptibility of the plant (Gouget *et al.,* 2006; Bouwmeester *et al.,* 2011). These examples not only illustrate the interdependency between the PM and the CW, they also highlight its importance during plant-pathogen-interactions.
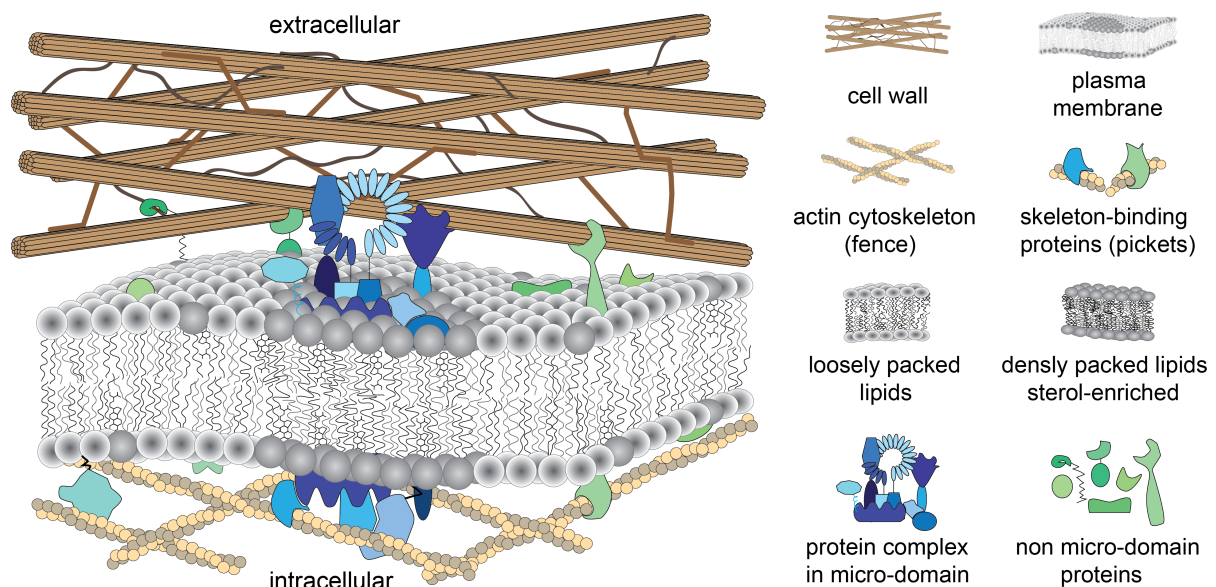
Fig. 2.3 Determinants for the compartmentalization of plant plasma membranes

Proteins and lipids are not freely diffusing along the entire PM. Their mobility is restricted by the intracellular membrane-associated actin cytoskeleton (fence) and associated proteins (pickets). Specific lipid compositions and lipid-protein interactions mediate another tier of compartmentalization. These membrane rafts are enriched in sterols. Even protein-protein interactions contribute to the compartmentalization. Additionally, the CW influences the dynamics of PM components. Together the CW, the PM and the cytoskeleton form the cell surface continuum of plants. Components are not drawn to scale.

2.2.6.   Plant Membrane Compartments

An increasing number of reports shows that several plant proteins are heterogeneously distributed at the PM and localize to distinct sub-compartments. However, the appearance of these domains can be highly divergent with respect to size, pattern, density and mobility (Sutter *et al.*, 2006; Lherminier *et al.*, 2009; Lefebvre *et al.*, 2010; Haney *et al.*, 2011; Demir *et al.*, 2013; Zhang *et al.*, 2013; Barberon *et al.*, 2014; Jarsch *et al.*, 2014; Luschnig & Vert, 2014; Wang *et al.*, 2015b; Mao *et al.*, 2016).

Cell polarity is known to play an important role for diverse cellular pathways, including cell-to-cell communication and directional transport of hormones or other small molecules (Wiśniewska *et al.*, 2006; Takano *et al.*, 2010; Barberon *et al.*, 2014; Mao *et al.*, 2016). Especially for many auxin-regulated developmental processes, the formation, maintenance and redirection of auxin concentration gradients are crucial (Benjamins & Scheres, 2008; Kleine-Vehn & Friml, 2008). These flexible rearrangements can be achieved by a variable polar distribution of PIN auxin efflux carrier at the cell surface. Apical, basal, inner lateral and outer lateral domains can be distinguished. Interestingly, the target domains of PINs are not only dependent on the PIN protein, but additionally on the cell type and distinct stimuli (Gälweiler *et al.,* 1998; Müller *et al.,* 1998; Friml *et al.*, 2002a; Friml *et al.*, 2002b; Wiśniewska *et al.*, 2006; Kleine-Vehn & Friml, 2008). Accordingly, the polarity of PINs is not based on polar transport of newly synthesized proteins, but is mainly caused by subsequent, spatial-defined recycling processes (Kleine-Vehn *et al.*, 2008; Kleine-Vehn *et al.*, 2011). In addition, their phosphorylation status (Friml *et al.*, 2004; Michniewicz *et al.*, 2007; Huang *et al.*, 2010; Zhang *et al.*, 2010), the CW (Feraru *et al.*, 2011) as well as sterol and lipid compositions (Willemsen *et al.*, 2003; Men *et al.*, 2008) influence their subcellular localization.

Besides continuously existing domains, other PM compartments can emerge upon a certain stimulus, such as the perception of phytopathogens (reviewed in Faulkner, 2015).
At the site of attempted penetration by filamentous pathogens, dome-shamed CW appositions, so-called papillae, are formed (Aist, 1976). These papillae are enriched in callose, cellulose and arabinoxylan as well as ROS, phenolic compounds and silicon (Aist, 1976; McLusky *et al.*, 1999; Chowdhury *et al.*, 2014). The formation of papillae is accompanied by several cellular modulations including polarization of organelles and rearrangements of the cytoskeleton below the penetration site (Gross *et al.*, 1993; Freytag *et*

al., 1994; Kobayashi *et al.,* 1994; Schmelzer, 2002). In addition, the clustering of sterols in the associated PMs results in raft-like features at the site of attempted invasion (Bhat *et al.,* 2005). Accordingly, several defense-related proteins have been shown to focally accumulate around the papillae, including PEN (PENETRATION) 1, 2, 3, SNAP33 (SOLUBLE N-ETHYLMALEIMIDE-SENSITIVE FACTOR ADAPTOR PROTEIN 33), VAMP722 (VESICLE-ASSOCIATED MEMBRANE PROTEIN 722) and ATL31 (TOXICOS EN LEVADURA 31) (Assaad *et al.,* 2004; Bhat *et al.,* 2005; Stein *et al.,* 2006; Kwon *et al.,* 2008; Meyer *et al.,* 2009; Underwood & Somerville, 2013; Maekawa *et al.,* 2014). All these rearrangements enable the formation of an induced, local defense platform against pathogen invasion.

Adapted pathogens, however, are able to overcome this barrier and subsequently develop specialized feeding structures within the plant cell. These so-called haustoria are enclosed by a plant-derived extra-haustorial membrane (EHM) (O'Connell & Panstruga, 2006). Even though the EHM is continuous with the PM, their appearance as well as their protein composition can be different (Gil & Gay, 1977; Koh *et al.,* 2005; Lu *et al.,* 2012b). Some PM marker proteins such as PIP1;4 (PLASMA MEMBRANE INTRINSIC PROTEIN 1;4) and ACA8 have been shown to be excluded from the EHM surrounding haustoria of various fungi and oomycetes (Lu *et al.,* 2012b). Contrary, PEN1, FLS2 and PDLP1 (PLASMODESMATA LOCATED PROTEIN 1) displayed a differential EHM-localization dependent on the invading pathogen (O'Connell & Panstruga, 2006; Lu *et al.,* 2012b; Caillaud *et al.,* 2014). This diversity suggests a specific targeting of PM proteins to the EHM rather than lateral diffusion or general recycling mechanisms. Accordingly, secretory vesicles and endosomal compartments accumulate around haustoria (Lu *et al.,* 2012b). In line with this, VAMP721/722 vesicles have been demonstrated to be essential for the targeted secretion of RPW8.2 (RESISTANCE TO POWDERY MILDEW 8.2) to the EHM of *Golovinomyces orontii* (Kim *et al.,* 2014). Wang and colleagues reported that the core EHM targeting signal, composed of the N-terminal TM-domain and two arginine (R)- or lysine (K)-enriched short motifs, is crucial and sufficient for the targeting of RPW8.2 to the EHM (Wang *et al.,* 2013). There, the unconventional non-NB-LRR type resistance protein confers a broad-spectrum resistance to divers species of powdery mildew fungi by the local induction of SA-dependent defense responses such as accumulation of callose and ROS (Xiao *et al.,* 2001; Wang *et al.,* 2009).

In addition to directional targeting, also a spatiotemporally regulated promoter activity can influence the subcellular localization of proteins such as the *Medicago truncatula* phosphate transporter MtPT4 (Pumplin *et al.,* 2012). *MtPT4* is exclusively expressed in roots colonized by arbuscular mycorrhizal (AM) fungi and, more precisely, in arbuscule-containing cells

(Harrison *et al.*, 2002). Arbuscules are highly branched, fungal structures that are known to be the sites of nutrient exchange during AM symbiosis (reviewed in Parniske, 2008). Accordingly, MtPT4 localizes specifically to the plant-derived periarbuscular membrane (PAM) surrounding fungal arbuscules (Harrison *et al.*, 2002). Interestingly, the PAM-localization of MtPT4 is dependent on the activity of its native promoter, since a continuous expression by a 35S promoter results in a mis-localization to the endoplasmic reticulum (Pumplin *et al.*, 2012). Additionally, several PM-localized transporters can be re-directed to the PAM when expressed from the PT4 promoter. Therefore, a strictly regulated expression coincident with arbuscule formation seems to be critical for the polar targeting of MtPT4 to the PAM.

Altogether, these data emphasize that specialized membrane compartments enable spatiotemporal-defined cellular responses during plant-microbe-interactions.

In addition to these rather large, locally restricted compartments, punctate micro-domains are distributed along the entire PM. Micro-domain-localized proteins have been shown to participate in different signaling pathways including hormone signaling, immunity and symbiosis (Lherminier *et al.*, 2009; Haney *et al.*, 2011; Demir *et al.*, 2013; Wang *et al.*, 2015b; Nagano *et al.*, 2016).

In 2013, Demir and colleagues reported that the calcium dependent protein kinase CPK21 is associated with DRMs in a sterol-dependent manner (Demir *et al.*, 2013). CPK21 was previously shown to be involved in ABA (abscisic acid)-signaling processes together with the phosphatase ABI1 (ABSCISIC-ACID INSENSITIVE 1) and the anion channel SLAC1 (SLOW ANION CHANNEL 1) (Geiger *et al.*, 2010). Additionally, CPK21 is able to phosphorylate and consequently activate the anion channel SLAH3 (SLAC1 HOMOLOG 3) in a Ca^{2+} and ABA-dependent manner (Geiger *et al.*, 2011). The co-expression of CPK21 with SLAH3 resulted in a re-localization of the latter into DRMs and in a complex formation in AtREM1.3-labeled micro-domains (Demir *et al.*, 2013). Intriguingly, the additional expression of ABI1 prevents the domain localization of the SLAH3/CPK21 complex and abolishes the activation of SLAH3. These results highlight the importance of micro-domains for the SLAH3-mediated anion transport in ABA signaling (Demir *et al.*, 2013).

In previous studies, the subcellular localization of individual proteins was investigated predominantly. The variable appearance of these sub-compartments as well as the involvement of micro-domain-localized proteins in distinct signaling pathways suggested the existence of multiple compartments. However, only recently the co-existence of various

micro-domains was proven in PMs of *Nicotiana benthamiana* and *Arabidopsis*. A plethora of diverse micro-domains was identified by the use of marker proteins of the multigene remorin family (Jarsch *et al.*, 2014).

2.3. Remorin Proteins

Remorins constitute a plant-specific multigene family that is present in all land plants and comprises 16 members in *Arabidopsis*. Based on their full-length amino acid sequences, they can be subdivided into six distinct groups (Raffaele *et al.*, 2007). In general, remorin proteins are characterized by their canonical structure. While their C-terminal regions are highly conserved, their N-terminal parts are extremely variable or even absent (group 3) (Raffaele *et al.*, 2007). Their C-terminal region contains a coiled-coil domain and is thought to be the main contributor for the *in vitro* assembly of oligomeric filamentous structures (Bariola *et al.*, 2004; Marín *et al.*, 2012; Yue *et al.*, 2014). In addition to homooligomers, several remorins are able to form heterodimers with closely related proteins (Marín *et al.*, 2012; Jarsch, 2014; Son *et al.*, 2014). However, also the N-terminal region influences the interaction among remorins and also with other proteins (Marín *et al.*, 2012; Tóth *et al.*, 2012). The N-terminal part is intrinsically disordered (ID) and therefore lacks any ordered secondary structure under physiological conditions (Raffaele *et al.*, 2007; Marín & Ott, 2012). Interestingly, binding to other proteins or post-translational phosphorylation events can induce the differential folding of ID segments (Iakoucheva *et al.*, 2004; Wright & Dyson, 2009). In line with the latter, the majority of all identified phospho-sites in remorin proteins are located in their disordered N-terminal region (Marín & Ott, 2012). Since so-called "hub" proteins often contain longer ID segments (Dunker *et al.*, 2005), it is likely that remorins act as molecular scaffolds and play a role for the assembly of active signaling platforms at the PM (Jarsch & Ott, 2011).

Remorin proteins do not contain a TM domain, but are attached to the inner leaflet of the PM through a combination of S-acylation, induced folding of the C-terminal anchor and protein-protein or protein-lipid interactions (Perraki *et al.*, 2012; Konrad *et al.*, 2014). Even though remorins were considered as micro-domain marker proteins for several years (Raffaele *et al.*, 2009; Lefebvre *et al.*, 2010; Demir *et al.*, 2013), the diversity of remorin-labeled compartments was shown only recently by investigating the subcellular localization of 15 *Arabidopsis* remorin proteins (Jarsch *et al.*, 2014). The majority localizes to large, laterally

stable domains that can differ in size, shape and distribution. In contrast, two group 1 remorins, AtREM1.2 and AtREM1.3 (hereafter REM1.2 and REM1.2), are predominantly targeted to rather small and highly mobile micro-domains. However, they are occasionally organized in larger, immobile compartments dependent on the tissue and the developmental stage, indicating a dynamic localization pattern (Jarsch *et al.*, 2014).

In addition, detailed co-expression analyses revealed a diverse range of coexisting domains at the PM. Interestingly, closely related remorins show an increased tendency for co-localization compared to less related proteins, suggesting a functional compartmentalization of the PM (Jarsch *et al.*, 2014).
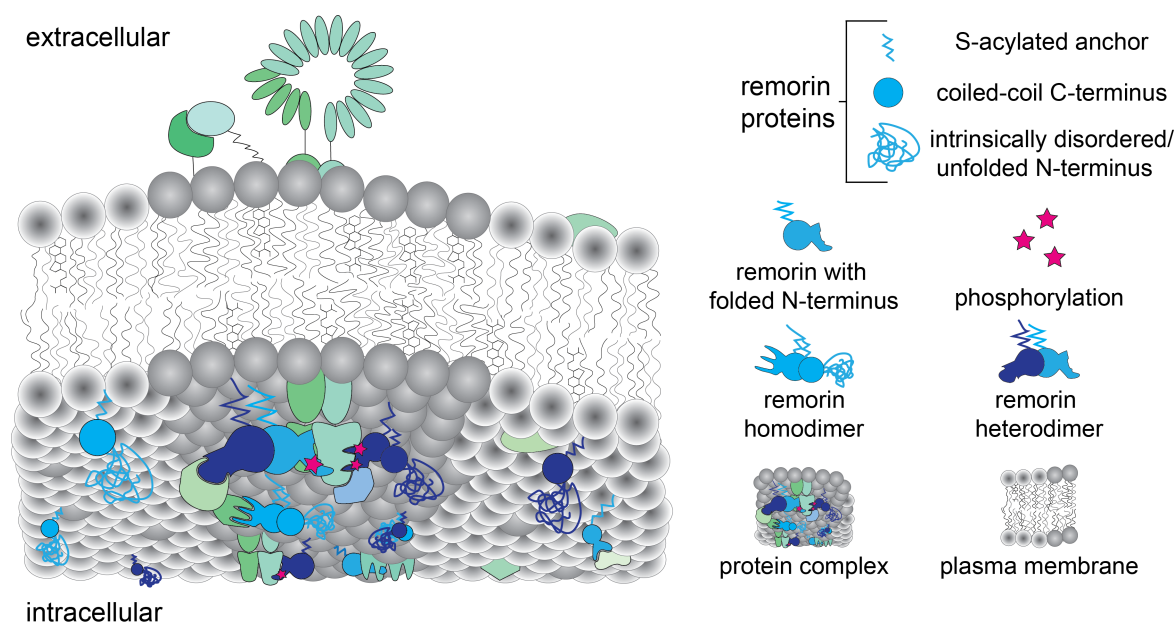
Fig. 2.4 Model of an active signaling platform mediated by scaffolding remorin proteins

Remorin proteins localize to the cytoplasmic leaflet of the PM via an S-acylated C-terminal anchor. Their localization to micro-domains is dependent on the sterol content of the PM. Remorins can form homooligomeric structures and heterodimeric complexes mainly mediated by their conserved C-terminal region. The intrinsically disordered N-terminal region has a stabilizing function and can undergo folding upon interaction or phosphorylation events. Remorins are hypothesized to act as scaffold proteins that play a role in the assembly of higher order protein complexes and the formation of active signaling hubs. Components are not drawn to scale.

So far, remorins of different species have been reported to participate in various abiotic and biotic stress-induced responses. Transcripts of the Foxtail Millet (*Setaria italica*) *SiREM6* and the Mulberry (*Morus indica*) *MiREM* are significantly up-regulated upon ABA treatment and

salt stress. Accordingly, the heterologous overexpression of both proteins confers an increased tolerance to salinity in *Arabidopsis* (Checker & Khurana, 2013; Yue *et al.*, 2014). Also the rice OsREM4.1 is up-regulated upon ABA treatment resulting in a negative regulation of BR signaling. Therefore, OsREM4.1 is assumed to mediate the interlinking of BR and ABA signaling pathways (Gui *et al.*, 2016).

In addition to abiotic responses, several remorins have been shown to play a role during beneficial as well as harmful plant-microbe-interactions.

The group 2 SYMREM1 (SYMBIOTIC REMORIN 1), for example, is involved in root nodule symbiosis between rhizobium bacteria and legumes. Accordingly, *SYMREM1* is exclusively expressed under symbiotic conditions, localizes to the plant-derived symbiosome membrane and is involved in the assembly of a symbiosis-related micro-domain at the PM (Lefebvre *et al.*, 2010; Tóth *et al.*, 2012; Stratil, 2016).

The *Zea mays* group 6 remorin ZmREM6.3 was reported to participate in quantitative disease resistance in maize (Jamann *et al.*, 2016). Furthermore, AtREM4.1 and AtREM4.2 play a negative role in plant defense, since double mutants display a reduced susceptibility against two geminiviruses (Son *et al.*, 2014). In contrast, the potato (*Solanum tuberosum*) StREM1.3 is a positive player in plant immunity against the *Potato virus X* (PVX) (Raffaele *et al.*, 2009). StREM1.3 accumulates at plasmodesmata (PD) and interacts with the viral, PD-localized movement protein TGBp1 (TRIPLE GENE BLOCK PROTEIN 1). Consequently, the ability of TGBp1 to increase the permeability of PD is obstructed and the cell-to-cell movement of PVX is reduced (Raffaele *et al.*, 2009; Perraki *et al.*, 2014). Even the rice remorin protein GSD1 (GRAIN SETTING DEFECT 1) was demonstrated to be important for the regulation of PD conductance during grain setting (Gui *et al.*, 2014), suggesting a common feature for several remorin proteins. StREM1.3 was additionally shown to act as a susceptibility factor in the interaction between *Nicotiana benthamiana* and *Phytophthora infestans*. Similar results were also obtained for the *Solanum lycopersicum* ortholog SiREM1.2 in tomato (Bozkurt *et al.*, 2014).

Also the *Arabidopsis* group 1 remorins REM1.2 and REM1.3 are assumed to be involved in plant immunity, even though a direct role has not been demonstrated so far (reviewed in Jarsch & Ott, 2011). Interestingly, both remorins belong to the 10 % most highly and ubiquitously expressed genes in *Arabidopsis* (Raffaele *et al.*, 2007). They are regulated upon pathogen infection and in an effector-triggered manner (Coaker *et al.*, 2004; Widjaja *et al.*, 2009). Moreover, flg22 treatments result in a differential phosphorylation pattern and their enrichment in DRMs (Benschop *et al.*, 2007; Keinath *et al.*, 2010). In addition, REM1.2

is phosphorylated upon expression of AvrRPM1 in an RPM1-dependent manner (Widjaja *et al.*, 2009). In line with this result, REM1.2 was demonstrated to interact with RIN4 (Liu *et al.*, 2009). Only recently, an interaction was shown between REM1.3 and HIR1 (HYPERSENSITIVE INDUCED REACTION 1), a protein assumed to participate in ETI-induced cell death. Even REM1.2 associates to the same complex at the PM, indicating the assembly of an immunity-related micro-domain (Lv *et al.*, 2017). Taken together, theses results suggest a role for REM1.2 and REM1.3 in plant immunity.

2.4. Aims of the Study

The variety of co-existing, remorin-labeled micro-domains suggests the functional compartmentalization of plant plasma membranes. Functioning as putative molecular scaffold that facilitate higher-order protein complex assemblies *in vivo*, remorin proteins are promising candidates for the identification of new signaling components involved in diverse cellular pathways. As group 1 remorins are presumed to play a role in plant defense-related signal transductions, REM1.2 was used as a bait to identify novel receptor-like kinases (RLKs) with a putative function in plant immunity.

One RLK, named RICKY1 (REMORIN INTERCTING KINASE IN YEAST 1), was found to specifically interact with REM1.2.

In this work, I aimed to functionally characterize the so far unknown RLK RICKY1 using a modern range of biochemical, cell biological and phenotypic methods.

I intended to examine the biological role of RICKY1, its localization pattern and the interdependency between RICKY1 and group 1 remorins.

I hypothesize that RICKY1 is a new player in plant immunity-related signaling pathways and associated with membrane micro-domains.

3. Results

3.1. Identification of New Interaction Partners of REM1.2

Several studies identified specific interactions between remorin proteins and receptor-like kinases at the PM of various plant species. These RLKs are involved in different cellular pathways including root nodule symbiosis, plant immunity and hormone signaling (Lefebvre *et al.*, 2010; Tóth *et al.*, 2012; Son *et al.*, 2014; Gui *et al.*, 2016). Remorins, as proposed scaffold proteins, seem to play a role during protein complex formation and the assembly of active signaling hubs to facilitate an efficient signal transduction (Stratil, 2016). This model provides the opportunity to elucidate complex signaling pathways by identifying new interaction partners of remorin proteins. As different studies indicate a role for group 1b remorins during plant defense (reviewed in Jarsch & Ott, 2011), AtREM1.2 was used in the GAL4 yeast two-hybrid (Y2H) system to identify new components of this pathway (Jarsch, 2014).

This method is based on the modular properties of many eukaryotic transcription factors (Hope & Struhl, 1986; Keegan *et al.*, 1986). The activation domain (AD) and the binding domain (BD) of GAL4 can be fused separately to two proteins of interest. If these proteins interact, the activation domain of GAL4 is recruited to the promoter of the *HIS3* reporter gene and as a consequence the gene expression is initiated. *HIS3* codes for an enzyme involved in the biosynthesis of histidine, whereby the histidine auxotrophy of the yeast strain PJ69-4a can be overcome (James *et al.*, 1996).

A targeted GAL4 Y2H screen was performed with REM1.2 against a library containing the cytoplasmic domains of RLKs putatively involved in plant immunity (provided by Birgit Kemmerling, University of Tübingen). Out of 55 clones only At1g53440 was able to specifically interact with REM1.2 and was called REMORIN INTERCTING KINASE IN YEAST 1 or short RICKY1.

The assay was repeated independently to verify the results obtained during the screen. Therefore, the cytosolic domain (CD) of RICKY1, fused to the binding domain of GAL4, was co-transformed with an AD-fused REM1.2 into PJ69-4a yeast cells. Both proteins were able to interact, as the transformants had the ability to grow on selective media lacking histidine (Fig. 3.1A).

Subsequently, the putative interaction of RICKY1 with REM1.3 was analyzed to test the specificity of the interaction with REM1.2. Yeast cells co-transformed with RICKY1 CD and REM1.3 were not able to grow on selective media. This indicates that the interaction of RICKY1 with REM1.2 is very specific in yeast. Additionally, this negative result showed that RICKY1 has no auto-activation ability.

As it is known that remorins are able to form homodimers (Bariola *et al.*, 2004), the interactions of REM1.2 with REM1.2 and REM1.3 with REM1.3 were used as positive controls. Both co-transformations led to yeast growth on selective media, also confirming the functionality of the REM1.3 construct.

Finally, proteins were extracted from the co-transformed yeast cells to verify that negative interaction results are not the consequence of lacking protein expression. All recombinant proteins could be detected with tag-specific antibodies (Fig. 3.1B).
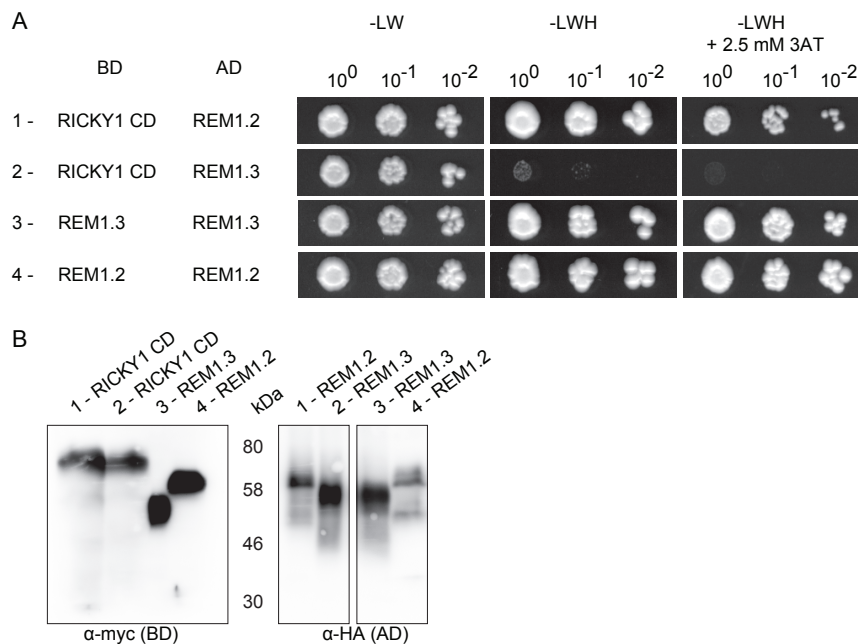
Fig. 3.1 The cytosolic domain of RICKY1 interacts specifically with REM1.2 in yeast

(A) GAL4 yeast two-hybrid (Y2H) assay of the cytosolic domain (CD) of RICKY1 with REM1.2 and REM1.3. Remorins were fused to the activation domain (AD) and RICKY1 was fused to the binding domain (BD) of GAL4. Transformants were grown on control medium (-LW) and selective medium (-LWH +/- 2.5 mM 3-AT) in three consecutive dilutions. The interactions of REM1.2/REM1.2 and REM1.3/REM1.3 were used as positive controls. L = leucine, W = tryptophan, H = histidine, 3-AT = 3-amino-1,2,4-triazole. (B) Expression analysis in yeast using immunoblot analysis. AD-fused proteins were visualized with an HA antibody and BD-fused proteins with a myc antibody.

3.2. Characterization of the Leucine-Rich Repeat Receptor-Like Kinase RICKY1

As RICKY1 was a protein with unknown function, an *in silico* analysis was performed to get a first indication of its putative function. The *RICKY1* gene spans 5604 bp and consists of 23 exons and 22 introns. Its locus is embedded in a cluster comprising three closely related genes on chromosome 1. At1g53420, At1g53430 as well as *RICKY1* encode LRR-RLKs belonging to the subgroup LRR VIII-2 based on the sequence of their kinase domains (Shiu & Bleecker, 2001b). Including the extracellular sequences in addition, 13 RLKs are assigned to this subgroup ((Gou *et al.*, 2010); Fig. 3.2A). The extracellular region of RICKY1 is predicted to contain a signal peptide, eleven LRRs and a malectin domain (MD) (Fig. 3.2B). This domain shows a high sequence similarity to the animal protein malectin, which was identified in *Xenopus laevis* for the first time (Schallus *et al.*, 2008). Malectin is an ER-membrane located protein that is specifically able to bind di-glycosylated glycans (Schallus *et al.*, 2010). It has been shown to participate in quality control mechanisms in the ER (Chen *et al.*, 2011; Galli *et al.*, 2011; Qin *et al.*, 2012). Additionally, RICKY1 contains a predicted transmembrane (TM) domain and a cytoplasmic protein kinase domain.

Two T-DNA insertion lines in the Col-0 background were obtained to investigate the role of RICKY1. Homozygous plants were identified (see 5.5.8) and the actual T-DNA insertion site was determined by sequencing. Accordingly, *ricky1-1* plants carry the T-DNA in their 21st exon and *ricky1-2* in the promoter region of *RICKY1,* 129 bp upstream of the ATG (Fig. 3.2C; Hofer, 2012). qPCR analyses were performed in 14-day-old seedlings to examine the *RICKY1* transcript in both mutant lines. After normalization to the housekeeping gene *Ubiquitin C*, both *ricky1* mutants showed a highly significant reduction in transcript level compared to Col-0 (Fig. 3.2D). Both knock-down mutants were used for further phenotypic analyses.
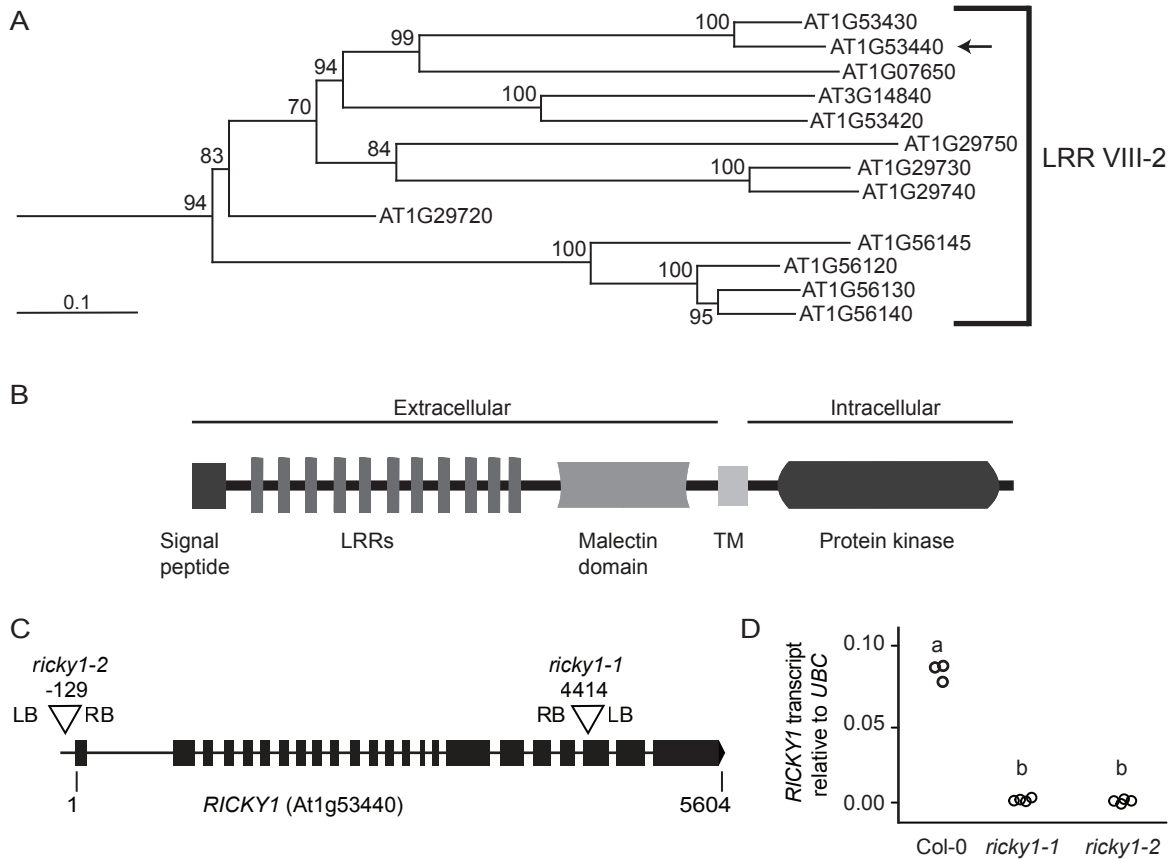
Fig. 3.2 *In silico* and transcriptional analysis

(A) Phylogenetic tree of LRR VIII-2 RLKs based on the full-length amino acid sequences analyzed by the Neighbor-joining method. Bootstrap values are given in percent. The scale bar represents the number of amino-acid substitutions per site. The arrow indicates RICKY1 (modified from (Gou *et al.*, 2010)). (B) Predicted protein structure of RICKY1 (UniProtKB/Pfam30.0). The RLK contains a signal peptide, eleven leucine-rich repeats (LRRs) and a malectin domain in its extracellular part and an intracellular protein kinase domain. Domain sizes are not to scale. TM = transmembrane domain. (C) Schematic view of the T-DNA insertion sites in the mutant lines *ricky1-1* and *ricky1-2* (see Hofer, 2012). The position of the T-DNAs (triangles) refers to the corresponding ATG (1). The orientation of the T-DNAs is indicated by LB (left border) and RB (right border). Exons are represented as black boxes, intros as black lines. (D) qPCR analysis of the *RICKY1* transcript in 14-day-old Col-0 and homozygous *ricky1* seedlings. The expression of *RICKY1* was normalized to *Ubiquitin C* (*UBC*). The transcript of *RICKY1* was highly down-regulated in both mutant backgrounds (n = 3 – 4). Statistical significance was assessed using one-way analysis of variance (ANOVA) followed by a Tukey HSD test (P≤ 0.001).

3.2.1.   Investigating a Putative Role of RICKY1 in Plant Development

In 2001, Shiu and Bleeker identified over 600 receptor-like kinases in the genome of *Arabidopsis* (Shiu & Bleecker, 2001b). So far, only a minority has been characterized. Among them, most RLKs are either involved in different developmental processes or play a role in biotic and abiotic stress responses. Some RLKs have been also shown to have dual functions (reviewed in Li & Tax, 2013; Osakabe *et al.*, 2013; Fan *et al.*, 2016).

3.2.1.1.   RICKY1 is not involved in plant development

First of all, it was investigated if the reduced RICKY1 levels have an impact on the development and growth of *ricky1* mutant plants. Therefore, different developmental stages were examined and compared to Col-0. Early stages were analyzed on seedlings grown on ½ MS plates (supplemented with 1 % sucrose) under long-day conditions. There was no significant difference between the lines regarding germination rates (Fig. 3.3A) and rosette diameters 14 days after germination (Fig. 3.3B). Later stages were analyzed on adult plants grown on soil under long-day conditions. Both mutant lines did not display an altered rosette diameter at floral transition (Fig. 3.3C). The transition from the vegetative to generative state was defined as the time point of shoot emergence. Also relating to primary bolt length (Fig. 3.3D), number of side bolts (Fig. 3.3E) and number of secondary bolts (Fig. 3.3F) the mutants did not show significant differences to the wild type. These data indicate that the absence of RICKY1 has no obvious effect on the development under normal growth conditions.
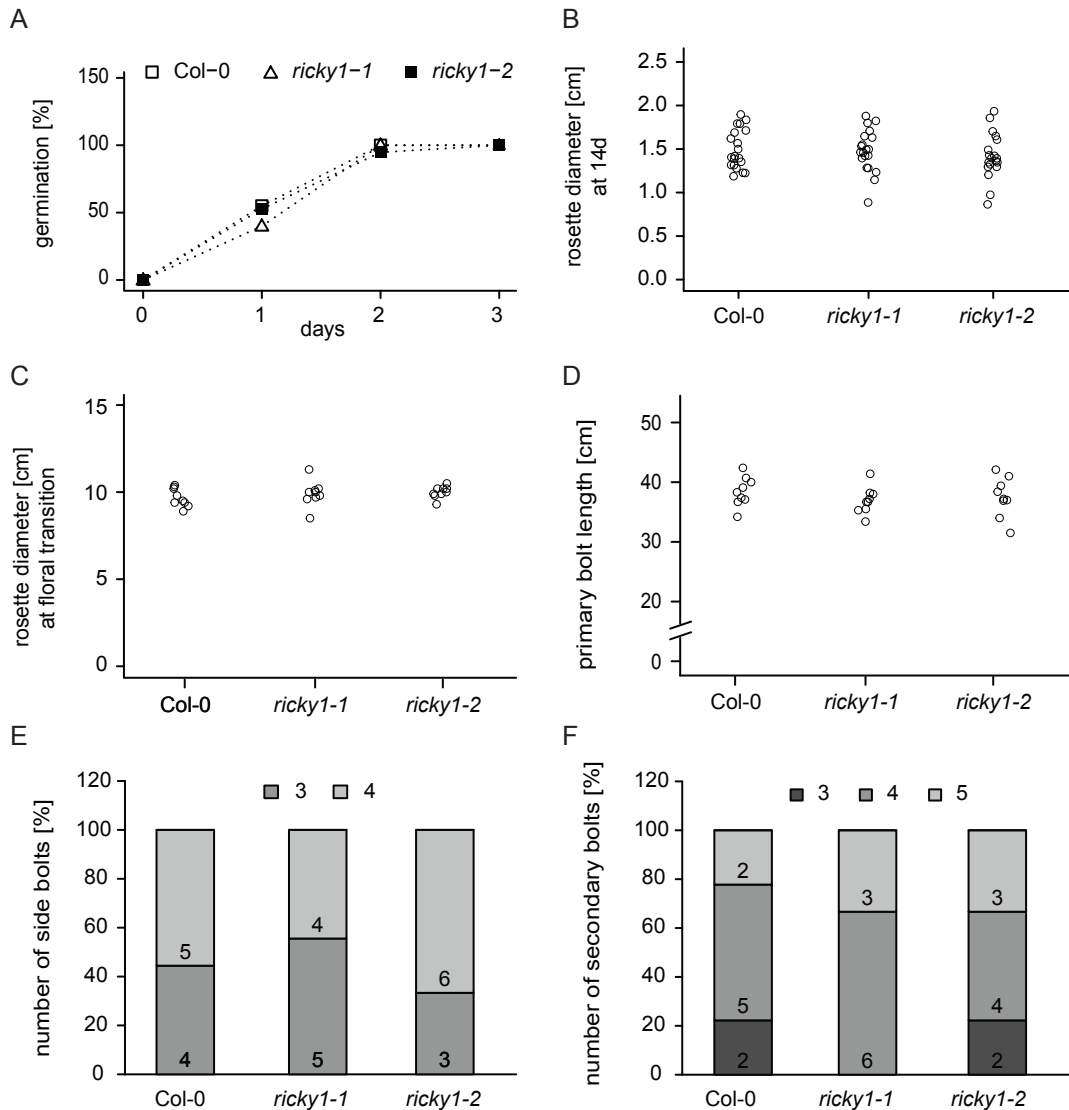
Fig. 3.3 *ricky1* mutants do not exhibit developmental defects

Different developmental stages were examined in Col-0 and *ricky1* mutants grown under long-day conditions on plate (½ MS + 1 % sucrose) (A,B; n = 20) and on soil (C-F; n = 9). (A) Germination rates were scored on the indicated days. (B,C) The diameter of rosettes was measured in 14-day-old seedlings (B) and adult plant at the time of floral transition (C). The primary bolt length (D), the number of side bolts on the primary bolt (E) and the number of secondary bolts (F) were analyzed in seven-week-old plants. (E,F) Total numbers are indicated additionally.
There was no significant difference between Col-0 and the *ricky1* mutants. Statistical significance was assessed using Fisher´s exact test (A,E,F) or one-way ANOVA (B-D), respectively.

3.2.1.2.   *ricky1* mutants are more resistant to auxin

In 2011, ten Hove and colleagues characterized T-DNA insertion lines of 69 root-expressed LRR-RLKs referring to their putative involvement in different abiotic stress pathways. Among others, their response to treatments with various hormones and osmotic compounds was analyzed. This study revealed a role for RICKY1 in auxin signaling, as 4 independent *ricky1*

T-DNA insertion lines showed a significant increase in root growth after application of the naturally occurring auxin IAA (Indole-3-acetic acid). Mutants that exhibited a greater than 20 % difference to the wild type were scored as resistant to the treatment (ten Hove *et al.*, 2011).

Because the lines *ricky1-1* and *ricky1-2* were not included in this study, we investigated if these mutants also display an auxin-related phenotype. Therefore, the effect of the synthetic auxin NAA (naphthaleneacetic acid) on the root growth of Col-0 and *ricky1* seedlings was examined. Four-day-old seedlings were challenged with different concentrations of NAA that are known to have an inhibitory effect on the root growth. Three days after the treatment with 100 and 200 nM NAA the mutant lines showed a significant increase in root length compared to Col-0. The primary roots were 4-7 % longer in *ricky1-1* and *ricky1-2* plants (Fig. 3.4A). A similar effect was observed 5 days after application of NAA with differences of 3-5 % (Fig. 3.4B). These results indicate that *ricky1-1* and *ricky1-2* are also significantly more resistant to NAA, even though the phenotype appeared milder compared to the published data (ten Hove *et al.*, 2011). This could be due to a slightly different experimental setup (see 5.5.17) or to the usage of NAA instead of IAA, since the synthetic auxin NAA has been shown to be more stable over time compared to the endogenous auxin IAA (Dunlap *et al.*, 1986; Dunlap & Robacker, 1988).
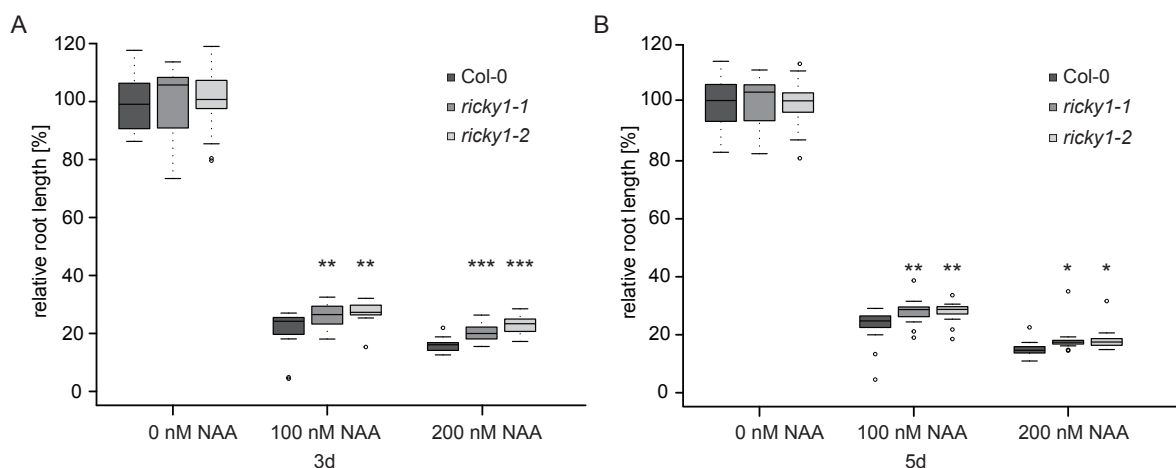
Fig. 3.4 *ricky1* mutants are more resistant to NAA

Col-0 and *ricky1* mutants were grown on ½ MS plates supplemented with 1 % sucrose. Four-day-old seedlings were challenged with different concentrations of NAA (Naphthaleneacetic acid) (n = 15,16). Pictures were taken after 3 (A) and 5 (B) days. The primary root length was measured using ImageJ. The averaged root length of each line without NAA was set to 100 percent, respectively. Statistical significance between the mutant lines and Col-0 within one treatment was assessed using one-way ANOVA followed by Dunnett´s multiple comparison test (* $P \leq 0.05$, ** $P \leq 0.01$, *** $P \leq 0.001$).

3.2.2.   Examining the Role of RICKY1 During Plant Immunity

In the following experiments, it was investigated if RICKY1 is indeed involved in plant immunity and, if so, where it can be placed in the signaling cascade. The MAMP flg22 was used to trigger early, intermediate and late defense responses (Gomez-Gomez *et al.*, 1999) and their integrity was analyzed in both *ricky1* mutant lines.

3.2.2.1.   *ricky1* mutants are not impaired in the flg22-induced ROS production

A very early response is the oxidative burst occurring only minutes after flg22 treatment. The production of ROS can be measured over time in relative light units (RLUs) using a luminol-based assay. Col-0 as well as both *ricky1* mutants displayed a flg22-specific reaction curve (Fig. 3.5A). The ROS production peaked 8 −12 minutes after treatment and decreased to background level 30 min later. A calculation of total RLUs produced over 35 minutes revealed no significant difference between *ricky1* mutants and Col-0 (Fig. 3.5B). These data indicate that RICKY1 is not involved in flg22-riggered oxidative burst.
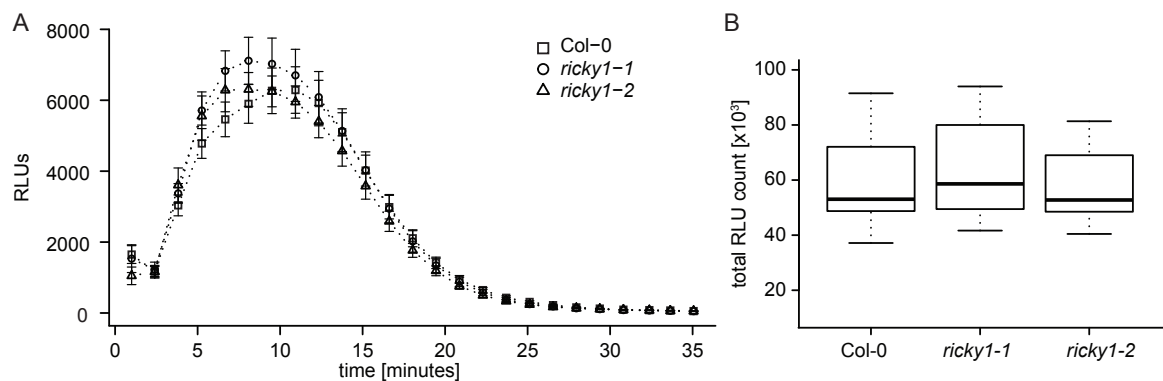
Fig. 3.5 RICKY1 is not involved in flg22-induced ROS production

Leaf discs of five-week-old *Arabidopsis* plants were treated with 100 nM flg22 and ROS production was measured over time as RLUs (relative light units) (n = 12). (A) Values represent mean RLUs +/- SE at different time points. (B) Values represent total RLUs measured over 35 minutes. Both *ricky1* mutants did not display a significant difference to Col-0. Statistical significance was assessed using one-way ANOVA.

3.2.2.2.   RICKY1 in not involved in the flg22-induced expression of defense marker genes

Another early to intermediate defense response is the increased expression of defense marker genes. It has been shown that MAMPs are able to induce the expression of genes involved in two distinct hormone-regulated defense pathways (Denoux *et al.*, 2008). The SA-dependent signaling mainly mediates resistance to biotrophic pathogen, whereas JA and ethylene ET play a role in defense mechanisms against necrotrophs (Glazebrook, 2005). Five-week-old plants were infiltrated with 1 μM flg22 or H_2O to analyze these defense responses. Leaves were harvested 1 h and 24 h after infiltration and qPCRs were performed to evaluate the expression of several defense marker genes. The expression of key components of both pathways was analyzed to check the integrity of both SA- and JA/ET-dependent signaling cascades.
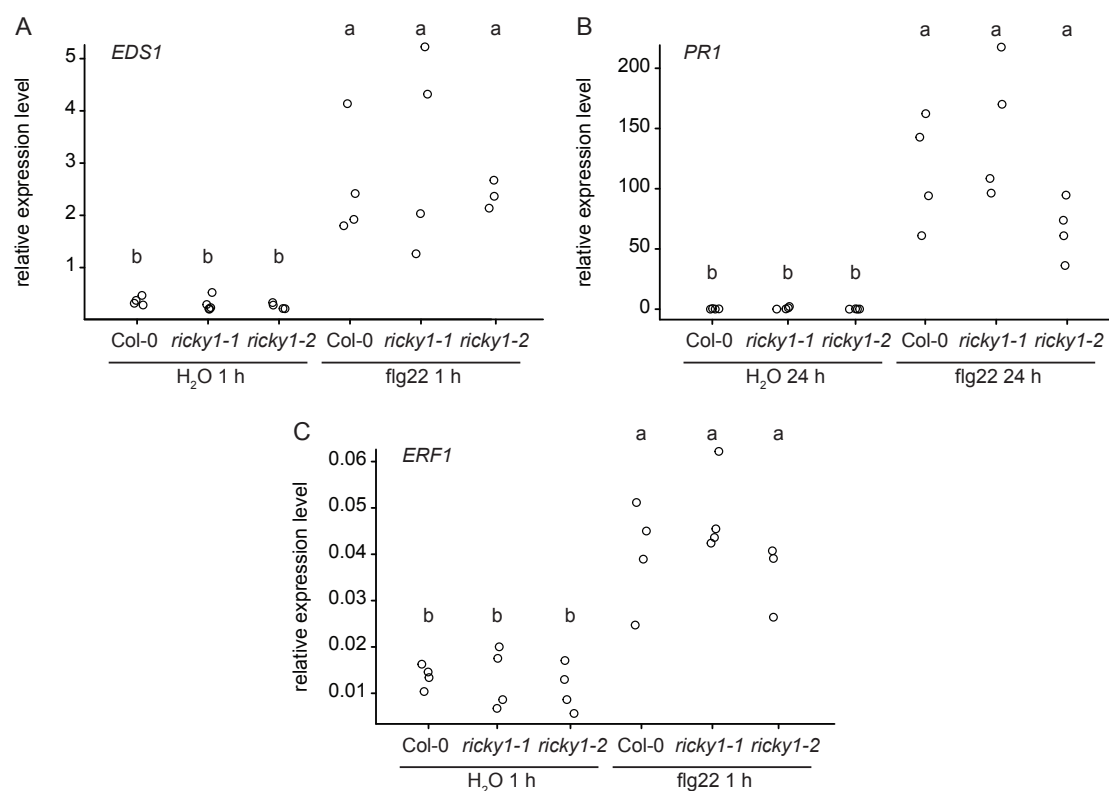
Fig. 3.6 *ricky1* mutants are not affected in the flg22-induced expression of defense marker genes

Five-week-old *Arabidopsis* leaves were infiltrated with H_2O or 1 μM flg22 and harvested 1 h (A,C) or 24 h (B) later (n = 3 – 4). Transcript levels of the marker genes, *EDS1* (A), *PR1* (B) and *ERF1* (C) were normalized to *UBC*. Col-0 and both *ricky1* mutants showed an increased defense gene expression after flg22 treatment, but *ricky1* mutants did not display an altered expression compared to Col-0 of the same treatment. Statistical significance was assessed using one-way ANOVA followed by a Tukey HSD test (P≤ 0.05 (C), P≤ 0.001 (A,B)).

The genes *EDS1* (*ENHANCED DISEASE SUSCEPTIBILITY 1*) and *PR1* (*PATHOGENESIS-RELATED PROTEIN 1*) play an important role during SA-dependent responses and are induced 1 h and 24 h after MAMP treatment, respectively (Denoux *et al.*, 2008).

Both genes are significantly induced after flg22 treatment, but neither the expression of the early nor of the late SA-related marker gene differed between both *ricky1* mutants and the wild type (Fig. 3.6A,B). Also the transcript of the early JA/ET-induced gene *ERF1* (*ETHYLENE RESPONSE FACTOR 1*) (Berrocal-Lobo *et al.*, 2002) was significantly increased after flg22 treatment, but did not show an altered expression between the lines (Fig. 3.6C). These results indicate that RICKY1 is not involved flg22-induced expression of defense-related marker genes.

3.2.2.3.   *ricky1* mutants are affected in the flg22-triggered production of callose

As *ricky1* mutants were not impaired in early and intermediate defense responses, the integrity of a later defense mechanism was examined. Hours after flg22 treatment an increased production of callose depositions can be detected (Gomez-Gomez *et al.*, 1999). Under this stress condition the (1,3)-β-glycan is mainly produced by the PM-localized callose synthase GSL5 and deposited between the PM and the CW (reviewed in Ellinger & Voigt, 2014).

Five-week-old wild type, *ricky1* and *fls2* mutant leaves were infiltrated with 1 μM flg22 or H_2O as control and harvested 24 h later to analyze the production of callose. Callose deposits were stained with methyl blue and one representative area per leaf was imaged using fluorescence microscopy (Fig. 3.7A,B). Subsequently, ImageJ was used to process all images and to analyze the number of callose depositions (Fig. 3.7C,D). Col-0 leaves treated with flg22 showed many callose deposits, whereas only isolated spots were visible in the *fls2* mutant. Both, *ricky1-1* and *ricky1-2* lines displayed an intermediate phenotype with several callose depositions (Fig. 3.7A). The counting of callose deposits revealed that in both *ricky1* mutants the number of callose spots was significantly decreased to 67 % compared to Col-0 (Fig. 3.7C). On the other hand, there was no significant difference between all lines in the mock-treated samples (Fig. 3.7B,D). These results suggest that RICKY1 plays a role in the flg22-induced callose production or later flg22-triggered processes.
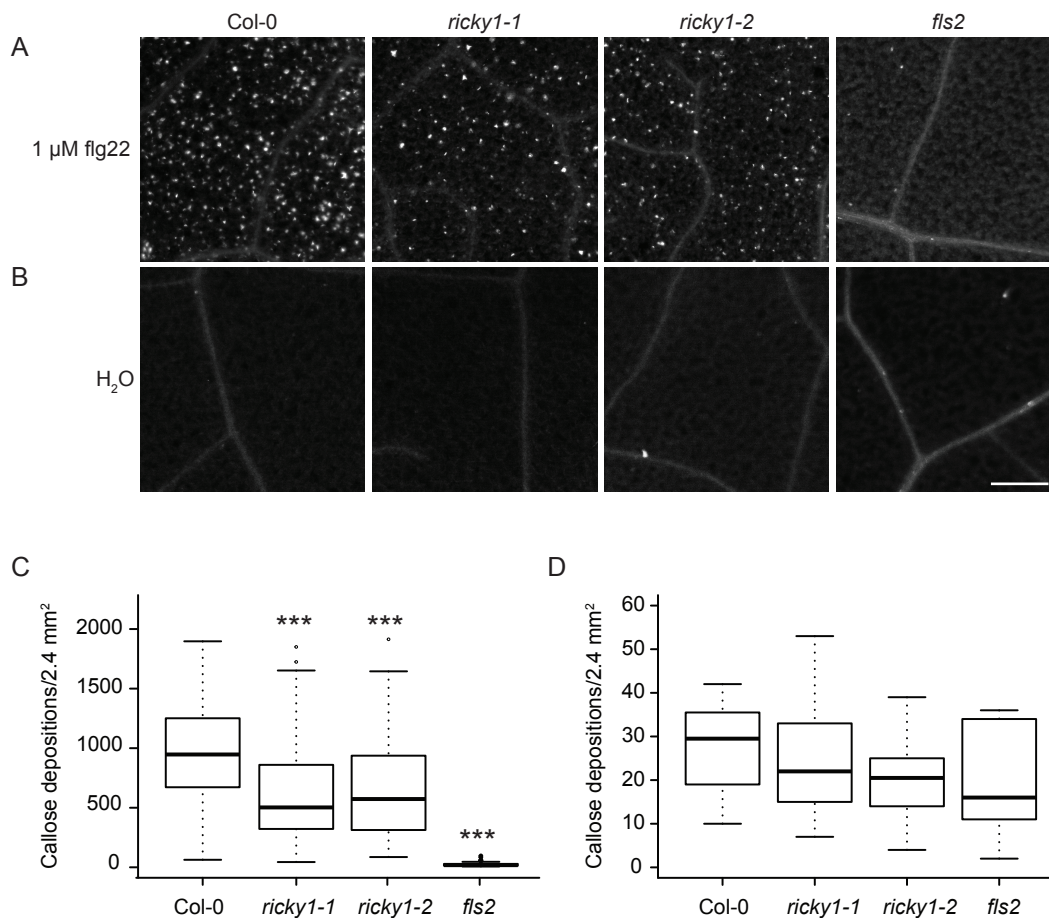
Fig. 3.7 RICKY1 is involved in flg22-induced callose deposition

Five-week-old *Arabidopsis* leaves were infiltrated with 1 μM flg22 ((A,C) n = 51 – 55) or H_2O ((B,D) n = 16 – 18) and harvested 24 h later. Callose depositions in Col-0, *ricky1-1*, *ricky1-2* and *fls2* were stained with methyl blue and analyzed using fluorescence microscopy. (A,B) Representative pictures. Bar = 200 μm. (C,D) The number of callose depositions was counted using ImageJ. Values represent the summary of 4 independent biological experiments. Both *ricky1* mutants showed a significant decrease in callose deposition after flg22 treatment (C), whereas there was no change in the mock control (D). Statistical significance was assessed using one-way ANOVA followed by Dunnett´s multiple comparison test (*** P≤ 0.001).

Subsequently, it was investigated if the observed callose phenotype of the *ricky1* mutants is caused by the T-DNA insertions in the *RICKY1* locus. Therefore, *ricky1-1* and *ricky1-2* plants were stably transformed with a genomic RICKY1-sGFP construct driven by its own promoter. Two independent complemented lines in the *ricky1-1* and in the *ricky1-2* mutant background were further analyzed, respectively.

A protein extraction from 14-day-old seedlings was performed to determine the protein levels of RICKY1-sGFP in all complemented lines. RICKY1-sGFP fusion proteins were detected using immunoblot analysis with a GFP antibody. Proteins extracted from Col-0 were used as

a negative control to distinguish between specific and unspecific signals. Two bands at about 75 and 175 kDa were specifically detected in all 4 complemented lines, but not in Col-0 (Fig. 3.8A). The strong signal at 175 kDa corresponds to the size of the full length RICKY1-sGFP fusion protein. The second signal at about 75 kDa could coincide with the predicted size of RICKY1-sGFP protein lacking the extracellular domains. All complemented lines showed a stable expression of RICKY1, whereby *RICKY1-sGFP/ricky1-2* plants exhibited lower protein amounts compared to the *RICKY1-sGFP/ricky1-1* lines. Equal loading was confirmed by the signal strength of the unspecific bands visible in all lanes.
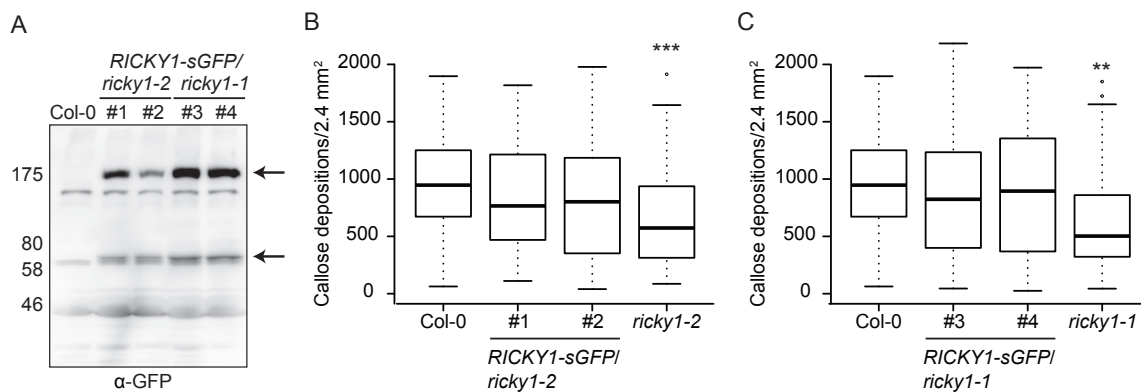
Fig. 3.8 The callose phenotype of the *ricky1* mutants can be partially complemented

ricky1 mutants were complemented with a GFP-tagged genomic *RICKY1* construct driven by its native promoter. Two homozygous complemented *ricky1-2* (#1, #2) and *ricky1-1* (#3, #4) lines were used for the determination of protein levels (A) and their ability to complement the callose phenotype of the mutants (B,C). (A) RICKY1-sGFP expression analysis of 14-day-old complemented *ricky1* seedlings using immunoblot analysis with a GFP antibody. Col-0 was used as a control. Arrows indicate specific bands. (B,C) Five-week-old *Arabidopsis* leaves were infiltrated with 1 μM flg22 and harvested 24 h later. Callose depositions were stained with methyl blue and analyzed using fluorescence microscopy. The number of callose depositions was counted using ImageJ. Values represent the summary of 4 independent biological experiments. Both complemented lines in the *ricky1-2* ((B) n = 50 – 54) and in the *ricky1-1* ((C) n = 51 – 56) background did not show a significant difference to Col-0, respectively. Statistical significance was assessed using one-way ANOVA followed by Dunnett´s multiple comparison test (** $P \leq 0.01$, *** $P \leq 0.001$).

All *RICKY1-sGFP/ricky1* lines were included in the callose assays shown in Fig. 3.7 to investigate if the lack of RICKY1 causes the callose phenotype in the *ricky1* mutants. None of the complemented lines showed a significant difference to Col-0 regarding the production of callose, contrary to both *ricky1* mutants (Fig. 3.8B,C). *RICKY1-sGFP/ricky1-2* plants displayed 83-86 % and *RICKY1-sGFP/ricky1-1* plants 92-94 % callose deposits compared to Col-0, respectively. As a consequence, it can be concluded that all complemented lines are able to partially rescue the *ricky1* phenotype. These results confirm that the decreased

callose production in the *ricky1* mutants is indeed caused by the loss of RICKY1. Additionally, they provide evidence for the functionality of the RICKY1-sGFP fusion protein.

3.2.2.4.   RICKY1 plays a role during plant defense against various pathogens

The results described above confirm a role for RICKY1 in flg22-induced defense mechanisms. Subsequently, it was investigated if the restricted immune response has an impact on the fitness of *ricky1* mutants, when they are challenged with plant pathogens. As flg22 is a conserved epitope of the bacterial flagellum, the hemibiotrophic bacterium *Pseudomonas syringae* pv. *tomato* (*Pto*) was used for first analyses (Katagiri *et al.*, 2002; Xin & He, 2013).

Bacteria of the *Pto* strain DC3000 were sprayed onto five-week-old Col-0, *ricky1* and *fls2* leaves and the bacterial growth was analyzed 3 days later. Both *ricky1* mutants showed a significant higher bacterial density compared to Col-0 and are therefore more susceptible to *Pseudomonas syringae* (Fig. 3.9). As the plants were less infected than *fls2* plants, they exhibited an intermediate phenotype.
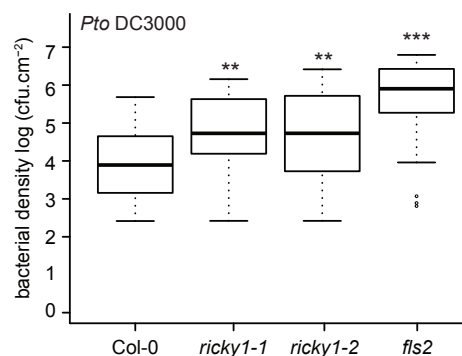
Fig. 3.9 *ricky1* mutants are more susceptible to *P. syringae*

Five-week-old plants were spray-inoculated with *Pseudomonas syringae* pv. *tomato* (*Pto*) DC3000 (OD_{600} = 0.02). Bacterial density was analyzed 3 days post infection (dpi) as colony forming units (cfu). Values represent the average of 3 independent biological experiments (n = 36). Both *ricky1* mutants showed a significantly increased bacterial growth compared to Col-0. Statistical significance was assessed using one-way ANOVA followed by Dunnett´s multiple comparison test (** P≤ 0.01, *** P≤ 0.001).

Subsequently, another phytopathogen was used to investigate if the reduced fitness of *ricky1* mutants is specific to infections with *Pseudomonas*. Therefore, a collaboration with the laboratory of Harald Keller (UMR-Institut Sophia Agrobiotech) was initiated. They analyzed the interaction of *ricky1* with the obligate biotroph *Hyaloperonospora arabidopsidis* (*Hpa*). The oomycete is a natural pathogen of *Arabidopsis* and causes the downy mildew disease (Koch & Slusarenko, 1990; Coates & Beynon, 2010).

Ten-day-old Col-0 and *ricky1* mutant seedlings were spray-inoculated with the *Hpa* strain Waco to examine if RICKY1 is involved in the defense pathway against the oomycete. The infection success of *Hpa* was evaluated by counting the number of spores using a hemocytometer. Both *ricky1* mutant lines showed a 20 % higher sporulation rate compared to Col-0 and are therefore more susceptible to the oomycete (Fig. 3.10).

These data clearly indicate that RICKY1 plays a general role in plant immunity and is involved in defense mechanisms against various pathogens.
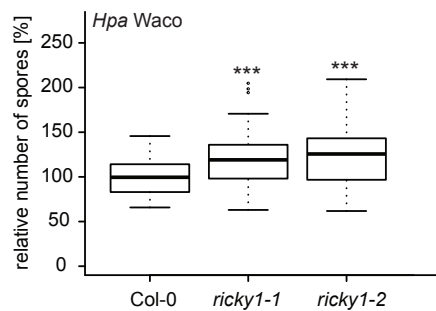
Fig. 3.10 *ricky1* mutants are more susceptible to *H. arabidopsidis*

Ten-day-old Arabidopsis seedlings were spray-inoculated with the oomycete *Hyaloperonospora arabidopsidis* (*Hpa*) isolate Waco at 40,000 spores/ml. The sporulation rate was determined with a hemocytometer 24 h after the induction of sporulation. The sporulation in Col-0 was defined as 100 %. Values represent the average of 3 independent biological experiments (n = 60). Both *ricky1* mutants showed significantly higher spore rates compared to Col-0. Statistical significance was assessed using one-way ANOVA followed by Dunnett´s multiple comparison test (*** P≤ 0.001). The experiments were performed by the collaborator Harald Keller.

3.2.3.   Cell Biological Characterization of RICKY1

Plant PMs separate the intracellular space from the outside environment and are therefore important for many cellular responses including plant immunity. They harbor RLKs that are able to perceive different MAMPs in the apoplast and are crucial to initiate different defense responses. Many of these mechanisms are also located at the PM (reviewed in Couto & Zipfel, 2016). The dynamic reorganization of the PM is essential to facilitate an efficient signal transduction that results in a suitable adaptation to changing conditions. Scaffold proteins, such as flotillins and remorin proteins, are thought to be involved in the formation of active signaling platforms at the PM (Jarsch & Ott, 2011). Pre-assembled protein complexes as well as stimulus-dependent lateral movement of proteins play a crucial role. Since this is a very dynamic process, the microscopy-based cell biological characterization of a protein can help to understand its biological function.

3.2.3.1.   RICKY1 localizes to the plasma membrane

The LRR-RLK RICKY1 contains one predicted transmembrane domain (Fig. 3.2B), but its actual subcellular localization has not been examined so far. Hence, the localization of RICKY1 was analyzed in the stable complemented *proRICKY1:RICKY1-sGFP/ricky1-1* line #3 (see Fig. 3.8). Five-week-old leaves were stained with the lipophilic dye FM4-64 that enables a counterstaining of the PM (Bolte *et al.*, 2004). Confocal laser scanning microscopy (CLSM) revealed a homogeneous distribution of the RICKY1-sGFP signal mainly at the PM (Fig. 3.11A), confirmed by the co-localization with FM4-64 (Fig. 3.11A´,A´´).
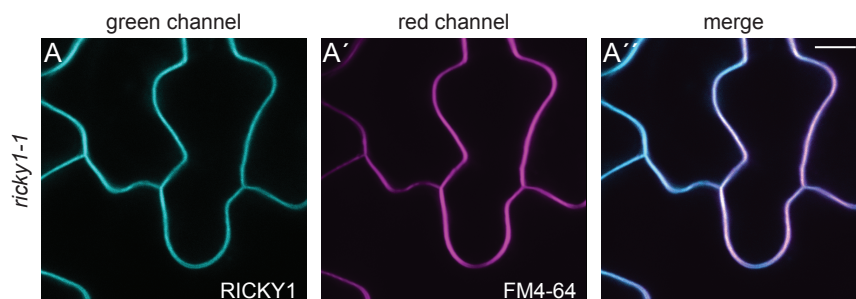
Fig. 3.11 RICKY1 localizes to the plasma membrane

Five-week-old *ricky1-1* plants expressing *RICKY1-sGFP* under its native promoter were stained with the styryl dye FM4-64. Epidermal cells were imaged using confocal microscopy. RICKY1-sGFP localized to the periphery of the cell (A) and co-localized with the PM marker FM4-64 (A´,A´´). Bar = 10 *μ*m.

In living cells, proteins are not insulated, but incorporated in a complex network of many different components that act together in one signaling pathway. For this reason, it is important to characterize proteins not only individually, but also consider proteins in their surrounding. Also putative interactions need to be investigated in their biological environment. Since RICKY1 was shown to interact with the remorin protein REM1.2 in the heterologous yeast system (see Fig. 3.1), the interaction should be verified *in planta*. *ProRICKY1:gRICKY1-sGFP/ricky1-1* #3 plants were additionally transformed with genomic constructs of *proREM1.2-mCherry-REM1.2* and *proREM1.3-mCherry-REM1.3* to enable a detailed characterization. CLSM confirmed the stable expression of RICKY1-sGFP and both mCherry-REM fusion proteins, and their co-localization at the PM (Fig. 3.12). These lines have been used for further cell biological analyses.
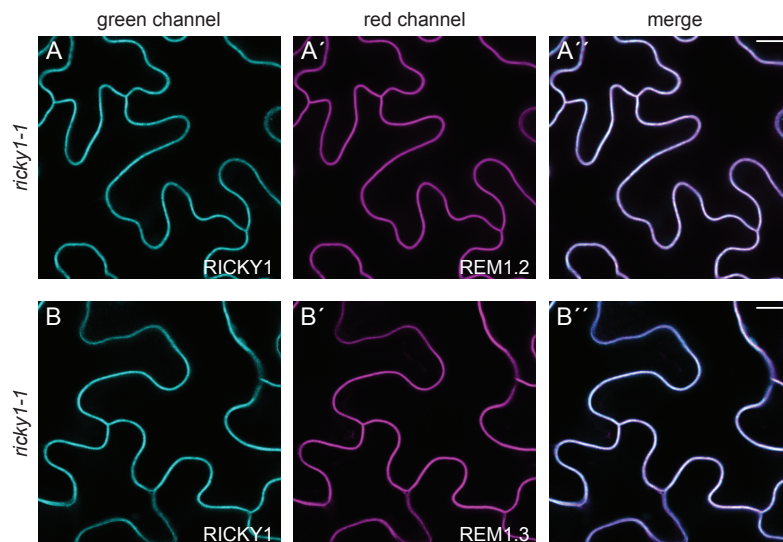
Fig. 3.12 RICKY1 co-localizes with REM1.2 and REM1.3 at the plasma membrane

Confocal microscopy of *ricky1-1* plants expressing *RICKY1-sGFP* and *mCherry-REM1.2* (A-A``) or *RICKY1-sGFP* and *mCherry-REM1.3* (B-B´´) under the control of their native promoters, respectively. RICKY1 co-localized with REM1.2 (A´´) and REM1.3 (B``) at the periphery of the cell. Bar = 10 μm.

3.2.3.2.   RICKY1 localizes to the sites of *Hyaloperonospora arabidopsidis* infection and around their haustoria

Plant membranes play an essential role during the invasion process of different pathogens. Accordingly, they undergo various changes in organization and composition to facilitate an efficient defense response. This especially applies for the actual host-pathogen interface like the site of haustoria formation. The invasive feeding structure, developed by fungi and oomycetes, is enveloped by a plant-derived EHM. Even though the EHM is continuous with

the PM, the protein composition can differ between them. In later stages haustoria get additionally enclosed by a host-derived encasement membrane (reviewed in Faulkner, 2015).

As RICKY1 was shown to be involved in plant immunity against *H. arabidopsidis* (Fig. 3.10), its subcellular localization was investigated after the infection with the oomycete. Therefore, 14-day-old *proRICKY1:gRICKY1-sGFP/ricky1-1* #3 seedlings were spray-inoculated with the *Hpa* isolate Noco2 and RICKY1 localization was analyzed 5 – 6 days after infection using CLSM. RICKY1-sGFP signals were visible at the PM and showed an accumulation at sites of oomycete structures (Fig. 3.13A). Additionally, RICKY1-GFP localized around the *Hpa* haustoria in many cases (Fig. 3.13B).
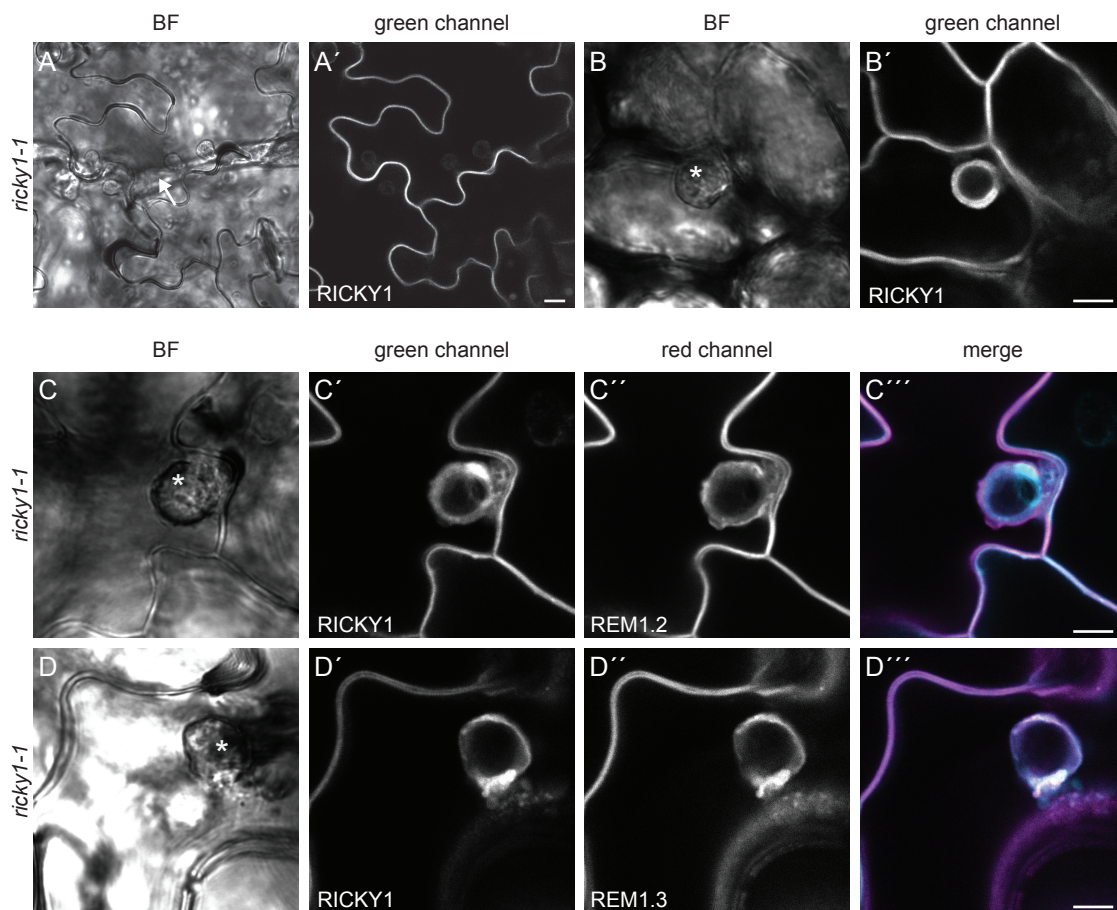
Fig. 3.13 RICKY1 localization is associated to oomycete structures

Confocal microscopy of *ricky1-1* mutants expressing *RICKY1-sGFP* (A,B), *RICKY1-sGFP* and *mCherry-REM1.2* (C-C´´´) or *RICKY1-sGFP* and *mCherry-REM1.3* (D-D´´´) under the control of their native promoters. 14-day-old seedlings were spray-inoculated with the *H. arabidopsidis* isolate Noco2 and haustoria were imaged 5-6 dpi. Bar = 10 *µ*m. Arrows and asterisks in bright field (BF) images indicate hyphae and haustoria, respectively.

To examine the localization of *Arabidopsis* remorin proteins during an *Hpa* infection, stable transgenic lines co-expressing *RICKY1-sGFP* and *mCherry-REM1.2* or *mCherry-REM1.3* were analyzed, respectively (Fig. 3.13C,D). REM1.2 (Fig. 3.13C) as well as REM1.3 (Fig. 3.13D) were localized at the PM and around the haustoria of *Hpa*. The same is true for the localization of RICKY1 in these co-expressing lines. The slightly variable patterning of RICKY1 at the haustoria could be due to different developmental stages of the haustoria and needs to be further investigated.

3.2.3.3.   RICKY1 co-localizes with REM1.2 and REM1.3 in micro-domains

Remorin proteins are well-accepted micro-domain marker proteins in different plant species (Raffaele *et al.*, 2009; Lefebvre *et al.*, 2010; Tóth *et al.*, 2012; Demir *et al.*, 2013; Gui *et al.*, 2014; Jarsch *et al.*, 2014). A recent study confirmed the variety of co-existing domains at the PM of *Arabidopsis.* Interestingly, the group 1 remorins REM1.2 and REM1.3 showed an exceptional patterning. Using confocal microscopy these remorins showed an occasionally occurring domain formation in a tissue-specific manner. A higher resolution in the z-axis and over time gained by total internal reflection microscopy (TIRFM), revealed the localization of REM1.2 and REM1.3 in small and mobile micro-domains also in other tissues (Jarsch *et al.*, 2014).

A collaboration with Sebastian Konrad was initiated to analyze the localization of RICKY1 more precisely and to investigate a putative co-localization with REM1.2 and REM1.3. *Arabidopsis* seedlings co-expressing *RICKY1-sGFP* and *mCherry-REM1.2* or *RICKY1-sGFP* and *mCherry-REM1.3* were examined using TIRF microscopy. Interestingly, RICKY1-sGFP signals were also observed in distinct domains at the surface of epidermal cells (Fig. 3.14A,B). These domains were, as well as the remorin-targeted domains, small and highly mobile.

Subsequently, ImageJ was used to investigate a putative co-localization of RICKY1 and the remorin proteins. The Pearson´s coefficient (Rr) displays the linear dependency of two datasets and ranges from -1 to 1. A value of -1 points to a complete negative correlation (exclusion) between two proteins, while a value of 1 suggests an absolute positive correlation (co-localization). Values around 0 indicate no correlation between two datasets (homogeneous distribution). For a statistical assumption, randomized simulations have to be performed and compared to the original dataset. Therefore, the Costes´ randomization was

applied to all GFP channels resulting in a randomized Pearson´s coefficient (rd Rr). Protein pairs with Rr > rd Rr are thereby scored as co-localizing, while pairs with Rr < rd Rr are regarded as excluding (Manders *et al.*, 1992; Costes *et al.*, 2004; Bolte & Cordelieres, 2006). The Pearson´s coefficient obtained for RICKY1 and REM1.2 was Rr = 0.590 (SE = 0.01; n = 20), indicating a positive correlation between both proteins. Since the randomized Pearson´s coefficient rd Rr = 0.00 (SE = 0.005; n = 20; P< 0.001) was significantly lower than Rr, it can be concluded that RICKY1 co-localizes with REM1.2. A similar result was observed for RICKY1 and REM1.3. The calculated Pearson´s coefficient Rr = 0.559 (SE = 0.018; n = 21) was significantly higher than the randomized value rd Rr = 0.00 (SE = 0.004; n = 21; P< 0.001). Hence, RICKY1-labeled micro-domains show a positive correlation with REM1.3.
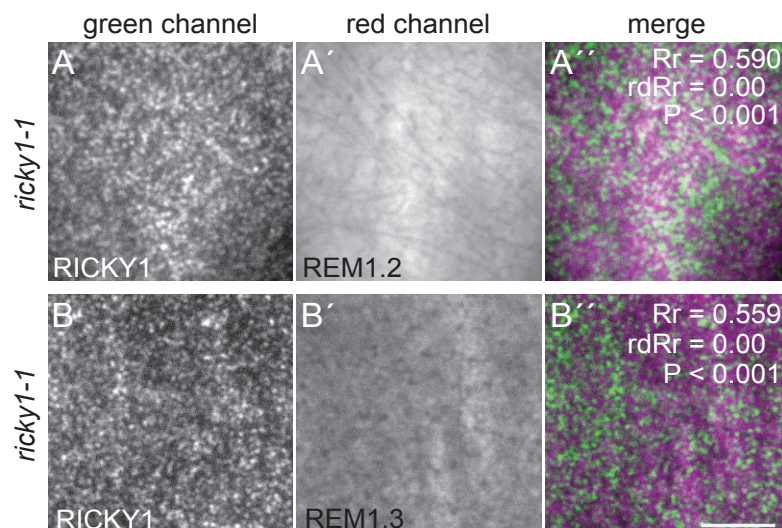
Fig. 3.14 RICKY1 co-localizes with REM1.2 and REM1.3 in micro-domains at the plasma membrane

Total internal reflection microscopy of stable transgenic *Arabidopsis* plants co-expressing *RICKY1-sGFP* and *mCherry-REM1.2* (A-A´´) or *RICKY1-sGFP* and *mCherry-REM1.3* (B-B´´) under the control of their native promoters (n = 20,21). Bar = 5 *µ*m. Co-localization was analyzed using ImageJ. Pearson´s coefficients (Rr) indicated a co-localization of RICKY1 with REM1.2 and REM1.3. Costes´ randomized Pearson´s coefficients (rd Rr) were calculated as controls. Statistical significance was assessed using a Student´s *t* test (P< 0.001). Image acquisition and data processing was performed by Sebastian Konrad.

3.2.3.4.   RICKY1 interacts with remorin proteins *in planta*

So far, the interaction of REM1.2 and RICKY1 has been shown in the heterologous Y2H system (Fig. 3.1). As both proteins co-localized in small domains at the PM (Fig. 3.14), it was of special interest if both proteins are able to interact *in planta*. Additionally, a putative interaction of RICKY1 with REM1.3 was investigated, as these proteins did not interact in yeast, but showed a positive correlation using TIRF microscopy.

First of all, the bimolecular fluorescence complementation (BiFC) system was used to examine the interaction in epidermal cells of *Nicotiana benthamiana*. This method has been widely used to analyze the interaction between remorin proteins and different RLKs (Tóth *et al.*, 2012; Jarsch *et al.*, 2014). Therefore, all proteins of interest were fused to non-fluorescent halves of the fluorophore YFP and transiently expressed under the control of the cauliflower mosaic virus promoter 35S.

Homo-oligomers of REM1.2 and REM1.3 were used as positive controls. Both, the co-expression of REM1.2 with REM1.2 (Fig. 3.15A,G) and of REM1.3 with REM1.3 (Fig. 3.15C,I) resulted in a homogeneous distribution of the YFP signal at the PM. In the following experiments, RICKY1 was fused to the N-terminal part of YFP (Yn) and remorins were fused to the C-terminal part of YFP (Yc). Cells co-expressing RICKY1 and REM1.2 showed fluorescence signals in distinct parts of the PM. These can be seen in overview pictures (Fig. 3.15B), as well as on the PM-surface (Fig. 3.15H). Similar patterns were observed in cells co-expressing RICKY1 and REM1.3 (Fig. 3.15D,J). These data indicate that RICKY1 interacts with REM1.2 and REM1.3 in distinct parts of the PM, even though all three proteins showed a homogeneous distribution using confocal microscopy (see Fig. 3.12, Fig. 3.15A,C,G,I).

To investigate the specificity of these interactions, the *Arabidopsis* group 6 remorin REM6.4 was used as control, because it was previously shown to localize to micro-domains (Jarsch *et al.*, 2014). A co-transformation of REM6.4 with RICKY1 did not reconstitute a functional YFP (Fig. 3.15F), indicating that both proteins are not interacting. To validate the functionality of the REM6.4 construct, its ability to form homo-dimers was examined. The co-expression of REM6.4 with REM6.4 resulted in YFP signals in distinct domains at the PM (Fig. 3.15E,K). The co-transformations of REM6.4/REM6.4 and RICKY1/REM6.4 were performed on the same leaf to exclude that the missing interaction is caused by problems with the *N. benthamiana* plants.

These results clearly demonstrate the specificity of the interaction between group 1 remorins and RICKY1 in the heterologous *N. benthamiana* system.
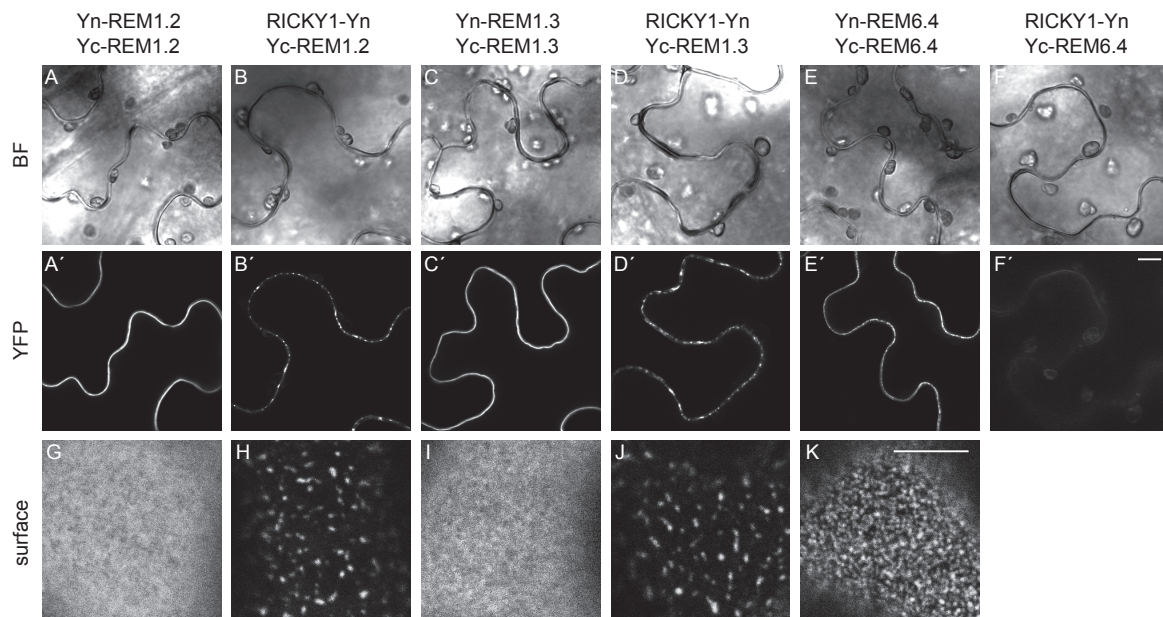
Fig. 3.15 RICKY1 interacts with REM1.2 and REM1.3 in distinct domains at the plasma membrane in *N. benthamiana*

Bimolecular fluorescence complementation (BiFC) in transiently transformed *N. benthamiana* cells. The fluorescence signal was analyzed in overview pictures (A-F,A´-F´) and on the upper plane of the PM (G-K) using confocal microscopy. All constructs were driven by the 35S promoter. Co-expressions of REM1.2/REM1.2 (A,A´,G), REM1.3/REM1.3 (C,C´,I) and REM6.4/REM6.4 (E,E´,K) were used as controls. REM1.2 and REM1.3 homo-oligomers showed a homogeneous distribution at the PM, whereas REM6.4 homo-oligomers localized in micro domains. Co-expression of RICKY1-Yn with Yc-REM1.2 (B,B´,H) and Yc-REM1.3 (D,D´,J) resulted in fluorescence signals in distinct domains at the PM. The co-expression of RICKY1-Yn with Yc-REM6.4 served as negative control. Bar = 10 μm. Yc = C-terminal half of YFP; Yn = N-terminal half of YFP

One critical aspect about BiFC is the irreversibility of an interaction (Kerppola, 2008). On the one hand this allows the analysis of weak or transient interactions, but it also inhibits a real-time detection of protein complex formation. As the localization of group 1 remorins is thought to be a very dynamic process (Jarsch *et al.*, 2014), the interaction of RICKY1 and remorin proteins was investigated using another imaging-based method.

The combination of fluorescence lifetime imaging (FLIM) and fluorescence resonance energy transfer (FRET) enables a temporal and spatial analysis of protein interactions in living plant cells. The method is based on the measurement of the lifetime of a donor

fluorophore in the presence and absence of a non-excited acceptor molecule. The fluorescence lifetime (τ) is defined as the period of time a fluorophore exists in an excited state prior to returning to the ground state again. The transfer of energy from the excited donor to a non-excited acceptor molecule can shorten this period significantly. Two molecules must be in close proximity of 1-10 nm to enable FRET, which correlates with the distance of two physically interacting proteins. In addition, a significant spectral overlap between the emission spectrum of the donor and the excitation spectrum of the acceptor is necessary (reviewed in Bücherl *et al.*, 2014).

As GFP and mCherry are a widely used fluorophore pair in FLIM-FRET measurements, *Arabidopsis* plants expressing *RICKY1-sGFP*, *RICKY1-sGFP* and *mCherry-REM1.2* or *RICKY1-sGFP* and *mCherry-REM1.3* were analyzed. All constructs were under the control of their native promoters, respectively. A pulsed multi-photon laser was used to excite the GFP fluorophores and the GFP lifetime of all pixels at the PM was calculated subsequently with the SPCM software. False color-coded overview images indicate the variable GFP lifetimes at the PM of all three lines (Fig. 3.16A). The code ranges from high τ values of 2.6 ns (red) to low τ values of 2.2 ns (blue). An increased area of reduced GFP lifetime was detectable in plants co-expressing *RICKY1-sGFP* and *mCherry-REM1.2* compared to control plants expressing *RICKY1-sGFP* alone or *RICKY1-sGFP* and *mCherry-REM1.3*.

The average GFP lifetime of each line was calculated and analyzed to make a statistical assumption. All three lines showed significant different GFP lifetimes, whereby *RICKY1-sGFP/mCherry-REM1.2* plants displayed a major reduction in τ compared to *RICKY1-sGFP* alone (Fig. 3.16B). Here, the calculated FRET efficiency was 4.1 %. In *RICKY1-sGFP/mCherry-REM1.3* co-expressing plants the FRET efficiency was 1.6 %.

Since this reduction was also significantly different to the control, the distribution of τ was investigated in more detail. Plotting the frequencies of all lifetimes revealed a clear shift to lower τ values in the *RICKY1-sGFP/mCherry-REM1.2* plants compared to the control as well as to the *RICKY1-sGFP/mCherry-REM1.3* plants (Fig. 3.16C). These data indicate that RICKY1 is physically interacting mainly with REM1.2, even though all three proteins co-localize in distinct domains at the PM (Fig. 3.14).
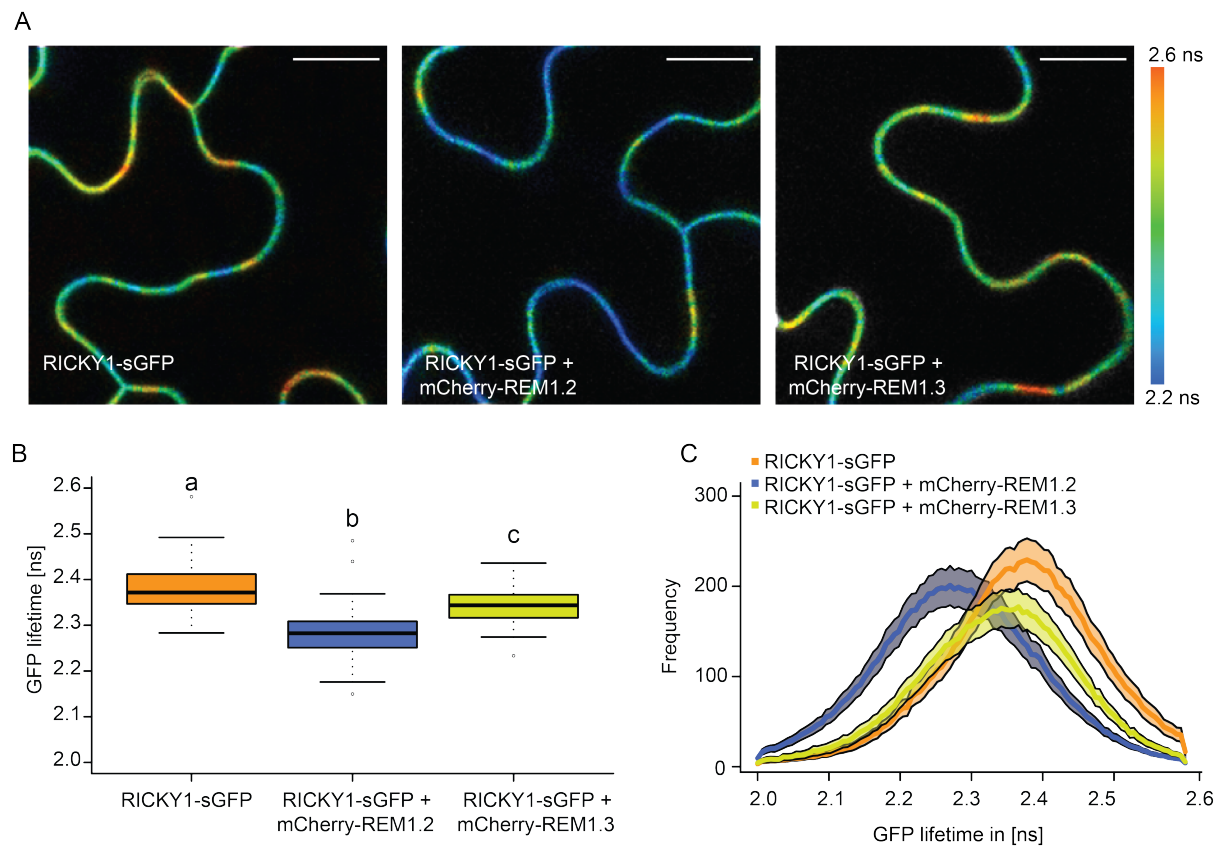
Fig. 3.16 RICKY1 interacts with REM1.2 at the PM of *Arabidopsis*

FLIM/FRET analysis in five-week-old *ricky1-1* plants expressing *RICKY1-sGFP*, *RICKY1-sGFP* and *mCherry-REM1.2* or *RICKY1-sGFP* and *mCherry-REM1.3* under the control of their native promoters, respectively (n = 50). (A) Representative pictures indicating GFP lifetimes (2.2 – 2.6 ns) at the PM with the corresponding color code. Bars = 10 μm. (B) Values represent the average GFP lifetime of all images. Statistical significance was assessed using one-way ANOVA followed by a Tukey HSD test (P≤ 0.001). The FRET efficiency between RICKY1-sGFP/mCherry-REM1.2 and RICKY1-sGFP/mCherry-REM1.3 was 4.1 % and 1.6 %, respectively. (C) Values represent the distribution of GFP lifetimes in all images. Shown is the average frequency +/- SE. Co-expression of RICKY1-sGFP and mCherry-REM1.2 led to a clear shift to lower GFP lifetimes compared to the RICKY1-sGFP alone control.

3.2.3.5.   Investigating the impact of REM1.2 on the localization and mobility of RICKY1

Increasing evidence indicates the impact of scaffold proteins on the localization pattern and dynamics of PM-localized proteins (Wang *et al.*, 2015b; Stratil, 2016). Therefore, it should be investigated if REM1.2 has an impact on the localization and mobility of RICKY1. Accordingly, *rem1.2-1* mutants were stable transformed with a genomic *RICKY1-sGFP* construct driven by its own promoter. *Rem1.2-1* plants have been shown previously to be knockout mutants (Jarsch *et al.*, 2014).

The subcellular localization of RICKY1 in this line was analyzed using confocal microscopy. RICKY1-sGFP fluorescence signal was detectable at the PM, which was confirmed by a co-localization with the styryl dye FM4-64 (Fig. 3.17A). *RICKY1-sGFP/rem1.2-1* plants were spray-inoculated with the *Hpa* isolate Noco2 to investigate its localization at a specialized membrane. Six days after infection RICKY1 localized around the haustorium as well as to the surrounding PM (Fig. 3.17B).

No obvious difference to the subcellular localization of RICKY1-sGFP in the *ricky1-1* mutant background was observed using confocal microscopy (see Fig. 3.11; Fig. 3.13). These data show that REM1.2 is not essential for the PM-localization of RICKY1 in *Arabidopsis*. The ability of RICKY1 to localize to micro-domains in the absence of REM1.2 needs to be further investigated using TIRF microscopy.
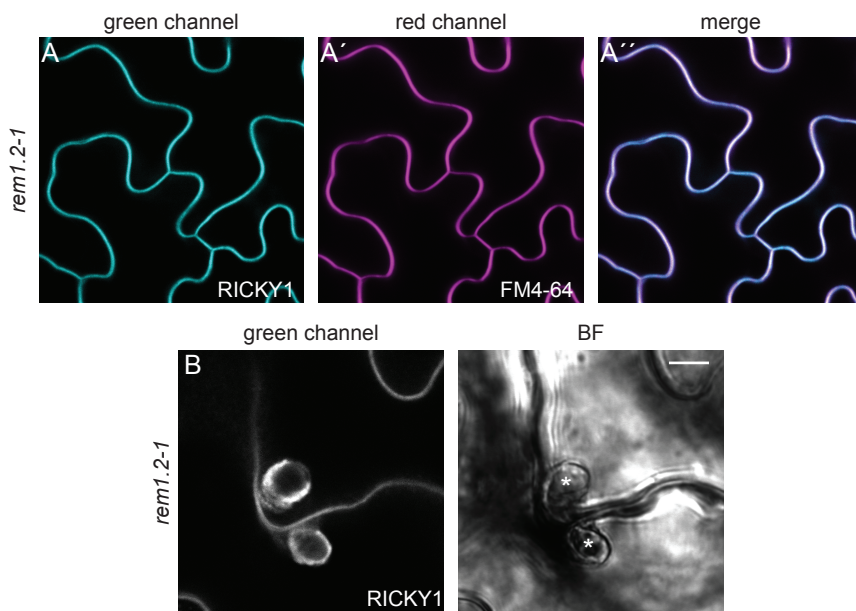
Fig. 3.17 REM1.2 has no obvious influence on the localization of RICKY1

Confocal microscopy of *Arabidopsis* plants expressing *proRICKY1:gRICKY1-sGFP* in the *rem1.2-1* mutant background. (A) Five-week-old plants were stained with the PM dye FM4-64 (A´). RICKY1-sGFP localized to the periphery of the cell (A) and co-localized with FM4-64 (A´,A´´). Bar = 10 µm. (B) 14-day-old seedlings were spray-inoculated with the *Hpa* isolate Noco2 and haustoria were images 6 dpi. RICKY1-sGFP localized around the haustorium. Bar = 10 µm. Asterisks in bright field (BF) images indicate haustoria.

In addition to the localization, the impact of REM1.2 on the dynamics of RICKY1 was examined. Therefore, the fluorescence recovery after photobleaching (FRAP) was analyzed in *RICKY1-sGFP/ricky1-1* and *RICKY1-sGFP/rem1.2-1* lines using confocal microscopy. This method is based on the irreversible photobleaching of a subset of fluorophores in a

defined area. By monitoring the fluorescence recovery through lateral diffusion of non-bleached fluorophores, the mobility of a fluorescently labeled protein of interest can be determined (De Los Santos *et al.*, 2015).

To examine the mobility of RICKY1 in both mutant backgrounds, two regions of interest (ROIs) were bleached per image and the recovery of fluorescence was documented over time. Non-bleached ROIs in the proximity were used as controls to compensate the bleaching over time. The calculation of fluorescence intensities was performed with ImageJ.

First, the relative normalized fluorescence intensities were plotted over time (Fig. 3.18A). RICKY1 was mobile in both lines, indicated by the final recovered intensities of 76 % and 82 % in *ricky1-1* and *rem1.2-1*, respectively. The mobile fraction of RICKY1-sGFP was calculated in both mutant backgrounds to statistically analyze the difference. This value displays the mobile portion of a protein population at the PM. The mobile fraction of RICKY1-sGFP was significantly higher in the *rem1.2-1* mutant background compared to the *ricky1-1* plants (Fig. 3.18).

These data clearly demonstrate the influence of REM1.2 on the mobility of RICKY1 at the PM.
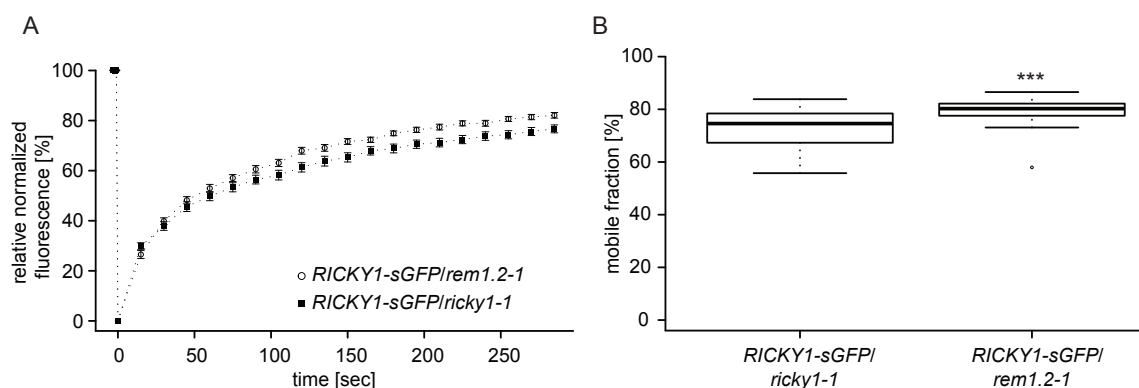
Fig. 3.18 REM1.2 has an impact on the mobility of RICKY1

Fluorescence recovery after photobleaching analysis in 14-day-old *Arabidopsis* plants expressing *proRICKY1:gRICKY1-sGFP* in the *ricky1-1* and the *rem1.2-1* mutant background, respectively (n = 27, 28). Fluorescence intensities of bleached ROIs (region of interest) were normalized to non-bleached ROIs in their vicinity. (A) Normalized pre-bleach intensities were set to 100 % and normalized recovery rates +/- SE are shown over time. (B) The calculated mobile fraction of RICKY1-sGFP was significantly higher in the *rem1.2-1* mutant background compared to the *ricky1-1* mutant background. Statistical significance was assessed using a Welch *t* test (*** P≤ 0.001).

3.2.4.   Investigating the Kinase Activity of RICKY1 and its Impact on Interactions and Localization

In 1989, a remorin protein was initially identified due to its differential phosphorylation after the treatment with polygalacturonides (Farmer *et al.*, 1989). Since then, several studies analyzed the interaction of remorins with different RLKs (Lefebvre *et al.*, 2010; Tóth *et al.*, 2012; Gui *et al.*, 2016) and showed their stimulus-dependent phosphorylation pattern (Benschop *et al.*, 2007; Keinath *et al.*, 2010; Gui *et al.*, 2016). These data indicate that phosphorylation is an important step for the dynamic regulation of remorin proteins.

3.2.4.1.   The interaction of RICKY1 and REM1.2 is phosphorylation-dependent

Following the *in planta* confirmation that RICKY1 physically interacts with REM1.2 (Fig. 3.16), the interaction itself was further characterized. For this, the heterologous yeast system was used. It enables a direct read-out of the interaction between RICKY1 and REM1.2 in absence of other plant proteins that could also influence the interplay of both proteins.

Remorins are characterized by the presence of a coiled-coil domain in their conserved C-terminal region (Raffaele *et al.*, 2007). Additionally, most of them contain a highly variable N-terminal region that is intrinsically disordered (Marín & Ott, 2012). A domain swap experiment was performed with REM1.2 and the non-interacting REM1.3 to specify which part of REM1.2 is crucial for the interaction with RICKY1. Consequently, the N-terminal region of REM1.2 was fused to the C-terminal part of REM1.3 (N-REM1.2/C-REM1.3) and the N-terminal part of REM1.3 was fused to the C-terminal domain of REM1.2 (N-REM1.3/C-REM1.2) (Fig. 3.19A).

The constructs were tested in a GAL4 Y2H experiment to analyze their ability to interact with the cytosolic domain of RICKY1. The interaction of RICKY1 CD and wild type REM1.2 served as a positive control (Fig. 3.19B). Co-transformations of RICKY1 with both domain swap constructs did not result in yeast growth on plates with a high stringency, although all recombinant proteins were expressed (Fig. 3.19C).

Even though the N-REM1.3/C-REM1.2 construct showed a weak growth on low stringency plates, these data clearly indicate that both the N- and the C-terminal regions of REM1.2 are needed for a proper interaction with RICKY1.
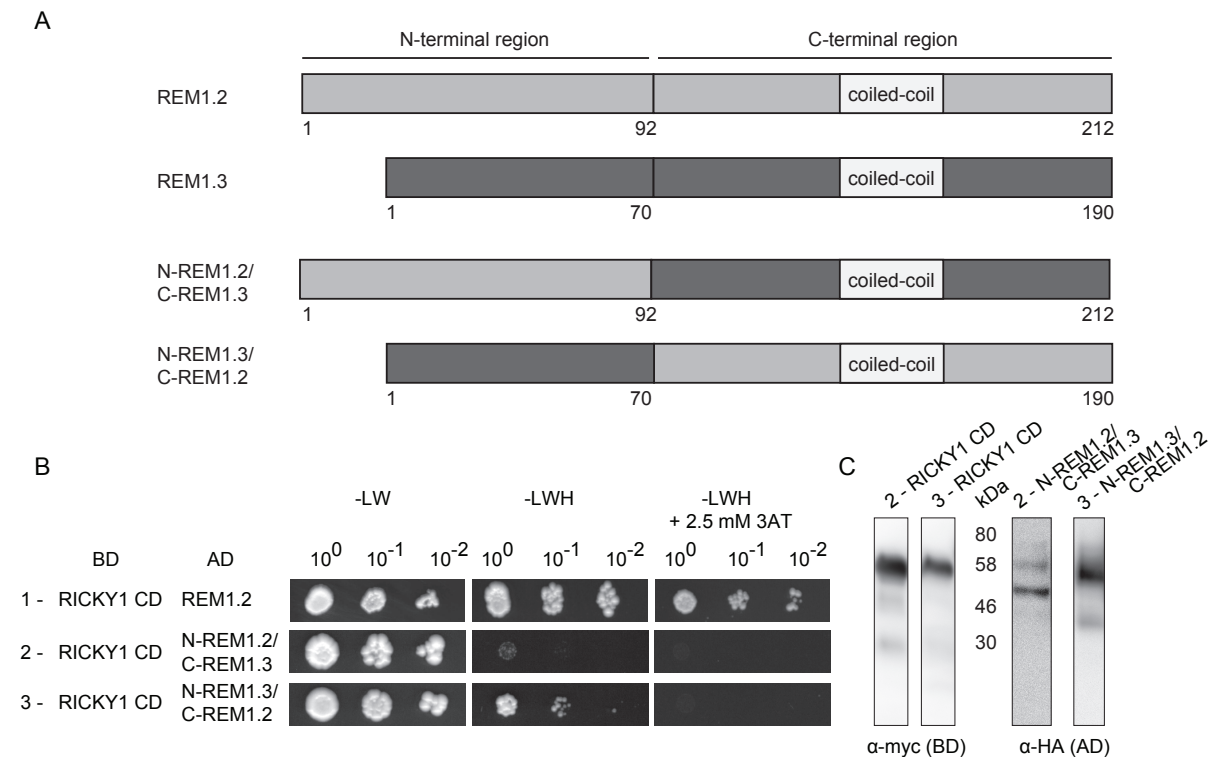
Fig. 3.19 The N- and the C-terminal region of REM1.2 are needed for a proper interaction with RICKY1 in yeast

(A) Schematic view of the protein structure of REM1.2 and REM1.3. For the domain swap experiment the N-terminal region of REM1.2 (AA 1-92) was fused to the C-terminal region of REM1.3 (AA 71-190) (N-REM1.2/C-REM1.3) and vice versa (N-REM1.3/C-REM1.2). The conserved coiled-coil domain is indicated in all constructs. (B) GAL4 Y2H assay between RICKY1 CD and chimeric remorin proteins. RICKY1 was fused to binding domain (BD) and the remorins to the activation domain (AD) of GAL4. Transformants were grown on control medium (-LW) and selective medium (-LWH +/- 2.5 mM 3-AT) in three consecutive dilutions. L = leucine, W = tryptophan, H = histidine, 3-AT = 3-amino-1,2,4-triazole. (B) The expression of proteins in yeast cells that did not grow on selective media was analyzed using immunoblot analysis. AD-fused proteins were visualized with an HA antibody and BD-fused proteins with a myc antibody.

It has been shown that the intrinsically disorder N-terminal region of remorin proteins harbors most of the identified *in vivo* phospho-sites (Marín & Ott, 2012). Since RICKY1 contains a predicted serine/threonine-protein kinase domain in its intracellular region (Fig. 3.2B), it was investigated if the interaction might be phosphorylation-dependent. Two approaches were followed up to answer this question.

First, the necessity of an active kinase domain was analyzed. For this, the conserved DFG motif in the kinase domain of RICKY1 was mutated to an NFG (D811N). This motif is located at the start of the activation segment and mediates polar contact to the phosphates of ATP (Hanks & Hunter, 1995; Johnson *et al.*, 1998). Mutations of the conserved aspartate are known to result in kinase-dead mutants (Yoshida & Parniske, 2005).

Second, the relevance of putative phospho-sites in REM1.2 was investigated. A sequence alignment of the N-termini of REM1.2 and the non-interacting REM1.3 was performed to identify phospho-sites that might be important for the interaction (Fig. 3.20A). Non-conserved *in vivo* phospho-sites present in REM1.2 and absent in REM1.3 were of special interest (see Marín & Ott, 2012). These serines and threonines were subsequently mutated to alanines to create phospho-ablative REM1.2 mutants. Accordingly, a quadruple (S11/S13/T18/T19A), a double (T41/T46A) and a single (T70A) mutant were generated.

The kinase-dead RICKY1 D811N as well as the three phospho-ablative mutants of REM1.2 were then tested in a GAL4 Y2H assay. The expression of recombinant proteins was confirmed by immunoblot analysis (Fig. 3.20C). The growth of yeast cells co-transformed with the active RICKY1 and wild type REM1.2 was used as positive control (Fig. 3.20B). The kinase-dead version of RICKY1 was no longer able to interact with REM1.2, indicating that the kinase activity of RICKY1 is essential for the interaction with REM1.2. The phospho-ablative mutants T41/T46A and T70A showed an interaction with RICKY1, while the quadruple mutant was not capable to interact with the kinase. This suggests that the region at the very beginning of REM1.2 is important for the interaction with RICKY1.

Accordingly, single phospho-ablative mutants were generated and additionally tested in a GAL4 Y2H experiment to specify the exact site of interaction. None of the single mutants showed an interaction with RICKY1 (Fig. 3.20B). This could imply that all four phospho-sites are involved in the interaction with RICKY1. Another explanation would be that a mutation in this intrinsically disordered region is sufficient to change the conformation of REM1.2 and to inhibit an interaction with RICKY1.

Additionally, the interaction of the quadruple mutant with the wild type REM1.2 was investigated to exclude that these mutations destroy the overall ability of REM1.2 to interact with other proteins. Since the co-transformed yeast cells were still able to grow on selective media, it can be concluded that this region is of special importance for the interaction with RICKY1.

A   Intrinsically disordered N-terminal region

REM1.3

MAEEQKTSKVDVESPAVLAPAKEPTPAP----------------------------------VEVADEKIHNPPP-------VESKALAVVEKPIEEHTPKKASSGSADRD

REM1.2

MAEEQK I ALESESPAKVTTPAPADTPAPAPAEIPAPAPAPTPADVTKDVAEEKIQNPPPEQIFDDSKALTVVEKPVEEPAPAKPASASLDRD

S11/S13/T18/T19   T41/T46   T70

B

C

α-myc (BD)   α-HA (AD)
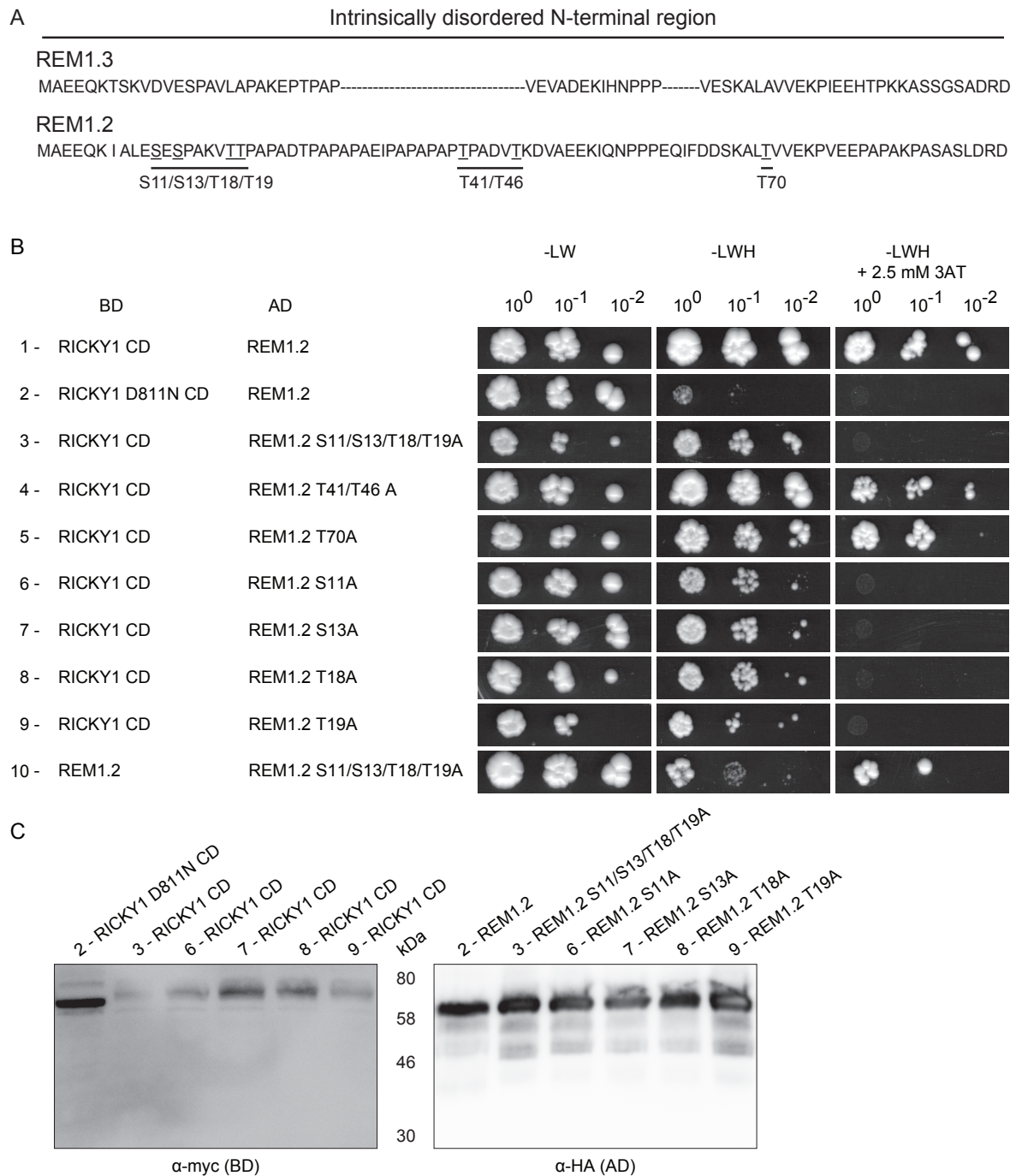
Fig. 3.20 The interaction of RICKY1 and REM1.2 is phosphorylation-dependent

(A) Amino acid sequence alignment of the N-terminal regions of REM1.2 and REM1.3 (Clustal Omega). Non-conserved phospho-sites present in REM1.2 but not in REM1.3 are underlined. These serines (S) and threonines (T) were mutated to alanines (A) to create phosho-ablative mutants of REM1.2. (B) GAL4 Y2H assay of RICKY1 wild type or kinase-dead (D811N) with REM1.2 wild type or phospho-ablative (S11/S13/T18/T19A, S11A, S13A, T18A, T19A, T41/T46A, T70A) mutants. Remorins were fused to the activation domain (AD) and the kinases to the binding domain (BD) of GAL4. Transformants were grown on control medium (-LW) and selective medium (-LWH +/- 2.5 mM 3-AT) in three consecutive dilutions. L = leucine, W = tryptophan, H = histidine, 3-AT = 3-amino-1,2,4-triazole. (C) The expression of proteins in yeast cells that did not grow on selective media was analyzed using immunoblot analysis (performed by the lab rotation student Michael Soutschek). AD-fused proteins were visualized with an HA antibody and BD-fused proteins with a myc antibody.

3.2.4.2.   RICKY1 is an active kinase

The previously shown interaction studies indicate that the interaction between RICKY1 and REM1.2 is dependent on phosphorylation (Fig. 3.20). However, the actual activity of the RICKY1 kinase domain has not been demonstrated so far. For this, the cytosolic domains of the active and the inactive RICKY1 were recombinantly expressed in *E. coli* cells. Therefore, both genes were cloned under the control of the T7 promoter for high-level protein expression (Studier & Moffatt, 1986) and should be transformed into Rosetta cells for an optimized codon-usage. Contrary to the inactive kinase, no successful transformation event was achieved for the active RICKY1. Even numerous repetitions with changed conditions (among others, lower growth temperatures, increasing glucose concentration, use of carbenicillin instead of ampicillin) did not solve the problem. This led to the conclusion that the active kinase might be toxic for the bacteria.

For this reason, the proteins were re-cloned under the control of the tightly regulated *tet* promoter, to reduce basal protein expression prior to induction (Skerra, 1994). Both constructs were successfully transformed into DH5α cells and protein expression was induced using anhydrotetracycline. Since the protein amount was too low to be detected via coomassie staining, the expression of recombinant proteins was verified by immunoblot analysis of the N-terminally fused Strep-tag. No proteins were detected in the non-induced control, compared to the induced samples (Fig. 3.21A). Interestingly, the active and the inactive kinase domains showed a different migration pattern, which was also visible for the RICKY1 variants expressed in yeast (Fig. 3.21C).

The higher molecular weight of the active protein could be due to post-translational modifications like phosphorylation. The protein was purified and subsequently incubated with different phosphorylation-specific antibodies to investigate if the active kinase is indeed phosphorylated. The tag-specific Strep antibody was used as control (Fig. 3.21B). RICKY1 could be detected with an antibody binding both, phosphorylated serines and threonines. For further specification, antibodies binding either phosphorylated serines or threonines were used. Compared to the α-phospho threonine, no signal was visible after incubation with the α-phospho serine antibody. These data indicate that the active kinase of RICKY1 contains at least one phosphorylated threonine residue.

Next, it was examined if the observed band shift was caused by the phosphorylation. Therefore, the purified active kinase was incubated with the fast alkaline phosphatase (FastAP) or a mock control. The migration behavior of the proteins was subsequently analyzed by SDS-PAGE and immunoblot analysis with Strep- and phospho Ser/Thr-specific

antibodies. A clear band shift was visible between the mock- and the phosphatase-treated kinase (Fig. 3.21C), comparable to the previously shown migration pattern of active and inactive RICKY1 proteins (Fig. 3.21A). The phosphorylation-specific antibody confirmed the dephosphorylation, since the FastAP-treated sample only showed a weak signal compared to the mock-treated control. The partially visible double bands might suggest that RICKY1 is phosphorylated at several residues.

Since the inactive kinase showed a lower molecular weight comparable to the dephosphorylated active kinase, it can be concluded that the phosphorylation of the active kinase was mainly caused by auto-phosphorylation and not by an endogenous kinase of *E. coli*.

Taken all together, these results indicate that RICKY1 contains a functional kinase domain and is able to auto-phosphorylate itself on at least one threonine residue in *E. coli*. Further studies need to be performed to examine the ability of RICKY1 to phosphorylate REM1.2.
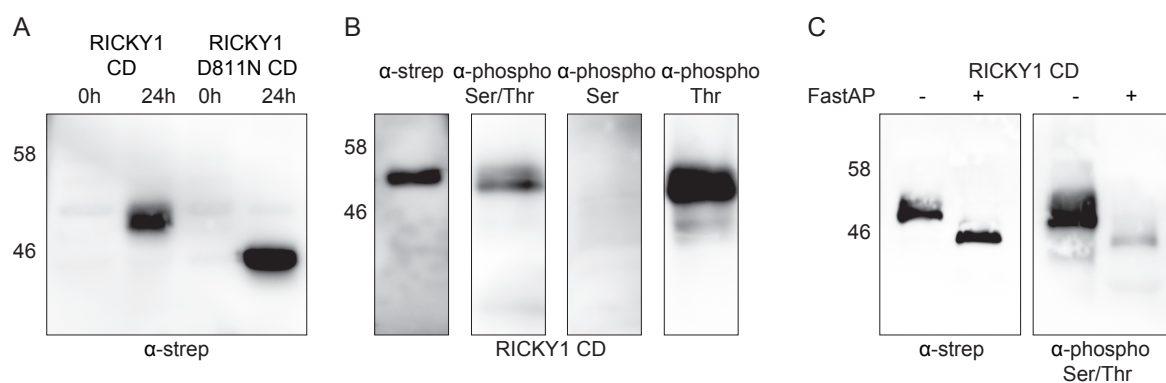
Fig. 3.21 RICKY1 is able to auto-phosphorylate itself on a threonine residue in *E. coli*

(A) Induced expression of the active and inactive (D811N) cytosolic domains (CD) of RICKY1 in *E. coli* DH5α cells. Proteins were N-terminally fused to a Strep-tag. The expression was induced with anhydrotetracycline and bacteria were harvest 24 h after induction. Samples were equalized to OD_{600} = 4 and loaded on a SDS-PAGE. Proteins were visualized using immunoblot detection with a Strep antibody. A clear band shift was visible comparing wild type and kinase-dead RICKY1. (B) Equal amounts of purified RICKY1 CD were detected with different phospho-antibodies and α-Strep as control. RICKY1 could be detected with phospho-threonine antibodies. (C) Purified RICKY1 was treated with a phosphatase (FastAP = fast alkaline phosphatase) or a mock control. Proteins were detected with Strep- and phospho-Ser/Thr antibodies. FastAP treated RICKY1 showed a clear band shift compared to the mock-treated control. Ser = serine, Thr = threonine, CD = cytosolic domain.

3.2.4.3. The localization and mobility of RICKY1 is not dependent on its kinase activity

Previous experiments showed that the mutation of the DFG motif in the kinase domain of RICKY1 results in an inactive kinase (Fig. 3.21) that is not longer able to interact with REM1.2 in yeast (Fig. 3.20). To analyze the importance of the kinase activity *in planta*, *ricky1-1* mutants were transformed with a genomic *RICKY1 D811N-sGFP* construct driven by its native promoter. First, it was investigated if the kinase-dead version of RICKY1 shows an altered subcellular localization compared to the active protein using confocal microscopy. Co-localization with the styryl dye FM4-64 revealed that RICKY1 D811N was still localized to the PM (Fig. 3.22A). Second, FRAP experiments were performed to analyze the mobility of the inactive in comparison to the active kinase. After normalization both RICKY1 variants displayed similar recovery curves (Fig. 3.22B) and a calculation of their mobile fractions revealed no significant difference between them (Fig. 3.22C). Both results indicate that the kinase activity of RICKY1 has no impact on its subcellular localization and mobility.
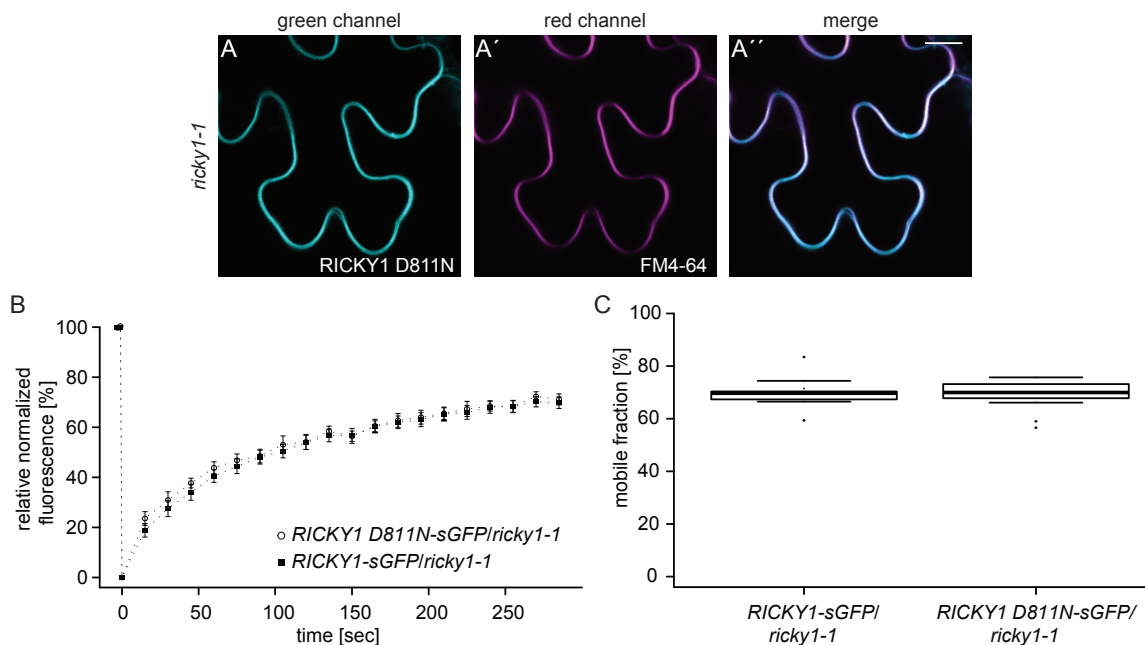
Fig. 3.22 The kinase activity of RICKY1 is not essential for its localization and mobility

Confocal microscopy of five-week-old *Arabidopsis* plants expressing *proRICKY1:gRICKY1 D811N-sGFP* or *proRICKY1:gRICKY1-sGFP* in the *ricky1-1* mutant background. (A-A´´) RICKY1 D811N-sGFP (A) co-localized with the PM dye FM4-64 (A´,A´´). Bar = 10 *μ*m. (B,C) Fluorescence recovery after photobleaching. Fluorescence intensities of bleached ROIs (region of interest) were normalized to non-bleached ROIs in their vicinity. (B) Normalized pre-bleach intensities were set to 100 % and normalized recovery rates +/- SE are shown over time. (C) There was no significant difference between active and inactive RICKY1 regarding the calculated mobile fraction. Statistical significance was assessed using a Student´s *t* test.

3.3. Characterization of the LRR-RLK At1g53430

RLKs represent a large monophyletic gene family with over 600 members in *Arabidopsis*. This corresponds to approximately 2.5 % of all protein-coding genes (Shiu & Bleecker, 2001b). Tandem as well as large-scale duplications of chromosomes seem to be responsible for this gene expansion (Shiu & Bleecker, 2001b; Shiu & Bleecker, 2003). Interestingly, a correlation was found between the function of RLKs and the number of duplication events. In contrast to RLKs participating in developmental processes, RLKs involved in plant immunity are often located in tandem clusters (Shiu *et al.*, 2004).

In the LRR subfamily VIII-2 73 % of all members, including *RICKY1*, are embedded into a gene cluster (Shiu & Bleecker, 2003). So far, the function of the majority of these proteins is still unknown. Only the LRR-RLK LIK1 (LYSM RLK1-INTERACTING KINASE 1; At3g14840) was shown to play a role during plant defense (Le *et al.*, 2014). Since closely related proteins are often involved in the same signaling pathway, we had a closer look at the members of this subgroup. Phylogenetic analyses identified the protein At1g53430 as the closest relative of RICKY1 (see Fig. 3.2; Shiu & Bleecker, 2001b; Gou *et al.*, 2010). An alignment of their full-length protein sequences revealed a similarity of 88 % (Clustal Omega). Considering only their kinase domains, both proteins showed a sequence similarity of 98 %.

In the following, the kinase At1g53430 was characterized especially regarding its putative function in plant immunity.

3.3.1.   At1g53430 is No Interaction Partner of Remorin Proteins in Yeast

Since RICKY1 and At1g53430 share a high sequence similarity especially in their C-terminal region, it was investigated whether the cytosolic domain of At1g53430 is able to interact with a remorin protein. For this purpose, the kinase was fused to the binding domain of GAL4 and co-transformed with AD-REM1.2 and AD-REM1.3 into the yeast strain PJ69-4a. While both co-transformed yeast cells grew slightly on SD –LWH plates, they were not capable to grow on media with higher stringency (Fig. 3.23A). Since even negative controls occasionally resulted in minor, unspecific yeast growth on low stringency plates (data not shown), only the growth on media with higher stringency was considered as interaction.

As the kinase showed no interaction with REM1.2 and REM1.3, it was called <u>R</u>ICKY1-<u>l</u>ike 1 or short RYL1. The homo-dimerization of REM1.2 and REM1.3 functioned as positive controls.
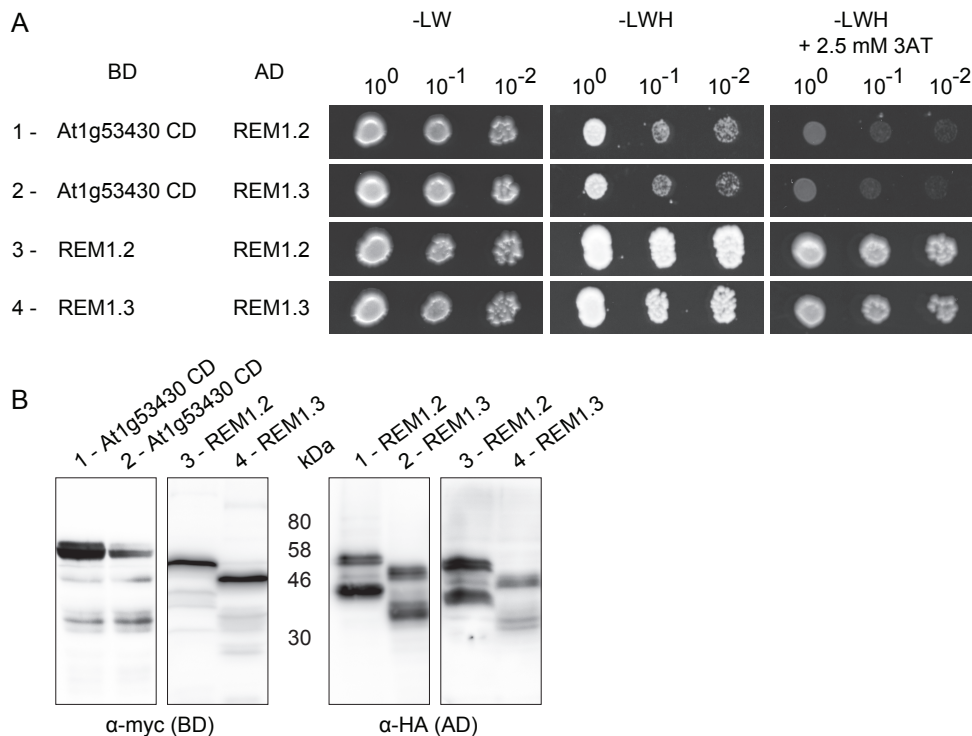
Fig. 3.23 RYL1 is not able to interact with remorin proteins in yeast

(A) GAL4 Y2H assay of the cytosolic domain (CD) of RYL1 with REM1.2 and REM1.3. Remorins were fused to the activation domain (AD) and RYL1 was fused to the binding domain (BD) of GAL4. Transformants were grown on control medium (-LW) and selective medium (-LWH +/- 2.5 mM 3-AT) in three consecutive dilutions. The interactions of REM1.2/REM1.2 and REM1.3/REM1.3 were used as positive controls. L = leucine, W = tryptophan, H = histidine, 3-AT = 3-amino-1,2,4-triazole.
(B) Expression analysis in yeast using immunoblot analysis. AD-fused proteins were visualized with an HA antibody and BD-fused proteins with a myc antibody.

3.3.2.   RYL1 is Involved in Plant Immunity

In the following experiments, the function of RYL1 was investigated. Therefore, a T-DNA insertion line in the Col-0 background was obtained and characterized. Sequencing of the *RYL1* locus revealed a T-DNA insertion in the 11th intron of *ryl1-1* mutant plants (Fig. 3.24A; Hofer, 2012). Quantitative RT-PCRs were performed to analyze if this gene disruption influences the expression of *RYL1*. 14-day-old *ryl1-1* seedlings showed a highly significant reduction in *RYL1* transcript levels compared to Col-0 (Fig. 3.24B). This knock-down line was subsequently used to examine the role of RYL1.

Fig. 3.24 *ryl1-1* plants show highly reduced *RYL1* transcript levels

(A) Schematic view of the T-DNA insertion site in the mutant line *ryl1-1* (Hofer, 2012). The position of the T-DNA (triangles) refers to the corresponding ATG (1). The orientation of the T-DNA is indicated by LB (left border) and RB (right border). Exons are represented as black boxes, introns as black lines. (B) qPCR analysis of the *RYL1* transcript in 14-day-old Col-0 and homozygous *ryl1-1* seedlings. The expression of *RYL1* was normalized to *UBC*. The transcript of *RYL1* was highly down-regulated in the mutant background (n = 4). Statistical significance was assessed using a Student´s *t* test (P≤ 0.001).

As RICKY1 was shown to be involved in plant immunity (see 3.2.2), it was investigated whether also RYL1 plays a role during plant defense. Similar to *ricky1* mutants, *ryl1-1* plants were challenged with the MAMP flg22 and the integrity of early, intermediate and late defense responses were analyzed.

Leaf discs of five-week-old Col-0, *ryl1-1* and *fls2* plants were floated with flg22 and the subsequent oxidative burst was measured over time. In contrast to *fls2* mutants, Col-0 as well as *ryl1-1* plants displayed flg22-specific response curves (Fig. 3.25A). The ROS production started only minutes after the application of flg22, reached its maximum after 8 minutes and decreased to background level 20 minutes later. A calculation of the total RLUs revealed no significant difference in ROS production between *ryl1-1* and Col-0 (Fig. 3.25B).

Next, the expression of SA- and JA/ET-dependent defense marker genes was investigated in five-week-old *ryl1-1* and Col-0 plants. The experiment was performed together with the *ricky1* mutants (see Fig. 3.6). Leaves were infiltrated with flg22 or H_2O and harvested 1 h or 24 h later. Transcript levels were analyzed using qPCR. The early JA/ET-regulated gene *ERF1* was significantly induced in the flg22-treated leaves of both lines compared to the mock controls (Fig. 3.25C). Nevertheless, the expression levels of *EFR1* in *ryl1-1* mutant plants were not significantly altered compared to wild type plants of the same treatment. Also the SA-dependent gene *PR1* was highly up-regulated 24 h after flg22 treatment compared to the mock control (Fig. 3.25D). However, no significant differences were observed between *ryl1-1* and Col-0 plants of the same treatment.

Taken together, these data indicate that early and intermediate flg22-triggered defense responses are not dependent on RYL1.
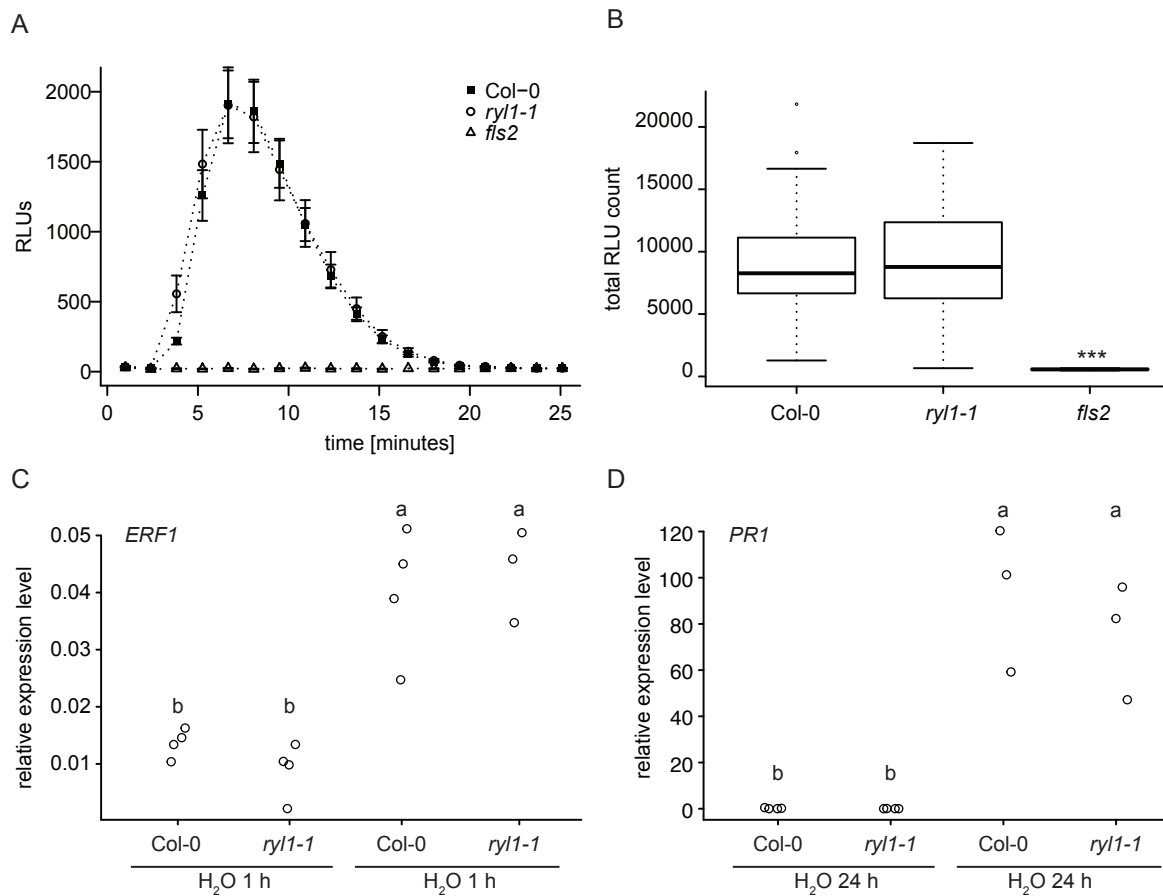
Fig. 3.25 *ryl1-1* is not impaired in early flg22-induced defense responses

(A,B) Leaf discs of five-week-old *Arabidopsis* plants were treated with 100 nM flg22 and ROS production was measured over time as RLUs (relative light units) (n = 21). (A) Values represent mean RLUs +/- SE at different time points. (B) Values represent total RLUs measured over 35 minutes. In contrast to *fls2, ryl1-1* plants did not display a significant difference to Col-0. Statistical significance was assessed using one-way ANOVA followed by Dunnett´s multiple comparison test (*** P≤ 0.001). (C,D) Five-week-old *Arabidopsis* leaves were infiltrated with H_2O or 1 μM flg22 and harvested 1 h (C) or 24 h (D) later (n = 3 − 4). Transcript levels of the marker genes *ERF1* (C) and *PR1* (D) were normalized to *UBC*. Col-0 and *ryl1-1* mutant plants showed an increased defense gene expression after flg22 treatment, but *ryl1-1* mutants did not display an altered expression compared to Col-0 of the same treatment. Statistical significance was assessed using one-way ANOVA followed by a Tukey HSD test (P≤ 0.05 (C), P≤ 0.001 (D)).

As it was shown that *ricky1* mutants were affected in the flg22-induced production of callose (see Fig. 3.7), this late defense mechanism was also analyzed in *ryl1-1* plants. Five-week-old Col-0, *ryl1-1* and *fls2* plants were infiltrated with flg22 or H_2O and harvested 24 h later. Fluorescence microscopy and a subsequent counting of callose depositions using ImageJ revealed that the callose production is significantly reduced to 55 % in flg22-treated *ryl1-1* mutant plants compared to Col-0 (Fig. 3.26A,C). Since the *fls2* mutants only showed isolated callose deposits, *ryl1-1* plants exhibited an intermediate phenotype.

On the other hand, no significant difference was observed between the mock-treated leaves of all three lines (Fig. 3.26B,D). These data clearly suggest the involvement of RYL1 in the flg22-induced production of callose.
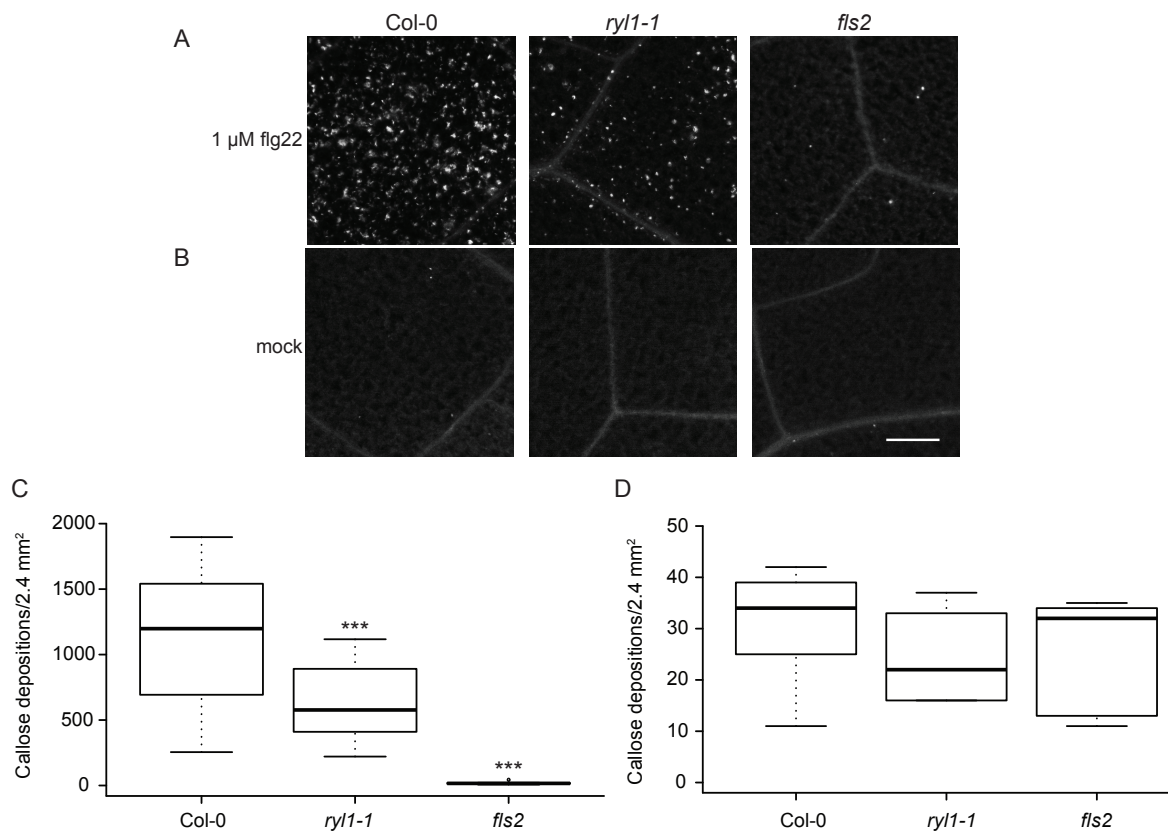
Fig. 3.26 RYL1 is involved in flg22-induced callose deposition

Five-week-old *Arabidopsis* leaves were infiltrated with 1 μM flg22 ((A,C) n = 13 – 15) or H_2O ((B,D n = 5)) and harvested 24 h later. Callose depositions in Col-0, *ryl1-1* and *fls2* were stained with methyl blue and analyzed using fluorescence microscopy. (A,B) Representative pictures. Bar = 200 μm. (C,D) The number of callose depositions was counted using ImageJ. Values represent the mean number of callose depositions. After flg22 treatment *ryl1-1* mutants showed a significant decrease in callose deposition (C), whereas there was no change in the mock control (D). Statistical significance was assessed using one-way ANOVA followed by Dunnett´s multiple comparison test (*** P≤ 0.001).

Subsequently, *ryl1-1* plants were challenged with various phytopathogens to analyze the importance of RYL1 during different infection processes. Five-week-old wild type, *ryl1-1* and *fls2* plants were spray-inoculated with the hemibiotrophic bacterium *Pto* DC3000. Leaf discs were harvested three days later to determine the bacterial growth in all lines. A highly significant increase in bacterial density was observed in *ryl1-1* and *fls2* mutants compared to Col-0 (Fig. 3.27A).
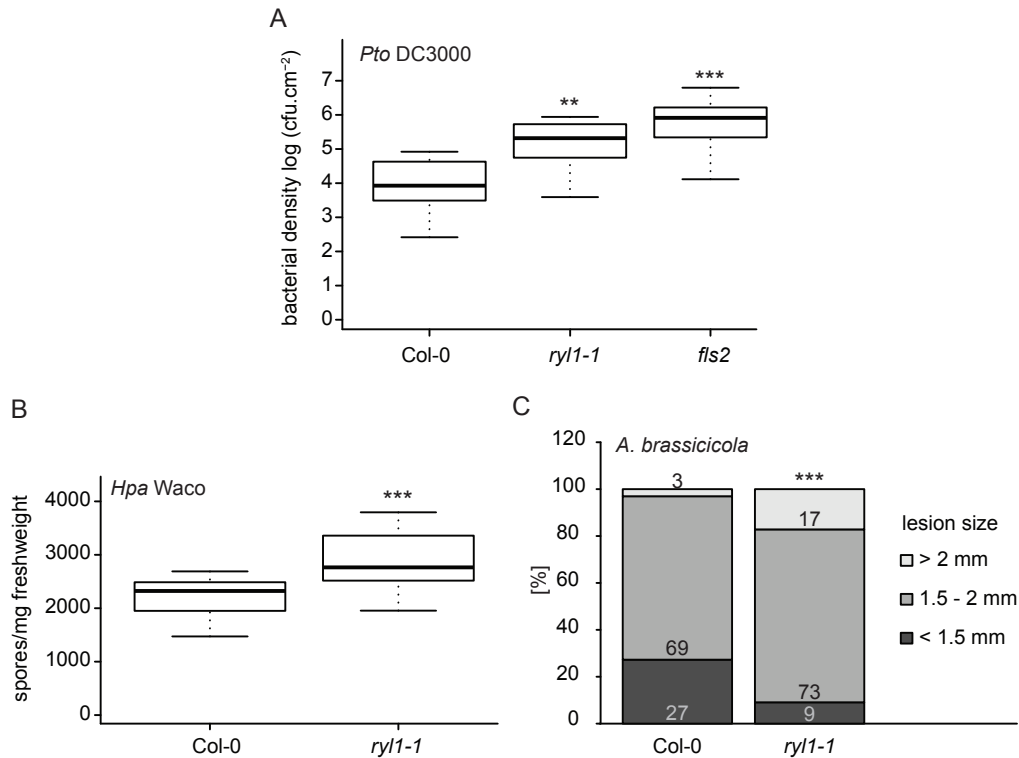
Fig. 3.27 *ryl1-1* is more susceptible to various pathogens

(A) Bacterial growth in *ryl1-1* mutant plants. Five-week-old plants were spray-inoculated with *Pseudomonas syringae* pv. *tomato* (*Pto*) DC3000 (OD_{600} = 0.02). Bacterial density was analyzed 3 dpi as colony forming units (cfu) (n = 12). The bacterial growth is significantly increased in *ryl1-1* plants compared to Col-0. *fls2* mutants were used as positive control. Statistical significance was assessed using one-way ANOVA followed by Dunnett´s multiple comparison test (** P≤ 0.01, *** P≤ 0.001).
(B) *Hpa* growth in *ryl1-1*. Ten-day-old *Arabidopsis* seedlings were spray-inoculated with the oomycete *Hpa* isolate Waco at 40,000 spores/ml. The sporulation rate was determined with a hemocytometer 24 h after the induction of sporulation. Values represent the average mean (n = 20). Spore rates were significantly higher in *ryl1-1* plants compared to Col-0. Statistical significance was assessed using a Student´s *t* test (*** P≤ 0.001). The experiment was performed by the collaborator Harald Keller.
(C) Distribution of lesion sizes in *Alternaria brassicicola* infected *ryl1-1* plants. 600 spores were dropped onto the leave surface of four-week-old *Arabidopsis* plants and lesion sizes were measured 4 - 5 days later. The graph represents a summary of 5 independent biological experiments (n = 99). Total numbers are indicated additionally. Lesion sizes were significantly altered in *ryl1-1* plants compared to Col-0. Statistical significance was assessed using Fisher´s exact test (*** P≤ 0.001). The experiments were performed by the collaborator Elisabeth Pabst.

The fitness of *ryl1-1* plants after the infection with other pathogens was analyzed by collaboration partners.

Harald Keller (UMR-Institut Sophia Agrobiotech) examined the interaction of wild type and *ryl1-1* plants with the biotrophic oomycete *Hyaloperonospora arabidopsidis*. Therefore, ten-day-old seedlings were spray-inoculated with the *Hpa* isolate Waco. The sporulation rate was determined seven days later using a hemocytometer. *ryl1-1* mutants showed a

significantly increased number of spores compared to Col-0 and are therefore more susceptible to the oomycete (Fig. 3.27B).

Additionally, the interaction of Col-0 and *ryl1-1* plants with *Alternaria brassicicola* was investigated by Elisabeth Pabst (Helmholtz Zentrum München). For this, spores of the necrotrophic fungus were dropped onto four-week-old *Arabidopsis* leaves. After 4 - 5 days, the severity of disease was determined by measuring the lesion diameters at the spots of infection. Lesions sizes differed significantly between *ryl1-1* leaves and Col-0 (Fig. 3.27C), indicating an increased susceptibility to the fungus.

Taken all together, these results indicate that RYL1 is involved in a general defense mechanism that is important to fend off various phytopathogens.

To confirm, that all shown phenotypes of *ryl1-1* plants are indeed caused by the T-DNA insertion in the *RYL1* locus, an independent *ryl1-2* allele was investigated by Sandy Niesik during her master thesis under my supervision (Niesik, 2016).

3.3.3.   Generating *ricky1/ryl1* Double Mutants

A comparison of *ricky1* and *ryl1* mutant phenotypes points to the fact that both proteins could be involved in the same signaling pathway (see 3.2.2 and 3.3.2). The mutants are not only affected in the same defense responses, also the severity of impairment is comparable between them. As both proteins are closely related (Fig. 3.2A) and share a high sequence similarity, they could play redundant roles during plant immunity. Therefore, *ricky1/ryl1* double mutants need to be generated and characterized to test this hypothesis.

However, the conventional genetic crossing is not suitable, since both genes lie next to each other on chromosome 1. In this case, double mutants can be created by several methods based on post-transcriptional gene silencing. The specific silencing of target genes can be induced by, among other, small non-coding microRNAs (miRNA) of 21-24 nucleotides. Longer, at least partially double stranded miRNA precursors are thereby processed by specific RNases of the Dicer family. The processed single-stranded miRNAs get then incorporated in the RNA-induced silencing complex (RISC) and mediate the specific cleavage of target mRNAs with complementary sequences (Chen, 2005).

By using the endogenous miRNA precurser MIR319a as template, artificial miRNAs (amiRNAs) can be genetically engineered to target any gene of interest. For the design of

amiRNAs, that exclusively silence *RICKY1* or *RYL1* transcripts, the Web microRNA Designer (WMD3) tool was used (Schwab *et al.*, 2006; Ossowski *et al.*, 2008). Following the WMD3 guidelines (see 5.2.6), two amiRNAs, targeting specific sequences in the kinase domain of *RICKY1* or *RYL1,* were cloned under the control of a 35S promoter, respectively (Fig. 3.28A,B).

First of all, the functionality of these constructs was tested transiently in *N. benthamiana* leaves. Therefore, the *proRICKY1:gRICKY1-sGFP* construct was expressed alone or together with the *35S:amiRICKY1* construct, and the GFP fluorescence was analyzed three days later using confocal microscopy. Co-expression of *RICKY1-sGFP* and *amiRICKY1* resulted in a highly reduced fluorescence compared to the *RICKY1-sGFP* alone control (Fig. 3.28C,D), showing the functionality of the *RICKY1* amiRNA.

The *amiRYL1* construct was co-transformed with *RICKY1-sGFP* to determine the specificity of the gene silencing. In contrast to *amiRICKY1*, no obvious changes in the GFP intensity were observed in cells co-expressing *RICKY1-sGFP* and *amiRYL1* (Fig. 3.28E). These results indicate a specific targeting of the *RICKY1* mRNA by *amiRICKY1*.

An examination of the *amiRYL1* construct was not viable in *N. benthamiana*, since no functional *proRYL1:gRYL1* construct was available.
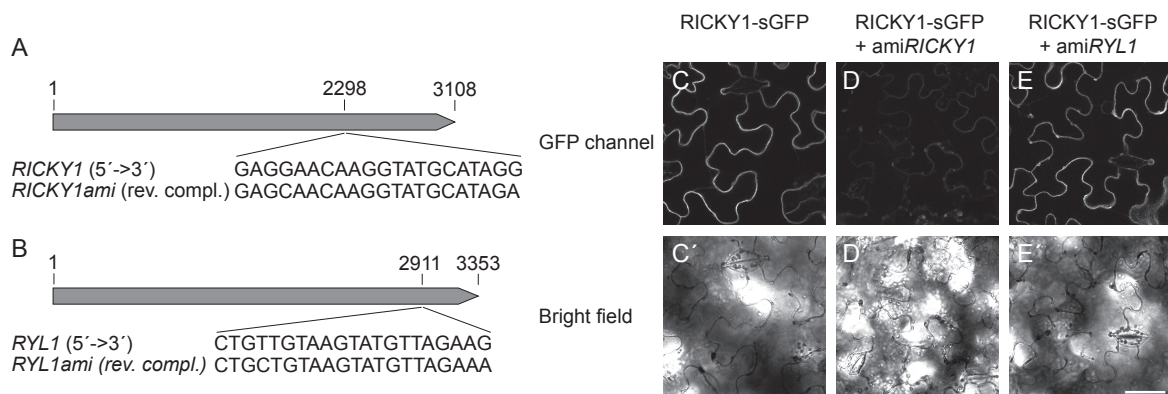
Fig. 3.28 Identification of artificial microRNA to specifically target *RICKY1* and *RYL1*

(A,B) Schematic view of *RICKY1* (A) and *RYL1* (B) mRNAs with the corresponding artificial microRNAs (amiRNAs). AmiRNAs were designed with the WMD3 tool of the Weigel lab. The binding sites of the amiRNAs and their sequences are indicated. (C,D) The functionality of the *RICKY1* amiRNA construct was tested transiently in *N. benthamiana*. The fluorescence signal of RICKY1-sGFP was analyzed in leaves expressing *proRICKY1:gRICKY1-sGFP* alone (C), together with the *amiRICKY1* construct (D) or as a control the *amiRYL1* construct (E). Co-expression with *amiRICKY1*, but not with *amiRYL1* led to decreased GFP signal at the PM. Bar = 50 µm.

Since the functionality as well as the specificity of *amiRICKY1* was demonstrated in the transient *N. benthamiana* system (see Fig. 3.28), both amiRNA constructs were subsequently transformed into *Arabidopsis* to generate *ricky1/ryl1* double mutants. To facilitate this process *ricky1-1* and *ryl1-1* single mutants were used as genetic background. Both lines were transformed with the amiRNA construct that targets the other gene, respectively.

23 stable transformed *amiRYL1/ricky1-1* and 31 *amiRICKY1/ryl1-1* T0 plants were identified and their *RICKY1* and *RYL1* transcript levels were determined immediately. Col-0 as well as non-transformed *ricky1-1* and *ryl1-1* single mutants were used as controls. As expected, all mutants showed a highly reduced transcript corresponding to their genetic background (Fig. 3.29). Concerning the expression of the amiRNA-targeted gene, a high variability in transcript levels was observed in both mutant backgrounds. As the relative expression level was based on one sample, only plants showing less than 30 % transcript compared to Col-0 were used for further propagation.
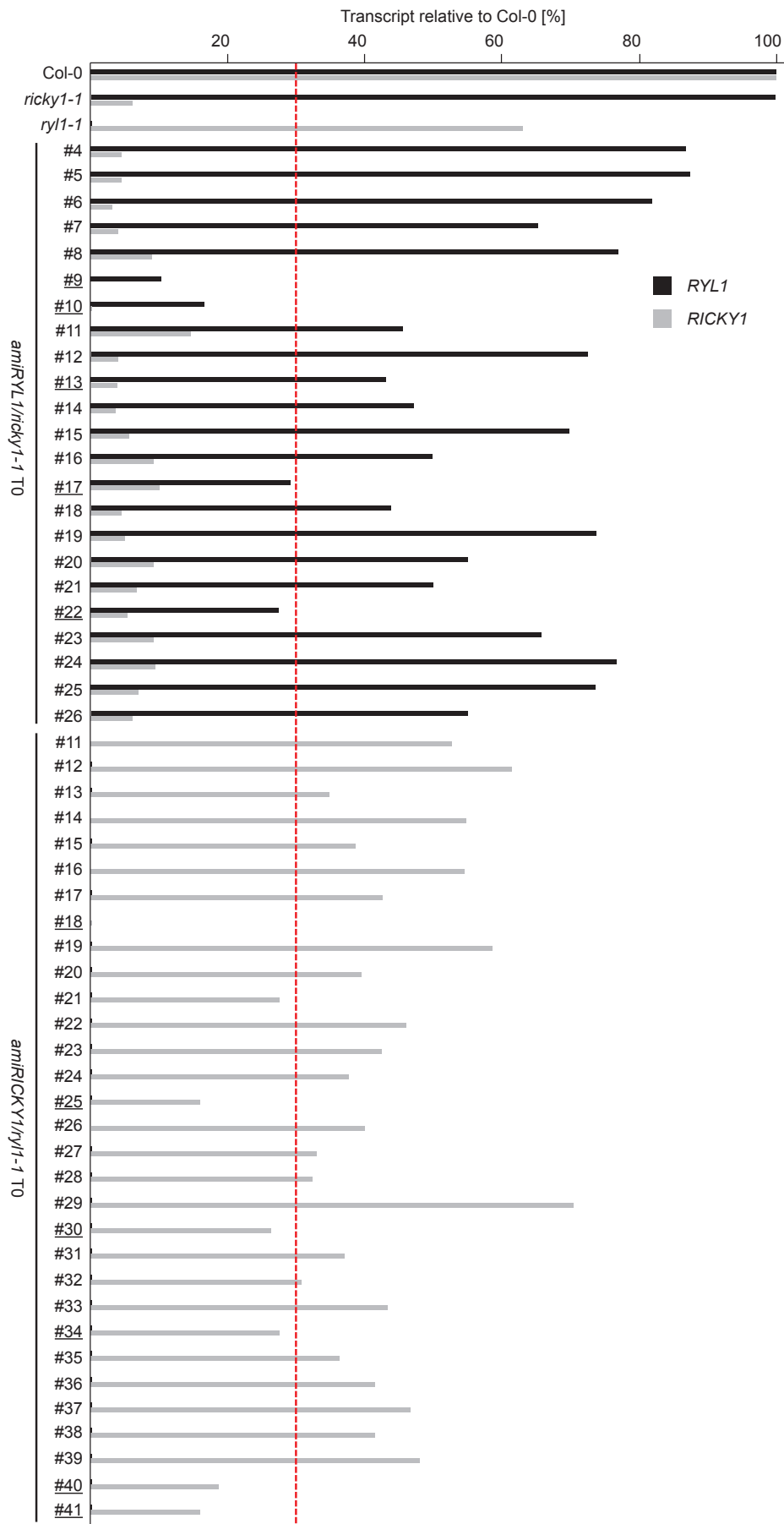
See legend on next page

Fig. 3.29 Identification of heterozygous amiRNA lines with reduced transcript levels

qPCR analysis of five-week-old heterozygous T0 *Arabidopsis* plants expressing 35S-driven *amiRICKY1* in the homozygous *ryl1-1* mutant background and *amiRYL1* in the homozygous *ricky1-1* mutant background. Col-0, *ricky1-1* and *ryl1-1* were used as controls (n = 1). Transcripts of *RICKY1* (grey bars) and *RYL1* (black bars) were normalized to *UBC*. Expression levels in Col-0 were set to 100 %. The red dotted line indicates 30 % transcript compared to Col-0. *amiRYL1* and *amiRICKY1* lines that showed reduced expression levels in the corresponding transcript (underlined) were used for further propagation.

Two generations later, homozygous plants were identified for five independent *amiRYL1/ricky1-1* (#9, 10, 13, 17, 22) and for four *amiRICKY1/ryl1-1* (#18, 30, 40, 41) lines. These plants were used to verify the gene silencing, shown in the heterozygous T0 plants (see Fig. 3.29), and to determine the actual transcript levels. Therefore, qPCRs were performed for Col-0, *ricky1-1, ryl1-1* and all double mutants.

First, *RICKY1* expression levels were analyzed in all lines. As expected, *ricky1-1* and all *amiRYL1/ricky1-1* plants showed a significant decrease in the *RICKY1* transcript compared to Col-0 (Fig. 3.30A). However, the transcript was not significantly different in *ryl1-1* and *amiRICKY1/ryl1-1* plants. The same was true for the expression of *RYL1*. It was significantly down-regulated in all plants in the *ryl1-1* background, but none of the *amiRYL1/ricky1-1* plants displayed a reduced transcript level compared to Col-0 (Fig. 3.30B). In contrast, all *amiRYL1/ricky1-1* lines even displayed a tendency for enhanced *RYL1* transcripts that was significant in *amiRYL1/ricky1-1* line #22. Unfortunately, no *ricky1/ryl1* double mutant could be generated using amiRNAs.
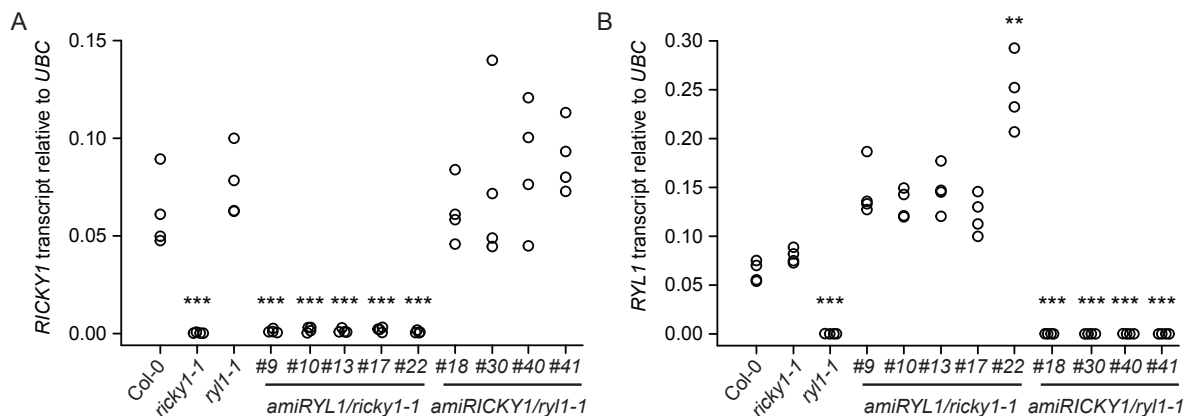
Fig. 3.30 Homozygous amiRNA lines do not show reduced transcript levels

qPCR analysis of 11-day-old homozygous *Arabidopsis* seedlings expressing 35S-driven *amiRICKY1* in the *ryl1-1* mutant background and *amiRYL1* in the *ricky1-1* mutant background. Col-0, *ricky1-1* and *ryl1-1* were used as controls (n = 4). Transcripts of *RICKY1* (A) and *RYL1* (B) were normalized to *UBC.* The corresponding transcript is not silenced in the homozygous *amiRYL1* and *amiRICKY1* lines, respectively. Statistical significance was assessed using one-way ANOVA followed by Dunnett´s multiple comparison test (** P≤ 0.01, *** P≤ 0.001).

3.4. *RICKY1* and *RYL1* are Up-Regulated Upon Infiltration

RICKY1 and RYL1 were demonstrated to be involved in flg22-induced defense responses (see 3.2.2 and 3.3.2). In line with these results, both transcripts have been shown to be slightly up-regulated in Ler-0 seedlings 30 min after flg22 treatment (Zipfel *et al.*, 2004). In the following, it was examined if *RICKY1* and *RYL1* are also differentially regulated at early and later time points in Col-0 plants. Therefore, both transcripts were determined in the defense marker gene expression experiment shown in Fig. 3.6. Here, five-week-old Col-0 leaves were infiltrated with 1 μM flg22 or H_2O and harvested 1 h and 24 h later.

No significant difference was observed regarding the expression of *RICKY1* in H_2O and flg22-treated leaves, harvested at the same time point (Fig. 3.31A). However, transcript levels in leaves harvested 24 h after infiltration were significantly reduced compared to samples harvested 1 h after infiltration, independent of the treatment.

The analysis of *RYL1* yielded similar results (Fig. 3.31B). No altered expression was observed between H_2O and flg22-treated leaves, but a significantly decreased transcript level was visible 24 h after infiltration compared to the earlier time point.

In these experiments the published flg22-triggered transcript induction of *RICKY1* and *RYL1* could not be repeated. This could be due to another *Arabidopsis* ecotype, the developmental stage of the plants or the method used for flg22 treatment (see Zipfel *et al.*, 2004 and 5.5.13). However, the time-dependent regulation of both transcripts after infiltration was unexpected, but interesting and was investigated more precisely.
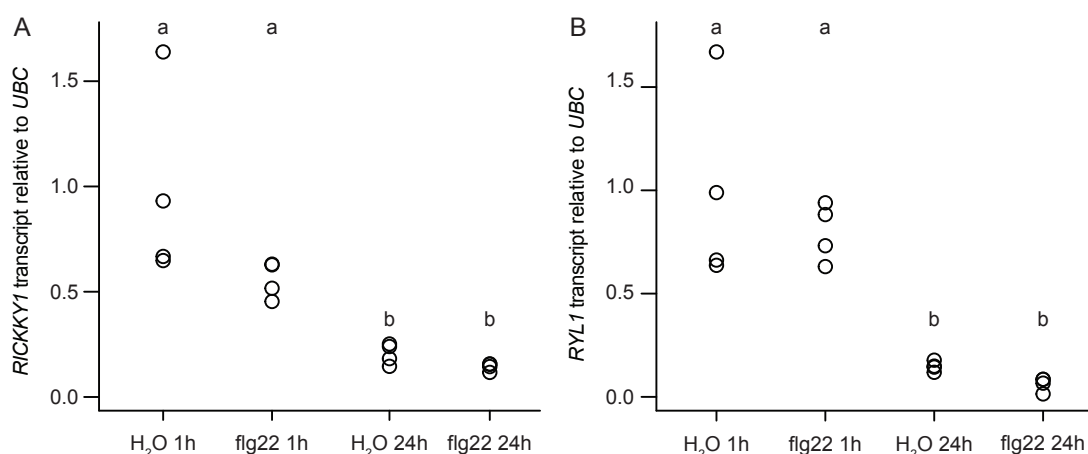
Fig. 3.31 *RICKY1* and *RYL1* transcripts are differently regulated 1 h and 24 h after infiltration

Five-week-old Col-0 plants were infiltrated with H_2O or flg22 and harvested 1 h and 24 h later. *RICKY1* (A) and *RYL1* (B) transcripts were analyzed using qPCR. Both transcripts were significantly lower 24 h after infiltration compared to 1 h after infiltration independent of the treatment. Statistical significance was assessed using one-way ANOVA followed by a Tukey HSD test (P $\leq$ 0.005).

Therefore, time course experiment with five-week-old Col-0 plants was performed to examine the differential regulation of *RICKY1* and *RYL1* in more detail. As the observed induction occurred independent of the applied solution (see Fig. 3.31), H_2O was used for the infiltration of *Arabidopsis* plants. Subsequently, leaves were harvested 15 min, 30 min, 1 h, 3 h, 6 h, 12 h and 24 h after infiltration as well as prior to infiltration (0 h). Quantitative PCRs were performed and all transcripts were calculated relative to the non-infiltrated control.

First, the *RICKY1* transcript levels were analyzed. The expression of *RICKY1* increased significantly 30 min after infiltration and reached its maximum of 4-fold induction after 1 h (Fig. 3.32A). The induction was durable within 12 h and decreased to control levels after 24 h.

Second, the *RYL1* expression levels were determined. Its increase started 30 min after infiltration and showed a highly significant 23-fold induction after 1 h (Fig. 3.32B). In contrast to *RICKY1*, the *RYL1* expression dropped to control levels already after 3 h.

In short, the differential regulation upon infiltration could be verified for both LRR-RLKs.

REM1.2 and REM1.3 have been shown to co-localize with RICKY1 in small micro-domains at the PM (see Fig. 3.14). Additionally, REM1.2 was demonstrated to be a direct interaction partner of RICKY1 (see Fig. 3.16). Hence, the expression of these genes was also examined. The transcript level of *REM1.2* was significantly enhanced 30 min after infiltration and exhibited a peak after 1 h with a 3-fold induction compared to the control. Subsequently, the transcript gradually declined to control levels (Fig. 3.32C).

REM1.3 displayed a similar pattern (Fig. 3.32D). Its transcript level showed a significant increase after 15 min and a maximum of 9-fold induction after 1 h. After 3 h the expression of *REM1.3* approximated progressively to control levels.

All analyzed genes exhibited a significantly induced expression after infiltration, which peaked after 1 h, and decreased to control levels after 24 h latest.
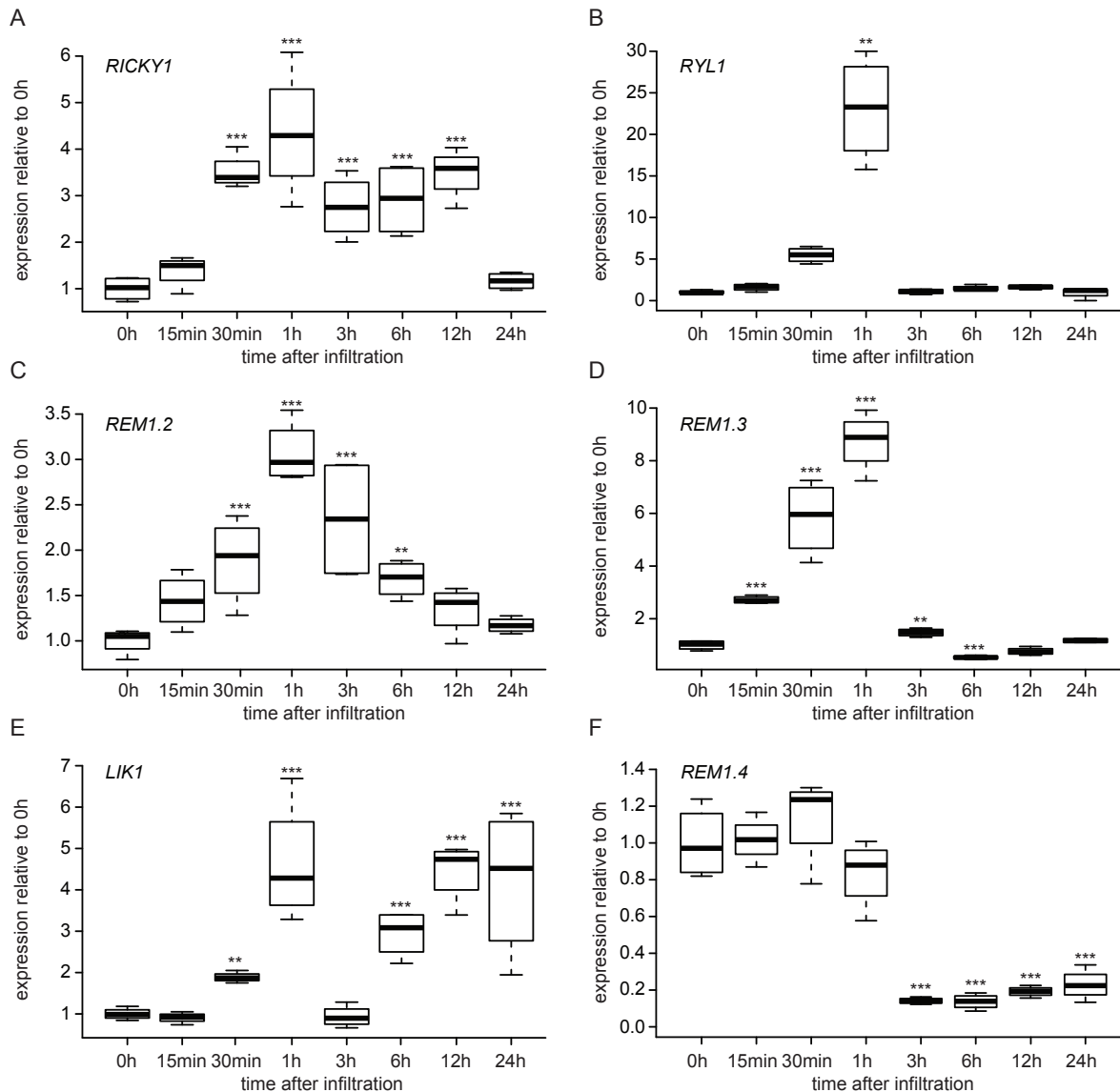
Fig. 3.32 *RICKY1, RYL1, REM1.2* and *REM1.3* are up-regulated upon infiltration

Five-week-old Col-0 leaves were infiltrated with H_2O and harvested at the indicated time points (n = 4). *RICKY1* (A), *RYL1* (B), *REM1.2* (C), *REM1.3* (D), *LIK1* (E) and *REM1.4* (F) transcripts were normalized to *UBC*. Transcripts in the non-infiltrated control (0 h) were set to 1, respectively. Statistical significance was assessed using one-way ANOVA followed by Dunnett´s multiple comparison test (** $P \leq 0.01$, *** $P \leq 0.001$).

In the following, additional transcripts were to ensure that the observed regulation is specific for these genes and not a common pattern.

On the one hand, the expression of another MD-containing LRR-RLK was investigated. LIK1 is related to RICKY1 and RYL1 (Fig. 3.2A) and has been demonstrated to be involved in plant immunity only recently (Le *et al.*, 2014). The transcript of *LIK1* showed a very dynamic pattern. It was significantly up-regulated after 30 min and 1 h, and decreased to control level

after 3 h (Fig. 3.32E). In contrast to *RICKY1* and *RYL1*, *LIK1* displayed an additional induction after 6 h, which was durable within 24 h.

On the other hand, the expression of another *Arabidopsis* remorin was examined. As REM1.2 and REM1.3, REM1.4 belongs to the subgroup 1 (Raffaele *et al.*, 2007), but recent studies indicated an involvement of REM1.4 homologues in abiotic stress responses (Checker & Khurana, 2013; Yue *et al.*, 2014). Accordingly, *REM1.4* showed a altered expression pattern after infiltration compared to *REM1.2* and *REM1.3.* The *REM1.4* transcript was significantly down-regulated to 20 % compared to the non-infiltrated control 3 h after infiltration and did not recover over time (Fig. 3.32F).

In summary, these results clearly demonstrate that the described differential regulation is specific for *RICKY1*, *RYL1*, *REM1.2* and *REM1.3*. This might indicate that these proteins are involved in a signaling pathway triggered by infiltration. An additional experiment was performed to investigate this in more detail.

Since the induced expression after infiltration was independent of the solution (see Fig. 3.31), the question arose about the actual trigger. Mechanical wounding of the leaf during the infiltration process might cause the altered gene expression.

Subsequently, five-week-old Col-0 leaves were wounded with a needle and harvested 1 h and 24 h later. As control, non-treated leaves (0 h) were used and their transcript levels were set to 1. In contrast to infiltration, mechanical wounding did not result in an induced expression of *RICKY1* after 1 h (Fig. 3.33A). However, 24 h later the expression of *RICKY1* was significantly reduced compared to the control. A similar pattern was observed for the expression of *RYL1* (Fig. 3.33B).

Additionally, the transcripts of *REM1.2* and *REM1.3* were examined. Both genes showed opposite tendencies regarding their regulation 1 h after wounding, but no significant differences were observed at this time point. However, the expression of *REM1.3* was significantly reduced after 24 h (Fig. 3.33C,D).

The transcript levels of *JAZ10* and *LOX3*, two wound-induced marker genes, were analyzed to ensure that the treatment worked in this experiment (Yan *et al.*, 2007; Wang *et al.*, 2008). As expected, both transcripts were significantly induced 1 h after mechanical wounding (Fig. 3.33E,F). They displayed a significant decrease 24 h after wounding compared to the non-treated control.

These data clearly demonstrate that the induced expression of *RICKY1*, *RYL1*, *REM1.2* and *REM1.3* upon infiltration (see Fig. 3.32) is not caused by mechanical wounding.
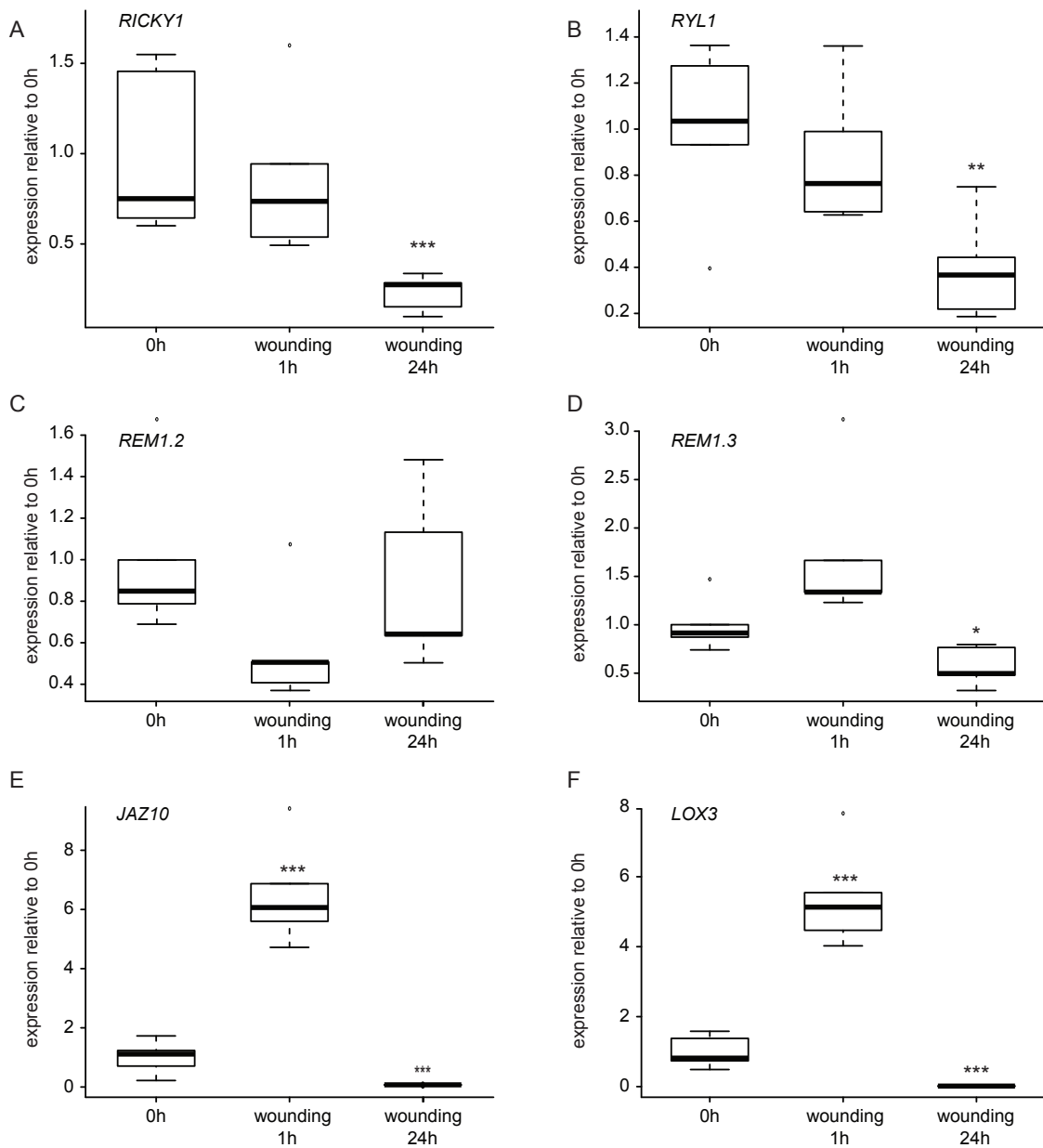
Fig. 3.33 *RICKY1*, *RYL1*, *REM1.2* and *REM1.3* are not up-regulated upon wounding

Five-week-old Col-0 leaves were wounded with a needle and harvested at the indicated time points. *RICKY1* (A), *RYL1* (B), *REM1.2* (C), *REM1.3* (D), *JAZ10* (E) and *LOX3* (F) transcripts were normalized to *UBC*. The wounding marker genes *JAZ10* and *LOX3* were used as controls. Transcripts in the non-wounded control (0 h) were set to 1, respectively. Statistical significance was assessed using one-way ANOVA followed by Dunnett´s multiple comparison test (* P≤ 0.05, ** P≤ 0.01, *** P≤ 0.001).

4. Discussion

Recent data demonstrates the co-existence of various micro-domains labeled by different remorin proteins at the PM of *Arabidopsis* (Jarsch *et al.*, 2014). Remorins are postulated to act as molecular scaffolds and play a role during the assembly of active signaling hubs (Jarsch & Ott, 2011). Interestingly, micro-domains targeted by closely related proteins show a high degree of co-localization, indicating a functional compartmentalization of the PM (Spira *et al.*, 2012; Jarsch *et al.*, 2014).

So far, remorins have been demonstrated to participate in several abiotic and biotic stress-related pathways (Raffaele *et al.*, 2009; Checker & Khurana, 2013; Gui *et al.*, 2016). Members of the remorin group 1 are thought to be involved in plant immunity (Coaker *et al.*, 2004; Benschop *et al.*, 2007; Liu *et al.*, 2009; Widjaja *et al.*, 2009; Keinath *et al.*, 2010; Jarsch & Ott, 2011), even though their actual function has not been determined so far.

We hypothesize that these remorins are promising candidates to explore the protein composition of a plant immunity-associated signaling platform. Consequently, REM1.2 was used as a bait to identify novel components of plant defense. Therein, the LRR-MD RLK RICKY1 was found to be a specific interaction partner of REM1.2 (Jarsch, 2014).

Here, I characterized RICKY1 with focus on its putative function in plant immunity and its subcellular organization.

4.1. RICKY1 in Plant Immunity

Plant defense is an elaborate, multi-layered system based on the early recognition of microbial pattern at the PM, followed by an immediate initiation of several defense mechanisms. First responses such as protein complex formation and early phosphorylation events start only seconds after perception of the bacterial elicitor flg22 (Gomez-Gomez *et al.*, 1999; Schulze *et al.*, 2010). Subsequently, downstream signaling cascades mediate further cellular modulations such as the increased production of ROS, the activation of MAPKs cascades and the enhanced callose synthesis. These responses occur minutes, hours or days later (Gomez-Gomez *et al.*, 1999; Bigeard *et al.*, 2015).

Interestingly, *ricky1* and *ryl1* plants display a reduction in late callose deposition upon flg22 application (Fig. 3.7, Fig. 3.8, Fig. 3.26), whereas earlier responses are not affected in the mutants (Fig. 3.5, Fig. 3.6, Fig. 3.25). This genetically locates both proteins downstream of

ROS production and MAPK activation, but upstream of callose deposition. Also the L-type lectin receptor kinase-V1.2 (LecRK-VI.2) was shown to be involved in distinct processes including stomatal closure, callose deposition, defense gene expression and MAPK activation. Other responses such as the dimerization of FLS2 and BAK1, the phosphorylation of BIK1 and ROS production are not impaired in *lecrk-VI.2* mutants (Singh *et al.*, 2012). In line with this, Smith and colleagues proposed at least three independent signaling pathways, rather than a single, linear cascade. They demonstrated an opposing role in plant immunity for the dynamin-related protein DRB2B, which is partially required for the flg22-induced endocytosis of FLS2. It acts as a negative regulator of RBOHD-dependent and as a positive regulator of RBOHD-independent processes, while it is not involved in the activation of MAPK signaling cascades (Smith *et al.*, 2014). Therefore, RICKY1 and RYL1 might be important for late signaling responses or even for a callose-specific pathway.

In the last years, the involvement of tryptophan-derived indole glucosinolate (IG) metabolites in flg22-induced callose deposition has been demonstrated (Clay *et al.*, 2009; Luna *et al.*, 2011). IGs are hydrolyzed by the peroxisome-localized myrosinase PEN2 (Lipka *et al.*, 2005; Bednarek *et al.*, 2009) and resulting metabolites are transported to the apoplast by the PM-localized ABC transporter PEN3 (Kobae *et al.*, 2006; Stein *et al.*, 2006; Bednarek *et al.*, 2009). In addition to their antimicrobial effect, IG breakdown products are involved in the induction of callose synthesis (Clay *et al.*, 2009). In line with this, Luna and colleagues proposed a function of callose in detoxification of toxic antimicrobial compounds (Luna *et al.*, 2011). PEN3 was shown to be phosphorylated downstream of activated MPK3 and MPK6 (Lassowskat *et al.*, 2014). But since PEN3 lacks a typical MAPK target site, another kinase downstream of MPK3/6 might be involved (Lassowskat *et al.*, 2014; Xu *et al.*, 2016). However, the biological function of this phosphorylation still needs to be investigated. It would be interesting to test, if RICKY1 or RYL1 might play a direct or indirect role in this process. Especially, because PEN3 is involved in the transport of the auxin precursor IBA (Strader & Bartel, 2009) and RICKY1 could play a role in auxin-related processes (Fig. 3.4; ten Hove *et al.*, 2011). As *ricky1* and *ryl1* mutants, also *pen3* plants are more susceptible to various pathogens of different lifestyles (Fig. 3.9, Fig. 3.10, Fig. 3.27; Stein *et al.*, 2006; Xin *et al.*, 2013). Additionally, PEN3 was shown to re-localize upon flg22 treatment (Underwood & Somerville, 2013) and *Blumeria graminis* f. sp. *hordei* (*Bgh*) infection (Stein *et al.*, 2006) to the site of PAMP detection and powdery mildew penetration, respectively. There, PEN3 displays a clear co-localization with callose deposits (Underwood & Somerville, 2013).

Callose synthesis is known to be active at sites of direct pathogen contact: in papillae, that are formed in response to filamentous pathogens penetrating the cell, and in encasements, which encompass haustoria of fungi and oomycetes (Voigt, 2014; Faulkner, 2015). The PM-localized callose synthase PMR4/GLS5 is responsible for callose depositions in papillae (Jacobs *et al.*, 2003; Nishimura *et al.*, 2003), haustorial encasements (Meyer *et al.*, 2009) as well as at sites of flg22 perception (Luna *et al.*, 2011). However, concerns have been raised about a role of callose in resistance against fungal pathogens, since *pmr4* mutants showed an enhanced resistance to *Bgh* and *Golovinomyces orontii* (Jacobs *et al.*, 2003; Nishimura *et al.*, 2003). Nevertheless, plants overexpressing PMR4 show a complete penetration resistance to *Golovinomyces cichoracearum* (Ellinger *et al.*, 2013). The increased production of callose leads to an extensive migration into pre-existing cellulose fibrils, that results in a resistance against CW hydrolyzing enzymes. This conjunction builds an effective physical barrier against a pathogenic invasion (Eggert *et al.*, 2014). These opposing results indicate the importance of a strict spatial and temporal activation of callose synthesis. This regulation might occur through protein interactions, complex formation or active vesicle-dependent transport to the site of attack (Meyer *et al.*, 2009; Ellinger *et al.*, 2013; Ellinger & Voigt, 2014). Also post-translational modifications play an important role. Distinct phospho-sites have been identified in PMR4, which are essential for the transport to the site of infection or the activation of PMR4. However, the corresponding kinase(s) have not been identified so far (Christian A. Voigt 2014, presented at the 16th MPMI conference). Since RICKY1 plays a role in callose deposition (Fig. 3.9, Fig. 3.10) and localizes to sites of growing oomycete structures (Fig. 3.13), it might be directly or indirectly involved in this process.

Upon *Hpa* infection, the localization of RICKY1 shows an increased signal at sites of hyphal growth (Fig. 3.13A), even though it is homogeneously distributed at the PM in uninfected leaves (Fig. 3.11). Additionally, RICKY1 signal accumulates at the haustorial neck and is visible around the haustoria. During host invasion, these specialized feeding structures remain enveloped by the plant-derived EHM. The EHM separates the haustorium from the host cytoplasm and serves as interface for the delivery of effectors to the host cell as well as for the nutrient uptake by the pathogen (Voegele & Mendgen, 2003; O'Connell & Panstruga, 2006). Mature haustoria are additionally enclosed by a double-layered encasement membrane that is enriched in callose (Soylu & Soylu, 2003; O'Connell & Panstruga, 2006). Even though the EHM as well as the encasement membrane are continuous with the host PM, their protein composition can be different. While several PM-localized proteins are excluded from the EHM, all analyzed PM proteins localize to the encasement, indicating distinct trafficking pathways (Koh *et al.*, 2005; Lu *et al.*, 2012b).

To examine, if RICKY1 localizes to the EHM or the encasement membrane, a detailed characterization was performed by Sandy Niesik (Niesik, 2016). Callose depositions start at the haustorial neck and gradually enclose the maturing haustorium (Meyer *et al.*, 2009; Micali *et al.*, 2011). A similar pattern was observed for RICKY1. A high degree of co-localization between RICKY1 and callose deposits indicates a localization of RICKY1 at the developing encasement rather then at the EHM (Niesik, 2016). It seems apparent that also REM1.2 and REM1.3 localize to the encasement membrane (Fig. 3.13C,D), but a detailed analysis is needed to verify their localization. In former studies, StREM1.3 was shown to localize to the EHM membrane of *Phytophthora infestans* (Lu *et al.*, 2012b; Bozkurt *et al.*, 2014), while it was excluded from the specialized, host-derived perihyphal membrane of *Colletotrichum higginsianum* (Richard O´Connell 2015, presented at 36th New Phytologist symposium). The varying protein composition at the interface of different pathogens highlights the complexity of plant-pathogen interactions and emphasizes the importance of detailed investigations. In the future it would be interesting to analyze the localization of RYL1 upon infection with *Hpa* and other filamentous pathogens. So far this was not feasible due to the lack of a functional native promoter construct.

4.2. RICKY1 and RYL1 – New Sensors of Cell Wall Integrity?

Plant CWs are load-bearing, but dynamic structures that play an important role during cell expansion and protection against various external stresses. They consist mainly of cellulose fibrils, hemicellulose, pectin, proteins and in secondary CWs also of lignin. The composition, however, is highly heterogeneous and depends on the developmental stage and on environmental conditions (Burton *et al.*, 2010).

To maintain cell wall integrity (CWI), plants need a sensitive and fine-tuned monitoring system for mechano-sensing, the perception of turgor pressure and the detection of CW damage. Chemical as well as physical signals could function as indicators of CWI (Hamann, 2012; Voxeur & Höfte, 2016).

These mechanisms are especially important during plant-microbe interactions, since phytopathogenic fungi and bacteria have to break the CW at a certain stage of their invasion. This happens independently of their lifestyle, even though the infection process differs between necrotrophic and biotrophic pathogens. While biotrophs need to keep their host cells alive and stay unperceived, necrotrophs live on and off dead tissue and can therefore use more destructive mechanisms (Bellincampi *et al.*, 2014). But nevertheless, all pathogens secrete specific CW-degrading enzymes that facilitate their invasion process and enable an

efficient nutrient uptake. As a consequence, the CW gets damaged and endogenous breakdown products can be perceived as DAMPs by corresponding PRR at the PM (Choi & Klessig, 2016). Well-studied examples are oligogalacturonides (OGs), which are released from the CW upon degradation of pectin homogalacturonan by fungal polygalacturonases (PG) (Cervone *et al.*, 1989; Ferrari *et al.*, 2013). Wall-associated kinases (WAKs) were shown to bind pectin polymers *in vitro* and *in planta* (Wagner & Kohorn, 2001; Decreux & Messiaen, 2005; Decreux *et al.*, 2006; Kohorn *et al.*, 2009; Brutus *et al.*, 2010). The perception of OGs leads to a wide range of defense responses including ROS production, the expression of defense marker genes and callose deposition (Bellincampi *et al.*, 2000; Denoux *et al.*, 2008; Galletti *et al.*, 2008). Interestingly, a potato remorin is differentially phosphorylated upon application of polygalacturonides (PGAs) within few minutes (Farmer *et al.*, 1989), indicating a role in this signaling pathway. However, the corresponding kinase has not been described so far.

In addition to their role in plant defense (Brutus *et al.*, 2010), WAKs are also involved in cell expansion (Lally *et al.*, 2001; Kohorn *et al.*, 2006) and might indirectly regulate turgor-sensitive processes (Kohorn *et al.*, 2009; Kohorn, 2016).

Even RICKY1 and RYL1 might participate in a CWI sensing process. A loss of both proteins results in an increased susceptibility to a biotrophic oomycete and hemibiotrophic bacteria (Fig. 3.9, Fig. 3.10, Fig. 3.27). Moreover, *ryl1* mutant plants are more susceptible to the necrotrophic fungi *Alternaria brassicicola* (Fig. 3.27), while *ricky1* mutants show only tendencies (data not shown). These data indicate the involvement of both proteins in general mechanism against pathogen infection. This could be also related to the perception of CW rearrangements or changes in the CW-PM continuum.

The enhanced expression of *RICKY1* and *RYL1* upon infiltration (Fig. 3.31, Fig. 3.32) supports this hypothesis. The induction is not caused by wounding itself (Fig. 3.33) and is also not dependent on the osmolarity of the solution, since the infiltration of ddH2O, tap water and mannitol results in a comparable increase of transcript levels (Lab rotation Sandy Niesik, 2016). This might indicate a link to mechano-sensing, but further analyses are needed to define the actual role of RICKY1 and RYL1. Interestingly, also REM1.2 and REM1.3 show similar expression pattern upon infiltration (Fig. 3.32, Fig. 3.33), suggesting an involvement in the same signaling pathway. In line with this, *rem1.2* and *rem1.3* single and double mutants show CW-related phenotypes in preliminary experiments (personal communication Macarena Marin, Thomas Ott). Both single mutants are more resistant to the cellulose synthesis inhibitor isoxaben and hydrated seeds of the double mutant display mucilage defects, which are also confirmed by mass spectrometry (personal communication

Clara Sánchez Rodriguez, Macarena Marin, Thomas Ott). Not only the amount of sugars is decreased in the non-adherent mucilage, also the sugar composition is altered in both, adherent and non-adherent mucilage compared to WT. These results suggest a function in CW-related processes.

Another hint for a putative role for RICKY1 and RYL1 during CWI maintenance is given by their protein structure. In addition to 11 predicted LRRs, both proteins contain a MD in their extracellular region (Fig. 3.2B). The animal protein malectin is anchored to the membrane of the endoplasmic reticulum and binds specifically to Glc2-N-glycans (Schallus *et al.*, 2008; Schallus *et al.*, 2010). In line with this, it was shown to play a role in the quality control via binding to misfolded proteins (Chen *et al.*, 2011; Galli *et al.*, 2011; Qin *et al.*, 2012). Because of the sequence similarity between the animal malectin protein and the plant MD, a binding of MD-RLKs to different carbohydrates in the apoplast seems to be reasonable, although it was not demonstrated so far.

Besides MDs, some plant RLKs as the CrRLK1Ls contain two malectin-like domains (MLD) in a tandem organization in their extracellular region (Boisson-Dernier *et al.*, 2011). Members of this family are thought to bind to the CW and act as sensors of CWI (Cheung & Wu, 2011). In line with this, several CrRLK1Ls have been shown to be involved in various growth- and stress-related pathways (Galindo-Trigo *et al.*, 2016). Mutations in the RLK *THE1 (THESEUS1)*, for example*,* were demonstrated to partially restore growth defects of the cellulose-deficient mutant *prc1-1,* without altering the cellulose content (Hematy *et al.*, 2007). In addition, a functional THE1 is needed for the oxidative burst triggered by the cellulose synthesis inhibitor isoxaben (Denness *et al.*, 2011), indicating a role for THE1 in CWI sensing.

Another well-studied example is the RLK *FER*, which was first identified as a regulator of the fertilization process (Huck *et al.*, 2003). Over the last years, FER was shown to be important for many cellular pathways, including root hair development and plant immunity (Duan *et al.*, 2010; Kessler *et al.*, 2010). In 2014, Haruta and colleagues identified FER as the receptor of the secreted peptide RALF, which plays a negative role in cell expansion (Haruta *et al.*, 2014). Interestingly, also *RICKY1* and *RYL1* transcripts are 3 – 4-fold up regulated upon RALF treatment, but corresponding mutants do not display a RALF-induced change in root growth compared to wild type plants (Haruta *et al.*, 2014). Nevertheless, they could be directly or indirectly involved in this pathway.

Additionally, FER was only recently shown to act as a mechano-sensor for different

mechanical stimuli (Shih *et al.*, 2014), supporting a function of FER in CWI. Altogether it is not surprising, that Wolf and Höfte raised the possibility that there is more then one ligand for FER (Wolf & Höfte, 2014), as it has been demonstrated already for mammalian receptors (Touhara, 1997; Pi & Quarles, 2012).

This could be also true for RICKY1 and RYL1, since they possess 11 predicted LRRs in addition to the MD. In contrast to the MD, that is thought to mediate binding to carbohydrates, LRR-containing kinases are known to preferentially bind peptides or proteins (Zipfel, 2014). Also other RLKs contain a MLD domain and few LRRs, arranged in reverse order compared to RICKY1. Members of this group play a role in different plant-microbe interactions, including harmful as well as beneficial interdependencies. IOS1 (IMPAIRED IN SUSCEPTIBILITY 1), for example, was shown to be involved in plant immunity and to act in BAK1-dependent and independent signaling pathways (Hok *et al.*, 2011; Yeh *et al.*, 2016). On the other side, the *Lotus japonicus* RLK SYMRK (SYMBIOSIS RECEPTOR-LIKE KINASE) is required for symbiosis with bacteria and fungi (Stracke *et al.*, 2002). Interestingly, the cleavage of the MLD was demonstrated to be important for the interaction of SYMRK with NFR5 (NOD FACTOR RECEPTOR 5) and its turnover at the PM (Antolin-Llovera *et al.*, 2014). Critical for the release of the MLD is a conserved "GDPC" motif connecting the MLD and the LRRs (Kosuta *et al.*, 2011; Antolin-Llovera *et al.*, 2014).

Also RICKY1 shows two specific bands after immunoblot analysis (Fig. 3.8A), whereby the sizes correspond to the full-length RICKY1 and a truncated protein lacking its whole extracellular domain (ΔLRR/MD) (Niesik, 2016). However, RICKY1 does not contain a "GDPC" motif in its extracellular region, indicating a different cleavage procedure. Intriguingly, a similar pattern also applies for FLS2 (pers. communication Daniel Couto, Zipfel lab). It remains to be investigated if the release of the whole extracellular region is a purification artifact or an actual ectodomain shedding, which was already demonstrated for AtCERK1 (Petutschnig *et al.*, 2014) and several mammalian receptors (Hayashida *et al.*, 2010; Higashiyama *et al.*, 2011).

In sum, members of the LRR subgroup VIII-2, such as RICKY1 and RYL1, might be good candidates for an additional group of CWI sensing RLKs in plants.

4.3. RICKY1 and RYL1 – Redundant Proteins or Interaction Partners?

Comparing the phenotypes of *ricky1* and *ryl1* mutants in plant immunity (Fig. 3.5, Fig. 3.6, Fig. 3.7, Fig. 3.9, Fig. 3.10, Fig. 3.25, Fig. 3.26, Fig. 3.27), it is obvious that both proteins are involved in the same defense responses. Additionally, also their gene expression is induced similarly following the treatments investigated in this study (Fig. 3.31, Fig. 3.32, Fig. 3.33). Since both proteins are closely related (Fig. 3.2A; Shiu & Bleecker, 2001b; Gou *et al.*, 2010) and share a high sequence similarity particularly in their kinase domain (98%) (Clustal Omega), it is likely that RICKY1 and RYL1 act at least partially redundant. This hypothesis would also provide an explanation for the mild phenotypes of both single mutants.

The functional redundancy between members of a protein family has been reported for many groups. Well-studied examples are the five SERK proteins in *Arabidopsis*. They have been shown to play relevant and often redundant roles as co-receptors in various signaling pathways. However, their genetic importance for distinct processes is unequal (Ma *et al.*, 2016). While single mutants often display only weak or even no obvious phenotypes, double, triple and quadruple mutants are known to have severe defects in male gametophyte development (Albrecht *et al.*, 2005; Colcombet *et al.*, 2005), BR signaling (Gou *et al.*, 2012) and stomatal patterning (Meng *et al.*, 2015).

Also the closely related CrRLK1Ls ANX1 (ANXUR 1) and ANX2 have been demonstrated to act redundantly in the pollen to maintain pollen tube integrity (Boisson-Dernier *et al.*, 2009; Miyazaki *et al.*, 2009). As RICKY1 and RYL1, ANX1 and ANX2 share a high amino acid sequence similarity of over 80 % in their extracellular domains, suggesting that both proteins bind the same ligand (Boisson-Dernier *et al.*, 2009; Miyazaki *et al.*, 2009; Boisson-Dernier *et al.*, 2011). This could be also the case for RICKY1 and RYL1, even though no putative ligand has been identified so far. This extends to the majority of over 600 RLKs in *Arabidopsis* (Shiu & Bleecker, 2001a), since only few ligand-RLK pairs have been identified by now (Butenko *et al.*, 2014).

However, a functional redundancy is not the only hypothesis to explain the putative interdependencies between RICKY1 and RYL1. Both proteins might also interact and form hetero-dimers that are essential for a distinct signaling process. Even the absence of one protein would then result in a diminished signaling step. The comparable degree of impairment of both single mutants in all analyzed responses supports this idea (Fig. 3.7, Fig. 3.9, Fig. 3.10, Fig. 3.26, Fig. 3.27).

To investigate the robustness of both hypotheses, the phenotypes of *ricky1/ryl1* double

mutants need to be examined. Because of their clustered gene loci, amiRNAs were used in this study to generate double mutants. However, even though heterozygous plant displayed decreased expression levels (Fig. 3.29), this effect was abolished in homozygous plants (Fig. 3.30). The reason for this could not be determined. The effect might be due to severe developmental defect in the double mutants, which are not discernable in the single mutants, or due to problems with the amiRNAs. Another method, such as the CRISPR/Cas9 system (Bortesi & Fischer, 2015), should be tested to clarify the interdependency between RICKY1 and RYL1. Additionally, it would be interesting to investigate the putative interaction of both proteins.

Besides RICKY1 and RYL1, only one member of the *Arabidopsis* LRR subgroup VIII-2 was characterized so far. The RLK LIK1 was identified in an Y2H-screen as an interaction partner of CERK1 (Le *et al.*, 2014). In contrast to *ricky1* and *ryl1* mutants, *lik1* plants show an enhanced immune response triggered by chitin and flg22 and are more resistant to *P. syringae*. In addition to its negative role in immunity against hemibiotrophs, LIK1 was demonstrated to act as a positive regulator against necrotrophic pathogens. Interestingly, the defects in *lik1* mutants are caused by a reduced expression of genes involved in JA and ET signaling pathways (Le *et al.*, 2014), while *ricky1* and *ryl1* mutants are not affected in the expression of defense marker genes (Fig. 3.6, Fig. 3.25). It would be interesting to investigate if RICKY1, RYL1 and LIK1 are either involved in the same or in an independent signaling pathway. Their mainly opposing phenotypes also suggest antagonistic functions. Therefore, *ricky1/lik1* and *ryl1/lik1* double mutants have been generated to analyze this in more detail.

Besides *Arabidopsis*, a LRR-MD RLK from barley, HvLEMK1, was only recently shown to contribute to non-host resistance in barley and to quantitative host resistance in wheat against the powdery mildew fungus *Blumeria graminis* f.sp. *tritici* (*Bgt*) (Rajaraman *et al.*, 2016). Taken together, it is likely, that the LRR subfamily VIII-2 displays another group of RLKs involved in plant immunity.

4.4. RICKY1 and Auxin Signaling

Hormones are not only known to orchestrate different developmental processes but also play an essential role for mediating responses to several stresses, including plant immunity (Verma *et al.*, 2016). A fine-tuned balance of growth and defense is reasonable, since induced defense mechanisms are energy-consuming processes (Walters & Heil, 2007;

Denance *et al.*, 2013). In addition to the key-regulators of defense, SA, JA and ET, also growth-related hormones such as auxin have been shown to play a role in plant immunity (Shigenaga & Argueso, 2016). The involvement of auxin in developmental and stress-related responses makes it a worthwhile target for manipulations during plant-pathogen interactions. Many bacteria have been shown to increase their virulence by the synthesis of auxin (Glickmann *et al.*, 1998) or the modulation of host auxin signaling by different effectors (Chen *et al.*, 2007; Evangelisti *et al.*, 2013). In contrast, plants down-regulate auxin responses for an increased resistance against biotrophic pathogens (Navarro *et al.*, 2006). Interestingly, RICKY1 was demonstrated to be involved in plant defense against various pathogens (Fig. 3.9, Fig. 3.10) and in auxin signaling (Fig. 3.4; ten Hove *et al.*, 2011). Ten Hove and colleagues observed an increased resistance to IAA and the polar transport inhibitor NPA (N-1-Naphthylphthalamic acid) in *ricky1* mutants. This coincidence is also true for other T-DNA lines corresponding to 6 distinct genes, including *PEPR1* and *ERECTA-LIKE 2* (*ERL2)* (ten Hove *et al.*, 2011). PEPR1, the receptor for the endogenous elicitors AtPeps (Huffaker *et al.*, 2006; Yamaguchi *et al.*, 2006; Bartels *et al.*, 2013), was additionally shown to be involved in several defense responses induced by ethylene (Liu *et al.*, 2013), flg22 and OGs (Gravino *et al.*, 2016). The LRR-RLK ERL2 is a functional paralog of ERECTA (ER) and acts synergistically and partially redundantly with ER and ERL1 in many development processes (Shpak *et al.*, 2004; Shpak *et al.*, 2005; Pillitteri *et al.*, 2007; Shpak, 2013) and plant immunity (Jorda *et al.*, 2016). Some of the developmental defects of *er/erl1/erl2* triple mutants are caused by an affected auxin transport (Chen *et al.*, 2013).

The involvement of single RLKs and whole receptor complexes in different signaling pathways enables an additional step of regulation. In addition, these multiple functions in plant development, hormone signaling and responses to various stresses emphasize the complexity of these cellular pathways. To which extent RICKY1 and also RYL1 might play a role in different signaling cascades needs to be further investigated.

4.5. The Interaction Between RICKY1 and Remorin Proteins

Remorins of various plant species have been shown to interact with receptor-like kinases involved in different signaling pathways (Lefebvre *et al.*, 2010; Tóth *et al.*, 2012; Jarsch, 2014; Son *et al.*, 2014; Gui *et al.*, 2016). We specifically searched for RLKs that interact with REM1.2 and have a putative function in plant defense (personal communication Birgit Kemmerling, University of Tübingen; Jarsch, 2014) to identify so far unknown components of

plant immunity. In this regard, the cytosolic domain of the LRR-RLK RICKY1 was identified as a specific interaction partner of REM1.2 in a Y2H screen (Fig. 3.1; Jarsch, 2014). Intriguingly, the closely related RYL1 is not able to interact with REM1.2 (Fig. 3.23), even though both kinase domains share a sequence identity of 98 %. Additionally, RICKY1 does not interact with REM1.3 (Fig. 3.1), the closest relative of REM1.2 (Raffaele *et al.*, 2007). Taken together, these data suggest a high specificity for the interaction between RICKY1 and REM1.2, at least in yeast. This is not surprising, since remorin proteins harbor a highly flexible ID region (Marín & Ott, 2012), which is known to mediate the binding to several interaction partners with a high specificity, but a low affinity (Dyson & Wright, 2005). This is also a common feature of transient interactions between kinases and substrates in different signaling pathways (Dyson & Wright, 2005; Mittag *et al.*, 2010). Interestingly, it was shown that many components of plant immunity harbor at least some ID regions (Marín & Ott, 2014). Predictions indicate that even RICKY1 contains two longer ID segments located at the end of its kinase domain and in its C-terminal tail (PONDR VL-XT). The latter was shown to be present in SERK1, SERK3, BRI1 as well as FLS2, suggesting a common feature for plant RLKs (aan den Toorn et al. 2012). The C-terminal tail itself is thought to be involved in common regulatory mechanisms (Wang *et al.*, 2005; aan den Toorn *et al.*, 2012).

Since it is known that phosphorylation often occurs in intrinsically disordered regions (Iakoucheva *et al.*, 2004), this could be also true for RICKY1 and might be a good indication for putative phosphorylation sites of RICKY1.

Stimulus-dependent phosphorylation events as well as the assembly of protein complexes are essential to facilitate a fast and efficient signal transduction. So-called "hub" proteins often contain ID regions to provide the plasticity for interactions with various proteins and are therefore central players for the formation of interaction networks (Dunker *et al.*, 2005; Dosztanyi *et al.*, 2006; Patil & Nakamura, 2006; Mittag *et al.*, 2010). This supports the idea that remorin proteins act as molecular scaffolds and mediate active signaling hubs at the PM (Jarsch & Ott, 2011). Especially, because group 1 remorins are differentially phosphorylated upon several stress-related stimuli (Farmer *et al.*, 1989; Benschop *et al.*, 2007; Widjaja *et al.*, 2009). Most of the phosphorylation sites are located in the ID N-terminal region (Marín & Ott, 2012). This might provide various interaction sites for different interaction partners dependent on the specific stimulus.

Only recently, it was demonstrated that the intrinsically disordered mammalian protein 4E-BP2 gets differentially folded upon phosphorylation, resulting in an altered binding behavior (Bah *et al.*, 2015). This might also apply for REM1.2, since phospho-ablative mutations in

the very N-terminal region interfere with its capability to interact with RICKY1 (Fig. 3.20). In addition, the kinase activity of RICKY1 is essential for the interaction, highlighting the importance of the post-translational modification. However, it still needs to be investigated if RICKY1 is actually able to directly phosphorylate REM1.2.

Also the interaction between OsREM4.1 and OsSERK1 is dependent on the phosphorylation status of OsREM4.1 (Gui *et al.*, 2016). While non-phosphorylated OsREM4.1 interacts with OsSERK1, the phosphorylation of OsREM4.1 by OsBRI1 causes a disassociation from the complex and enables an interaction of OsBRI1 with OsSERK1. This mechanism was shown to regulate the antagonistic functions of ABA and BR signaling in rice. Interestingly, only the N-terminal region of OsREM4.1 is crucial for the interaction with OsSERK1 (Gui *et al.*, 2016). In contrast, the C-terminal region of REM1.3 is essential for the interaction with different importin α isoforms, while the N-terminal region might be involved in stabilizing the interaction (Marín *et al.*, 2012). This also applies for the interaction of LjSYMREM1 with the RLKs NFR1, NFR5 and SYMRK (Tóth *et al.*, 2012). However, for a proper interaction of RICKY1 and REM1.2 both the N- and the C-terminal domain are important (Fig. 3.19). Additionally, the REM1.2/REM1.3 domain swap experiments emphasize the specificity of the interaction between RICKY1 and REM1.2 in yeast.

The interplay between RICKY1 and REM1.2 was also investigated in the homologous *Arabidopsis* system to monitor both proteins in their biological context.

In planta, remorins are known to localize to the PM and are well-accepted micro-domain marker proteins (Raffaele *et al.*, 2009; Lefebvre *et al.*, 2010; Tóth *et al.*, 2012; Demir *et al.*, 2013; Jarsch *et al.*, 2014). Only recently, Jarsch and colleagues observed REM1.2 and REM1.3 mainly in small and highly mobile micro-domains below the resolution limit of confocal microscopy (Jarsch *et al.*, 2014). Even RICKY1 localizes to the PM (Fig. 3.11) and is organized in small and dynamic domains that can be visualized using TIRF microscopy (Fig. 3.14A,B). Interestingly, RICKY1-labelled micro-domains co-localize with REM1.2 and REM1.3 (Fig. 3.14). Since both remorins are able to form heterooligomers (Jarsch, 2014), it can be hypothesized that all three proteins might be part of a higher order protein complex at the PM.

This is supported by the data obtained by image-based *in planta* interaction studies. BiFC analyses reveal a close proximity of RICKY1 with REM1.2 and REM1.3 in distinct sub-compartments of the PM (Fig. 3.15). A similar pattern was also observed for LjSYMREM1 and NFR1 (Tóth *et al.*, 2012) as well as for AtREM6.4 and BAK1 (Jarsch, 2014), indicating a common feature for the interaction of remorin proteins with receptor-like kinases. However,

using a higher temporal and spatial resolution, a direct interaction was mainly demonstrated for RICKY1 and REM1.2 (Fig. 3.16). Taken together it is likely, that RICKY1, REM1.2 and REM1.3 are part of a protein complex and REM1.2 mediates an indirect interaction between RICKY1 and REM1.3.

To which extent the kinase activity of RICKY1 and the phospho-sites of REM1.2 are important for the interaction *in planta* still needs to be validated. Therefore, *Arabidopsis* plants expressing kinase-dead RICKY1 and wild type REM1.2 or a phospho-ablative mutant have been generated and should be used for further FLIM/FRET analyses. Even other micro-domain-localized proteins or external stimuli might positively or negatively influence the interaction of RICKY1 and REM1.2 *in planta*.

4.6. Micro-Domains at the Plasma Membrane

Over the last years, several cell biological studies identified multiple proteins that are organized in distinct sub-compartments of the PM. In addition to accepted families of micro-domain marker proteins like remorins (Raffaele *et al.*, 2009; Lefebvre *et al.*, 2010; Tóth *et al.*, 2012; Demir *et al.*, 2013; Jarsch *et al.*, 2014) and flotillins (Haney & Long, 2010; Haney *et al.*, 2011; Li, RL *et al.*, 2012), also other proteins such as the potassium channel KAT1 (Sutter *et al.*, 2006; Reuff *et al.*, 2010), the NADPH oxidase RBOHD (Lherminier *et al.*, 2009) and the receptor BRI1 (Wang *et al.*, 2015b) have been shown to localize to micro-domains.

However, only recently the coexistence of diverse micro-domains has been demonstrated for yeast (Spira *et al.*, 2012) and for plants (Jarsch *et al.*, 2014). The majority of *Arabidopsis* remorin proteins were shown to mainly localize to laterally stable micro-domains (Jarsch *et al.*, 2014). Only group 1 remorins display a more homogeneous distribution, but are nevertheless organized in small and highly dynamic structures detectable using TIRF microscopy. Occasionally, REM1.2 and REM1.3 are targeted to larger, immobile domains in elongating hypocotyl cells (Jarsch *et al.*, 2014). In this context, it has to be noted that Demir and colleagues observed large, static REM1.2- and REM1.3-labeled micro-domains also in other tissues. Interestingly, immobile REM1.2-targeted micro-domains show a clear co-localization with REM1.3 (Demir *et al.*, 2013). This emphasizes again their putative involvement in the same signaling pathway.

Taken together, it can be concluded that the localization of group 1 remorins seems to be a very dynamic process. It might be that the re-localization of REM1.2 and REM1.3 into larger complexes is dependent on a certain stimulus or on a developmental stage. If or to which extent the re-localization is essential for their function remains to be investigated.

Under the conditions used in our lab, REM1.2 and REM1.3 localize to static micro-domains only in elongating hypocotyl cells (Jarsch *et al.*, 2014). Since the hypocotyl has a complete embryonic origin, cell growth relies entirely on cell expansion rather than on cortical and epidermal cell divisions (Gendreau *et al.*, 1997). Therefore, a tremendous remodeling of the CW network occurs that also comprises a change in CW thickness (Refregier *et al.*, 2004; Derbyshire *et al.*, 2007; Boron & Vissenberg, 2014). The altered hypocotyl growth in PME (pectin methylesterase) and PG mutants highlights the importance of pectin metabolism for this process (Derbyshire *et al.*, 2007; Guenin *et al.*, 2011; Xiao *et al.*, 2017). Since preliminary results indicate a putative involvement of group 1 remorins in CW-related processes, including pectin metabolism (personal communication Macarena Marin, Thomas Ott, Clara Sánchez Rodriguez), it might be interesting to investigate if the re-localization of REM1.2 and REM1.3 plays a role during the expansion of hypocotyl cells. Additionally, it could be worthwhile to have a closer look at the localization of RICKY1 in elongating hypocotyl cells. Especially, because CW rearrangements have an impact on the CW-PM continuum (Pogorelko *et al.*, 2013) and RICKY1 might be involved in a CWI-sensing pathway.

Even the CW itself is known to influence the dynamics of PM-localized proteins. Many plant proteins as the potassium channel KAT1 (Sutter *et al.*, 2006; Reuff *et al.*, 2010) and the boric acid/borate transporter BOR1 (Takano *et al.*, 2010) have been reported to contain a relatively high immobile fraction. In 2012, Martinière and colleagues nicely demonstrated the low lateral mobility of 11 out of 13 tested PM proteins (Martinière *et al.*, 2012). Proteins that are inserted in the outer leaflet and contain an extracellular region are less mobile compared to those that are inserted in the inner leaflet. FRAP experiments in protoplasts and plasmolysed cells revealed an increased mobility of proteins that protrude into the CW space, emphasizing the impact of the CW on the immobilization of PM proteins. In contrast, protein-protein interactions and the cytoskeleton showed only minor effect on the protein dynamics in this study (Martinière *et al.*, 2012).

Even though remorins attach to the cytosolic leaflet of the PM (Raffaele *et al.*, 2009), the mobility of the relatively static potato remorin StREM1.3 is highly increased in *Arabidopsis* protoplasts compared to mesophyll cells (Blachutzik *et al.*, 2015). Nevertheless, StREM1.3 is still organized in distinct micro-domains at the PM, indicating that the formation and the maintenance of StREM1.3-labeled micro-domains are not dependent on the CW. However, some proteins within these micro-domains might be linked to or stabilized by the CW and could influence the mobility of StREM1.3 (Blachutzik *et al.*, 2015).

Not only the CW also the cytoskeleton is interconnected with the PM and contributes to the cell surface continuum (Baluška *et al.,* 2003; Denness *et al.,* 2011; McKenna *et al.,* 2014). In the animal field, the impact of the actin cytoskeleton on the sub-compartmentalization of the PM is widely accepted (Chichili & Rodgers, 2009; Kusumi *et al.,* 2012; Dinic *et al.,* 2013). Szymanski and colleagues demonstrated the differential distribution of several *Arabidopsis* proteins between DRM and DSM (detergent-soluble membrane) fractions upon disruption of the cytoskeleton (Szymanski *et al.,* 2015). Among them, REM1.2 and REM1.3 show a clear shift from DRM to DSM fractions after treatment with cytochalasin D, an inhibitor of actin polymerization (Cooper, 1987). Also the treatment with oryzalin, a microtubule-depolymerizing agent (Morejohn *et al.,* 1987), leads to a depletion of the remorins from the DRM, but not to an increase in the DSM fraction (Szymanski *et al.,* 2015). These results are also confirmed cell biologically. The disruption of the actin filament results in a significant reduction of REM1.2-labeled micro-domains, while the depolymerization of microtubules leads to less, but larger micro-domains. The authors concluded that actin is essential for the organization of REM1.2 in micro-domains, whereas the disruption of microtubules might relocate REM1.2-targeted micro-domains within the PM (Szymanski *et al.,* 2015). In contrast, the localization of AtREM6.6 (At1g13920) in filament-like structures seems to be dependent on microtubules, but independent of actin (Jarsch *et al.,* 2014), suggesting multiple mechanisms for different remorins. In line with this, the rice remorin GSD1 was shown to interact with the desmotubule-associated actin binding protein OsACT1 (ACTIN1), which affects the conductance of PD (Gui *et al.,* 2014; Gui *et al.,* 2015). It has not been determined so far, if also other remorins interact with components of the cytoskeleton.

In sum, recent data revealed the impact of the CW and the cytoskeleton on the localization and dynamics of remorin proteins. The question arises to which extent remorins as putative scaffold proteins contribute to the localization and mobility of other proteins within distinct sub-compartments.

Even RICKY1 is organized in small, very dynamic micro-domains at the PM (Fig. 3.14A,B). FRAP experiments additionally revealed a high lateral mobility of RICKY1 (Fig. 3.18). Interestingly, the mobility of RICKY1 is affected by REM1.2, since RICKY1 shows an increased mobile fraction in *rem1.2* mutants (Fig. 3.18). Besides the absent interaction, the lack of the scaffold protein could impair the formation of protein complexes or result in de-stabilized protein complexes within these micro-domains. However, if the absence of REM1.2 has an effect on the localization of RICKY1 to micro-domains needs to be further investigated using TIRF microscopy.

In contrast, the kinase activity of RICKY1 has no impact on its mobility (Fig. 3.22), even though it is essential for the interaction with REM1.2 in yeast (Fig. 3.20). This might be a hint that the increased mobility of RICKY1 in *rem1.2* is rather due to the instability of the hub than to the absent interaction with REM1.2. Especially, because it can be assumed that RICKY1 interacts with several other PM-localized proteins even independent of its kinase activity.

As we hypothesize that REM1.2 and REM1.3 act in concert to mediate active signaling hubs, it would be interesting to characterize the mobility of RICKY1 in *rem1.2/rem1.3* double mutants. This line has already been generated and can be used for further experiments. These results can help to understand the function of group 1 remorins as scaffold proteins.

The mobility of several PM-localized proteins is additionally dependent on the environmental conditions. The receptor FLS2, for example, was shown to be highly dynamic under resting conditions, but its mobility significantly decreased upon flg22 treatment (Ali *et al.*, 2007). The authors suggested that this is caused by an altered interaction behavior or the re-localization to micro-domains. A similar pattern was observed for the *Medicago truncatula* RLK LYK3. Highly mobile LYK3-labeled micro-domains are immobilized after inoculation with the symbiotic bacterium *Sinorhizobium meliloti*. In addition, the static LYK3-targeted micro-domains co-localize with FLOT4 (Haney *et al.*, 2011). Recent results indicate that the formation of these symbiosis-associated micro-domains is additionally dependent on SYMREM1 (Stratil, 2016). These results again emphasize the importance of remorin proteins as molecular scaffolds for the assembly of active signaling hubs.

It can be speculated that also RICKY1 re-localizes in larger, laterally stable domains dependent on the developmental stage or the environmental conditions. However, the appropriate stimulus has not been identified so far.

Increasing evidence indicates that the compartmentalization of proteins involved in one signaling pathway might be crucial for a spatiotemporal efficient process (Spira *et al.*, 2012; Jarsch *et al.*, 2014; McKenna *et al.*, 2014; Tapken & Murphy, 2015).

Only recently, Nagano and colleagues demonstrated the importance of micro-domains for the chitin-induced immunity in rice (Nagano *et al.*, 2016). The knockdown (KD) of two fatty acid 2-hydroxylases *FAH1* and *FAH2* results in less abundant micro-domains and an increased susceptibility to the rice blast fungus *Magnaporthe oryzae*. Detailed analyses revealed that multiple defense-related proteins, including the RAC/ROP small GTPase RAC1 and several RBOHs, are decreased in DRM fractions of OsFAH1/2-KD plants upon chitin treatment. The altered localization and dynamics of these proteins leads to a diminished

chitin-induced ROS production. In sum, this study nicely demonstrates that micro-domains are crucial for the chitin-induced ROS signaling and immunity mediated by the RAC1-RBOHB/H pathway (Nagano *et al.*, 2016).

To which extent the subcellular organization of RICKY1 might be crucial for its function, still needs to be further investigated.

The data obtained in this study support our main idea that remorins are promising baits to identify new, so far uncharacterized components of diverse signaling hubs.

Here, I demonstrated the importance of the REM1.2-interacting LRR-MD RLK RICKY1 for plant immunity. Interestingly, RICKY1 plays a role at later stages of defense. So far, the main focus of research is on early signaling events at the PM. Therefore, the further characterization of RICKY1, RYL1 and their targets might help to elucidate downstream signaling pathways. Furthermore, their putative function as CWI sensors suggest that members of the subgroup LRR VIII-2 are promising candidates for future studies. In this regard, it might be of special importance to examine the function of their malectin domain.

Additionally, I was able to show, that RICKY1 is associated with membrane micro-domains and that its mobility is influenced by the scaffold protein REM1.2. This provides the opportunity to further investigate the significance of micro-domains as active signaling platforms in plant defense.

5. Material and Methods

5.1. Media

5.1.1.　Bacterial Media

5.1.1.1.　LB medium for *Escherichia coli* and *Agrobacterium tumefaciens*

Amount	Component
1 % (w/v)	Bacto trypton
0.5 % (w/v)	Bacto yeast extract
1 % (w/v)	NaCl
1.3 % (w/v)	Bacto agar (for solid medium)

Combined ingredients were autoclaved for 20 min at 120 °C.

Antibiotics were added prior to use.

5.1.1.2.　Kings B medium for *Pseudomonas syringae*

Amount	Component
2 % (w/v)	Bacto peptone
1.5 % (w/v)	K_2HPO_4
1.5 % (w/v)	$MgSO_4$ (add after autoclaving)
1 % (w/v)	Bacto agar

Adjust pH 7.2

Combined ingredients were autoclaved for 20 min at 120 °C. 1 M $MgSO_4$ was sterile filtrated and added prior to use. Rifampicin was added to a final concentration of 50 µg/ml.

5.1.2.   Yeast Media

5.1.2.1.   YPAD medium

Amount	Component
1 % (w/v)	Bacto yeast extract
2 % (w/v)	Bacto peptone
0.004 % (w/v)	Adenine sulfate
2 % (v/v)	Glucose monohydrate (add after autoclaving)
2 % (w/v)	Bacto agar (for solid medium)

Combined ingredients were autoclaved for 20 min at 120 °C. Glucose was autoclaved separately as a 20 % stock solution for 15 min at 115 °C and added prior to use.

5.1.2.2.   Selective dropout (SD) medium

Amount	Component
20 ml	10 x Yeast nitrogen base ((YNB); 67 g/l)
20 ml	10 x AA-stock solution (w/o leucine, tryptophan, histidine, adenine)
10 ml	40 % Glucose
150 ml	H_2O (for liquid medium) or bacto agar (4 g/ 150 ml)
8 ml	25 x adenine stock solution
400 μl	500 % histidine stock solution (for SD –LW plates)
x	3-amino-1,2,4-triazole (3-AT)

All components were sterilized separately and combined directly before use. YNB was sterile filtrated and 40 % glucose was autoclaved for 15 min at 115 °C. The AA-stock solution and water/agar were autoclaved for 20 min at 120 °C.

5.1.3.   Plant Media

5.1.3.1.   ½ MS medium

Amount	Component
0.22 %	Basal Salt Mixture Murashige & Skoog Medium
1 %	Sucrose
0.8 %	Bacto agar (for solid medium)

Adjust pH 5.8

Combined ingredients were autoclaved for 20 min at 120 °C.

Antibiotics and hormones were added prior to use.

5.2. Cloning

5.2.1.   Polymerase Chain Reaction (PCR)

5.2.1.1.   Analytical PCR

Standard PCRs for the verification of transformed bacterial strains and for genotyping of genomic DNAs were performed with *Taq*-polymerase. The annealing temperature as well as the elongation time was optimized for each PCR individually.

PCR reaction mix (20 μl)

Amount	Component
2 μl	Standard *Taq* buffer (10x)
0.6 μl	Forward Primer (10 μM)
0.6 μl	Reverse Primer (10 μM)
0.4 μl	MgCl$_2$ (50 mM)
0.4 μl	dNTPs (10 mM)
0.05 μl	*Taq*-polymerase
x	DNA template (10-100 ng) or bacteria

Standard PCR program

Step	Temperature	Time
1. Initial denaturation	95 °C	2 min
2. Denaturation	95 °C	30 sec
3. Annealing	x	30 sec
4. Elongation	72 °C	60 sec/kb
5. Final Elongation	72 °C	5 min

Steps 2 – 4 were repeated 29 times.

5.2.1.2. Preparative PCR

PCRs for preparative amplification of sequences from cDNA or genomic DNA were performed with Phusion HF polymerase. The annealing temperature as well as the elongation time was optimized for each PCR individually. A detailed primer list can be found in the appendix.

PCR reaction mix (20 μl)

Amount	Component
4 μl	HF-buffer (5x)
0.6 μl	Forward Primer (10 μM)
0.6 μl	Reverse Primer (10 μM)
0.4 μl	MgCl$_2$ (50 mM)
0.4 μl	dNTPs (10 mM)
0.2 μl	Phusion-polymerase
10 ng	DNA template

Standard PCR program

Step	Temperature	Time
1. Initial denaturation	98 °C	2 min
2. Denaturation	98 °C	30 sec
3. Annealing	x	30 sec
4. Elongation	72 °C	20 sec/kb
5. Final Elongation	72 °C	5 min

Steps 2 – 4 were repeated 34 times.

5.2.2. Cloning of Entry Vectors

Gene-specific primers with specific overhangs were used for the amplification of target genes from cDNA (5.3) or genomic DNA (5.5.7).

BP-overhangs were used for the subsequent BP-cloning (Invitrogen) into Gateway-compatible entry vectors (pDONR207, pDONRzeo) following the manufacturer´s instructions. For type IIS restriction enzyme-based cloning strategies, all corresponding recognition sites in the construct were mutated prior to cloning. BsaI recognition sites were added to the primers for the subsequent cloning into the modified, Gateway-compatible pENTR_D BsaI:GW:BsaI vector (see Morbitzer *et al.*, 2011). BpiI and BsaI recognition sites were added to the primers for subsequent Golden Gate cloning (see Binder *et al.*, 2014). A complete list of all generated entry clones can be found in the appendix.

5.2.3. Transformation of *E. coli*

Chemically competent *E. coli* cells were thawed on ice prior to the addition of DNA (5 μl LR reaction, 10 ng plasmid DNA). After incubation on ice for 10 minutes, a heat shock at 42 °C was performed for 90 sec. Back on ice, 250 μl LB medium was added and the cells were incubated at 37 °C for 1 h with gentle shaking. Subsequently, cells were plated onto LB plates containing the appropriate antibiotic selection and incubated oN at 37 °C. Transformants were verified by analytical PCR (colony PCR) and grown oN in liquid culture (37 °C, 180 rpm). Plasmids were isolated with the GeneJet Plasmid MiniPrep Kit (Thermo Scientific) following the manufacturer´s instructions.

5.2.4. Cloning of Expression Vectors

Gateway-compatible expression vectors were cloned following the manufacturer´s instructions. Golden Gate-compatible expression vectors were assembled as described in (Binder *et al.*, 2014). A complete list of all generated expression clones can be found in the appendix.

5.2.5.   Transformation of *A. tumefaciens*

Electro-competent *A. tumefaciens* cells were thawed on ice prior to the addition of 50 ng plasmid DNA. The electroporation was conducted in electroporation cuvettes with 1.8 kV. Subsequently, 500 μl LB were added and cells were incubated at 28 °C for 2 h with gentle shaking. Afterwards, cells were plated onto LB plates containing the appropriate antibiotic selection and incubated for two days at 28 °C. Transformants were verified by analytical PCR (colony PCR).

5.2.6.   Generation of Artificial MicroRNAs (amiRNAs)

AmiRNAs were designed following the guidelines of the web tool WMD3 (Web MicroRNA Designer) (see Ossowski *et al.,* 2008). The amiRNA-containing precursor was generated by overlapping PCRs using the plasmid pRS300 as template. Overhangs containing BsaI sites were used to clone the constructs into the vector pENTR_D BsaI:GW:BsaI. The vector pGWB2 was used for the *in planta* expression.

5.3. RNA, cDNA, qPCR

5.3.1.   RNA Extraction from *A. thaliana*

Total RNA was extracted from 14-day-old seedlings or five-week-old leaves using the Spectrum™ Plant Total RNA Kit (Sigma-Aldrich) following the manufacturer´s instructions. RNA was eluted with 30 μl DEPC-treated H_2O. The quality of the RNA was analyzed via agarose gels and the absorbance of UV-visible light.

5.3.2.   DNase Treatment of RNA

1 μg RNA was treated with DNase I (Invitrogen) according to the instructions provided by the manufacturer. The success of the treatment was subsequently verified by performing a test qRT-PCR (5.3.4).

5.3.3. cDNA Synthesis

The DNA-free RNA was used for cDNA synthesis (Invitrogen, Superscript® IV First-Strand Synthesis System) following the manufacturer´s instructions. The cDNAs were subsequently diluted 1:5.

5.3.4. Quantitative Real-Time PCR (qPCR)

Quantitative real-time PCRs were performed using a 96-well Real-Time PCR machine (Bio-Rad, CFX96). Two technical replicates and at least three biological replicates were used. The *AtUBC* gene was used as housekeeping gene. Standard qRT-PCRs were performed with an annealing temperature of 60 °C and without an elongation step.
A list of all qPCR primer used in this study can be found in the appendix.

Master mix

Amount	Component
5 μl	SYBR^{TM} Green Master Mix
1 μl	Forward Primer (1 μM)
1 μl	Reverse Primer (1 μM)
2 μl	H_2O
1 μl	cDNA (1:5 diluted)

Standart qPCR program

Step	Temperature	Time
1. Initial denaturation	95 °C	3 min
2. Denaturation	95 °C	10 sec
3. Annealing	60 °C	30 sec
4. Denaturation	95 °C	10 sec
4. Generation of melt curve	65 °C – 95° C Increase 0.5 °C/cycle	5 sec

Steps 2 – 3 were repeated 39 times.

5.4. Protein Work

5.4.1.　Protein Separation via SDS-PAGE

Proteins samples were mixed with the appropriate amount of SDS loading dye and boiled for 5 min at 95 °C prior to loading on a 10 % SDS-Polyacrylamide gel, if not indicated differently. The electrophoresis was performed for 1 – 2 h at 150 V in 1 x SDS running buffer. Subsequently, gels were either stained with coomassie (0.1 % in a solution containing 40 % ethanol and 10 % acetic acid) or used for western blot analysis (5.4.2).

6 x SDS loading dye

Amount	Component
350 mM	Tris-HCl pH 6.8
30 %	Glycerol
10 %	SDS
0.012 %	Bromophenol blue
600 mM	DTT (add freshly before use)

Stacking gel

Amount	Component
180 mM	Tris-HCl pH 6.8
5 %	Acrylamide
0.1 %	SDS
0.1 %	APS
0.1 %	TEMED

Separation gel 10 %

Amount	Component
360 mM	Tris-HCl pH 8.8
10 %	Acrylamide
0.1 %	SDS
0.1 %	APS
0.04 %	TEMED

10 x SDS running buffer

Amount	Component
3 % (w/v)	Tris
14.4 % (w/v)	Glycine
1 %	SDS

5.4.2.   Western Blot Analysis

Proteins were transferred onto ethanol-activated PVDF (polyvinylidene fluoride) membranes using 1 x transfer buffer for 3 h at 100 V and 4 °C or over night at 35 V and 4 °C. The subsequent handling of the membrane was performed following the manufacturer´s suggestions for the first antibody. The membranes were blocked in milk or BSA for 1 – 2 h at room temperature. The first antibody was applied to the membrane over night at 4 °C. After three washing steps the membrane was incubated with the respective HRP-conjugated second antibody for 2 – 3 h at room temperature. Following three washing steps, the membrane was incubated with the SuperSignal® West Femto Maximum Sensitivity substrate (Pierce) and chemiluminescence was detected using a fusion detection camera (Peqlab).

10 x Transfer buffer for small proteins

Amount	Component
3 % (w/v)	Tris
14.4 % (w/v)	Glycine

Adjust pH 8.3

Prior to use ethanol was added to a final concentration of 20 %. A final concentration of 10 % ethanol and 0.01 % SDS was used to optimize the transfer of large proteins.

5.4.3.   Expression of Recombinant Proteins in *E. coli*

For the recombinant expression of RLKs, the cytosolic domains were cloned into the pASK-IBA7 plus vector under the control of the tetA promoter. All proteins were expressed as *Strep*-tag II fusion proteins in *E. coli* DH5α cells. Liquid cultures were grown at 37 °C until OD_{600} reached 0.6 – 0.8. The expression of recombinant proteins was induced with 200 μg/l anhydrotetracycline for 24 h at 16 °C. Samples were taken before and 24 h after induction and analyzed using SDS-PAGE followed by immunoblot analysis (5.4.2).

5.4.4.   Purification of Recombinant Proteins from *E. coli*

Strep-tag II-fused recombinant proteins were expressed in the DH5α strain (5.4.3). Cells were harvested by centrifugation (15 min, 4000 x g, 4 °C), resuspended with the appropriate amount of STE buffer (containing 100 μg/ml lysozyme and protease inhibitors) and incubated on ice for 15 min. Subsequently, 5 mM DTT and 1.5 % N-lauroylsarcosine were added and mixed by vigorous shaking. A French press was used to break the cells (3 times 1260 psi) and cell debris was removed by centrifugation (15 min, 9500 x g, 4 °C). The supernatant was immediately loaded onto equilibrated Strep-tactin® sepharose® containing columns. The sepharose was washed 5 times with 2 CV buffer W and bound proteins were subsequently eluted 6 times with 0.5 CV buffer E. The purification was analyzed using SDS-PAGE followed by immunoblot analysis (5.4.2)

STE buffer

Amount	Component
10 mM	Tris pH 8
150 mM	NaCl
1 mM	EDTA

Buffer W

Amount	Component
100 mM	Tris pH 8
150 mM	NaCl
1 mM	EDTA

Buffer E

Amount	Component
100 mM	Tris pH 8
150 mM	NaCl
1 mM	EDTA
2.5 mM	Desthiobiotin

5.4.5.   *In vitro* Phosphatase Assay

20 μl purified RICKY1 protein (5.4.4) were incubated with 1 x FastAP reaction buffer and 7 μl FastAP (Thermosensitive Alkaline Phosphatase) (Thermo scientific) for 1 h at 37 °C. The reaction was stopped by adding the appropriate amount of SDS loading dye and boiling for 5 min. The dephosphorylation was analyzed using SDS-PAGE followed by immunoblot analysis with tag- and phospho-specific antibodies (5.4.2)

5.5. Plant Work

5.5.1.   Sterilization of *A. thaliana* Seeds

Arabidopsis seeds were incubated in 70 % ethanol (+ 0.05 % Tween 20) for 10 min with continuous shaking. The solution was replaced twice with 96 % ethanol and twice with sterile ddH$_2$O for two minutes each. Subsequently, the seeds were transferred to ½ MS plates supplemented with 1 % sucrose (5.1.3.1) and vernalized for two to five days at 4 °C in the dark.

5.5.2.   *A. thaliana* Growth Conditions

Sterilized *Arabidopsis* seeds were germinated on plate (5.5.1) under long-day conditions (16 h light/ 8 h darkness, 22 °C/ 18 °C). Seedlings designated for growth on earth were transferred 2 days after germination. Plants used for seed production were grown under long-day conditions in the greenhouse for 8 weeks. Plants for elicitor treatments and

infection assays were grown under short-day conditions (8 h light / 16 h darkness, 20 °C/ 18 °C) in walk-in chambers, if not indicated differently.

5.5.3.   *N. benthamiana* Growth Conditions

N. benthamiana plants were grown for 3 – 4 weeks in a walk-in chamber under long-day (16 h light/ 8 h darkness) conditions.

5.5.4.   Generation of Stable Transgenic *A. thaliana* Plants

Plants designated for stable transformation with *A. tumefaciens* were grown under short-day conditions for 5 – 6 weeks in a walk-in chamber. Plants were transferred to long-day conditions in the greenhouse to induce floral transition. The primary bolt was cut one week prior to floral dipping (Clough & Bent, 1998). In brief, 250 ml liquid medium was inoculated with *A. tumefaciens* (50 ml liquid culture, grown oN) and grown for 4 h at 28 °C with gentle shaking. Bacterial cells were harvested and resuspended in dipping solution. Plants were dipped into the solution, covered with a big and incubated over night in the dark.
On the next day, the plants were transferred to the greenhouse for seed production.

Dipping solution

Amount	Component
5 %	Sucrose
0.05 %	Silvett-77
x	Bacterial pellet

5.5.5.   Identification of Transformed *A. thaliana* Plants

Transgenic plants carrying the *bar* gene as transformation marker were sown on soil and grown under long-day conditions in the greenhouse. The gardeners sprayed the seedlings twice with BASTA (0.25 % in water). Resistant plants were brought to seed production.
Transgenic plants carrying the *hpt* gene as transformation marker were identified according to (Harrison *et al.*, 2006). In brief, seeds were sterilized (5.5.1) and transferred to ½ MS

plates containing 1 % sucrose and 15 μg/ml hygromycin B (5.1.3.1). Following stratification (2 days, 4 °C, darkness), the seedlings were incubated for 6 h in a walk-in chamber under white light. After 2 days incubation in the dark, the seedlings were grown under long-day conditions for 2 additional days. Resistant seedlings were transferred to soil and brought to seed production.

5.5.6.   Generation of Genetic Crosses

Homozygous parental lines were grown in the greenhouse under long-day conditions until they start flowering. All open flowers, young flower buds and seed pots were removed in the designated mother plants. Pistils were dissected and pollinated with open flowers of the designated father plant. The pollination was repeated on the two following days. Seeds of the fertilized pistils were harvested and F1 plants were analyzed by PCR (5.5.8).

5.5.7.   DNA Extraction from *A. thaliana*

Arabidopsis plants were grown for 3 – 4 weeks under long-day conditions. One leaf per plant was harvested, ground in liquid nitrogen and mixed with 500 μl extraction buffer. Cell debris was removed by centrifugation (10 min, high speed, benchtop centrifuge). The supernatant was supplemented with isopropanol (1:1), mixed by inversion and spun down (15 min, top speed, benchtop centrifuge). The pellet was dried for 30 min and subsequently resuspendend in H_2O with gentle shaking for 30 min. Leftover cell debris was removed by centrifugation (10 min, top speed, benchtop centrifuge).

DNA extraction buffer

Amount	Component
200 mM	Tris/HCl pH 9
400 mM	LiCl
25 mM	EDTA
1 %	SDS

5.5.8.   Genotyping Procedure for T-DNA Insertion Lines

T-DNA insertion lines ordered from ABRC/NASC and plant lines derived from genetic crosses were genotyped. Therefore, DNA of 3 – 4-week-old plants was extracted (5.5.7) and used for PCR amplification (5.2.1.1). In total, three PCRs were performed to clarify the genotypes of all plants. Gene-specific primers that span the annotated T-DNA insertion site were used to amplify the wild type allele. A T-DNA specific primer was combined with the gene-specific forward and the reverse primer to identify the orientation of the T-DNA. The mutant allele amplicons were sent for sequencing (following the guidelines of the sequencing service faculty of biology) to verify the exact insertion site.

5.5.9.   Transient Transformation of *N. benthamiana* Leaves

A. tumefaciens carrying the construct of interest were grown oN in liquid LB under appropriate antibiotic selection. Bacteria were harvested and resuspended in infiltration solution to obtain the desired OD_{600} for infiltration. The viral silencing inhibitor P19 was used with a final OD_{600} of 0.1. The bacterial solutions were incubated for 2 h in the dark prior to infiltration. The youngest, fully expanded leaves of 3 – 4-week-old *N. benthamiana* plants were syringe-infiltrated and grown for three additional days under long-day conditions. Protein expression was analyzed using confocal microscopy (5.7).

Infiltration solution

Amount	Component
150 μM	Acetosyringone
10 mM	$MgCl_2$
10 mM	MES/KOH pH 5.6
x	Bacterial Pellet

5.5.10.   Whole Protein Extraction from *A. thaliana*

Arabidopsis seedlings were grown on ½ MS plates supplemented with 1 % sucrose (5.1.3.1) for 14 days under long-day conditions. 8 – 10 seedlings per line were harvested, pooled and ground in liquid nitrogen. 2 x volume Waadt buffer were added to the plant powder prior to

boiling at 95 °C for 5 min. Leftover cell debris was removed by centrifugation (30 min, 16,000 x g, 4 °C). The supernatant was mixed with 2x SDS loading dye (5.4.1), boiled for 5 min at 95 °C and subsequently loaded on a SDS-PAGE (5.4.1).

Waadt buffer

Amount	Component
62.5 mM	Tris
2 %	SDS
10 %	Glycerol
5 %	β-Mercaptoethanol
1 x	Protease inhibitor cocktail

5.5.11.   ROS Burst Assay

Plants were grown for 4 – 5 weeks in a walk-in chamber under short-day conditions.

One leaf disc per plant was harvested with a cork borer (diameter 4 mm), transferred to a new, white 96-well plate and floated oN in sterile H_2O. On the next day, H_2O was replaced by 100 μl ROS reaction mixture and the luminescence was measured using a 96-well plate reader (30 °C, 0.5 s measurement/well, 5 s shaking/ plate, 30 – 35 cycles).

ROS reaction mixture

Amount	Component
10 μg/ml	Horseradish peroxidase
400 μM	Luminol pH 11
100 nM	flg22

5.5.12.   Callose Deposition Assay

Plants were grown for 4 – 5 weeks in a walk-in chamber under short-day conditions. One day prior to the experiment the plants were not watered. One leaf per plant was syringe-infiltration with 1 μM flg22 or H_2O, respectively. Leaves discs were harvested 24 h later with a puncher (diameter 4 mm) and cleared oN in an ethanol : acetic acid (6 : 1) solution. After several washing steps (once with 50 % and 30 % ethanol and twice with H_2O for 1 h,

respectively) the leaves were stained with methyl blue (0.05 % in 67 mM K_2HPO_4 pH 9.2) oN in darkness. Callose deposits were visualizes using fluorescence microscopy (Leica DMI 6000B, A4 filter, 5x objective) and one representative picture was taken per leaf disc. Image processing and analyses were performed using ImageJ/FIJI (1.46r). Pictures were background subtracted (rolling ball of 10 pixels) and filtered (Gaussian blur of 1 pixel) prior to automatic thresholding. The number of callose depositions was counted using the "analyze particles" function of ImageJ.

5.5.13.   Marker Gene Expression

Five-week-old *Arabidopsis* leaves were used for the analysis of gene expression upon a certain stimulus. Leaves were infiltrated with 1 μM flg22 and water (as control) for the examination of the defense marker genes. Leaves were infiltrated with water or wounded with a needle to analyze the stress induction. Here, non-infiltrated and non-wounded leaves were used as controls. Leaves were harvested at the indicated time points and handled as described in 5.3.

5.5.14.   Infection with *P. syringae*

Arabidopsis plants were grown for 4 – 5 weeks in a walk-in chamber under short-day conditions. *P. syringae* bacteria were grown in liquid culture (containing the respective antibiotic selection) until $OD_{600} = 0.6 – 0.9$. The plants were spray-inoculated with an OD_{600} of 0.02 (in 10 mM $MgCl_2$ containing 0.04 % Silwet L-77). After spraying, the plants were kept under high humidity for three days in a binder chamber. Two leaf discs (diameter 4 mm) per plant were pooled and ground in 10 mM $MgCl_2$. Serial dilutions were dropped to Kings B medium containing the appropriate antibiotic selection (5.1.1.2) and colonies were counted 2 – 3 days after incubation at 28 °C.

5.5.15.   Infection with *H. arabidopsidis*

For the evaluation of oomycete haustoria, plants were grown for 14 days in a walk-in chamber under long-day conditions. 10 – 15 seedlings were planted in one pot. *Hpa* Noco2 spores were freshly harvested from Col-0 plants one week after infection. Therefore, infected

leaves were collected, washed with sterile H_2O and mixed by vigorous shaking. After filtration through miracloth, the liquid was sprayed onto *Arabidopsis* seedlings. The seedlings were kept under high humidity for six days in a binder chamber. Haustoria were images using confocal microscopy (5.7).

The evaluation of *Hpa* sporulation was performed by Harald Keller (UMR-Institut Sophia Agrobiotech). In brief, 10-day-old seedlings were spray-inoculated to saturation with a spore suspension from the *H. arabidopsidis* isolate Waco at 40,000 spores mL^{-1}. Plants were kept in a growth cabinet at 16 °C for six days with a 12 h photoperiod. Sporulation was induced by spraying plants with water and keeping them for 24 h under high humidity, and the sporulation rate was determined with a hemocytometer.

5.5.16.   Infection with *A. brassicicola*

Elisabeth Pabst (Helmholtz Zentrum München) performed the infection assays with *A. brassicicola*. In brief, 600 spores of *A. brassicicola* were dropped onto four-week-old *A. thaliana* leaves. After 4 – 5 days, the severity of disease was determined by measuring the lesion diameters at the spots of infection.

5.5.17.   Auxin Root Growth Inhibition Assay

Arabidopsis seeds were grown vertically on ½ MS plates containing 1 % sucrose (5.1.3.1) for 3 – 4 days under long-day conditions. Subsequently, the seedlings were transferred to ½ MS plates supplemented with 1 % sucrose and different concentrations of naphthaleneacetic acid (NAA). The length of the primary root was marked on day 0 as control and on day 3 and day 5. Plates were scanned and the root growth was analyzed using ImageJ.

5.5.18.   Developmental Phenotyping

All seeds were germinated on ½ MS plates supplemented with 1 % sucrose (5.1.3.1). Seedlings designated for the examination of germinations rates and rosette diameter at 14 days were grown on plate under long-day conditions. The phenotyping of later development stages was performed on adult plant grown under long-day conditions in the greenhouse.

The transition from the vegetative to generative state (floral transition) was defined as the time point of shoot emergence.

5.6. Yeast Work

5.6.1.   Yeast Transformation

Remorins were cloned into the pGADT7 vector containing the activation domain (AD) of GAL4 to perform the GAL4 yeast two-hybrid interaction assays. The cytosolic domains of all kinases were cloned into the pGBKT7 vector containing the binding domain (BD) of GAL4. 200 ng of both plasmids were combined and mixed with 300 μl of the yeast transformation master mix.

The strain PJ69-4a was grown in 20 ml liquid YPAD (5.1.2.1) until it reached OD_{600} = 0.6. Cells were harvested, dissolved in 1 ml sterile water and 100 μl were immediately added to the master mix. After vigorous shaking for at least 1 minute, the cells were incubated for 45 min at 42 °C. Subsequently, the cells were harvested, resuspended in 0.9 % NaCl and plated on SD medium (5.1.2.2) lacking leucine and tryptophan. The transformation efficiency was analyzed after 2 – 3 days incubation at 28 °C.

Yeast transformation master mix

Amount	Component
240 μl	50 % PEG 3350
36 μl	1 M LiAc
30 μl	2 mg/mg denatured single-stranded DNA

5.6.2.   GAL4 Yeast Two-Hybrid Drop Assay

PJ69-4a cells were co-transformed with AD- and BD-fused constructs of interest (5.6.1). At least 10 colonies per combination were pooled and grown over night in 100 μl liquid SD –LW medium (5.1.2.2) at 28 °C. On the next day, the cells were diluted to a final OD_{600} of 1. Five serial dilutions were performed and dropped onto SD -LW, SD -LWH and SD -LWH

+ 2.5 mM 3-amino-1,2,4-triazole (3-AT) plates using a stamp. Yeast growth was analyzed after 3 days incubation at 28 °C.

5.6.3.   Protein Extraction from Yeast

20 ml of SD -LW liquid medium (5.1.2.2) were inoculated with yeast cells grown on SD -LW plates of the GAL4 Y2H drop assay (5.6.2). After 16 – 20 h shaking at 28 °C, the cells were harvested and washed with 1 mM EDTA. The pellet was dissolved with 200 μl 2 M NaOH and incubated on ice for 10 min. Subsequently, 200 μl 50 % TCA were added, mixed and incubated on ice for 2 h. The cells were harvested (20 min, 14,000 x g, 4 °C) and washed with 200 μl ice-cold acetone. Following another centrifugation step (20 min, 14,000 x g, 4 °C), the cells were resuspended with 200 μl 5 % SDS and equal amounts of SDS sample buffer were added. Cells were incubated for 15 min at 37 °C with gently shaking and cell debris was removed by centrifugation (5 min, 14,000 x g, RT). The supernatant was analyzed using SDS-PAGE (5.4.1) followed by immunoblot analysis (5.4.2).

Yeast SDS sample buffer

Amount	Component
25 mM	Tris-HCl pH 6.8
9 M	Urea
1 mM	EDTA
1 %	SDS
0.7 M	β-Mercaptoethanol
10 %	Glycerol
0.01 %	Bromphenol blue

5.7. Confocal Laser Scanning Microscopy (CLSM)

For microscopic analyses, *A. thaliana* and *N. benthamiana* leaves were infiltrated with H_2O prior to harvest (puncher 4 mm diameter). Leaf discs were mounted on glass slides and immediately imaged using a Leica TCS SP5 confocal microscope. GFP was excited with the Argon laser (AR) at 488 nm and the emission was detected between 500 and 550 nm. YFP

was excited with a wavelength of 514 nm (AR) and the emission was detected at 525 – 599 nm. mCherry was excited at 561 nm using the Diode Pumped Solid State (DPSS) laser and the emission was detected at 570 – 640 nm. Samples, co-expressing two fluorophores, were imaged using the sequential mode between frames. Images were taken with a Leica DFC350FX digital camera.

5.7.1.   FM4-64 Staining of the Plasma Membrane

100 μg FM4-64 powder were resolved in 165 μl DMSO. Prior to use the stock solution was diluted 1:10 with H_2O (final concentration: 100 μM). Leaf discs were floated in FM4-64 for 15 – 20 minutes prior to image acquisition. The excitation was performed at 561 nm with the DPSS laser and the emission was detected between 570 and 640 nm.

5.7.2.   Bimolecular Fluorescence Complementation (BiFC)

BiFC experiments were transiently performed in *N. benthamiana* leaves (5.5.9). Therefore, all remorin constructs were N-terminally fused to the N- and C-terminal part of YFP (Yn or Yc), while RICKY1 constructs were C-terminally fused to Yn. All constructs were under the control of the 35S promoter (pAMPAT vector series). Remorins were infiltrated with a final OD_{600} of 0.005 and RICKY1 with a final OD_{600} of 0.2. The expression was analyzed three days after infiltration using confocal microscopy (5.7).

5.7.3.   Fluorescence Lifetime Imaging and Fluorescence Resonance Energy Transfer (FLIM-FRET)

FLIM-FRET experiments were performed in five-week-old stable transformed *A. thaliana* plants expressing *RICKY1-sGFP*, *RICKY1-sGFP* and *mCherryREM1.2* or *RICKY1-sGFP* and *mCherry-REM1.3* under the control of their native promoters, respectively. The fluorescence of H_2O-infiltrated leaf discs was first verified as described above (5.7). FLIM measurements were performed with a Ti:Sapphire (Mai Tai) picosecond-pulse multi-photon laser and a fast FLIM photomultiplier (Becker & Hickl, Berlin, Germany). The 63x lens (zoom 4 – 6) was used for imaging. Image acquisition was performed with a pixel format of 256x256 and a pinhole set to 9.89. GFP was excited with a wavelength of 900 nm (12.5 %,

21 % Gain, 20 % Offset, 80 MHz pulsing) and fluorescence was detected between 495 – 570 nm.

Data acquisition was performed with the predefined setup, 256_256_80.hz-256tch, of the SPCM software. Photons were counted for 64 cycles (3 s/cycle). Fluorophore lifetimes were subsequently analyzed using the SPCImage software version 2.80. Therefore, a ROI was dragged around the PM excluding chloroplasts and obvious artifacts. The "hot spot" was positioned manually to calculate the Instrument Response Function (IRF) for the fitting procedure. For an optimized signal to noise ratio, pixels were binned by factor 6. Additionally, a threshold value of 20 was used for all pictures. The χ^2 fit should be close to 1. The fluorescence decay matrix was calculated to obtain the average lifetime of GFP per image. Values between 2000 and 2600 ns were taken into consideration. In addition, the frequency of all lifetimes was exported. The FRET efficiency was calculated using the formula: $(1-(lifetime_{with\ acceptor}/ lifetime_{without\ acceptor}))*100$.

5.7.4. Fluorescence Recovery After Photo Bleaching (FRAP)

FRAP experiments to compare the mobility of RICKY1-sGFP in the *ricky1-1* and the *rem1.2-1* mutant backgrounds were performed in 14-day-old seedlings. Five-week-old plants were used to compare the dynamics of RICKY1-sGFP and RICKY1 D811N-sGFP (both in *ricky1-1*). The imaging was performed in the FRAP Wizard software with AR laser power of 40 %. The 20x lens (zoom 15) and a pixel format of 512x512 were used for image acquisition. Three pre-bleach images were taken (1.293 s/frame). Subsequently, two ROIs (2 *μ*m x 2 *μ*m) were bleached per image (seedlings: 15 frames, laser 488 nm 100 %, 476 nm 100 %; adult plants: RICKY1-sGFP: 20 frames, laser 488 nm 100 %, 476 nm 100 %; RICKY1 D811N-sGFP: 10 frames, laser 488 nm 100 %) and recovery was imaged in 15 s intervals over 20 frames.

FRAP calculation were performed using ImageJ and R studio. In brief, fluorescence values in a bleached area were normalized to a control ROI in the proximity. Normalized values were fitted using the formula y = A*(1- exp(-b*x)). Mobile fractions (mf = $A*100/I_I$; with I_I = initial fluorescence intensity) were calculated.

5.8. Total Internal Reflection Fluorescence (TIRF) Microscopy

Sebastian Konrad (LMU München) performed the TIRF microscopy as well as the subsequent co-localization analyses.

In brief, a planar gel pad of Carolina Observation Gel (Carolina Biological Supply, Item No. # 132700) was created by pressing a small ball of gel between two glass slides. Leaves where infiltrated with perfluorodecalin and mounted on the gel as described in (Littlejohn *et al.*, 2014). TIRF illumination was generated in a Delta Vision Elite (GE, Healthcare, Applied Precision) system with an Olympus IX-71 microscope, equipped with an Insight SSI(TM) solid state illumination system and an X4 laser module. Images were taken with an Olympus UAPON 100XOTIRF 1.49 NA oil immersion objective and recorded with a CoolSnap HQ2 CCD camera (Photometrics, Tucson, USA). GFP was excited with the 488 nm laser line and emission was detected with a 525/48 nm bandpass filter. mCherry was excited with the 542 nm laser line and emission was detected with a 597/45 nm bandpass filter. Image exposure time and TIRF angle were adjusted according to sample fluorescence intensity and specimen location.

Pearson's colocalization of at least 20 images where determined using the ImageJ plugin JACoP (Bolte & Cordelieres, 2006). A Costes randomization was conducted for every image to evaluate these parameters. Therefore, pixel blocks of the GFP channels were randomly distributed resulting in artificial images that were again compared with the corresponding mCherry channel. P-values of the Costes randomization always yielded a highly significant difference from the original images (P= >99%).

5.9. Statistical Analyses

The program "R studio" (0.99.486 © 2009 – 2015 R Studio Inc.) was used for graphical presentation and statistical analyses. Therefore, the packages "multcomp" (Hothorn *et al.*, 2008), "multcompview" and "car" (Fox & Weisberg, 2011) were used. If two samples with equal variances were compared, a Student´s *t*-test was performed. A Welch *t*-test was performed, if the samples had unequal variances. If more than two samples were analyzed, a one-way analysis of variance (ANOVA) followed by a Tukey HSD test (all vs. all) or a Duunett´s multiple comparison test (all vs. one) was performed. The Fisher´s exact test was used to assess the independency of a certain characteristic in different samples. Values obtained by qPCR were transformed logarithmically prior to statistical analysis.

5.10.   Web Tools

Name	Link*	Purpose of use
Clustal Omega	http://www.ebi.ac.uk/Tools/msa/clustalo/	Protein alignment
UniProtKB	http://www.uniprot.org/help/uniprotkb	Prediction of protein domains
Pfam30.0	http://pfam.xfam.org/	Prediction of protein domains
PONDR VL-XT	http://www.pondr.com/	Prediction of ID regions
WMD3	http://wmd3.weigelworld.org/cgi-bin/webapp.cgi	Design of amiRNAs

* 26.02.2017

6. Abbreviations

3-AT	3-amino-1,2,4-triazole
35S	Promoter of the Cauliflower mosaic virus
α-	Anti-
AD	Activation domain
A. thaliana	*Arabidopsis thaliana*
A. tumefaciens	*Agrobacterium tumefaciens*
ABA	Abscisic acid
ABI1	ABSCISIC-ACID INSENSITIVE 1
ABRC	Arabidopsis Biological Resource Center
ACA8	ARABIDOPSIS-AUTOINHIBITED CA2+ ATPASE 8
ACT1	ACTIN 1
AM	Arbuscular mycorrhiza
amiRNA	Artificial microRNA
ANX	ANXUR
APS	Ammoniumperoxodisulphate
ATL31	TOXICOS EN LEVADURA 31
ATP	Adenosine 5′-triphosphate
Avr	Avirulence
BAK1	BRI1-ASSOCIATED RECEPTOR KINASE
BD	Binding domain
Bgh	*Blumeria graminis* f. sp. *hordei*
Bgt	*Blumeria graminis* f. sp. *tritici*
BiFC	Bimolecular fluorescence complementation
BIK1	BOTRYTIS-INDUCED KINASE 1
BOR1	BORON TRANSPORTER 1
BR	brassinosteroid
BRI1	BRASSINOSTEROID INSENSITIVE 1
BSA	Bovine serum albumin
C-terminus	Carboxy-terminus
Ca^{2+}	Calcium
CD	Cytosolic domain
cDNA	Coding DNA
CDPK/CPK	CALCIUM-DEPENDENT PROTEIN KINASE
CEBiP	CHITIN ELICITOR-BINDING PROTEIN
CERK1	CHITIN ELICITOR RECEPTOR KINASE 1
CesA	Cellulose synthase
Cfu	Colony forming unit
Cl^-	Chloride
CLSM	Confocal laser scanning microscopy
COR	Coronatine
CRISPR	Clustered Regularly Interspaced Short Palindromic Repeats
CSC	Cellulose synthase complex
CSI1	CELLULOSE SYNTHASE-INTERACTIVE PROTEIN 1
CW	Cell wall
CWI	Cell wall integrity
D/Asp	Aspartic acid
DAMP	DAMAGE-ASSOCIATED MOLECULAR PATTERN
DEX	Dexamethasone
DIM	Detergent-insoluble membrane
Dm	Double mutant
DNA	Deoxyribonucleic acid
dNTP	Di-nucleotide triphosphate

DOPE	1,2-dioleoyl-sn-glycero-3-phosphoethanolamine
DORN1	DOES NOT RESPOND TO NUCLEOTIDES 1
dpi	Days post infection
DRM	Detergent-resistant membrane
DSM	Detergent-soluble membrane
DTT	Dithiothreitol
E. coli	*Escherichia coli*
ECD	Extracellular domains
EDS1	ENHANCED DISEASE SUSCEPTIBILITY 1
EDTA	Ethylenediaminetetraacetic acid
EFR	EF-TU RECEPTOR
EF-TU	Elongation factor thermo unstable
EHM	Extra-haustorial membrane
ERF	ETHYLENE RESPONSE FACTOR 1
ERL	ERECTA-LIKE
ET	Ethylene
ETI	Effector-triggered immunity
ETS	Effector-triggered susceptibility
FLIM	Fluorescence lifetime imaging
FLOT	Flotillin
FLS2	FLAGELLIN SENSING 2
FRAP	Fluorescence recovery after photobleaching
FRET	Fluorescence resonance energy transfer
G/Gly	Glycin
GAL4	Galactose-responsive transcription factor
gDNA	Genomic DNA
GFP	Green fluorescence protein
GPI	Glycosylphosphatidylinositol
GSD1	GRAIN SETTING DEFECT 1
GSL	GLUCAN SYNTHASE-LIKE
GW	Gateway
H	Histidine
h	hour(s)
HAE/HSL2	HAESA/HAE-LIKE 2
Hpa	*Hyaloperonospora arabidopsidis*
HR	Hypersensitive response
HRP	Horseradish peroxidase
HygB	Hygromycin B
IAA	Indole-3-acetic acid
ID	Intrinsic disorder
IG	Indole glucosinolate
IOS1	IMPAIRED IN SUSCEPTIBILITY 1
IRAK	IL-1 RECEPTOR-ASSOCIATED KINASE
JA	Jasmonic acid
K/Lys	Lysine
K^+	Potassium
Kan	Kanamycin
KAT1	*ARABIDOPSIS THALIANA* K^+ CHANNEL
Kb	Kilobase
KD	Knockdown
L	Leucine
LecRK	Lectin receptor kinase
LIK1	LYSM RLK1-INTERACTING KINASE 1
LORE	LIPOOLIGOSACCHARIDE-SPECIFIC REDUCED ELICITATION
LPS	Lipopolysaccharides
LRR	Leucine-rich repeat
LYM	LysM DOMAIN-CONTAINING GPI-ANCHORED PROTEIN
LYK	LYSIN MOTIF RECEPTOR LIKE KINASE

LysM	Lysin motif
M	Molar
M. truncatula	*Medicago truncatula*
MAMP	Microbe-associated molecular pattern
MAPK	Mitogen-activated protein kinase
MD	Malectin domain
mg	Milligram
MEKK1	MAPK/ERK KINASE KINASE 1
MES	2-(N-morpholino)ethanesulfonic acid
MgCl$_2$	Magnesium chloride
MgSO$_4$	Magnesium sulphate
MKK	MITOGEN-ACTIVATED PROTEIN KINASE KINASE
min	Minute(s)
ml	Millilitre
MLD	Malectin-like domain
μm	micrometer
MPK	MITOGEN-ACTIVATED PROTEIN KINASE
MS	Murashige Skoog
MSK	Membrane-associated cytoskeleton
MtPT4	*Medicago truncatula* phosphate transporter 4
N. benthamiana	*Nicotiana benthamiana*
N-terminus	Amino-terminus
NAA	Naphthaleneacetic acid
NASC	Nottingham Arabidopsis Stock Center
NB-LRR	Nucleotide-binding-LRR
NFR	NOD FACTOR RECEPTOR
NPA	N-1-Naphthylphthalamic Acid
OD	Optical density
OGs	Oligogalacturonides
oN	over night
ORF	Open reading frame
PAGE	Polyacrylamide gel electrophoresis
PAM	Periarbuscular membrane
PAMP	Pathogen-associated molecular pattern
PBL	AVRPPHB SUSCEPTIBLE 1 (PBS1)-like
PCR	Polymerase chain reaction
PD	Plasmodesmata
PDLP1	PLASMODESMATA LOCATED PROTEIN 1
PEG	Polyethylene glycol
PEN	PENETRATION
PEPR	PEP1 RECEPTOR
PG	Polygalacturonase
PGAs	Polygalacturonides
PGN	Peptidoglycan
PIN	PINFORMED
PIP	PLASMA MEMBRANE INTRINSIC PROTEIN
PM	Plasma membrane
PME	Pectin methylesterase
PMR4	POWDERY MILDEW RESISTANT 4
PR1	PATHOGENESIS-RELATED PROTEIN 1
PRR	Pattern-recognition receptor
Pro	Promoter
PSKR1	PHYTOSULFOKINE (PSK) RECEPTOR 1
PTI	PAMP-triggered immunity
Pto	*Pseudomonas syringae* pv. *tomato*
qPCR	quantitative PCR
R/Arg	Arginine
R gene	Resistance gene

RALF	RAPID ALKALINIZATION FACTOR
RBOHD	RESPIRATORY BURST OXIDASE HOMOLOG D
Rd	randomized
RICKY1	REMORIN INTERACTING KINASE IN YEAST
RIN4	RPM1 INTERACTING PROTEIN 4
REM	Remorin
RIPK	RPM1-INDUCED PROTEIN KINASE
RK	Receptor kinase
RLCK	Receptor-like cytoplasmic kinase
RLK	Receptor-like kinase
RLP	Receptor-like protein
RLU	Relative light units
ROI	region of interest
ROS	Reactive oxygen species
RPM1	RESISTANCE TO PSEUDOMONAS SYRINGAE PV. MACULICOLA
RPS2	RESISTANCE TO PSEUDOMONAS SYRINGAE 2
RPW8.2	RESISTANCE TO POWDERY MILDEW 8.2
Rr	Pearson´s coefficient
RT	Room temperature
RYL1	RICKY1-LIKE 1
SA	Salicylic acid
SD	Selective dropout
SDS	Sodium dodecyl-sulphate
SE	Standard error
S/Ser	Serine
SERK	SOMATIC EMBRYOGENESIS RECEPTOR KINASE
SLAC1	SLOW ANION CHANNEL 1
SLAH3	SLAC1 HOMOLOG 3
SNAP33	SOLUBLE N-ETHYLMALEIMIDE-SENSITIVE FACTOR ADAPTOR PROTEIN 33
SYMREM	SYMBIOTIC REMORIN 1
SYMRK	SYMBIOSIS RECEPTOR-LIKE KINASE
T/Thr	Threonine
T-DNA	Transfer DNA
TEMED	Tetramethylethylenediamine
THE1	THESEUS1
TIR	Toll-interleukin 1 (IL-1) receptor
TIRF	Total internal reflection fluorescence microscopy
TLR	TOLL-LIKE RECEPTOR
TM	Transmembrane
UBC	Ubiquitin C
V	Volt
VAMP722	VESICLE-ASSOCIATED MEMBRANE PROTEIN 722
W	Tryptophan
WAK	WALL-ASSOCIATED KINASE
WT	Wild type
Y2H	Yeast two-hybrid
Yc	C-terminal part of the yellow fluorescence protein
Yn	N-terminal part of the yellow fluorescence protein
YNB	Yeast nitrogen base
τ	Fluorescence lifetime

7. Literature

aan den Toorn M, Huijbers MME, de Vries SC, van Mierlo CPM. 2012. The Arabidopsis thaliana SERK1 Kinase Domain Spontaneously Refolds to an Active State In Vitro. *Plos One* **7**(12): e50907.

Aderem A, Ulevitch RJ. 2000. Toll-like receptors in the induction of the innate immune response. *Nature* **406**(6797): 782-787.

Aist JR. 1976. Papillae and Related Wound Plugs of Plant-Cells. *Annual Review of Phytopathology* **14**: 145-163.

Albrecht C, Russinova E, Hecht V, Baaijens E, de Vries S. 2005. The Arabidopsis thaliana SOMATIC EMBRYOGENESIS RECEPTOR-LIKE KINASES1 and 2 control male sporogenesis. *Plant Cell* **17**(12): 3337-3349.

Ali GS, Prasad KVSK, Day I, Reddy ASN. 2007. Ligand-dependent reduction in the membrane mobility of FLAGELLIN SENSITIVE2, an Arabidopsis receptor-like kinase. *Plant and Cell Physiology* **48**(11): 1601-1611.

Antolin-Llovera M, Ried MK, Parniske M. 2014. Cleavage of the SYMBIOSIS RECEPTOR-LIKE KINASE Ectodomain Promotes Complex Formation with Nod Factor Receptor 5. *Current Biology* **24**(4): 422-427.

Asai T, Tena G, Plotnikova J, Willmann MR, Chiu WL, Gomez-Gomez L, Boller T, Ausubel FM, Sheen J. 2002. MAP kinase signalling cascade in Arabidopsis innate immunity. *Nature* **415**(6875): 977-983.

Assaad FF, Qiu JL, Youngs H, Ehrhardt D, Zimmerli L, Kalde M, Wanner G, Peck SC, Edwards H, Ramonell K, et al. 2004. The PEN1 syntaxin defines a novel cellular compartment upon fungal attack and is required for the timely assembly of papillae\. *Molecular Biology of the Cell* **15**(11): 5118-5129.

Axtell MJ, Chisholm ST, Dahlbeck D, Staskawicz BJ. 2003. Genetic and molecular evidence that the Pseudomonas syringae type III effector protein AvrRpt2 is a cysteine protease. *Molecular Microbiology* **49**(6): 1537-1546.

Axtell MJ, Staskawicz BJ. 2003. Initiation of RPS2-specified disease resistance in Arabidopsis is coupled to the AvrRpt2-directed elimination of RIN4. *Cell* **112**(3): 369-377.

Bah A, Vernon RM, Siddiqui Z, Krzeminski M, Muhandiram R, Zhao C, Sonenberg N, Kay LE, Forman-Kay JD. 2015. Folding of an intrinsically disordered protein by phosphorylation as a regulatory switch. *Nature* **519**(7541): 106-109.

Baluška F, Šamaj J, Wojtaszek P, Volkmann D, Menzel D. 2003. Cytoskeleton-plasma membrane-cell wall continuum in plants. Emerging links revisited. *Plant Physiology* **133**(2): 482-491.

Barberon M, Dubeaux G, Kolb C, Isono E, Zelazny E, Vert G. 2014. Polarization of IRON-REGULATED TRANSPORTER 1 (IRT1) to the plant-soil interface plays crucial role in metal homeostasis. *Proceedings of the National Academy of Sciences of the United States of America* **111**(22): 8293-8298.

Bariola PA, Retelska D, Stasiak A, Kammerer RA, Fleming A, Hijri M, Franks S, Farmer EE. 2004. Remorins form a novel family of coiled coil-forming oligomeric and filamentous proteins associated with apical, vascular and embryonic tissues in plants. *Plant Molecular Biology* **55**(4): 579-594.

Bartels S, Lori M, Mbengue M, van Verk M, Klauser D, Hander T, Boni R, Robatzek S, Boller T. 2013. The family of Peps and their precursors in Arabidopsis: differential expression and localization but similar induction of pattern-triggered immune responses. *Journal of Experimental Botany* **64**(17): 5309-5321.

Beauzamy L, Nakayama N, Boudaoud A. 2014. Flowers under pressure: ins and outs of turgor regulation in development. *Annals of Botany* **114**(7): 1517-1533.

Bednarek P, Pislewska-Bednarek M, Svatos A, Schneider B, Doubsky J, Mansurova M, Humphry M, Consonni C, Panstruga R, Sanchez-Vallet A, et al. 2009. A Glucosinolate Metabolism Pathway in Living Plant Cells Mediates Broad-Spectrum Antifungal Defense. *Science* **323**(5910): 101-106.

Bellincampi D, Cervone F, Lionetti V. 2014. Plant cell wall dynamics and wall-related susceptibility in plant-pathogen interactions. *Frontiers in Plant Science* **5**(228).

Bellincampi D, Dipierro N, Salvi G, Cervone F, De Lorenzo G. 2000. Extracellular H2O2 induced by oligogalacturonides is not involved in the inhibition of the auxin-regulated rolB gene expression in tobacco leaf explants. *Plant Physiology* **122**(4): 1379-1385.

Bender CL, Alarcon-Chaidez F, Gross DC. 1999. Pseudomonas syringae phytotoxins: Mode of action, regulation, and biosynthesis by peptide and polyketide synthetases. *Microbiology and Molecular Biology Reviews* **63**(2): 266-292.

Benjamins R, Scheres B. 2008. Auxin: The looping star in plant development. *Annual Review of Plant Biology* **59**: 443-465.

Benschop JJ, Mohammed S, O'Flaherty M, Heck AJR, Slijper M, Menke FLH. 2007. Quantitative phosphoproteomics of early elicitor signaling in Arabidopsis. *Molecular & Cellular Proteomics* **6**(7): 1198-1214.

Bent AF, Kunkel BN, Dahlbeck D, Brown KL, Schmidt R, Giraudat J, Leung J, Staskawicz BJ. 1994. Rps2 of Arabidopsis-Thaliana - a Leucine-Rich Repeat Class of Plant-Disease Resistance Genes. *Science* **265**(5180): 1856-1860.

Berchtold D, Walther TC. 2009. TORC2 Plasma Membrane Localization Is Essential for Cell Viability and Restricted to a Distinct Domain. *Molecular Biology of the Cell* **20**(5): 1565-1575.

Berrocal-Lobo M, Molina A, Solano R. 2002. Constitutive expression of ETHYLENE-RESPONSE-FACTOR1 in Arabidopsis confers resistance to several necrotrophic fungi. *Plant J* **29**(1): 23-32.

Bethke G, Pecher P, Eschen-Lippold L, Tsuda K, Katagiri F, Glazebrook J, Scheel D, Lee J. 2012. Activation of the Arabidopsis thaliana Mitogen-Activated Protein Kinase MPK11 by the Flagellin-Derived Elicitor Peptide, flg22. *Molecular Plant-Microbe Interactions* **25**(4): 471-480.

Bhat RA, Miklis M, Schmelzer E, Schulze-Lefert P, Panstruga R. 2005. Recruitment and interaction dynamics of plant penetration resistance components in a plasma membrane microdomain. *Proc Natl Acad Sci U S A* **102**(8): 3135-3140.

Bigeard J, Colcombet J, Hirt H. 2015. Signaling Mechanisms in Pattern-Triggered Immunity (PTI). *Molecular Plant* **8**(4): 521-539.

Binder A, Lambert J, Morbitzer R, Popp C, Ott T, Lahaye T, Parniske M. 2014. A modular plasmid assembly kit for multigene expression, gene silencing and silencing rescue in plants. *Plos One* **9**(2): e88218.

Blachutzik JO, Kreuzer I, Hedrich R, Harms GS. 2015. Mobility of Group 1b Remorins in Membrane Nanodomains Differs Significantly between Mesophyll Cells and Protoplasts. *J Plant Biochem Physiol* **3**(153).

Blume B, Nurnberger T, Nass N, Scheel D. 2000. Receptor-mediated increase in cytoplasmic free calcium required for activation of pathogen defense in parsley. *Plant Cell* **12**(8): 1425-1440.

Boisson-Dernier A, Kessler SA, Grossniklaus U. 2011. The walls have ears: the role of plant CrRLK1Ls in sensing and transducing extracellular signals. *Journal of Experimental Botany* **62**(5): 1581-1591.

Boisson-Dernier A, Roy S, Kritsas K, Grobei MA, Jaciubek M, Schroeder JI, Grossniklaus U. 2009. Disruption of the pollen-expressed FERONIA homologs ANXUR1 and ANXUR2 triggers pollen tube discharge. *Development* **136**(19): 3279-3288.

Boller T. 1995. Chemoperception of Microbial Signals in Plant-Cells. *Annual Review of Plant Physiology and Plant Molecular Biology* **46**: 189-214.

Boller T, Felix G. 2009. A renaissance of elicitors: perception of microbe-associated molecular patterns and danger signals by pattern-recognition receptors. *Annu Rev Plant Biol* **60**: 379-406.

Bolte S, Cordelieres FP. 2006. A guided tour into subcellular colocalization analysis in light microscopy. *Journal of Microscopy* **224**: 213-232.

Bolte S, Talbot C, Boutte Y, Catrice O, Read ND, Satiat-Jeunemaitre B. 2004. FM-dyes as experimental probes for dissecting vesicle trafficking in living plant cells. *Journal of Microscopy* **214**: 159-173.

Boron AK, Vissenberg K. 2014. The Arabidopsis thaliana hypocotyl, a model to identify and study control mechanisms of cellular expansion. *Plant Cell Reports* **33**(5): 697-706.

Bortesi L, Fischer R. 2015. The CRISPR/Cas9 system for plant genome editing and beyond. *Biotechnology Advances* **33**(1): 41-52.

Boudsocq M, Sheen J. 2013. CDPKs in immune and stress signaling. *Trends Plant Sci* **18**(1): 30-40.

Boudsocq M, Willmann MR, McCormack M, Lee H, Shan L, He P, Bush J, Cheng SH, Sheen J. 2010. Differential innate immune signalling via Ca(2+) sensor protein kinases. *Nature* **464**(7287): 418-422.

Bouwmeester K, de Sain M, Weide R, Gouget A, Klamer S, Canut H, Govers F. 2011. The Lectin Receptor Kinase LecRK-I.9 Is a Novel Phytophthora Resistance Component and a Potential Host Target for a RXLR Effector. *Plos Pathogens* **7**(3): e1001327.

Bozkurt TO, Richardson A, Dagdas YF, Mongrand S, Kamoun S, Raffaele S. 2014. The Plant Membrane-Associated REMORIN1.3 Accumulates in Discrete Perihaustorial Domains and Enhances Susceptibility to Phytophthora infestans. *Plant Physiology* **165**(3): 1005-1018.

Bradley DJ, Kjellbom P, Lamb CJ. 1992. Elicitor-Induced and Wound-Induced Oxidative Cross-Linking of a Proline-Rich Plant-Cell Wall Protein - a Novel, Rapid Defense Response. *Cell* **70**(1): 21-30.

Bringmann M, Li EY, Sampathkumar A, Kocabek T, Hauser MT, Persson S. 2012. POM-POM2/CELLULOSE SYNTHASE INTERACTING1 Is Essential for the Functional Association of Cellulose Synthase and Microtubules in Arabidopsis. *Plant Cell* **24**(1): 163-177.

Broekgaarden C, Caarls L, Vos IA, Pieterse CMJ, Van Wees SCM. 2015. Ethylene: Traffic Controller on Hormonal Crossroads to Defense. *Plant Physiology* **169**(4): 2371-2379.

Brown DA. 2006. Lipid rafts, detergent-resistant membranes, and raft targeting signals. *Physiology* **21**: 430-439.

Brown DA, London E. 1998. Functions of lipid rafts in biological membranes. *Annual Review of Cell and Developmental Biology* **14**: 111-136.

Brown DA, Rose JK. 1992. Sorting of Gpi-Anchored Proteins to Glycolipid-Enriched Membrane Subdomains during Transport to the Apical Cell-Surface. *Cell* **68**(3): 533-544.

Brutus A, Sicilia F, Macone A, Cervone F, De Lorenzo G. 2010. A domain swap approach reveals a role of the plant wall-associated kinase 1 (WAK1) as a receptor of oligogalacturonides. *Proceedings of the National Academy of Sciences of the United States of America* **107**(20): 9452-9457.

Bücherl CA, Bader A, Westphal AH, Laptenok SP, Borst JW. 2014. FRET-FLIM applications in plant systems. *Protoplasma* **251**(2): 383-394.

Burton RA, Gidley MJ, Fincher GB. 2010. Heterogeneity in the chemistry, structure and function of plant cell walls. *Nature Chemical Biology* **6**(10): 724-732.

Butenko MA, Wildhagen M, Albert M, Jehle A, Kalbacher H, Aalen RB, Felix G. 2014. Tools and Strategies to Match Peptide-Ligand Receptor Pairs. *Plant Cell* **26**(5): 1838-1847.

Büttner D. 2016. Behind the lines-actions of bacterial type III effector proteins in plant cells. *Fems Microbiology Reviews* **40**(6): 894-937.

Cai RM, Lewis J, Yan SC, Liu HJ, Clarke CR, Campanile F, Almeida NF, Studholme DJ, Lindeberg M, Schneider D, et al. 2011. The Plant Pathogen Pseudomonas syringae pv. tomato Is Genetically Monomorphic and under Strong Selection to Evade Tomato Immunity. *Plos Pathogens* **7**(8).

Caillaud MC, Wirthmueller L, Sklenar J, Findlay K, Piquerez SJM, Jones AME, Robatzek S, Jones JDG, Faulkner C. 2014. The Plasmodesmal Protein PDLP1 Localises to Haustoria-Associated Membranes during Downy Mildew Infection and Regulates Callose Deposition. *Plos Pathogens* **10**(11).

Campos ML, Kang JH, Howe GA. 2014. Jasmonate-Triggered Plant Immunity. *Journal of Chemical Ecology* **40**(7): 657-675.

Canut H, Carrasco A, Galaud JP, Cassan C, Bouyssou H, Vita N, Ferrara P, Pont-Lezica R. 1998. High affinity RGD-binding sites at the plasma membrane of Arabidopsis thaliana links the cell wall. *Plant Journal* **16**(1): 63-71.

Cao YR, Liang Y, Tanaka K, Nguyen CT, Jedrzejczak RP, Joachimiak A, Stacey G. 2014. The kinase LYK5 is a major chitin receptor in Arabidopsis and forms a chitin-induced complex with related kinase CERK1. *Elife* **3**.

Casey PJ. 1995. Protein Lipidation in Cell Signaling. *Science* **268**(5208): 221-225.

Cervone F, Hahn MG, Delorenzo G, Darvill A, Albersheim P. 1989. Host-Pathogen Interactions. XXXIII. A Plant Protein Converts a Fungal Pathogenesis Factor into an Elicitor of Plant Defense Responses. *Plant Physiology* **90**(2): 542-548.

Cesari S, Bernoux M, Moncuquet P, Kroj T, Dodds PN. 2014. A novel conserved mechanism for plant NLR protein pairs: the "integrated decoy" hypothesis. *Frontiers in Plant Science* **5**(606).

Checker VG, Khurana P. 2013. Molecular and functional characterization of mulberry EST encoding remorin (MiREM) involved in abiotic stress. *Plant Cell Reports* **32**(11): 1729-1741.

Chen MK, Wilson RL, Palme K, Ditengou FA, Shpak ED. 2013. ERECTA Family Genes Regulate Auxin Transport in the Shoot Apical Meristem and Forming Leaf Primordia. *Plant Physiology* **162**(4): 1978-1991.

Chen XM. 2005. microRNA biogenesis and function in plants. *Febs Letters* **579**(26): 5923-5931.

Chen Y, Hu D, Yabe R, Tateno H, Qin SY, Matsumoto N, Hirabayashi J, Yamamoto K. 2011. Role of malectin in Glc(2)Man(9)GlcNAc(2)-dependent quality control of alpha 1-antitrypsin. *Molecular Biology of the Cell* **22**(19): 3559-3570.

Chen ZY, Agnew JL, Cohen JD, He P, Shan LB, Sheen J, Kunkel BN. 2007. Pseudomonas syringae type III effector AvrRpt2 alters Arabidopsis thaliana auxin physiology. *Proceedings of the National Academy of Sciences of the United States of America* **104**(50): 20131-20136.

Cheung AY, Wu HM. 2011. THESEUS 1, FERONIA and relatives: a family of cell wall-sensing receptor kinases? *Curr Opin Plant Biol* **14**(6): 632-641.

Chichili GR, Rodgers W. 2009. Cytoskeleton-membrane interactions in membrane raft structure. *Cell Mol Life Sci* **66**(14): 2319-2328.

Chinchilla D, Bauer Z, Regenass M, Boller T, Felix G. 2006. The Arabidopsis receptor kinase FLS2 binds flg22 and determines the specificity of flagellin perception. *Plant Cell* **18**(2): 465-476.

Chinchilla D, Zipfel C, Robatzek S, Kemmerling B, Nurnberger T, Jones JDG, Felix G, Boller T. 2007. A flagellin-induced complex of the receptor FLS2 and BAK1 initiates plant defence. *Nature* **448**(7152): 497-501.

Chisholm ST, Dahlbeck D, Krishnamurthy N, Day B, Sjolander K, Staskawicz BJ. 2005. Molecular characterization of proteolytic cleavage sites of the Pseudomonas syringae effector AvrRpt2. *Proceedings of the National Academy of Sciences of the United States of America* **102**(6): 2087-2092.

Choi HW, Klessig DF. 2016. DAMPs, MAMPs, and NAMPs in plant innate immunity. *BMC Plant Biol* **16**(1): 232-241.

Choi J, Tanaka K, Cao YR, Qi Y, Qiu J, Liang Y, Lee SY, Stacey G. 2014. Identification of a Plant Receptor for Extracellular ATP. *Science* **343**(6168): 290-294.

Choi WG, Toyota M, Kim SH, Hilleary R, Gilroy S. 2014. Salt stress-induced Ca2+ waves are associated with rapid, long-distance root-to-shoot signaling in plants. *Proceedings of the National Academy of Sciences of the United States of America* **111**(17): 6497-6502.

Chowdhury J, Henderson M, Schweizer P, Burton RA, Fincher GB, Little A. 2014. Differential accumulation of callose, arabinoxylan and cellulose in nonpenetrated versus penetrated papillae on leaves of barley infected with Blumeria graminis f. sp hordei. *New Phytologist* **204**(3): 650-660.

Clarke CR, Chinchilla D, Hind SR, Taguchi F, Miki R, Ichinose Y, Martin GB, Leman S, Felix G, Vinatzer BA. 2013. Allelic variation in two distinct Pseudomonas syringae flagellin epitopes modulates the strength of plant immune responses but not bacterial motility. *New Phytologist* **200**(3): 847-860.

Clay NK, Adio AM, Denoux C, Jander G, Ausubel FM. 2009. Glucosinolate Metabolites Required for an Arabidopsis Innate Immune Response. *Science* **323**(5910): 95-101.

Clough SJ, Bent AF. 1998. Floral dip: a simplified method for Agrobacterium-mediated transformation of Arabidopsis thaliana. *Plant J* **16**(6): 735-743.

Coaker GL, Willard B, Kinter M, Stockinger EJ, Francis DM. 2004. Proteomic analysis of resistance mediated by Rcm 2.0 and Rcm 5.1, two loci controlling resistance to bacterial canker of tomato. *Molecular Plant-Microbe Interactions* **17**(9): 1019-1028.

Coates ME, Beynon JL. 2010. Hyaloperonospora arabidopsidis as a Pathogen Model. *Annual Review of Phytopathology* **48**: 329-345.

Colcombet J, Boisson-Dernier A, Ros-Palau R, Vera CE, Schroeder JI. 2005. Arabidopsis SOMATIC EMBRYOGENESIS RECEPTOR KINASES1 and 2 are essential for tapetum development and microspore maturation. *Plant Cell* **17**(12): 3350-3361.

Cooper JA. 1987. Effects of Cytochalasin and Phalloidin on Actin. *Journal of Cell Biology* **105**(4): 1473-1478.

Cosgrove DJ. 2016. Catalysts of plant cell wall loosening. *F1000Res* **5**.

Coster HGL, Steudle E, Zimmermann U. 1977. Turgor Pressure Sensing in Plant-Cell Membranes. *Plant Physiology* **58**(5): 636-643.

Costes SV, Daelemans D, Cho EH, Dobbin Z, Pavlakis G, Lockett S. 2004. Automatic and quantitative measurement of protein-protein colocalization in live cells. *Biophysical Journal* **86**(6): 3993-4003.

Couto D, Zipfel C. 2016. Regulation of pattern recognition receptor signalling in plants. *Nature Reviews Immunology* **16**(9): 537-552.

Cui W, Lee JY. 2016. Arabidopsis callose synthases CalS1/8 regulate plasmodesmal permeability during stress. *Nat Plants* **2**(5): 16034.

Cunnac S, Chakravarthy S, Kvitko BH, Russell AB, Martin GB, Collmer A. 2011. Genetic disassembly and combinatorial reassembly identify a minimal functional repertoire of type III effectors in Pseudomonas syringae. *Proc Natl Acad Sci U S A* **108**(7): 2975-2980.

Dark A, Demidchik V, Richards SL, Shabala S, Davies JM. 2011. Release of extracellular purines from plant roots and effect on ion fluxes. *Plant Signal Behav* **6**(11): 1855-1857.

De Los Santos C, Chang CW, Mycek MA, Cardullo RA. 2015. FRAP, FLIM, and FRET: Detection and analysis of cellular dynamics on a molecular scale using fluorescence microscopy. *Molecular Reproduction and Development* **82**(7-8): 587-604.

Decreux A, Messiaen J. 2005. Wall-associated kinase WAK1 interacts with cell wall pectins in a calcium-induced conformation. *Plant and Cell Physiology* **46**(2): 268-278.

Decreux A, Thomas A, Spies B, Brasseur R, Van Cutsem P, Messiaen J. 2006. In vitro characterization of the homogalacturonan-binding domain of the wall-associated kinase WAK1 using site-directed mutagenesis. *Phytochemistry* **67**(11): 1068-1079.

Demir F, Horntrich C, Blachutzik JO, Scherzer S, Reinders Y, Kierszniowska S, Schulze WX, Harms GS, Hedrich R, Geiger D, et al. 2013. Arabidopsis nanodomain-delimited ABA signaling pathway regulates the anion channel SLAH3. *Proceedings of the National Academy of Sciences of the United States of America* **110**(20): 8296-8301.

Denance N, Sanchez-Vallet A, Goffner D, Molina A. 2013. Disease resistance or growth: the role of plant hormones in balancing immune responses and fitness costs. *Frontiers in Plant Science* **4**(155).

Denness L, McKenna JF, Segonzac C, Wormit A, Madhou P, Bennett M, Mansfield J, Zipfel C, Hamann T. 2011. Cell Wall Damage-Induced Lignin Biosynthesis Is Regulated by a Reactive Oxygen Species- and Jasmonic Acid-Dependent Process in Arabidopsis. *Plant Physiology* **156**(3): 1364-1374.

Denoux C, Galletti R, Mammarella N, Gopalan S, Werck D, De Lorenzo G, Ferrari S, Ausubel FM, Dewdney J. 2008. Activation of defense response pathways by OGs and Flg22 elicitors in Arabidopsis seedlings. *Molecular Plant* **1**(3): 423-445.

Derbyshire P, McCann MC, Roberts K. 2007. Restricted cell elongation in Arabidopsis hypocotyls is associated with a reduced average pectin esterification level. *Bmc Plant Biology* **7**(31).

Devaux PF, Morris R. 2004. Transmembrane asymmetry and lateral domains in biological membranes. *Traffic* **5**(4): 241-246.

Dinic J, Ashrafzadeh P, Parmryd I. 2013. Actin filaments attachment at the plasma membrane in live cells cause the formation of ordered lipid domains. *Biochimica Et Biophysica Acta-Biomembranes* **1828**(3): 1102-1111.

Dosztanyi Z, Chen J, Dunker AK, Simon I, Tompa P. 2006. Disorder and sequence repeats in hub proteins and their implications for network evolution. *Journal of Proteome Research* **5**(11): 2985-2995.

Duan Q, Kita D, Li C, Cheung AY, Wu HM. 2010. FERONIA receptor-like kinase regulates RHO GTPase signaling of root hair development. *Proc Natl Acad Sci U S A* **107**(41): 17821-17826.

Dubiella U, Seybold H, Durian G, Komander E, Lassig R, Witte CP, Schulze WX, Romeis T. 2013. Calcium-dependent protein kinase/NADPH oxidase activation circuit is required for rapid defense signal propagation. *Proceedings of the National Academy of Sciences of the United States of America* **110**(21): 8744-8749.

Dunker AK, Cortese MS, Romero P, Iakoucheva LM, Uversky VN. 2005. Flexible nets - The roles of intrinsic disorder in protein interaction networks. *Febs Journal* **272**(20): 5129-5148.

Dunlap JR, Kresovich S, Mcgee RE. 1986. The Effect of Salt Concentration on Auxin Stability in Culture Media. *Plant Physiology* **81**(3): 934-936.

Dunlap JR, Robacker KM. 1988. Nutrient Salts Promote Light-Induced Degradation of Indole-3-Acetic-Acid in Tissue-Culture Media. *Plant Physiology* **88**(2): 379-382.

Dyson HJ, Wright PE. 2005. Intrinsically unstructured proteins and their functions. *Nature Reviews Molecular Cell Biology* **6**(3): 197-208.

Eggert D, Naumann M, Reimer R, Voigt CA. 2014. Nanoscale glucan polymer network causes pathogen resistance. *Scientific Reports* **4**(4159).

Ellinger D, Naumann M, Falter C, Zwikowics C, Jamrow T, Manisseri C, Somerville SC, Voigt CA. 2013. Elevated Early Callose Deposition Results in Complete Penetration Resistance to Powdery Mildew in Arabidopsis. *Plant Physiology* **161**(3): 1433-1444.

Ellinger D, Voigt CA. 2014. Callose biosynthesis in arabidopsis with a focus on pathogen response: what we have learned within the last decade. *Annals of Botany* **114**(6): 1349-1358.

Endler A, Kesten C, Schneider R, Zhang Y, Ivakov A, Froehlich A, Funke N, Persson S. 2015. A Mechanism for Sustained Cellulose Synthesis during Salt Stress. *Cell* **162**(6): 1353-1364.

Enns LC, Kanaoka MM, Torii KU, Comai L, Okada K, Cleland RE. 2005. Two callose synthases, GSL1 and GSL5, play an essential and redundant role in plant and pollen development and in fertility. *Plant Molecular Biology* **58**(3): 333-349.

Evangelisti E, Govetto B, Minet-Kebdani N, Kuhn ML, Attard A, Ponchet M, Panabieres F, Gourgues M. 2013. The Phytophthora parasitica RXLR effector Penetration-Specific Effector 1 favours Arabidopsis thaliana infection by interfering with auxin physiology. *New Phytologist* **199**(2): 476-489.

Fan M, Wang M, Bai MY. 2016. Diverse roles of SERK family genes in plant growth, development and defense response. *Sci China Life Sci* **59**(9): 889-896.

Farmer EE, Pearce G, Ryan CA. 1989. In vitro phosphorylation of plant plasma membrane proteins in response to the proteinase inhibitor inducing factor. *Proc Natl Acad Sci U S A* **86**(5): 1539-1542.

Faulkner C. 2015. A cellular backline: specialization of host membranes for defence. *Journal of Experimental Botany* **66**(6): 1565-1571.

Felix G, Duran JD, Volko S, Boller T. 1999. Plants have a sensitive perception system for the most conserved domain of bacterial flagellin. *Plant Journal* **18**(3): 265-276.

Feraru E, Feraru MI, Kleine-Vehn J, Martiniere A, Mouille G, Vanneste S, Vernhettes S, Runions J, Friml J. 2011. PIN Polarity Maintenance by the Cell Wall in Arabidopsis. *Current Biology* **21**(4): 338-343.

Ferrari S, Savatin DV, Sicilia F, Gramegna G, Cervone F, De Lorenzo G. 2013. Oligogalacturonides: plant damage-associated molecular patterns and regulators of growth and development. *Frontiers in Plant Science* **4**(49).

Flor HH. 1971. Current Status of Gene-for-Gene Concept. *Annual Review of Phytopathology* **9**: 275-296.

Fonseca S, Chini A, Hamberg M, Adie B, Porzel A, Kramell R, Miersch O, Wasternack C, Solano R. 2009. (+)-7-iso-Jasmonoyl-L-isoleucine is the endogenous bioactive jasmonate. *Nature Chemical Biology* **5**(5): 344-350.

Fox J, Weisberg S. 2011. *An R Companion to Applied Regression*: Thousand Oaks CA: Sage.

Frei dit Frey N, Mbengue M, Kwaaitaal M, Nitsch L, Altenbach D, Häweker H, Lozano-Duran R, Njo MF, Beeckman T, Huettel B, et al. 2012. Plasma Membrane Calcium ATPases Are Important Components of Receptor-Mediated Signaling in Plant Immune Responses and Development. *Plant Physiology* **159**(2): 798-809.

Freytag S, Arabatzis N, Hahlbrock K, Schmelzer E. 1994. Reversible Cytoplasmic Rearrangements Precede Wall Apposition, Hypersensitive Cell-Death and Defense-Related Gene Activation in Potato Phytophthora-Infestans Interactions. *Planta* **194**(1): 123-135.

Friml J, Benkova E, Blilou I, Wisniewska J, Hamann T, Ljung K, Woody S, Sandberg G, Scheres B, Jurgens G, et al. 2002a. AtPIN4 mediates sink-driven auxin gradients and root patterning in Arabidopsis. *Cell* **108**(5): 661-673.

Friml J, Wisniewska J, Benkova E, Mendgen K, Palme K. 2002b. Lateral relocation of auxin efflux regulator PIN3 mediates tropism in Arabidopsis. *Nature* **415**(6873): 806-809.

Friml J, Yang X, Michniewicz M, Weijers D, Quint A, Tietz O, Benjamins R, Ouwerkerk PBF, Ljung K, Sandberg G, et al. 2004. A PINOID-dependent binary switch in apical-basal PIN polar targeting directs auxin efflux. *Science* **306**(5697): 862-865.

Frye LD, Edidin M. 1970. Rapid Intermixing of Cell Surface Antigens after Formation of Mouse-Human Heterokaryons. *Journal of Cell Science* **7**(2): 319-335.

Fujiwara T, Ritchie K, Murakoshi H, Jacobson K, Kusumi A. 2002. Phospholipids undergo hop diffusion in compartmentalized cell membrane. *Journal of Cell Biology* **157**(6): 1071-1081.

Fujiwara TK, Iwasawa K, Kalay Z, Tsunoyama TA, Watanabe Y, Umemura YM, Murakoshi H, Suzuki KG, Nemoto YL, Morone N, et al. 2016. Confined diffusion of transmembrane

proteins and lipids induced by the same actin meshwork lining the plasma membrane. *Molecular Biology of the Cell* **27**(7): 1101-1119.

Galindo-Trigo S, Gray JE, Smith LM. 2016. Conserved Roles of CrRLK1L Receptor-Like Kinases in Cell Expansion and Reproduction from Algae to Angiosperms. *Frontiers in Plant Science* **7**(1269).

Galletti R, Denoux C, Gambetta S, Dewdney J, Ausubel FM, De Lorenzo G, Ferrari S. 2008. The AtrbohD-Mediated Oxidative Burst Elicited by Oligogalacturonides in Arabidopsis Is Dispensable for the Activation of Defense Responses Effective against Botrytis cinerea. *Plant Physiology* **148**(3): 1695-1706.

Galli C, Bernasconi R, Solda T, Calanca V, Molinari M. 2011. Malectin Participates in a Backup Glycoprotein Quality Control Pathway in the Mammalian ER. *Plos One* **6**(1).

Gälweiler L, Guan CH, Müller A, Wisman E, Mendgen K, Yephremov A, Palme K. 1998. Regulation of polar auxin transport by AtPIN1 in Arabidopsis vascular tissue. *Science* **282**(5397): 2226-2230.

Gao XQ, Chen X, Lin WW, Chen SX, Lu DP, Niu YJ, Li L, Cheng C, McCormack M, Sheen J, et al. 2013. Bifurcation of Arabidopsis NLR Immune Signaling via Ca2+-Dependent Protein Kinases. *Plos Pathogens* **9**(1).

Geiger D, Maierhofer T, AL-Rasheid KAS, Scherzer S, Mumm P, Liese A, Ache P, Wellmann C, Marten I, Grill E, et al. 2011. Stomatal Closure by Fast Abscisic Acid Signaling Is Mediated by the Guard Cell Anion Channel SLAH3 and the Receptor RCAR1. *Science Signaling* **4**(173).

Geiger D, Scherzer S, Mumm P, Marten I, Ache P, Matschi S, Liese A, Wellmann C, Al-Rasheid KAS, Grill E, et al. 2010. Guard cell anion channel SLAC1 is regulated by CDPK protein kinases with distinct Ca2+ affinities. *Proceedings of the National Academy of Sciences of the United States of America* **107**(17): 8023-8028.

Gendreau E, Traas J, Desnos T, Grandjean O, Caboche M, Hofte H. 1997. Cellular basis of hypocotyl growth in Arabidopsis thaliana. *Plant Physiology* **114**(1): 295-305.

Geng XQ, Jin L, Shimada M, Kim MG, Mackey D. 2014. The phytotoxin coronatine is a multifunctional component of the virulence armament of Pseudomonas syringae. *Planta* **240**(6): 1149-1165.

Gil F, Gay JL. 1977. Ultrastructural and Physiological Properties of Host Interfacial Components of Haustoria of Erysiphe-Pisi In vivo and In vitro. *Physiological Plant Pathology* **10**(1): 1-12.

Gill US, Lee S, Mysore KS. 2015. Host versus nonhost resistance: distinct wars with similar arsenals. *Phytopathology* **105**(5): 580-587.

Gilroy S, Suzuki N, Miller G, Choi WG, Toyota M, Devireddy AR, Mittler R. 2014. A tidal wave of signals: calcium and ROS at the forefront of rapid systemic signaling. *Trends in Plant Science* **19**(10): 623-630.

Gimenez-Ibanez S, Hann DR, Ntoukakis V, Petutschnig E, Lipka V, Rathjen JP. 2009a. AvrPtoB targets the LysM receptor kinase CERK1 to promote bacterial virulence on plants. *Current Biology* **19**(5): 423-429.

Gimenez-Ibanez S, Ntoukakis V, Rathjen JP. 2009b. The LysM receptor kinase CERK1 mediates bacterial perception in Arabidopsis. *Plant Signal Behav* **4**(6): 539-541.

Glazebrook J. 2005. Contrasting mechanisms of defense against biotrophic and necrotrophic pathogens. *Annu Rev Phytopathol* **43**: 205-227.

Glickmann E, Gardan L, Jacquet S, Hussain S, Elasri M, Petit A, Dessaux Y. 1998. Auxin production is a common feature of most pathovars of Pseudomonas syringae. *Molecular Plant-Microbe Interactions* **11**(2): 156-162.

Gomez-Gomez L, Boller T. 2000. FLS2: an LRR receptor-like kinase involved in the perception of the bacterial elicitor flagellin in Arabidopsis. *Molecular Cell* **5**(6): 1003-1011.

Gomez-Gomez L, Felix G, Boller T. 1999. A single locus determines sensitivity to bacterial flagellin in Arabidopsis thaliana. *Plant J* **18**(3): 277-284.

Gou X, He K, Yang H, Yuan T, Lin H, Clouse SD, Li J. 2010. Genome-wide cloning and sequence analysis of leucine-rich repeat receptor-like protein kinase genes in Arabidopsis thaliana. *BMC Genomics* **11**(19).

Gou XP, Yin HJ, He K, Du JB, Yi J, Xu SB, Lin HH, Clouse SD, Li J. 2012. Genetic Evidence for an Indispensable Role of Somatic Embryogenesis Receptor Kinases in Brassinosteroid Signaling. *Plos Genetics* **8**(1).

Gouget A, Senchou V, Govers F, Sanson A, Barre A, Rouge P, Pont-Lezica RP, Canut H. 2006. Lectin receptor kinases participate in protein-protein interactions to mediate plasma membrane-cell wall adhesions in Arabidopsis. *Plant Physiology* **140**(1): 81-90.

Gravino M, Locci F, Tundo S, Cervone F, Savatin DV, De Lorenzo G. 2016. Immune responses induced by oligogalacturonides are differentially affected by AvrPto and loss of BAK1/BKK1 and PEPR1/PEPR2. *Mol Plant Pathol.*

Green ER, Mecsas J. 2016. Bacterial Secretion Systems: An Overview. *Microbiology Spectrum* **4**(1).

Gross P, Julius C, Schmelzer E, Hahlbrock K. 1993. Translocation of Cytoplasm and Nucleus to Fungal Penetration Sites Is Associated with Depolymerization of Microtubules and Defense Gene Activation in Infected, Cultured Parsley Cells. *Embo Journal* **12**(5): 1735-1744.

Gu Y, Kaplinsky N, Bringmann M, Cobb A, Carroll A, Sampathkumar A, Baskin TI, Persson S, Somerville CR. 2010. Identification of a cellulose synthase-associated protein required for cellulose biosynthesis. *Proceedings of the National Academy of Sciences of the United States of America* **107**(29): 12866-12871.

Gudesblat GE, Iusem ND, Morris PC. 2007. Guard cell-specific inhibition of Arabidopsis MPK3 expression causes abnormal stomatal responses to abscisic acid and hydrogen peroxide. *New Phytologist* **173**(4): 713-721.

Guenin S, Mareck A, Rayon C, Lamour R, Ndong YA, Domon JM, Senechal F, Fournet F, Jamet E, Canut H, et al. 2011. Identification of pectin methylesterase 3 as a basic pectin methylesterase isoform involved in adventitious rooting in Arabidopsis thaliana. *New Phytologist* **192**(1): 114-126.

Gui JS, Liu C, Shen JH, Li LG. 2014. Grain setting defect1, Encoding a Remorin Protein, Affects the Grain Setting in Rice through Regulating Plasmodesmatal Conductance. *Plant Physiology* **166**(3): 1463-1478.

Gui JS, Zheng S, Liu C, Shen JH, Li JM, Li LG. 2016. OsREM4.1 Interacts with OsSERK1 to Coordinate the Interlinking between Abscisic Acid and Brassinosteroid Signaling in Rice. *Developmental Cell* **38**(2): 202-213.

Gui JS, Zheng S, Shen JH, Li LG. 2015. Grain setting defect1 (GSD1) function in rice depends on S-acylation and interacts with actin 1 (OsACT1) at its C-terminal. *Frontiers in Plant Science* **6**(804).

Hamann T. 2012. Plant cell wall integrity maintenance as an essential component of biotic stress response mechanisms. *Frontiers in Plant Science* **3**(77).

Han L, Li GJ, Yang KY, Mao GH, Wang RQ, Liu YD, Zhang SQ. 2010. Mitogen-activated protein kinase 3 and 6 regulate Botrytis cinerea-induced ethylene production in Arabidopsis. *Plant Journal* **64**(1): 114-127.

Haney CH, Long SR. 2010. Plant flotillins are required for infection by nitrogen-fixing bacteria. *Proceedings of the National Academy of Sciences of the United States of America* **107**(1): 478-483.

Haney CH, Riely BK, Tricoli DM, Cook DR, Ehrhardt DW, Long SR. 2011. Symbiotic Rhizobia Bacteria Trigger a Change in Localization and Dynamics of the Medicago truncatula Receptor Kinase LYK3. *Plant Cell* **23**(7): 2774-2787.

Hanks SK, Hunter T. 1995. Protein Kinases .6. The Eukaryotic Protein-Kinase Superfamily - Kinase (Catalytic) Domain-Structure and Classification. *Faseb Journal* **9**(8): 576-596.

Hann DR, Rathjen JP. 2007. Early events in the pathogenicity of Pseudomonas syringae on Nicotiana benthamiana. *Plant J* **49**(4): 607-618.

Hansen JD, Vojtech LN, Laing KJ. 2011. Sensing disease and danger: A survey of vertebrate PRRs and their origins. *Developmental and Comparative Immunology* **35**(9): 886-897.

Harrison MJ, Dewbre GR, Liu J. 2002. A phosphate transporter from Medicago truncatula involved in the acquisition of phosphate released by arbuscular mycorrhizal fungi. *Plant Cell* **14**(10): 2413-2429.

Harrison SJ, Mott EK, Parsley K, Aspinall S, Gray JC, Cottage A. 2006. A rapid and robust method of identifying transformed Arabidopsis thaliana seedlings following floral dip transformation. *Plant Methods* **2**(19).

Haruta M, Sabat G, Stecker K, Minkoff BB, Sussman MR. 2014. A Peptide Hormone and Its Receptor Protein Kinase Regulate Plant Cell Expansion. *Science* **343**(6169): 408-411.

Hayafune M, Berisio R, Marchetti R, Silipo A, Kayama M, Desaki Y, Arima S, Squeglia F, Ruggiero A, Tokuyasu K, et al. 2014. Chitin-induced activation of immune signaling by the

rice receptor CEBiP relies on a unique sandwich-type dimerization. *Proc Natl Acad Sci U S A* **111**(3): E404-413.

Hayashi F, Smith KD, Ozinsky A, Hawn TR, Yi EC, Goodlett DR, Eng JK, Akira S, Underhill DM, Aderem A. 2001. The innate immune response to bacterial flagellin is mediated by Toll-like receptor 5. *Nature* **410**(6832): 1099-1103.

Hayashida K, Bartlett AH, Chen Y, Park PW. 2010. Molecular and cellular mechanisms of ectodomain shedding. *Anat Rec (Hoboken)* **293**(6): 925-937.

Heerklotz H. 2002. Triton promotes domain formation in lipid raft mixtures. *Biophysical Journal* **83**(5): 2693-2701.

Hematy K, Sado PE, Van Tuinen A, Rochange S, Desnos T, Balzergue S, Pelletier S, Renou JP, Höfte H. 2007. A receptor-like kinase mediates the response of Arabidopsis cells to the inhibition of cellulose synthesis. *Current Biology* **17**(11): 922-931.

Higashiyama S, Nanba D, Nakayama H, Inoue H, Fukuda S. 2011. Ectodomain shedding and remnant peptide signalling of EGFRs and their ligands. *Journal of Biochemistry* **150**(1): 15-22.

Hind SR, Strickler SR, Boyle PC, Dunham DM, Bao Z, O'Doherty IM, Baccile JA, Hoki JS, Viox EG, Clarke CR, et al. 2016. Tomato receptor FLAGELLIN-SENSING 3 binds flgII-28 and activates the plant immune system. *Nat Plants* **2**(16128).

Hofer CA. 2012. *Funktionale Charakterisierung von Rezeptorkinasen während der Pathogenerkennung.* Master thesis, Ludwig-Maximilians-Universität München.

Hok S, Danchin EGJ, Allasia V, Panabieres F, Attard A, Keller H. 2011. An Arabidopsis (malectin-like) leucine-rich repeat receptor-like kinase contributes to downy mildew disease. *Plant Cell and Environment* **34**(11): 1944-1957.

Hong Z, Delauney AJ, Verma DP. 2001. A cell plate-specific callose synthase and its interaction with phragmoplastin. *Plant Cell* **13**(4): 755-768.

Hope IA, Struhl K. 1986. Functional Dissection of a Eukaryotic Transcriptional Activator Protein, Gcn4 of Yeast. *Cell* **46**(6): 885-894.

Hothorn T, Bretz F, Westfall P. 2008. Simultaneous inference in general parametric models. *Biometrical Journal* **50**(3): 346-363.

Huang F, Zago MK, Abas L, van Marion A, Galvan-Ampudia CS, Offringa R. 2010. Phosphorylation of Conserved PIN Motifs Directs Arabidopsis PIN1 Polarity and Auxin Transport. *Plant Cell* **22**(4): 1129-1142.

Huck N, Moore JM, Federer M, Grossniklaus U. 2003. The Arabidopsis mutant feronia disrupts the female gametophytic control of pollen tube reception. *Development* **130**(10): 2149-2159.

Huffaker A, Pearce G, Ryan CA. 2006. An endogenous peptide signal in Arabidopsis activates components of the innate immune response. *Proceedings of the National Academy of Sciences of the United States of America* **103**(26): 10098-10103.

Huot B, Yao J, Montgomery BL, He SY. 2014. Growth-Defense Tradeoffs in Plants: A Balancing Act to Optimize Fitness. *Molecular Plant* **7**(8): 1267-1287.

Iakoucheva LM, Radivojac P, Brown CJ, O'Connor TR, Sikes JG, Obradovic Z, Dunker AK. 2004. The importance of intrinsic disorder for protein phosphorylation. *Nucleic Acids Research* **32**(3): 1037-1049.

Ichimura K, Casais C, Peck SC, Shinozaki K, Shirasu K. 2006. MEKK1 is required for MPK4 activation and regulates tissue-specific and temperature-dependent cell death in Arabidopsis. *Journal of Biological Chemistry* **281**(48): 36969-36976.

Ichimura K, Shinozaki K, Tena G, Sheen J, Henry Y, Champion A, Kreis M, Zhang SQ, Hirt H, Wilson C, et al. 2002. Mitogen-activated protein kinase cascades in plants: a new nomenclature. *Trends in Plant Science* **7**(7): 301-308.

Ishihama N, Yamada R, Yoshioka M, Katou S, Yoshioka H. 2011. Phosphorylation of the Nicotiana benthamiana WRKY8 transcription factor by MAPK functions in the defense response. *Plant Cell* **23**(3): 1153-1170.

Jacobs AK, Lipka V, Burton RA, Panstruga R, Strizhov N, Schulze-Lefert P, Fincher GB. 2003. An Arabidopsis callose synthase, GSL5, is required for wound and papillary callose formation. *Plant Cell* **15**(11): 2503-2513.

Jamann TM, Luo XY, Morales L, Kolkman JM, Chung CL, Nelson RJ. 2016. A remorin gene is implicated in quantitative disease resistance in maize. *Theoretical and Applied Genetics* **129**(3): 591-602.

James P, Halladay J, Craig EA. 1996. Genomic libraries and a host strain designed for highly efficient two-hybrid selection in yeast. *Genetics* **144**(4): 1425-1436.

Jammes F, Song C, Shin D, Munemasa S, Takeda K, Gu D, Cho D, Lee S, Giordo R, Sritubtim S, et al. 2009. MAP kinases MPK9 and MPK12 are preferentially expressed in guard cells and positively regulate ROS-mediated ABA signaling. *Proc Natl Acad Sci U S A* **106**(48): 20520-20525.

Janes PW, Ley SC, Magee AI. 1999. Aggregation of lipid rafts accompanies signaling via the T cell antigen receptor. *Journal of Cell Biology* **147**(2): 447-461.

Jarsch IK. 2014. *Remorin proteins in Arabidopsis thaliana: Markers for diverse membrane microdomain with roles in plant-microbe interactions.* Ludwig-Maximilians-Universität München.

Jarsch IK, Konrad SSA, Stratil TF, Urbanus SL, Szymanski W, Braun P, Braun KH, Ott T. 2014. Plasma Membranes Are Subcompartmentalized into a Plethora of Coexisting and Diverse Microdomains in Arabidopsis and Nicotiana benthamiana. *Plant Cell* **26**(4): 1698-1711.

Jarsch IK, Ott T. 2011. Perspectives on Remorin Proteins, Membrane Rafts, and Their Role During Plant-Microbe Interactions. *Molecular Plant-Microbe Interactions* **24**(1): 7-12.

Jeworutzki E, Roelfsema MRG, Anschutz U, Krol E, Elzenga JTM, Felix G, Boller T, Hedrich R, Becker D. 2010. Early signaling through the Arabidopsis pattern recognition receptors FLS2 and EFR involves Ca2+-associated opening of plasma membrane anion channels. *Plant Journal* **62**(3): 367-378.

Johnson LN, Lowe ED, Noble MEM, Owen DJ. 1998. The structural basis for substrate recognition and control by protein kinases. *Febs Letters* **430**(1-2): 1-11.

Jones JD, Dangl JL. 2006. The plant immune system. *Nature* **444**(7117): 323-329.

Jorda L, Sopena-Torres S, Escudero V, Nunez-Corcuera B, Delgado-Cerezo M, Torii KU, Molina A. 2016. ERECTA and BAK1 Receptor Like Kinases Interact to Regulate Immune Responses in Arabidopsis. *Frontiers in Plant Science* **7**(897).

Kadota Y, Shirasu K, Zipfel C. 2015. Regulation of the NADPH Oxidase RBOHD During Plant Immunity. *Plant and Cell Physiology* **56**(8): 1472-1480.

Kadota Y, Sklenar J, Derbyshire P, Stransfeld L, Asai S, Ntoukakis V, Jones JD, Shirasu K, Menke F, Jones A, et al. 2014. Direct regulation of the NADPH oxidase RBOHD by the PRR-associated kinase BIK1 during plant immunity. *Molecular Cell* **54**(1): 43-55.

Katagiri F, Thilmony R, He SY. 2002. The Arabidopsis thaliana-pseudomonas syringae interaction. *Arabidopsis Book* **1**: e0039.

Katembe WJ, Swatzell LJ, Makaroff CA, Kiss JZ. 1997. Immunolocalization of integrin-like proteins in Arabidopsis and Chara. *Physiol Plant* **99**(1): 7-14.

Kawai T, Akira S. 2010. The role of pattern-recognition receptors in innate immunity: update on Toll-like receptors. *Nature Immunology* **11**(5): 373-384.

Kazan K, Lyons R. 2014. Intervention of Phytohormone Pathways by Pathogen Effectors. *Plant Cell* **26**(6): 2285-2309.

Keegan L, Gill G, Ptashne M. 1986. Separation of DNA-Binding from the Transcription-Activating Function of a Eukaryotic Regulatory Protein. *Science* **231**(4739): 699-704.

Keinath NF, Kierszniowska S, Lorek J, Bourdais G, Kessler SA, Shimosato-Asano H, Grossniklaus U, Schulze WX, Robatzek S, Panstruga R. 2010. PAMP (Pathogen-associated Molecular Pattern)-induced Changes in Plasma Membrane Compartmentalization Reveal Novel Components of Plant Immunity. *Journal of Biological Chemistry* **285**(50): 39140-39149.

Kerppola TK. 2008. Biomolecular fluorescence complementation (BiFC) analysis as a probe of protein interactions in living cells. *Annual Review of Biophysics* **37**: 465-487.

Kessler SA, Shimosato-Asano H, Keinath NF, Wuest SE, Ingram G, Panstruga R, Grossniklaus U. 2010. Conserved Molecular Components for Pollen Tube Reception and Fungal Invasion. *Science* **330**(6006): 968-971.

Khan M, Subramaniam R, Desveaux D. 2016. Of guards, decoys, baits and traps: pathogen perception in plants by type III effector sensors. *Curr Opin Microbiol* **29**: 49-55.

Kierszniowska S, Seiwert B, Schulze WX. 2009. Definition of Arabidopsis Sterol-rich Membrane Microdomains by Differential Treatment with Methyl-beta-cyclodextrin and Quantitative Proteomics. *Molecular & Cellular Proteomics* **8**(4): 612-623.

Kim CY, Zhang S. 2004. Activation of a mitogen-activated protein kinase cascade induces WRKY family of transcription factors and defense genes in tobacco. *Plant J* **38**(1): 142-151.

Kim H, O'Connell R, Maekawa-Yoshikawa M, Uemura T, Neumann U, Schulze-Lefert P. 2014. The powdery mildew resistance protein RPW8.2 is carried on VAMP721/722 vesicles to the extrahaustorial membrane of haustorial complexes. *Plant Journal* **79**(5): 835-847.

Kim HS, Desveaux D, Singer AU, Patel P, Sondek J, Dangl JL. 2005. The Pseudomonas syringae effector AvrRpt2 cleaves its C-terminally acylated target, RIN4, from Arabidopsis membranes to block RPM1 activation. *Proc Natl Acad Sci U S A* **102**(18): 6496-6501.

Kleine-Vehn J, Dhonukshe P, Sauer M, Brewer PB, Wisniewska J, Paciorek T, Benkova E, Friml J. 2008. ARF GEF-dependent transcytosis and polar delivery of PIN auxin carriers in Arabidopsis. *Current Biology* **18**(7): 526-531.

Kleine-Vehn J, Friml J. 2008. Polar Targeting and Endocytic Recycling in Auxin-Dependent Plant Development. *Annual Review of Cell and Developmental Biology* **24**: 447-473.

Kleine-Vehn J, Wabnik K, Martiniere A, Langowski L, Willig K, Naramoto S, Leitner J, Tanaka H, Jakobs S, Robert S, et al. 2011. Recycling, clustering, and endocytosis jointly maintain PIN auxin carrier polarity at the plasma membrane. *Molecular Systems Biology* **7**(540).

Kobae Y, Sekino T, Yoshioka H, Nakagawa T, Martinoia E, Maeshima M. 2006. Loss of AtPDR8, a plasma membrane ABC transporter of Arabidopsis thaliana, causes hypersensitive cell death upon pathogen infection. *Plant Cell Physiol* **47**(3): 309-318.

Kobayashi I, Kobayashi Y, Hardham AR. 1994. Dynamic Reorganization of Microtubules and Microfilaments in Flax Cells during the Resistance Response to Flax Rust Infection. *Planta* **195**(2): 237-247.

Koch E, Slusarenko A. 1990. Arabidopsis Is Susceptible to Infection by a Downy Mildew Fungus. *Plant Cell* **2**(5): 437-445.

Koh S, Andre A, Edwards H, Ehrhardt D, Somerville S. 2005. Arabidopsis thaliana subcellular responses to compatible Erysiphe cichoracearum infections. *Plant Journal* **44**(3): 516-529.

Kohorn BD. 2016. Cell wall-associated kinases and pectin perception. *Journal of Experimental Botany* **67**(2): 489-494.

Kohorn BD, Johansen S, Shishido A, Todorova T, Martinez R, Defeo E, Obregon P. 2009. Pectin activation of MAP kinase and gene expression is WAK2 dependent. *Plant Journal* **60**(6): 974-982.

Kohorn BD, Kobayashi M, Johansen S, Riese J, Huang LF, Koch K, Fu S, Dotson A, Byers N. 2006. An Arabidopsis cell wall-associated kinase required for invertase activity and cell growth. *Plant Journal* **46**(2): 307-316.

Konrad SSA, Popp C, Stratil TF, Jarsch IK, Thallmair V, Folgmann J, Marin M, Ott T. 2014. S-acylation anchors remorin proteins to the plasma membrane but does not primarily determine their localization in membrane microdomains. *New Phytologist* **203**(3): 758-769.

Kosuta S, Held M, Hossain MS, Morieri G, Macgillivary A, Johansen C, Antolin-Llovera M, Parniske M, Oldroyd GE, Downie AJ, et al. 2011. Lotus japonicus symRK-14 uncouples the cortical and epidermal symbiotic program. *Plant J* **67**(5): 929-940.

Krol E, Mentzel T, Chinchilla D, Boller T, Felix G, Kemmerling B, Postel S, Arents M, Jeworutzki E, Al-Rasheid KAS, et al. 2010. Perception of the Arabidopsis Danger Signal Peptide 1 Involves the Pattern Recognition Receptor AtPEPR1 and Its Close Homologue AtPEPR2. *Journal of Biological Chemistry* **285**(18): 13471-13479.

Kumar D. 2014. Salicylic acid signaling in disease resistance. *Plant Science* **228**: 127-134.

Kunze G, Zipfel C, Robatzek S, Niehaus K, Boller T, Felix G. 2004. The N terminus of bacterial elongation factor Tu elicits innate immunity in Arabidopsis plants. *Plant Cell* **16**(12): 3496-3507.

Kusumi A, Fujiwara TK, Morone N, Yoshida KJ, Chadda R, Xie M, Kasai RS, Suzuki KGN. 2012. Membrane mechanisms for signal transduction: The coupling of the meso-scale raft domains to membrane-skeleton-induced compartments and dynamic protein complexes. *Seminars in Cell & Developmental Biology* **23**(2): 126-144.

Kusumi A, Nakada C, Ritchie K, Murase K, Suzuki K, Murakoshi H, Kasai RS, Kondo J, Fujiwara T. 2005. Paradigm shift of the plasma membrane concept from the two-dimensional continuum fluid to the partitioned fluid: High-speed single-molecule tracking of membrane molecules. *Annual Review of Biophysics and Biomolecular Structure* **34**: 351-378.

Kwon C, Neu C, Pajonk S, Yun HS, Lipka U, Humphry M, Bau S, Straus M, Kwaaitaal M, Rampelt H, et al. 2008. Co-option of a default secretory pathway for plant immune responses. *Nature* **451**(7180): 835-841.

Lacombe S, Rougon-Cardoso A, Sherwood E, Peeters N, Dahlbeck D, van Esse HP, Smoker M, Rallapalli G, Thomma BPHJ, Staskawicz B, et al. 2010. Interfamily transfer of a plant pattern-recognition receptor confers broad-spectrum bacterial resistance. *Nature Biotechnology* **28**(4): 365-370.

Ladha S, Mackie AR, Harvey LJ, Clark DC, Lea EJA, Brullemans M, Duclohier H. 1996. Lateral diffusion in planar lipid bilayers: A fluorescence recovery after photobleaching investigation of its modulation by lipid composition, cholesterol, or alamethicin content and divalent cations. *Biophysical Journal* **71**(3): 1364-1373.

Lally D, Ingmire P, Tong HY, He ZH. 2001. Antisense expression of a cell wall-associated protein kinase, WAK4, inhibits cell elongation and alters morphology. *Plant Cell* **13**(6): 1317-1331.

Lassowskat I, Bottcher C, Eschen-Lippold L, Scheel D, Lee J. 2014. Sustained mitogen-activated protein kinase activation reprograms defense metabolism and phosphoprotein profile in Arabidopsis thaliana. *Frontiers in Plant Science* **5**(554).

Lauwers E, Grossmann G, Andre B. 2007. Evidence for coupled biogenesis of yeast Gap1 permease and sphingolipids: Essential role in transport activity and normal control by ubiquitination. *Molecular Biology of the Cell* **18**(8): 3068-3080.

Le MH, Cao YR, Zhang XC, Stacey G. 2014. LIK1, A CERK1-Interacting Kinase, Regulates Plant Immune Responses in Arabidopsis. *Plos One* **9**(7).

Lecourieux D, Mazars C, Pauly N, Ranjeva R, Pugin A. 2002. Analysis and effects of cytosolic free calcium increases in response to elicitors in Nicotiana plumbaginifolia cells. *Plant Cell* **14**(10): 2627-2641.

Lee D, Bourdais G, Yu G, Robatzek S, Coaker G. 2015. Phosphorylation of the Plant Immune Regulator RPM1-INTERACTING PROTEIN4 Enhances Plant Plasma Membrane H+-ATPase Activity and Inhibits Flagellin-Triggered Immune Responses in Arabidopsis. *Plant Cell* **27**(7): 2042-2056.

Lee GM, Zhang F, Ishihara A, Mcneil CL, Jacobson KA. 1993. Unconfined Lateral Diffusion and an Estimate of Pericellular Matrix Viscosity Revealed by Measuring the Mobility of Gold-Tagged Lipids. *Journal of Cell Biology* **120**(1): 25-35.

Lefebvre B, Timmers T, Mbengue M, Moreau S, Herve C, Toth K, Bittencourt-Silvestre J, Klaus D, Deslandes L, Godiard L, et al. 2010. A remorin protein interacts with symbiotic receptors and regulates bacterial infection. *Proceedings of the National Academy of Sciences of the United States of America* **107**(5): 2343-2348.

Lherminier J, Elmayan T, Fromentin J, Elaraqui KT, Vesa S, Morel J, Verrier JL, Cailleteau B, Blein JP, Simon-Plas F. 2009. NADPH Oxidase-Mediated Reactive Oxygen Species Production: Subcellular Localization and Reassessment of Its Role in Plant Defense. *Molecular Plant-Microbe Interactions* **22**(7): 868-881.

Li GJ, Meng XZ, Wang RG, Mao GH, Han L, Liu YD, Zhang SQ. 2012. Dual-Level Regulation of ACC Synthase Activity by MPK3/MPK6 Cascade and Its Downstream WRKY Transcription Factor during Ethylene Induction in Arabidopsis. *Plos Genetics* **8**(6).

Li J, Tax FE. 2013. Receptor-Like Kinases: Key Regulators of Plant Development and Defense. *Journal of Integrative Plant Biology* **55**(12): 1184-1187.

Li J, Wen JQ, Lease KA, Doke JT, Tax FE, Walker JC. 2002. BAK1, an Arabidopsis LRR receptor-like protein kinase, interacts with BRI1 and modulates brassinosteroid signaling. *Cell* **110**(2): 213-222.

Li L, Li M, Yu L, Zhou Z, Liang X, Liu Z, Cai G, Gao L, Zhang X, Wang Y, et al. 2014. The FLS2-associated kinase BIK1 directly phosphorylates the NADPH oxidase RbohD to control plant immunity. *Cell Host & Microbe* **15**(3): 329-338.

Li RL, Liu P, Wan YL, Chen T, Wang QL, Mettbach U, Baluska F, Samaj J, Fang XH, Lucas WJ, et al. 2012. A Membrane Microdomain-Associated Protein, Arabidopsis Flot1, Is Involved in a Clathrin-Independent Endocytic Pathway and Is Required for Seedling Development. *Plant Cell* **24**(5): 2105-2122.

Lin W, Lu D, Gao X, Jiang S, Ma X, Wang Z, Mengiste T, He P, Shan L. 2013a. Inverse modulation of plant immune and brassinosteroid signaling pathways by the receptor-like cytoplasmic kinase BIK1. *Proc Natl Acad Sci U S A* **110**(29): 12114-12119.

Lin W, Ma X, Shan L, He P. 2013b. Big roles of small kinases: the complex functions of receptor-like cytoplasmic kinases in plant immunity and development. *Journal of Integrative Plant Biology* **55**(12): 1188-1197.

Lindblom G, Johansson LBA, Arvidson G. 1981. Effect of Cholesterol in Membranes - Pulsed Nuclear Magnetic-Resonance Measurements of Lipid Lateral Diffusion. *Biochemistry* **20**(8): 2204-2207.

Lindeberg M, Cunnac S, Collmer A. 2012. Pseudomonas syringae type III effector repertoires: last words in endless arguments. *Trends in Microbiology* **20**(4): 199-208.

Lingwood D, Simons K. 2010. Lipid Rafts As a Membrane-Organizing Principle. *Science* **327**(5961): 46-50.

Lipka V, Dittgen J, Bednarek P, Bhat R, Wiermer M, Stein M, Landtag J, Brandt W, Rosahl S, Scheel D, et al. 2005. Pre- and postinvasion defenses both contribute to nonhost resistance in Arabidopsis. *Science* **310**(5751): 1180-1183.

Littlejohn GR, Mansfield JC, Christmas JT, Witterick E, Fricker MD, Grant MR, Smirnoff N, Everson RM, Moger J, Love J. 2014. An update: improvements in imaging perfluorocarbon-mounted plant leaves with implications for studies of plant pathology, physiology, development and cell biology. *Frontiers in Plant Science* **5**.

Liu J, Elmore JM, Fuglsang AT, Palmgren MG, Staskawicz BJ, Coaker G. 2009. RIN4 functions with plasma membrane H+-ATPases to regulate stomatal apertures during pathogen attack. *PLoS Biol* **7**(6): e1000139.

Liu J, Elmore JM, Lin ZJ, Coaker G. 2011. A receptor-like cytoplasmic kinase phosphorylates the host target RIN4, leading to the activation of a plant innate immune receptor. *Cell Host & Microbe* **9**(2): 137-146.

Liu T, Liu Z, Song C, Hu Y, Han Z, She J, Fan F, Wang J, Jin C, Chang J, et al. 2012. Chitin-induced dimerization activates a plant immune receptor. *Science* **336**(6085): 1160-1164.

Liu Z, Wu Y, Yang F, Zhang Y, Chen S, Xie Q, Tian X, Zhou JM. 2013. BIK1 interacts with PEPRs to mediate ethylene-induced immunity. *Proc Natl Acad Sci U S A* **110**(15): 6205-6210.

Liu ZY, Persson S, Sanchez-Rodriguez C. 2015a. At the border: the plasma membrane-cell wall continuum. *Journal of Experimental Botany* **66**(6): 1553-1563.

Liu ZY, Persson S, Zhang Y. 2015b. The connection of cytoskeletal network with plasma membrane and the cell wall. *Journal of Integrative Plant Biology* **57**(4): 330-340.

Lu B, Wang J, Zhang Y, Wang HC, Liang JS, Zhang JH. 2012a. AT14A mediates the cell wall-plasma membrane-cytoskeleton continuum in Arabidopsis thaliana cells. *Journal of Experimental Botany* **63**(11): 4061-4069.

Lu D, Wu S, Gao X, Zhang Y, Shan L, He P. 2010. A receptor-like cytoplasmic kinase, BIK1, associates with a flagellin receptor complex to initiate plant innate immunity. *Proc Natl Acad Sci U S A* **107**(1): 496-501.

Lu YJ, Schornack S, Spallek T, Geldner N, Chory J, Schellmann S, Schumacher K, Kamoun S, Robatzek S. 2012b. Patterns of plant subcellular responses to successful oomycete infections reveal differences in host cell reprogramming and endocytic trafficking. *Cellular Microbiology* **14**(5): 682-697.

Luna E, Pastor V, Robert J, Flors V, Mauch-Mani B, Ton J. 2011. Callose Deposition: A Multifaceted Plant Defense Response. *Molecular Plant-Microbe Interactions* **24**(2): 183-193.

Luschnig C, Vert G. 2014. The dynamics of plant plasma membrane proteins: PINs and beyond. *Development* **141**(15): 2924-2938.

Lv X, Jing Y, Xiao J, Zhang Y, Zhu Y, Julian R, Lin J. 2017. Membrane microdomains and the cytoskeleton constrain AtHIR1 dynamics and facilitate the formation of an AtHIR1-associated immune complex. *Plant J.*

Ma X, Xu G, He P, Shan L. 2016. SERKing Coreceptors for Receptors. *Trends Plant Sci* **21**(12): 1017-1033.

Macho AP, Boutrot F, Rathjen JP, Zipfel C. 2012. ASPARTATE OXIDASE Plays an Important Role in Arabidopsis Stomatal Immunity. *Plant Physiology* **159**(4): 1845-1856.

Macho AP, Zipfel C. 2014. Plant PRRs and the Activation of Innate Immune Signaling. *Molecular Cell* **54**(2): 263-272.

Mackey D, Belkhadir Y, Alonso JM, Ecker JR, Dangl JL. 2003. Arabidopsis RIN4 is a target of the type III virulence effector AvrRpt2 and modulates RPS2-mediated resistance. *Cell* **112**(3): 379-389.

Mackey D, Holt BF, Wiig A, Dangl JL. 2002. RIN4 interacts with Pseudomonas syringae type III effector molecules and is required for RPM1-mediated resistance in Arabidopsis. *Cell* **108**(6): 743-754.

Maekawa S, Inada N, Yasuda S, Fukao Y, Fujiwara M, Sato T, Yamaguchi J. 2014. The Carbon/Nitrogen Regulator ARABIDOPSIS TOXICOS EN LEVADURA31 Controls Papilla Formation in Response to Powdery Mildew Fungi Penetration by Interacting with SYNTAXIN OF PLANTS121 in Arabidopsis. *Plant Physiology* **164**(2): 879-887.

Malinovsky FG, Fangel JU, Willats WG. 2014. The role of the cell wall in plant immunity. *Frontiers in Plant Science* **5**(178).

Malínská K, Malínský J, Opekarová M, Tanner W. 2003. Visualization of protein compartmentation within the plasma membrane of living yeast cells. *Molecular Biology of the Cell* **14**(11): 4427-4436.

Malinsky J, Opekarová M, Grossmann G, Tanner W. 2013. Membrane Microdomains, Rafts, and Detergent-Resistant Membranes in Plants and Fungi. *Annual Review of Plant Biology* **64**: 501-529.

Manders EMM, Stap J, Brakenhoff GJ, Vandriel R, Aten JA. 1992. Dynamics of 3-Dimensional Replication Patterns during the S-Phase, Analyzed by Double Labeling of DNA and Confocal Microscopy. *Journal of Cell Science* **103**: 857-862.

Mao G, Meng X, Liu Y, Zheng Z, Chen Z, Zhang S. 2011. Phosphorylation of a WRKY transcription factor by two pathogen-responsive MAPKs drives phytoalexin biosynthesis in Arabidopsis. *Plant Cell* **23**(4): 1639-1653.

Mao H, Nakamura M, Viotti C, Grebe M. 2016. A Framework for Lateral Membrane Trafficking and Polar Tethering of the PEN3 ATP-Binding Cassette Transporter. *Plant Physiology* **172**(4): 2245-2260.

Marín M, Ott T. 2012. Phosphorylation of intrinsically disordered regions in remorin proteins. *Frontiers in Plant Science* **3**(86).

Marín M, Ott T. 2014. Intrinsic Disorder in Plant Proteins and Phytopathogenic Bacterial Effectors. *Chemical Reviews* **114**(13): 6912-6932.

Marín M, Thallmair V, Ott T. 2012. The Intrinsically Disordered N-terminal Region of AtREM1.3 Remorin Protein Mediates Protein-Protein Interactions. *Journal of Biological Chemistry* **287**(47): 39982-39991.

Martinière A, Gayral P, Hawes C, Runions J. 2011. Building bridges: formin1 of Arabidopsis forms a connection between the cell wall and the actin cytoskeleton. *Plant Journal* **66**(2): 354-365.

Martinière A, Lavagi I, Nageswaran G, Rolfe DJ, Maneta-Peyret L, Luu DT, Botchway SW, Webb SED, Mongrand S, Maurel C, et al. 2012. Cell wall constrains lateral diffusion of plant plasma-membrane proteins. *Proceedings of the National Academy of Sciences of the United States of America* **109**(31): 12805-12810.

Matos JL, Fiori CS, Silva-Filho MC, Moura DS. 2008. A conserved dibasic site is essential for correct processing of the peptide hormone AtRALF1 in Arabidopsis thaliana. *Febs Letters* **582**: 3343-3347.

McFarlane HE, Doring A, Persson S. 2014. The Cell Biology of Cellulose Synthesis. *Annual Review of Plant Biology, Vol 65* **65**: 69-94.

McKenna JF, Tolmie AF, Runions J. 2014. Across the great divide: the plant cell surface continuum. *Current Opinion in Plant Biology* **22**: 132-140.

McLusky SR, Bennett MH, Beale MH, Lewis MJ, Gaskin P, Mansfield JW. 1999. Cell wall alterations and localized accumulation of feruloyl-3 '-methoxytyramine in onion epidermis at sites of attempted penetration by Botrytis allii are associated with actin polarisation, peroxidase activity and suppression of flavonoid biosynthesis. *Plant Journal* **17**(5): 523-534.

Medzhitov R, Janeway CA. 2002. Decoding the patterns of self and nonself by the innate immune system. *Science* **296**(5566): 298-300.

Melotto M, Underwood W, Koczan J, Nomura K, He SY. 2006. Plant stomata function in innate immunity against bacterial invasion. *Cell* **126**(5): 969-980.

Men SZ, Boutte Y, Ikeda Y, Li XG, Palme K, Stierhof YD, Hartmann MA, Moritz T, Grebe M. 2008. Sterol-dependent endocytosis mediates post-cytokinetic acquisition of PIN2 auxin efflux carrier polarity. *Nature Cell Biology* **10**(2): 237-244.

Meng XZ, Chen X, Mang HG, Liu CL, Yu X, Gao XQ, Torii KU, He P, Shan LB. 2015. Differential Function of Arabidopsis SERK Family Receptor-like Kinases in Stomatal Patterning. *Current Biology* **25**(18): 2361-2372.

Meng XZ, Zhang SQ. 2013. MAPK Cascades in Plant Disease Resistance Signaling. *Annual Review of Phytopathology, Vol 51* **51**: 245-266.

Meng XZ, Zhou JG, Tang J, Li B, de Oliveira MVV, Chai JJ, He P, Shan LB. 2016. Ligand-Induced Receptor-like Kinase Complex Regulates Floral Organ Abscission in Arabidopsis. *Cell Reports* **14**(6): 1330-1338.

Meyer D, Pajonk S, Micali C, O'Connell R, Schulze-Lefert P. 2009. Extracellular transport and integration of plant secretory proteins into pathogen-induced cell wall compartments. *Plant Journal* **57**(6): 986-999.

Micali CO, Neumann U, Grunewald D, Panstruga R, O'Connell R. 2011. Biogenesis of a specialized plant-fungal interface during host cell internalization of Golovinomyces orontii haustoria. *Cellular Microbiology* **13**(2): 210-226.

Michniewicz M, Zago MK, Abas L, Weijers D, Schweighofer A, Meskiene I, Heisler MG, Ohno C, Zhang J, Huang F, et al. 2007. Antagonistic regulation of PIN phosphorylation by PP2A and PINOID directs auxin flux. *Cell* **130**(6): 1044-1056.

Miedes E, Vanholme R, Boerjan W, Molina A. 2014. The role of the secondary cell wall in plant resistance to pathogens. *Frontiers in Plant Science* **5**(358).

Miller G, Schlauch K, Tam R, Cortes D, Torres MA, Shulaev V, Dangl JL, Mittler R. 2009. The Plant NADPH Oxidase RBOHD Mediates Rapid Systemic Signaling in Response to Diverse Stimuli. *Science Signaling* **2**(84).

Mindrinos M, Katagiri F, Yu GL, Ausubel FM. 1994. The A. Thaliana Disease Resistance Gene Rps2 Encodes a Protein Containing a Nucleotide-Binding Site and Leucine-Rich Repeats. *Cell* **78**(6): 1089-1099.

Mitchell RE. 1982. Coronatine Production by Some Phytopathogenic Pseudomonads. *Physiological Plant Pathology* **20**(1): 83-89.

Mittag T, Kay LE, Forman-Kay JD. 2010. Protein dynamics and conformational disorder in molecular recognition. *Journal of Molecular Recognition* **23**(2): 105-116.

Miya A, Albert P, Shinya T, Desaki Y, Ichimura K, Shirasu K, Narusaka Y, Kawakami N, Kaku H, Shibuya N. 2007. CERK1, a LysM receptor kinase, is essential for chitin elicitor signaling in Arabidopsis. *Proceedings of the National Academy of Sciences of the United States of America* **104**(49): 19613-19618.

Miyazaki S, Murata T, Sakurai-Ozato N, Kubo M, Demura T, Fukuda H, Hasebe M. 2009. ANXUR1 and 2, sister genes to FERONIA/SIRENE, are male factors for coordinated fertilization. *Current Biology* **19**(15): 1327-1331.

Mizel SB, West AP, Hantgan RR. 2003. Identification of a sequence in human toll-like receptor 5 required for the binding of Gram-negative flagellin. *Journal of Biological Chemistry* **278**(26): 23624-23629.

Monaghan J, Zipfel C. 2012. Plant pattern recognition receptor complexes at the plasma membrane. *Current Opinion in Plant Biology* **15**(4): 349-357.

Mongrand S, Morel J, Laroche J, Claverol S, Carde JP, Hartmann MA, Bonneu M, Simon-Plas F, Lessire R, Bessoule JJ. 2004. Lipid rafts in higher plant cells - Purification and characterization of triton X-100-insoluble microdomains from tobacco plasma membrane. *Journal of Biological Chemistry* **279**(35): 36277-36286.

Morbitzer R, Elsaesser J, Hausner J, Lahaye T. 2011. Assembly of custom TALE-type DNA binding domains by modular cloning. *Nucleic Acids Research* **39**(13): 5790-5799.

Morejohn LC, Bureau TE, Mole-Bajer J, Bajer AS, Fosket DE. 1987. Oryzalin, a dinitroaniline herbicide, binds to plant tubulin and inhibits microtubule polymerization in vitro. *Planta* **172**(2): 252-264.

Mueller SC, Brown RM. 1980. Evidence for an Intramembrane Component Associated with a Cellulose Microfibril-Synthesizing Complex in Higher-Plants. *Journal of Cell Biology* **84**(2): 315-326.

Mueller SC, Brown RM, Scott TK. 1976. Cellulosic Microfibrils - Nascent Stages of Synthesis in a Higher Plant-Cell. *Science* **194**(4268): 949-951.

Müller A, Guan CH, Gälweiler L, Tänzler P, Huijser P, Marchant A, Parry G, Bennett M, Wisman E, Palme K. 1998. AtPIN2 defines a locus of Arabidopsis for root gravitropism control. *Embo Journal* **17**(23): 6903-6911.

Munro S. 2003. Lipid rafts: Elusive or illusive? *Cell* **115**(4): 377-388.

Murase K, Fujiwara T, Umemura Y, Suzuki K, Iino R, Yamashita H, Saito M, Murakoshi H, Ritchie K, Kusumi A. 2004. Ultrafine membrane compartments for molecular diffusion as revealed by single molecule techniques. *Biophysical Journal* **86**(6): 4075-4093.

Nagano M, Ishikawa T, Fujiwara M, Fukao Y, Kawano Y, Kawai-Yamada M, Shimamoto K. 2016. Plasma Membrane Microdomains Are Essential for Rac1-RbohB/H-Mediated Immunity in Rice. *Plant Cell* **28**(8): 1966-1983.

Nakagami H, Soukupova H, Schikora A, Zarsky V, Hirt H. 2006. A mitogen-activated protein kinase kinase kinase mediates reactive oxygen species homeostasis in Arabidopsis. *Journal of Biological Chemistry* **281**(50): 38697-38704.

Nam KH, Li JM. 2002. BRI1/BAK1, a receptor kinase pair mediating brassinosteroid signaling. *Cell* **110**(2): 203-212.

Navarro L, Dunoyer P, Jay F, Arnold B, Dharmasiri N, Estelle M, Voinnet O, Jones JDG. 2006. A plant miRNA contributes to antibacterial resistance by repressing auxin signaling. *Science* **312**(5772): 436-439.

Neyen C, Lemaitre B. 2016. Sensing Gram-negative bacteria: a phylogenetic perspective. *Curr Opin Immunol* **38**: 8-17.

Niesik SS. 2016. *Functional characterisation of the Arabidopsis thaliana receptor-like kinase RICKY1 during immune responses.* Master thesis, Ludwig-Maximilians-Universität München.

Nishimura MT, Stein M, Hou BH, Vogel JP, Edwards H, Somerville SC. 2003. Loss of a callose synthase results in salicylic acid-dependent disease resistance. *Science* **301**(5635): 969-972.

Nühse TS, Bottrill AR, Jones AME, Peck SC. 2007. Quantitative phosphoproteomic analysis of plasma membrane proteins reveals regulatory mechanisms of plant innate immune responses. *Plant Journal* **51**(5): 931-940.

Nühse TS, Peck SC, Hirt H, Boller T. 2000. Microbial elicitors induce activation and dual phosphorylation of the Arabidopsis thaliana MAPK 6. *Journal of Biological Chemistry* **275**(11): 7521-7526.

Nürnberger T, Brunner F, Kemmerling B, Piater L. 2004. Innate immunity in plants and animals: striking similarities and obvious differences. *Immunol Rev* **198**: 249-266.

O'Connell RJ, Panstruga R. 2006. Tete a tete inside a plant cell: establishing compatibility between plants and biotrophic fungi and oomycetes. *New Phytologist* **171**(4): 699-718.

O'Neill LAJ, Bowie AG. 2007. The family of five: TIR-domain-containing adaptors in Toll-like receptor signalling. *Nature Reviews Immunology* **7**(5): 353-364.

Osakabe Y, Yamaguchi-Shinozaki K, Shinozaki K, Tran LSP. 2013. Sensing the environment: key roles of membrane-localized kinases in plant perception and response to abiotic stress. *Journal of Experimental Botany* **64**(2): 445-458.

Ossowski S, Schwab R, Weigel D. 2008. Gene silencing in plants using artificial microRNAs and other small RNAs. *Plant Journal* **53**(4): 674-690.

Paredez AR, Persson S, Ehrhardt DW, Somerville CR. 2008. Genetic evidence that cellulose synthase activity influences microtubule cortical array organization. *Plant Physiology* **147**(4): 1723-1734.

Paredez AR, Somerville CR, Ehrhardt DW. 2006. Visualization of cellulose synthase demonstrates functional association with microtubules. *Science* **312**(5779): 1491-1495.

Parniske M. 2008. Arbuscular mycorrhiza: the mother of plant root endosymbioses. *Nature Reviews Microbiology* **6**(10): 763-775.

Parton RG, Simons K. 2007. The multiple faces of caveolae. *Nat Rev Mol Cell Biol* **8**(3): 185-194.

Patil A, Nakamura H. 2006. Disordered domains and high surface charge confer hubs with the ability to interact with multiple proteins in interaction networks. *Febs Letters* **580**(8): 2041-2045.

Peaucelle A, Braybrook S, Hofte H. 2012. Cell wall mechanics and growth control in plants: the role of pectins revisited. *Frontiers in Plant Science* **3**(121).

Pei ZM, Murata Y, Benning G, Thomine S, Klusener B, Allen GJ, Grill E, Schroeder JI. 2000. Calcium channels activated by hydrogen peroxide mediate abscisic acid signalling in guard cells. *Nature* **406**(6797): 731-734.

Perraki A, Binaghi M, Mecchia MA, Gronnier J, German-Retana S, Mongrand S, Bayer E, Zelada AM, Germain V. 2014. StRemorin1.3 hampers Potato virus X TGBp1 ability to increase plasmodesmata permeability, but does not interfere with its silencing suppressor activity. *Febs Letters* **588**(9): 1699-1705.

Perraki A, Cacas JL, Crowet JM, Lins L, Castroviejo M, German-Retana S, Mongrand S, Raffaele S. 2012. Plasma Membrane Localization of Solanum tuberosum Remorin from Group 1, Homolog 3 Is Mediated by Conformational Changes in a Novel C-Terminal Anchor and Required for the Restriction of Potato Virus X Movement. *Plant Physiology* **160**(2): 624-637.

Petersen M, Brodersen P, Naested H, Andreasson E, Lindhart U, Johansen B, Nielsen HB, Lacy M, Austin MJ, Parker JE, et al. 2000. Arabidopsis MAP kinase 4 negatively regulates systemic acquired resistance. *Cell* **103**(7): 1111-1120.

Petre B, Kamoun S. 2014. How Do Filamentous Pathogens Deliver Effector Proteins into Plant Cells? *Plos Biology* **12**(2).

Petutschnig EK, Jones AME, Serazetdinova L, Lipka U, Lipka V. 2010. The Lysin Motif Receptor-like Kinase (LysM-RLK) CERK1 Is a Major Chitin-binding Protein in Arabidopsis thaliana and Subject to Chitin-induced Phosphorylation. *Journal of Biological Chemistry* **285**(37): 28902-28911.

Petutschnig EK, Stolze M, Lipka U, Kopischke M, Horlacher J, Valerius O, Rozhon W, Gust AA, Kemmerling B, Poppenberger B, et al. 2014. A novel Arabidopsis CHITIN ELICITOR RECEPTOR KINASE 1 (CERK1) mutant with enhanced pathogen-induced cell death and altered receptor processing. *New Phytologist* **204**(4): 955-967.

Pi M, Quarles LD. 2012. Multiligand Specificity and Wide Tissue Expression of GPRC6A Reveals New Endocrine Networks. *Endocrinology* **153**(5): 2062-2069.

Piasecka A, Jedrzejczak-Rey N, Bednarek P. 2015. Secondary metabolites in plant innate immunity: conserved function of divergent chemicals. *New Phytologist* **206**(3): 948-964.

Pike LJ. 2006. Rafts defined: a report on the Keystone Symposium on Lipid Rafts and Cell Function. *Journal of Lipid Research* **47**(7): 1597-1598.

Pillitteri LJ, Bemis SM, Shpak ED, Torii KU. 2007. Haploinsufficiency after successive loss of signaling reveals a role for ERECTA-family genes in Arabidopsis ovule development. *Development* **134**(17): 3099-3109.

Pitzschke A, Hirt H. 2009. Disentangling the complexity of mitogen-activated protein kinases and reactive oxygen species signaling. *Plant Physiology* **149**(2): 606-615.

Pogorelko G, Lionetti V, Bellincampi D, Zabotina O. 2013. Cell wall integrity: targeted post-synthetic modifications to reveal its role in plant growth and defense against pathogens. *Plant Signal Behav* **8**(9).

Postel S, Kufner I, Beuter C, Mazzotta S, Schwedt A, Borlotti A, Halter T, Kemmerling B, Nurnberger T. 2010. The multifunctional leucine-rich repeat receptor kinase BAK1 is implicated in Arabidopsis development and immunity. *European Journal of Cell Biology* **89**(2-3): 169-174.

Pumplin N, Zhang XC, Noar RD, Harrison MJ. 2012. Polar localization of a symbiosis-specific phosphate transporter is mediated by a transient reorientation of secretion. *Proceedings of the National Academy of Sciences of the United States of America* **109**(11): E665-E672.

Qin SY, Hu D, Matsumoto K, Takeda K, Matsumoto N, Yamaguchi Y, Yamamoto K. 2012. Malectin Forms a Complex with Ribophorin I for Enhanced Association with Misfolded Glycoproteins. *Journal of Biological Chemistry* **287**(45): 38080-38089.

Qiu JL, Zhou L, Yun BW, Nielsen HB, Fiil BK, Petersen K, MacKinlay J, Loake GJ, Mundy J, Morris PC. 2008. Arabidopsis mitogen-activated protein kinase kinases MKK1 and MKK2 have overlapping functions in defense signaling mediated by MEKK1, MPK4, and MKS1. *Plant Physiology* **148**(1): 212-222.

Raffaele S, Bayer E, Lafarge D, Cluzet S, Retana SG, Boubekeur T, Leborgne-Castel N, Carde JP, Lherminier J, Noirot E, et al. 2009. Remorin, a Solanaceae Protein Resident in Membrane Rafts and Plasmodesmata, Impairs Potato virus X Movement. *Plant Cell* **21**(5): 1541-1555.

Raffaele S, Mongrand S, Gamas P, Niebel A, Ott T. 2007. Genome-wide annotation of remorins, a plant-specific protein family: Evolutionary and functional perspectives. *Plant Physiology* **145**(3): 593-600.

Rajaraman J, Douchkov D, Hensel G, Stefanato FL, Gordon A, Ereful N, Caldararu OF, Petrescu AJ, Kumlehn J, Boyd LA, et al. 2016. An LRR/Malectin Receptor-Like Kinase Mediates Resistance to Non-adapted and Adapted Powdery Mildew Fungi in Barley and Wheat. *Frontiers in Plant Science* **7**(1836).

Ranf S, Eschen-Lippold L, Frohlich K, Westphal L, Scheel D, Lee J. 2014. Microbe-associated molecular pattern-induced calcium signaling requires the receptor-like cytoplasmic kinases, PBL1 and BIK1. *BMC Plant Biol* **14**(374).

Ranf S, Gisch N, Schaffer M, Illig T, Westphal L, Knirel YA, Sanchez-Carballo PM, Zahringer U, Huckelhoven R, Lee J, et al. 2015. A lectin S-domain receptor kinase mediates lipopolysaccharide sensing in Arabidopsis thaliana. *Nature Immunology* **16**(4): 426-433.

Refregier G, Pelletier S, Jaillard D, Hofte H. 2004. Interaction between wall deposition and cell elongation in dark-grown hypocotyl cells in Arabidopsis. *Plant Physiology* **135**(2): 959-968.

Ren D, Liu Y, Yang KY, Han L, Mao G, Glazebrook J, Zhang S. 2008. A fungal-responsive MAPK cascade regulates phytoalexin biosynthesis in Arabidopsis. *Proc Natl Acad Sci U S A* **105**(14): 5638-5643.

Ren DT, Yang HP, Zhang SQ. 2002. Cell death mediated by MAPK is associated with hydrogen peroxide production in Arabidopsis. *Journal of Biological Chemistry* **277**(1): 559-565.

Rentel MC, Knight MR. 2004. Oxidative stress-induced calcium signaling in Arabidopsis. *Plant Physiology* **135**(3): 1471-1479.

Reuff M, Mikosch M, Homann U. 2010. Trafficking, lateral mobility and segregation of the plant K plus channel KAT1. *Plant Biology* **12**: 99-104.

Richmond TA, Somerville CR. 2000. The cellulose synthase superfamily. *Plant Physiology* **124**(2): 495-498.

Robatzek S, Bittel P, Chinchilla D, Kochner P, Felix G, Shiu SH, Boller T. 2007. Molecular identification and characterization of the tomato flagellin receptor LeFLS2, an orthologue of Arabidopsis FLS2 exhibiting characteristically different perception specificities. *Plant Molecular Biology* **64**(5): 539-547.

Ronald PC, Beutler B. 2010. Plant and Animal Sensors of Conserved Microbial Signatures. *Science* **330**(6007): 1061-1064.

Ross A, Yamada K, Hiruma K, Yamashita-Yamada M, Lu X, Takano Y, Tsuda K, Saijo Y. 2014. The Arabidopsis PEPR pathway couples local and systemic plant immunity. *Embo Journal* **33**(1): 62-75.

Ruoslahti E. 1996. RGD and other recognition sequences for integrins. *Annual Review of Cell and Developmental Biology* **12**: 697-715.

Russell AR, Ashfield T, Innes RW. 2015. Pseudomonas syringae Effector AvrPphB Suppresses AvrB-Induced Activation of RPM1 but Not AvrRpm1-Induced Activation. *Mol Plant Microbe Interact* **28**(6): 727-735.

Sako Y, Kusumi A. 1994. Compartmentalized Structure of the Plasma-Membrane for Receptor Movements as Revealed by a Nanometer-Level Motion Analysis. *Journal of Cell Biology* **125**(6): 1251-1264.

Samiee KT, Moran-Mirabal JM, Cheung YK, Craighead HG. 2006. Zero mode waveguides for single-molecule spectroscopy on lipid membranes. *Biophysical Journal* **90**(9): 3288-3299.

Sampathkumar A, Gutierrez R, McFarlane HE, Bringmann M, Lindeboom J, Emons AM, Samuels L, Ketelaar T, Ehrhardt DW, Persson S. 2013. Patterning and Lifetime of Plasma Membrane-Localized Cellulose Synthase Is Dependent on Actin Organization in Arabidopsis Interphase Cells. *Plant Physiology* **162**(2): 675-688.

Schallus T, Feher K, Sternberg U, Rybin V, Muhle-Goll C. 2010. Analysis of the specific interactions between the lectin domain of malectin and diglucosides. *Glycobiology* **20**(8): 1010-1020.

Schallus T, Jaeckh C, Feher K, Palma AS, Liu Y, Simpson JC, Mackeen M, Stier G, Gibson TJ, Feizi T, et al. 2008. Malectin: A novel carbohydrate-binding protein of the endoplasmic reticulum and a candidate player in the early steps of protein N-glycosylation. *Molecular Biology of the Cell* **19**(8): 3404-3414.

Schindler M, Meiners S, Cheresh DA. 1989. Rgd-Dependent Linkage between Plant-Cell Wall and Plasma-Membrane - Consequences for Growth. *Journal of Cell Biology* **108**(5): 1955-1965.

Schmelzer E. 2002. Cell polarization, a crucial process in fungal defence. *Trends Plant Sci* **7**(9): 411-415.

Schroeder RJ, Ahmed SN, Zhu YZ, London E, Brown DA. 1998. Cholesterol and sphingolipid enhance the Triton X-100 insolubility of glycosylphosphatidylinositol-anchored proteins by promoting the formation of detergent-insoluble ordered membrane domains. *Journal of Biological Chemistry* **273**(2): 1150-1157.

Schulz P, Herde M, Romeis T. 2013. Calcium-Dependent Protein Kinases: Hubs in Plant Stress Signaling and Development. *Plant Physiology* **163**(2): 523-530.

Schulze B, Mentzel T, Jehle AK, Mueller K, Beeler S, Boller T, Felix G, Chinchilla D. 2010. Rapid Heteromerization and Phosphorylation of Ligand-activated Plant Transmembrane Receptors and Their Associated Kinase BAK1. *Journal of Biological Chemistry* **285**(13): 9444-9451.

Schwab R, Ossowski S, Riester M, Warthmann N, Weigel D. 2006. Highly specific gene silencing by artificial microRNAs in Arabidopsis. *Plant Cell* **18**(5): 1121-1133.

Schwessinger B, Roux M, Kadota Y, Ntoukakis V, Sklenar J, Jones A, Zipfel C. 2011. Phosphorylation-dependent differential regulation of plant growth, cell death, and innate immunity by the regulatory receptor-like kinase BAK1. *Plos Genetics* **7**(4): e1002046.

Senchou V, Weide R, Carrasco A, Bouyssou H, Pont-Lezica R, Govers F, Canut H. 2004. High affinity recognition of a Phytophthora protein by Arabidopsis via an RGD motif. *Cellular and Molecular Life Sciences* **61**(4): 502-509.

Serrano M, Coluccia F, Torres M, L'Haridon F, Metraux JP. 2014. The cuticle and plant defense to pathogens. *Frontiers in Plant Science* **5**(274).

Shan LB, He P, Li JM, Heese A, Peck SC, Nurnberger T, Martin GB, Sheen J. 2008. Bacterial effectors target the common signaling partner BAK1 to disrupt multiple MAMP receptor-signaling complexes and impede plant immunity. *Cell Host & Microbe* **4**(1): 17-27.

Sheetz MP, Schindler M, Koppel DE. 1980. Lateral Mobility of Integral Membrane-Proteins Is Increased in Spherocytic Erythrocytes. *Nature* **285**(5765): 510-512.

Shigenaga AM, Argueso CT. 2016. No hormone to rule them all: Interactions of plant hormones during the responses of plants to pathogens. *Seminars in Cell & Developmental Biology* **56**: 174-189.

Shih HW, Miller ND, Dai C, Spalding EP, Monshausen GB. 2014. The Receptor-like Kinase FERONIA Is Required for Mechanical Signal Transduction in Arabidopsis Seedlings. *Current Biology* **24**(16): 1887-1892.

Shimizu T, Nakano T, Takamizawa D, Desaki Y, Ishii-Minami N, Nishizawa Y, Minami E, Okada K, Yamane H, Kaku H, et al. 2010. Two LysM receptor molecules, CEBiP and OsCERK1, cooperatively regulate chitin elicitor signaling in rice. *Plant J* **64**(2): 204-214.

Shiu SH, Bleecker AB. 2001a. Plant receptor-like kinase gene family: diversity, function, and signaling. *Sci STKE* **2001**(113).

Shiu SH, Bleecker AB. 2001b. Receptor-like kinases from Arabidopsis form a monophyletic gene family related to animal receptor kinases. *Proceedings of the National Academy of Sciences of the United States of America* **98**(19): 10763-10768.

Shiu SH, Bleecker AB. 2003. Expansion of the receptor-like kinase/Pelle gene family and receptor-like proteins in Arabidopsis. *Plant Physiology* **132**(2): 530-543.

Shiu SH, Karlowski WM, Pan RS, Tzeng YH, Mayer KFX, Li WH. 2004. Comparative analysis of the receptor-like kinase family in Arabidopsis and rice. *Plant Cell* **16**(5): 1220-1234.

Shpak ED. 2013. Diverse Roles of ERECTA Family Genes in Plant Development. *Journal of Integrative Plant Biology* **55**(12): 1238-1250.

Shpak ED, Berthiaume CT, Hill EJ, Torii KU. 2004. Synergistic interaction of three ERECTA-family receptor-like kinases controls Arabidopsis organ growth and flower development by promoting cell proliferation. *Development* **131**(7): 1491-1501.

Shpak ED, McAbee JM, Pillitteri LJ, Torii KU. 2005. Stomatal patterning and differentiation by synergistic interactions of receptor kinases. *Science* **309**(5732): 290-293.

Simons K, Ikonen E. 1997. Functional rafts in cell membranes. *Nature* **387**(6633): 569-572.

Singer SJ, Nicolson GL. 1972. The Fluid Mosaic Model of the Structure of Cell Membranes. *Science* **175**(4023): 720-731.

Singh P, Kuo YC, Mishra S, Tsai CH, Chien CC, Chen CW, Desclos-Theveniau M, Chu PW, Schulze B, Chinchilla D, et al. 2012. The Lectin Receptor Kinase-VI.2 Is Required for Priming and Positively Regulates Arabidopsis Pattern-Triggered Immunity. *Plant Cell* **24**(3): 1256-1270.

Skerra A. 1994. Use of the Tetracycline Promoter for the Tightly Regulated Production of a Murine Antibody Fragment in Escherichia-Coli. *Gene* **151**(1-2): 131-135.

Skibbens JE, Roth MG, Matlin KS. 1989. Differential extractability of influenza virus hemagglutinin during intracellular transport in polarized epithelial cells and nonpolar fibroblasts. *Journal of Cell Biology* **108**(3): 821-832.

Smith JM, Leslie ME, Robinson SJ, Korasick DA, Zhang T, Backues SK, Cornish PV, Koo AJ, Bednarek SY, Heese A. 2014. Loss of Arabidopsis thaliana Dynamin-Related Protein 2B Reveals Separation of Innate Immune Signaling Pathways. *Plos Pathogens* **10**(12).

Smith KD, Andersen-Nissen E, Hayashi F, Strobe K, Bergman MA, Barrett SLR, Cookson BT, Aderem A. 2003. Toll-like receptor 5 recognizes a conserved site on flagellin required for protofilament formation and bacterial motility. *Nature Immunology* **4**(12): 1247-1253.

Somssich M, Ma QJ, Weidtkamp-Peters S, Stahl Y, Felekyan S, Bleckmann A, Seidel CAM, Simon R. 2015. Real-time dynamics of peptide ligand-dependent receptor complex formation in planta. *Science Signaling* **8**(388).

Son S, Oh CJ, An CS. 2014. Arabidopsis thaliana Remorins Interact with SnRK1 and Play a Role in Susceptibility to Beet Curly Top Virus and Beet Severe Curly Top Virus. *Plant Pathology Journal* **30**(3): 269-278.

Soylu EM, Soylu S. 2003. Light and electron microscopy of the compatible interaction between Arabidopsis and the downy mildew pathogen Peronospora parasitica. *Journal of Phytopathology* **151**(6): 300-306.

Spira F, Mueller NS, Beck G, von Olshausen P, Beig J, Wedlich-Söldner R. 2012. Patchwork organization of the yeast plasma membrane into numerous coexisting domains. *Nature Cell Biology* **14**(6): 640-648.

Spoel SH, Dong X. 2012. How do plants achieve immunity? Defence without specialized immune cells. *Nature Reviews Immunology* **12**(2): 89-100.

Stegmann M, Monaghan J, Smakowska-Luzan E, Rovenich H, Lehner A, Holton N, Belkhadir Y, Zipfel C. 2017. The receptor kinase FER is a RALF-regulated scaffold controlling plant immune signaling. *Science* **355**(6322): 287-289.

Stein M, Dittgen J, Sanchez-Rodriguez C, Hou BH, Molina A, Schulze-Lefert P, Lipka V, Somerville S. 2006. Arabidopsis PEN3/PDR8, an ATP binding cassette transporter, contributes to nonhost resistance to inappropriate pathogens that enter by direct penetration. *Plant Cell* **18**(3): 731-746.

Stier A, Sackmann E. 1973. Spin labels as enzyme substrates. Heterogeneous lipid distribution in liver microsomal membranes. *Biochimica Et Biophysica Acta* **311**(3): 400-408.

Stracke S, Kistner C, Yoshida S, Mulder L, Sato S, Kaneko T, Tabata S, Sandal N, Stougaard J, Szczyglowski K, et al. 2002. A plant receptor-like kinase required for both bacterial and fungal symbiosis. *Nature* **417**(6892): 959-962.

Strader LC, Bartel B. 2009. The Arabidopsis PLEIOTROPIC DRUG RESISTANCE8/ABCG36 ATP Binding Cassette Transporter Modulates Sensitivity to the Auxin Precursor Indole-3-Butyric Acid. *Plant Cell* **21**(7): 1992-2007.

Stratil TF. 2016. *The Formation of an Infection-related Membrane Domain is Controlled by the Sequential Recruitment of Scaffold and Receptor Proteins.* PhD thesis, Ludwig-Maximilians-Universität München.

Studier FW, Moffatt BA. 1986. Use of Bacteriophage-T7 Rna-Polymerase to Direct Selective High-Level Expression of Cloned Genes. *Journal of Molecular Biology* **189**(1): 113-130.

Suarez-Rodriguez MC, Adams-Phillips L, Liu YD, Wang HC, Su SH, Jester PJ, Zhang SQ, Bent AF, Krysan PJ. 2007. MEKK1 is required for flg22-induced MPK4 activation in Arabidopsis plants. *Plant Physiology* **143**(2): 661-669.

Sun YD, Li L, Macho AP, Han ZF, Hu ZH, Zipfel C, Zhou JM, Chai JJ. 2013. Structural Basis for flg22-Induced Activation of the Arabidopsis FLS2-BAK1 Immune Complex. *Science* **342**(6158): 624-628.

Sutter JU, Campanoni P, Tyrrell M, Blatt MR. 2006. Selective mobility and sensitivity to SNAREs is exhibited by the Arabidopsis KAT1 K+ channel at the plasma membrane. *Plant Cell* **18**(4): 935-954.

Suzuki KGN, Fujiwara TK, Sanematsu F, Iino R, Edidin M, Kusumi A. 2007. GPI-anchored receptor clusters transiently recruit Lyn and G alpha for temporary cluster immobilization and Lyn activation: single-molecule tracking study 1. *Journal of Cell Biology* **177**(4): 717-730.

Szymanski WG, Zauber H, Erban A, Gorka M, Wu XN, Schulze WX. 2015. Cytoskeletal Components Define Protein Location to Membrane Microdomains. *Molecular & Cellular Proteomics* **14**(9): 2493-2509.

Takahashi F, Yoshida R, Ichimura K, Mizoguchi T, Seo S, Yonezawa M, Maruyama K, Yamaguchi-Shinozaki K, Shinozaki K. 2007. The mitogen-activated protein kinase cascade MKK3-MPK6 is an important part of the jasmonate signal transduction pathway in Arabidopsis. *Plant Cell* **19**(3): 805-818.

Takai R, Isogai A, Takayama S, Che FS. 2008. Analysis of flagellin perception mediated by flg22 receptor OsFLS2 in rice. *Mol Plant Microbe Interact* **21**(12): 1635-1642.

Takano J, Tanaka M, Toyoda A, Miwa K, Kasai K, Fuji K, Onouchi H, Naito S, Fujiwara T. 2010. Polar localization and degradation of Arabidopsis boron transporters through distinct trafficking pathways. *Proc Natl Acad Sci U S A* **107**(11): 5220-5225.

Tanaka K, Gilroy S, Jones AM, Stacey G. 2010. Extracellular ATP signaling in plants. *Trends Cell Biol* **20**(10): 601-608.

Tanner W, Malinsky J, Opekarova M. 2011. In Plant and Animal Cells, Detergent-Resistant Membranes Do Not Define Functional Membrane Rafts. *Plant Cell* **23**(4): 1191-1193.

Tapken W, Murphy AS. 2015. Membrane nanodomains in plants: capturing form, function, and movement. *Journal of Experimental Botany* **66**(6): 1573-1586.

ten Hove CA, Bochdanovits Z, Jansweijer VMA, Koning FG, Berke L, Sanchez-Perez GF, Scheres B, Heidstra R. 2011. Probing the roles of LRR RLK genes in Arabidopsis thaliana roots using a custom T-DNA insertion set. *Plant Molecular Biology* **76**(1-2): 69-83.

Thomma BPHJ, Eggermont K, Penninckx IAMA, Mauch-Mani B, Vogelsang R, Cammue BPA, Broekaert WF. 1998. Separate jasmonate-dependent and salicylate-dependent defense-response pathways in Arabidopsis are essential for resistance to distinct microbial pathogens. *Proceedings of the National Academy of Sciences of the United States of America* **95**(25): 15107-15111.

Thordal-Christensen H. 2003. Fresh insights into processes of nonhost resistance. *Current Opinion in Plant Biology* **6**(4): 351-357.

Tóth K, Stratil TF, Madsen EB, Ye JY, Popp C, Antolin-Llovera M, Grossmann C, Jensen ON, Schussler A, Parniske M, et al. 2012. Functional Domain Analysis of the Remorin Protein LjSYMREM1 in Lotus japonicus. *Plos One* **7**(1).

Touhara K. 1997. Binding of multiple ligands to pleckstrin homology domain regulates membrane translocation and enzyme activity of beta-adrenergic receptor kinase. *Febs Letters* **417**(2): 243-248.

Trda L, Fernandez O, Boutrot F, Heloir MC, Kelloniemi J, Daire X, Adrian M, Clement C, Zipfel C, Dorey S, et al. 2014. The grapevine flagellin receptor VvFLS2 differentially recognizes flagellin-derived epitopes from the endophytic growth-promoting bacterium Burkholderia phytofirmans and plant pathogenic bacteria. *New Phytologist* **201**(4): 1371-1384.

Tsuji A, Kawasaki K, Ohnishi S, Merkle H, Kusumi A. 1988. Regulation of band 3 mobilities in erythrocyte ghost membranes by protein association and cytoskeletal meshwork. *Biochemistry* **27**(19): 7447-7452.

Tsuji A, Ohnishi S. 1986. Restriction of the lateral motion of band 3 in the erythrocyte membrane by the cytoskeletal network: dependence on spectrin association state. *Biochemistry* **25**(20): 6133-6139.

Ullrich M, Bereswill S, Volksch B, Fritsche W, Geider K. 1993. Molecular Characterization of Field Isolates of Pseudomonas-Syringae Pv Glycinea Differing in Coronatine Production. *Journal of General Microbiology* **139**: 1927-1937.

Underwood W, Somerville SC. 2013. Perception of conserved pathogen elicitors at the plasma membrane leads to relocalization of the Arabidopsis PEN3 transporter. *Proceedings of the National Academy of Sciences of the United States of America* **110**(30): 12492-12497.

Urbanus SL, Ott T. 2012. Plasticity of plasma membrane compartmentalization during plant immune responses. *Frontiers in Plant Science* **3**: 181.

Van der Biezen EA, Jones JD. 1998. Plant disease-resistance proteins and the gene-for-gene concept. *Trends Biochem Sci* **23**(12): 454-456.

Van Meer G. 1989. Lipid Traffic in Animal-Cells. *Annual Review of Cell Biology* **5**: 247-275.

Veluchamy S, Hind SR, Dunham DM, Martin GB, Panthee DR. 2014. Natural Variation for Responsiveness to flg22, flgII-28, and csp22 and Pseudomonas syringae pv. tomato in Heirloom Tomatoes. *Plos One* **9**(9).

Verma V, Ravindran P, Kumar PP. 2016. Plant hormone-mediated regulation of stress responses. *BMC Plant Biol* **16**: 86.

Veronese P, Nakagami H, Bluhm B, Abuqamar S, Chen X, Salmeron J, Dietrich RA, Hirt H, Mengiste T. 2006. The membrane-anchored BOTRYTIS-INDUCED KINASE1 plays distinct roles in Arabidopsis resistance to necrotrophic and biotrophic pathogens. *Plant Cell* **18**(1): 257-273.

Voegele RT, Mendgen K. 2003. Rust haustoria: nutrient uptake and beyond. *New Phytologist* **159**(1): 93-100.

Voigt CA. 2014. Callose-mediated resistance to pathogenic intruders in plant defense-related papillae. *Frontiers in Plant Science* **5**(168).

Voxeur A, Höfte H. 2016. Cell wall integrity signaling in plants: "To grow or not to grow that's the question". *Glycobiology* **26**(9): 950-960.

Wagner TA, Kohorn BD. 2001. Wall-associated kinases are expressed throughout plant development and are required for cell expansion. *Plant Cell* **13**(2): 303-318.

Walters D, Heil M. 2007. Costs and trade-offs associated with induced resistance. *Physiological and Molecular Plant Pathology* **71**(1-3): 3-17.

Wan J, Zhang XC, Neece D, Ramonell KM, Clough S, Kim SY, Stacey MG, Stacey G. 2008. A LysM receptor-like kinase plays a critical role in chitin signaling and fungal resistance in Arabidopsis. *Plant Cell* **20**(2): 471-481.

Wang JZ, Li HJ, Han ZF, Zhang HQ, Wang T, Lin GZ, Chang JB, Yang WC, Chai JJ. 2015a. Allosteric receptor activation by the plant peptide hormone phytosulfokine. *Nature* **525**(7568): 265-268.

Wang L, Li H, Lv XQ, Chen T, Li RL, Xue YQ, Jiang JJ, Jin B, Baluska F, Samaj J, et al. 2015b. Spatiotemporal Dynamics of the BRI1 Receptor and its Regulation by Membrane Microdomains in Living Arabidopsis Cells. *Molecular Plant* **8**(9): 1334-1349.

Wang WM, Wen YQ, Berkey R, Xiao SY. 2009. Specific Targeting of the Arabidopsis Resistance Protein RPW8.2 to the Interfacial Membrane Encasing the Fungal Haustorium Renders Broad-Spectrum Resistance to Powdery Mildew. *Plant Cell* **21**(9): 2898-2913.

Wang WM, Zhang Y, Wen YQ, Berkey R, Ma XF, Pan ZY, Bendigeri D, King H, Zhang Q, Xiao SY. 2013. A Comprehensive Mutational Analysis of the Arabidopsis Resistance Protein RPW8.2 Reveals Key Amino Acids for Defense Activation and Protein Targeting. *Plant Cell* **25**(10): 4242-4261.

Wang XL, Li XQ, Meisenhelder J, Hunter T, Yoshida S, Asami T, Chory J. 2005. Autoregulation and homodimerization are involved in the activation of the plant steroid receptor BRI1. *Developmental Cell* **8**(6): 855-865.

Wang Z, Cao GG, Wang XL, Miao J, Liu XT, Chen ZL, Qu LJ, Gu HG. 2008. Identification and characterization of COI1-dependent transcription factor genes involved in JA-mediated response to wounding in Arabidopsis plants. *Plant Cell Reports* **27**(1): 125-135.

Weiler EW, Kutchan TM, Gorba T, Brodschelm W, Niesel U, Bublitz F. 1994. The Pseudomonas Phytotoxin Coronatine Mimics Octadecanoid Signaling Molecules of Higher-Plants. *Febs Letters* **345**(1): 9-13.

Widjaja I, Naumann K, Roth U, Wolf N, Mackey D, Dangl JL, Scheel D, Lee J. 2009. Combining subproteome enrichment and Rubisco depletion enables identification of low abundance proteins differentially regulated during plant defense. *Proteomics* **9**(1): 138-147.

Willemsen V, Friml J, Grebe M, van den Toorn A, Palme K, Scheres B. 2003. Cell polarity and PIN protein positioning in Arabidopsis require STEROL METHYLTRANSFERASE1 function. *Plant Cell* **15**(3): 612-625.

Willmann R, Lajunen HM, Erbs G, Newman MA, Kolb D, Tsuda K, Katagiri F, Fliegmann J, Bono JJ, Cullimore JV, et al. 2011. Arabidopsis lysin-motif proteins LYM1 LYM3 CERK1 mediate bacterial peptidoglycan sensing and immunity to bacterial infection. *Proceedings of the National Academy of Sciences of the United States of America* **108**(49): 19824-19829.

Wiśniewska J, Xu J, Seifertova D, Brewer PB, Ruzicka K, Blilou I, Rouquie D, Benkova E, Scheres B, Friml J. 2006. Polar PIN localization directs auxin flow in plants. *Science* **312**(5775): 883-883.

Wolf S, Höfte H. 2014. Growth Control: A Saga of Cell Walls, ROS, and Peptide Receptors. *Plant Cell* **26**(5): 1848-1856.

Wright PE, Dyson HJ. 2009. Linking folding and binding. *Current Opinion in Structural Biology* **19**(1): 31-38.

Wu J, Kurten EL, Monshausen G, Hummel GM, Gilroy S, Baldwin IT. 2007. NaRALF, a peptide signal essential for the regulation of root hair tip apoplastic pH in Nicotiana attenuata, is required for root hair development and plant growth in native soils. *Plant J* **52**(5): 877-890.

Xiao C, Barnes WJ, Zamil MS, Yi H, Puri VM, Anderson CT. 2017. Activation tagging of Arabidopsis POLYGALACTURONASE INVOLVED IN EXPANSION2 promotes hypocotyl elongation, leaf expansion, stem lignification, mechanical stiffening, and lodging. *Plant J*.

Xiao SY, Ellwood S, Calis O, Patrick E, Li TX, Coleman M, Turner JG. 2001. Broad-spectrum mildew resistance in Arabidopsis thaliana mediated by RPW8. *Science* **291**(5501): 118-120.

Xin XF, He SY. 2013. Pseudomonas syringae pv. tomato DC3000: a model pathogen for probing disease susceptibility and hormone signaling in plants. *Annu Rev Phytopathol* **51**: 473-498.

Xin XF, Nomura K, Underwood W, He SY. 2013. Induction and Suppression of PEN3 Focal Accumulation During Pseudomonas syringae pv. tomato DC3000 Infection of Arabidopsis. *Molecular Plant-Microbe Interactions* **26**(8): 861-867.

Xu J, Li Y, Wang Y, Liu H, Lei L, Yang H, Liu G, Ren D. 2008. Activation of MAPK kinase 9 induces ethylene and camalexin biosynthesis and enhances sensitivity to salt stress in Arabidopsis. *Journal of Biological Chemistry* **283**(40): 26996-27006.

Xu J, Meng J, Meng XZ, Zhao YT, Liu JM, Sun TF, Liu YD, Wang QM, Zhang SQ. 2016. Pathogen-Responsive MPK3 and MPK6 Reprogram the Biosynthesis of Indole Glucosinolates and Their Derivatives in Arabidopsis Immunity. *Plant Cell* **28**(5): 1144-1162.

Yamada K, Yamaguchi K, Shirakawa T, Nakagami H, Mine A, Ishikawa K, Fujiwara M, Narusaka M, Narusaka Y, Ichimura K, et al. 2016. The Arabidopsis CERK1-associated kinase PBL27 connects chitin perception to MAPK activation. *Embo Journal* **35**(22): 2468-2483.

Yamaguchi Y, Huffaker A, Bryan AC, Tax FE, Ryan CA. 2010. PEPR2 Is a Second Receptor for the Pep1 and Pep2 Peptides and Contributes to Defense Responses in Arabidopsis. *Plant Cell* **22**(2): 508-522.

Yamaguchi Y, Pearce G, Ryan CA. 2006. The cell surface leucine-rich repeat receptor for AtPep1, an endoaenous peptide elicitor in Arabidopsis, is functional in transgenic tobacco cells. *Proceedings of the National Academy of Sciences of the United States of America* **103**(26): 10104-10109.

Yan YX, Stolz S, Chetelat A, Reymond P, Pagni M, Dubugnon L, Farmer EE. 2007. A downstream mediator in the growth repression limb of the jasmonate pathway. *Plant Cell* **19**(8): 2470-2483.

Yeh YH, Panzeri D, Kadota Y, Huang YC, Huang PY, Tao CN, Roux M, Chien HC, Chin TC, Chu PW, et al. 2016. The Arabidopsis Malectin-Like/LRR-RLK IOS1 Is Critical for BAK1-Dependent and BAK1-Independent Pattern-Triggered Immunity. *Plant Cell* **28**(7): 1701-1721.

Yoshida S, Parniske M. 2005. Regulation of plant symbiosis receptor kinase through serine and threonine phosphorylation. *Journal of Biological Chemistry* **280**(10): 9203-9209.

Yue J, Li C, Liu YW, Yu JJ. 2014. A Remorin Gene SiREM6, the Target Gene of SiARDP, from Foxtail Millet (Setaria italica) Promotes High Salt Tolerance in Transgenic Arabidopsis. *Plos One* **9**(6).

Zhang J, Nodzynski T, Pencik A, Rolcik J, Friml J. 2010. PIN phosphorylation is sufficient to mediate PIN polarity and direct auxin transport. *Proceedings of the National Academy of Sciences of the United States of America* **107**(2): 918-922.

Zhang J, Shao F, Li Y, Cui H, Chen L, Li H, Zou Y, Long C, Lan L, Chai J, et al. 2007. A Pseudomonas syringae effector inactivates MAPKs to suppress PAMP-induced immunity in plants. *Cell Host & Microbe* **1**(3): 175-185.

Zhang Y, Immink R, Liu CM, Emons AM, Ketelaar T. 2013. The Arabidopsis exocyst subunit SEC3A is essential for embryo development and accumulates in transient puncta at the plasma membrane. *New Phytologist* **199**(1): 74-88.

Zheng XY, Spivey NW, Zeng WQ, Liu PP, Fu ZQ, Klessig DF, He SY, Dong XN. 2012. Coronatine Promotes Pseudomonas syringae Virulence in Plants by Activating a Signaling Cascade that Inhibits Salicylic Acid Accumulation. *Cell Host & Microbe* **11**(6): 587-596.

Zipfel C. 2014. Plant pattern-recognition receptors. *Trends in Immunology* **35**(7): 345-351.

Zipfel C, Felix G. 2005. Plants and animals: a different taste for microbes? *Curr Opin Plant Biol* **8**(4): 353-360.

Zipfel C, Kunze G, Chinchilla D, Caniard A, Jones JDG, Boller T, Felix G. 2006. Perception of the bacterial PAMP EF-Tu by the receptor EFR restricts Agrobacterium-mediated transformation. *Cell* **125**(4): 749-760.

Zipfel C, Robatzek S, Navarro L, Oakeley EJ, Jones JDG, Felix G, Boller T. 2004. Bacterial disease resistance in Arabidopsis through flagellin perception. *Nature* **428**(6984): 764-767.

Zurzolo C, van Meer G, Mayor S. 2003. The order of rafts - Conference on microdomains, lipid rafts and caveolae. *Embo Reports* **4**(12): 1117-1121.

8. Appendix

Table 1 List of all used *A. thaliana* lines ordered from NASC/ABRC

Ecotype	Background	Marker	Transgene	SALK/SAIL number
Col-0	*ricky1-1*	Kan	SALK T-DNA	SALK_130548.42.45.x
Col-0	*ricky1-2*	Kan	SALK T-DNA	SALK_057812.14.90.x
Col-0	*ryl1-1*	Kan	SALK T-DNA	SALK_047602.23.65.n
Col-0	*ryl1-2*	Kan	SALK T-DNA	SALK_129312C
Col-0	*rem1.2-1*	Kan	SALK T-DNA	SALK_117637.50.50.x
Col-0	*rem1.3-2*	Kan	SALK T-DNA	SALK_117448.53.95.x
Col-0	*lik1-5* (N648255)	Kan	SALK T-DNA	SALK_148255
Col-0	*fls2*	Kan	SAIL T-DNA	SAIL-691C04

Table 2 List of genetic crosses generated in this study

Ecotype	Parental line I	Parental line II
Col-0	*ricky1-1*	*lik1-5*
Col-0	*ryl1-1*	*lik1-5*

Table 3 List of transgenic lines created in this study

Ecotype	Background	Marker	Transgene
Col-0	*ricky1-1*	Kan	SALK T-DNA
		Basta	*proRICKY1:gRICKY1-sGFP*
Col-0	*ricky1-1*	Kan	SALK T-DNA
		Basta	*proRICKY1:gRICKY1-sGFP*
		HygB	*proREM1.2-mCherry-gREM1.2*
Col-0	*ricky1-1*	Kan	SALK T-DNA
		Basta	*proRICKY1:gRICKY1-sGFP*
		HygB	*proREM1.3-mCherry-gREM1.3*

Col-0	*ricky1-1*	Kan	SALK T-DNA
		Basta	*proRICKY1:gRICKY1 D811N-sGFP*
Col-0	*ricky1-1*	Kan	SALK T-DNA
		Basta	*proRICKY1:gRICKY1 D811N-sGFP*
		HygB	*proREM1.2-mCherry-gREM1.2*
Col-0	*ricky1-1*	Kan	SALK T-DNA
		Basta	*proRICKY1:gRICKY1 D811N-sGFP*
		HygB	*proREM1.3-mCherry-gREM1.3*
Col-0	*ricky1-1*	Kan	SALK T-DNA
		Basta	*proRICKY1:gRICKY1 D811N-sGFP*
		HygB	*proREM1.2-mCherry-gREM1.2*
			S11,S13,T18/T19A
Col-0	*ricky1-1*	Kan	SALK T-DNA
		HygB	*35S:amiRYL1*
Col-0	*ricky1-2*	Kan	SALK T-DNA
		Basta	*proRICKY1:gRICKY1-sGFP*
Col-0	*ricky1-2*	Kan	SALK T-DNA
		Basta	*proRICKY1:gRICKY1 D811N-sGFP*
Col-0	*ryl1-1*	Kan	SALK T-DNA
		HygB	*35S:amiRICKY1*
Col-0	*rem1.2-1*	Kan	SALK T-DNA
		Basta	*proRICKY1:gRICKY1-sGFP*
Col-0	*rem1.2-1/*	Kan	SALK T-DNA
	*rem1.3-2 **	Basta	*proRICKY1:gRICKY1-sGFP*

* Double mutants generated by Iris Jarsch

Table 4 Bacterial and yeast strains used in this study

Species	**Strain**	**Purpose of use**
Escherichia coli	DB3.1	Plasmid multiplication and maintenance
Escherichia coli	DH5α	Plasmid multiplication and maintenance, Heterologous expression of RICKY1 CD/RICKY1 D811N CD

Escherichia coli	TOP10	Plasmid multiplication and maintenance
Escherichia coli	Rosetta	Heterologous overexpression
Agrobacterium tumefaciens	Agl1	Stable transformation of *A. thaliana* and transient expression of *N. benthamiana*
Agrobacterium tumefaciens	GV3101	Stable transformation of *A. thaliana* and transient expression of *N. benthamiana*
Saccharomyces cerevisiae	PJ69-4a	GAL4 yeast two-hybrid interaction assay

Table 5 Constructs used in this study

Insert	Vector	Description
REM1.2 cDNA +stop	pGADT7	GAL4 Y2H assay (Iris Jarsch)
REM1.3 cDNA +stop	pGADT7	GAL4 Y2H assay (Iris Jarsch)
REM1.2 cDNA +stop	pGBKT7	GAL4 Y2H assay (Iris Jarsch)
REM1.3 cDNA +stop	pGBKT7	GAL4 Y2H assay (Iris Jarsch)
REM1.2 cDNA +stop	pAMPAT 35S:Yn:GW	*In planta* expression, BiFC (Iris Jarsch)
REM1.2 cDNA +stop	pAMPAT 35S:Yc:GW	*In planta* expression, BiFC (Iris Jarsch)
REM1.3 cDNA +stop	pAMPAT 35S:Yn:GW	*In planta* expression, BiFC (Iris Jarsch)
REM1.3 cDNA +stop	pAMPAT 35S:Yc:GW	*In planta* expression, BiFC (Iris Jarsch)
N-REM1.3/C-REM1.2 +stop	pENTR_D BsaI:GW:BsaI	Domain swap, entry clone
N-REM1.3/C-REM1.2 +stop	pGADT7	Domain swap, GAL4 Y2H assay
N-REM1.3/C-REM1.2 +stop	pENTR_D BsaI:GW:BsaI	Domain swap, entry clone
N-REM1.3/C-REM1.2 +stop	pGADT7	Domain swap, GAL4 Y2H assay
REM1.2 S11A +stop	pKS	Entry clone, phospho-mutant

REM1.2 S13A +stop	pKS	Entry clone, phospho-mutant
REM1.2 T18A +stop	pKS	Entry clone, phospho-mutant
REM1.2 T19A +stop	pKS	Entry clone, phospho-mutant
REM1.2 S11A +stop	pGADT7	GAL4 Y2H assay, phospho-mutant
REM1.2 S13A +stop	pGADT7	GAL4 Y2H assay, phospho-mutant
REM1.2 T18A +stop	pGADT7	GAL4 Y2H assay, phospho-mutant
REM1.2 T19A +stop	pGADT7	GAL4 Y2H assay, phospho-mutant
REM1.2 T41/T46A +stop	pGADT7	GAL4 Y2H assay, phospho-mutant
REM1.2 S11/S13/T18/T19A +stop	pGADT7	GAL4 Y2H assay, phospho-mutant
REM6.4 cDNA +stop	pAMPAT 35S:Yn:GW	*In planta* expression, BiFC
REM6.4 cDNA +stop	pAMPAT 35S:Yc:GW	*In planta* expression, BiFC
RICKY1 CD +stop	pDONRzeo	Enry clone (Birgit Kemmerling)
RYL1 CD +stop	pDONRzeo	Enry clone (Birgit Kemmerling)
RICKY1 CD +stop	pGADT7	GAL4 Y2H assay (Birgit Kemmerling)
RICKY1 CD +stop	pGBKT7	GAL4 Y2H assay (Birgit Kemmerling)
RYL1 CD +stop	pGADT7	GAL4 Y2H assay (Birgit Kemmerling)
RYL1 CD +stop	pGBKT7	GAL4 Y2H assay (Birgit Kemmerling)
RICKY1 D811N CD +stop	pDONRzeo	Entry clone, Kinase-dead RICKY1
RICKY1 D811N CD +stop	pGBKT7	GAL4 Y2H assay, Kinase-dead RICKY1

RICKY1 CD +stop	pASK IBA7 plus	Heterologous overexpression, BsaI free
RICKY1 D811N CD +stop	pASK IBA7 plus	Heterologous overexpression, Kinase-dead RICKY1, BsaI free
RICKY1 cDNA	pDONR207	Entry clone
RICKY1 cDNA	pAMPAT 35S:GW:Yn	*In planta* expression, BiFC
RICKY1 cDNA	pAMPAT 35S:GW:Yc	*In planta* expression, BiFC
RICKY1 cDNA	pDONR207	Entry clone, BsaI free
proRICKY1:gRICKY1 ORF	pENTR_D BsaI:GW:BsaI	BsaI free entry clone
proRICKY1:gRICKY1 ORF	pGWB604	*In planta* expression, C-terminal sGFP tag, BsaI free
proRICKY1:gRICKY1 D811N ORF	pENTR_D BsaI:GW:BsaI	Entry clone, BsaI free
proRICKY1:gRICKY1 D811N ORF	pGWB604	*In planta* expression, C-terminal sGFP tag, BsaI free
proREM1.2-mcherry-gREM1.2 ORF +stop	pGWB1	*In planta* expression, BsaI free (Sebastian Konrad)
proREM1.3-mcherry-gREM1.3 ORF +stop	pGWB1	*In planta* expression, BsaI free (Sebastian Konrad)
proREM1.2-mcherry-gREM1.2 ORF S11/S13/T18/T19A +stop	pGWB1	*In planta* expression, BsaI free, phospho-mutant
amiRICKY1	pENTR_D BsaI:GW:BsaI	Entry clone
amiRYL1	pENTR_D BsaI:GW:BsaI	Entry clone
amiRICKY1	pGWB2	*In planta* expression, amiRNA
amiRYL1	pGWB2	*In planta* expression, amiRNA

Table 6 Primers used in tis study for cloning

Purpose	Forward Primer	Reverse Primer
Cloning RICKY1 cDNA	GGGGACAAGTTTGTACAAAAAAGC AGGCTCCATGGGTTTCTTTTTCTCG ACCC	GGGGACCACTTTGTACAAGAAAGCT GGGTTCTCAATCTCCACATCAGTAA GATC
Cloning proRICKY1:gRICKY1 BsaI free, Fragment 1	GGTCTCGCACCCCCTTGTAAATCTA TTTGCCGC	GGTCTCGGAGAAGAGAGGGAGATA AGAAG
Cloning proRICKY1:gRICKY1 BsaI free, Fragment 2	GGTCTCGTCTCAATCGCTTAGTCTC TTTG	GGTCTCGCAACAATTCAGTCTTTAC CAACAG
Cloning proRICKY1:gRICKY1 BsaI free, Fragment 3	GGTCTCGGTTGTTAATTTGCAGAGA TCTC	GGTCTCGAGATGGGTTTGTACAGAG TAAAGC
Cloning proRICKY1:gRICKY1 BsaI free, Fragment 4	GGTCTCGATCTCCAACATTAAGACC ACCG	GGTCTCGCCTTCTCAATCTCCACAT CAGTAAGATC
D811N mutation	CTAATTTTGGTCTAGCGAAACTCG	AGATCTTAGCATTTAGAGACAGATC
amiRYL1 Fragment 1	TTTGGTCTCTCACCCTGCAAGGCG ATTAAGTTGGGTAAC	GAATTCTAAGATACTTACAGTAGTCT ACATATATATTCCT
amiRYL1 Fragment 2	GACTACTGTAAGTATCTTAGAATTC ACAGGTCGTGATATG	GACTGCTGTAAGTATGTTAGAAATC AAAGAGAATCAATGA
amiRYL1 Fragment 3	GATTTCTAACATACTTACAGCAGTC TCTCTTTTGTATTCC	AAAGGTCTCACCTTGCGGATAACAA TTTCACACAGGAAACA
Assembly amiRNAs	TTTGGTCTCTCACCCTGCAAGGCG ATTAAGTTGGGTAAC	AAAGGTCTCACCTTGCGGATAACAA TTTCACACAGGAAACA
amiRICKY1 Fragment 1	TTTGGTCTCTCACCCTGCAAGGCG ATTAAGTTGGGTAAC	GAACTATGCTTACCTTGTTGTTCTCT ACATATATATTCCT
amiRICKY1 Fragment 2	GAGAACAACAAGGTAAGCATAGTT CACAGGTCGTGATATG	GAGAGCAACAAGGTATGCATAGATC AAAGAGAATCAATGA
amiRICKY1 Fragment 3	GATCTATGCATACCTTGTTGCTCTC TCTCTTTTGTATTCC	AAAGGTCTCACCTTGCGGATAACAA TTTCACACAGGAAACA
Mutation of the BsaI site in RICKY1 cDNA	TTAAGACCACCGATGTCATCTG	TGTTGGAGATGGGTTTGTACAG
Cloning RICKY1 CD	TTTGGTCTCTGCGCAGGCTAACAG GTTACTTAGG	AAAGGTCTCTTATCATTACTCAATCT CCACATCAG
Mutation REM1.2	GCGAAGGTTGCGGCTCCTG	CGGAGCTTCTGCTTCTAACG

S11/S13/T18/T19A		
Mutation REM1.2 S11A	GAAGGTTACGACTCCTGCTCC	GCCGGAGATTCtGCTTCTAAC
Mutation REM1.2 S13A	GAAGGTTACGACTCCTGCTCC	GCCGGAGCTTCTGATTCTAAC
Mutation REM1.2 T18A	GAAGGTTGCGACTCCTGCTC	GCCGGAGATTCTGATTCTAAC
Mutation REM1.2 T19A	GAAGGTTACGGCTCCTGCTC	GCCGGAGATTCTGATTCTAAC
Mutation REM1.2 T41/T46A	GATGTCGCGAAAGACGTTGC	AGCCGGAGCCGGAGCTGG
N-REM1.2 for domain swap	TTTGGTCTCTCACCATGGCGGAGG AACAGAAGATAGC	AAAGGTCTCAATCTCTATCGAGCGA TGCAGAC
N-REM1.3 for domain swap	TTTGGTCTCTCACCATGGCGGAGG AGCAAAAGAC	AAAGGTCTCAATCTCTATCGGCCGA ACCAG
C-REM1.2 for domain swap	TTTGGTCTCTAGATGTTAAGCTAGC TGATTTGTC	AAAGGTCTCACCTTTTAGAAACATCC ACAAGTTG
C-REM1.3 for domain swap	TTTGGTCTCTAGATGTGATACTTGC CGACTTGG	AAAGGTCTCACCTTTTAGAAACATCC ACACGTTGC

Table 7 Primers used in this study for genotyping

	Forward Primer	**Reverse Primer**
ricky1-1 gene specific	CAAGACCTGATTGTTTCTTAC TTTC	CTCAATCTCCACATCAGTAAG ATC
ricky1-2 gene specific	CTTAGGTGGAAAAGAAGTGG ATG	CTCAATCTCCACATCAGTAAG ATC
ryl1-1 gene specific	GAAGACACTGTAAGTCAAACT CTG	CAAGCACCATTGAACACTATA CAC
lik1-5 gene specific	GGAAGTTCTGTTGGTACAGT GG	CTCGTAAACTAGCAGGAGCTG
T-DNA specific primer	-------	ATTTTGCCGATTTCGGAAC

Table 8 qPCR primers used in this study

Gene	Forward Primer	Reverse Primer
RICKY1	GTCCACGAGGAACAAGGTA	GTATTCTCTTCTTCATCGAGTTTC
RYL1	GATTTTGGTCTAGCTAAACTCAAC	GTAAACATCTGCCTTGTCTGTC
REM1.2	GGAAGCAGAAGAGAGAAGAGC	CACTTTACAGTTACGAAGTCTTG
REM1.3	AAAGGCAACGTGTGGATGT	CAAGACACAAACGACCAAACA
REM1.4	GGAATTAGCAGCCAAGTACCG	TGTTTCCCCATCGAGATGAT
LIK1	CCTTCTTGACTGGGTGCACG	CGAGCATACTCACCACCGTC
EDS1	CGAAGGGGACATAGATTGGA	ATGTACGGCCCTGTGTCTTC
FRK1	ATCTTCGCTTGGAGCTTCTC	TGCGGCGCAAGGACTAGAG
PR1	TTCTTCCCTCGAAAGCTCAA	AAGGCCCACCAGAGTGTATG
LOX3	TGGAAATGAGTGCCGCCGCA	GTAGCGTTCAACATAGGTTCG
JAZ10	ATCCCGATTTCTCCGGTCCA	ACTTTCTCCTTGCGATGGGAAGA
UBC	CTGCGACTCAGGGAATCTTCTAA	TTGTGCCATTGAATTGAACCC

9. Danksagung

10. Curriculum vitae

Personal Information

___

Name   Corinna Anna Buschle

Birth name   Hofer

Email

Current Position

___

Since 10/2012   PHD student in the research group of Prof. Dr. Thomas Ott

                 Ludwig-Maximilians-Universität Munich, Germany

                 Albert-Ludwigs-Universität Freiburg, Germany

Education

___

10/2010 – 07/2012   Master of Science, Biology, LMU Munich

                     Master thesis in the lab of Dr. Thomas Ott

10/2007 – 07/2010   Bachelor of Science, Biology, LMU Munich

                     Bachelor thesis in the lab of Dr. Cordelia Bolle

09/1998 – 07/2007   Hans-Carossa-Gymnasium, Landshut

                     Abitur